



Multiplicative Expansion of the Pool of Fully Synthetic Tetracycline Antibiotics

Citation

Wright, Peter Maughan. 2012. Multiplicative Expansion of the Pool of Fully Synthetic Tetracycline Antibiotics. Doctoral dissertation, Harvard University.

Permanent link

<http://nrs.harvard.edu/urn-3:HUL.InstRepos:10364587>

Terms of Use

This article was downloaded from Harvard University's DASH repository, and is made available under the terms and conditions applicable to Other Posted Material, as set forth at <http://nrs.harvard.edu/urn-3:HUL.InstRepos:dash.current.terms-of-use#LAA>

Share Your Story

The Harvard community has made this article openly available.
Please share how this access benefits you. [Submit a story](#).

[Accessibility](#)

© 2012 – Peter Maughan Wright

All rights reserved.

Multiplicative Expansion of the Pool of Fully Synthetic Tetracycline Antibiotics

Abstract

This thesis describes the development of chemical pathways for the preparation of more than 80 novel fully synthetic tetracyclines with structural variability at positions C5 and C5a. Progress toward the synthesis of 5-hetero-tetracyclines, another new class of tetracycline antibiotics, is also described. The results detailed herein – including successful C-ring-forming Michael–Claisen cyclizations of numerous modified AB precursors with just a few of the extraordinarily diverse D-ring precursors known to be effective nucleophiles in this key coupling reaction – represent the first steps toward a multiplicative expansion of the pool of fully synthetic tetracyclines.

Novel and versatile β -functionalization reaction sequences employing tris(methylthio)methylithium and 2-lithio-1,3-dithiane have been developed to transform the AB enone **10** (the key precursor to fully synthetic tetracyclines) into a diverse range of β -substituted AB enone products, including a highly efficient, single-operation method for the synthesis of a β -methyl ester-substituted AB enone (**20**). It is demonstrated that the six-membered C ring of tetracyclines comprising a C5a quaternary carbon center (e.g. **29**) can be assembled by stereocontrolled coupling reactions of β -substituted AB enones and *o*-toluate ester anion D-ring precursors. A C5a–C11a-bridged cyclopropane tetracycline precursor (**37**) was found to undergo efficient and regioselective ring-opening reactions with a range of nucleophiles in the presence

of magnesium bromide, thus providing another avenue for the preparation of fully synthetic tetracyclines containing an all-carbon quaternary center at position C5a.

The AB enone **10** has also been transformed into structurally diverse γ -substituted AB precursors, which in turn have been converted into fully synthetic tetracyclines with unprecedented modifications at position C5, including 5-fluorotetracyclines such as **94**. Numerous fully synthetic tetracyclines and tetracycline precursors have been shown to serve as diversifiable branch-points, allowing maximally expedient synthesis of C5- and C5a-substituted tetracyclines by late-stage diversification.

The substrate scope of the Michael–Claisen cyclization reaction has been expanded to include new heterocyclic enone electrophiles such as dihydro-4-pyridones, affording cycloadducts such as **142**. In this way, the viability of an iterative Michael–Claisen strategy for constructing 5-hetero-tetracyclines has been established. Numerous examples in this thesis serve to further demonstrate the broad applicability of the Michael–Claisen cyclization reaction as a powerful method for the assembly of stereochemically complex six-membered rings.

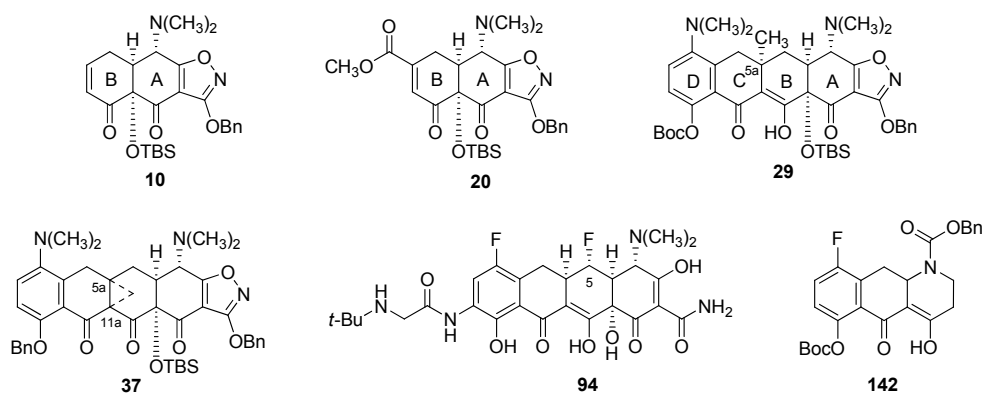


Table of Contents

Abstract	iii
Table of Contents	v
Acknowledgements	vii
List of Abbreviations	ix
Chapter 1 Introduction	1
Introduction	2
Michael–Claisen Reaction Sequences	10
Antibacterial Action of Tetracyclines	14
Tetracycline Resistance	24
Chapter 2 Synthesis of C5a-Substituted Tetracyclines	31
Introduction	32
Results	36
Antibacterial Activities	52
Conclusion	63
Experimental Section	64

Catalog of Spectra	128
Chapter 3 Synthesis of C5-Substituted Tetracyclines	153
Introduction	154
Results	158
Antibacterial Activities	171
Conclusion	185
Experimental Section	186
Catalog of Spectra	254
Chapter 4 Progress Toward the Synthesis of 5-Hetero-Tetracyclines	276
Introduction	277
Retrosynthetic Strategy and Background	282
Results	286
Conclusion	295
Experimental Section	296
Catalog of Spectra	333

Acknowledgements

First, I would like to thank my thesis advisor, Professor Andrew Myers. I am extremely grateful for Andy's mentorship, his incredible commitment to the tetracycline project, his ability to pay such close attention to the smallest details (of experiments and written communication) while never losing sight of the big picture, and his singular talent for inspiring metaphors. I would also like to thank Professors Eric Jacobsen and Tobias Ritter for serving on my Graduate Advising Committee. I have always enjoyed our interactions and it has been a privilege to carry out chemistry research in the same department as academics of their caliber.

Throughout my tenure in the Myers group I have been fortunate to be surrounded by brilliant chemists and great people. I would particularly like to thank Jon Mortison and Evan Hecker for being extremely helpful and entertaining baymates. I also thank the other recent members of "Team Tetracycline" – Fan Liu, Robin Sussman, David Kummer, and Amelie Dion – for being fantastic co-workers. I especially acknowledge Simon Lewis for his incredible patience while teaching me basic experimental techniques during my first stint in the Myers group as an undergraduate summer student.

I would like to express heartfelt thanks to Diana Eck and Dorothy Austin, the Masters of Lowell House, for giving me the opportunity to live and work in their wonderful community as a resident tutor. Lowell House breathed new life into my graduate school experience and has provided me with so many friends and memories I will cherish for a long time to come.

I thank my mother, Angela, for giving me a fantastic start in life and for her constant love and support, even from such a long distance. Finally, I would like to thank Professor George

Fleet, my organic chemistry tutor at St. John's College, Oxford, a wonderful teacher and mentor who opened my eyes to where chemistry could take me.

List of Abbreviations

Å	angstrom
AB	<i>Acinetobacter baumannii</i>
BC	<i>Burkholderia cenocepacia</i>
Bn	benzyl
Boc	<i>tert</i> -butyl carbonate
DBU	1,8-diazabicyclo[5.4.0]undec-7-ene
DCE	1,2-dichloroethane
DEAD	diethyl azodicarboxylate
DMAP	4-dimethylaminopyridine
DMF	dimethylformamide
DMSO	dimethyl sulfoxide
EC	<i>Escherichia coli</i>
EF	<i>Enterococcus faecalis</i>
equiv	equivalent
ESI	electrospray ionization

Et	ethyl
FDA	Food and Drug Administration
FTIR	Fourier transform infrared
g	gram
HMPA	hexamethylphosphoramide
HRMS	high-resolution mass spectrometry
Hz	hertz
IBX	2-iodoxybenzoic acid
<i>J</i>	coupling constant (in Hz)
KHMDS	potassium hexamethyldisilazide
KP	<i>Klebsiella pneumoniae</i>
LDA	lithium diisopropylamide
LiHMDS	lithium hexamethyldisilazide
M	molar (moles/liter)
mg	milligram
MHz	megahertz

MIC	minimum inhibitory concentration
mL	milliliter
mmol	millimole
NaHMDS	sodium hexamethyldisilazide
NBS	<i>N</i> -bromosuccinimide
NCS	<i>N</i> -chlorosuccinimide
NIS	<i>N</i> -iodosuccinimide
NMR	nuclear magnetic resonance
nOe	nuclear Overhauser effect
PA	<i>Pseudomonas aeruginosa</i>
Pd	palladium
Ph	phenyl
PM	<i>Proteus mirabilis</i>
ppm	parts per million
Pr	propyl
<i>R</i>	rectus (Cahn-Ingold-Prelog system)

Rf	retention factor
<i>S</i>	sinister (Cahn-Ingold-Prelog system)
SA	<i>Staphylococcus aureus</i>
SM	<i>Stenotrophomonas maltophilia</i>
SP	<i>Streptococcus pneumoniae</i>
TBS	<i>tert</i> -butyldimethylsilyl
TBSOTf	<i>tert</i> -butyldimethylsilyl trifluoromethanesulfonate
Tf ₂ O	trifluoromethanesulfonic anhydride
TFA	trifluoroacetic acid
THF	tetrahydrofuran
TLC	thin-layer chromatography
TMEDA	<i>N,N,N',N'</i> -tetramethylethylenediamine
TMSCl	chlorotrimethylsilane
UV	ultraviolet

Chapter 1

Introduction

Introduction

The tetracyclines are a class of broad-spectrum antibiotics that have been widely used in human and veterinary medicine for more than 50 years.¹ The first tetracycline antibiotic was discovered in 1948 when Benjamin Duggar of Lederle Laboratories isolated the natural product chlorotetracycline (Aureomycin®, **1**, Figure 1.1) from the culture broth of a novel species of *Streptomyces*.² Within two years a research team from Chas. Pfizer and Co. had isolated a second natural tetracycline, oxytetracycline (Terramycin®, **2**),³ and in 1953 tetracycline itself (**3**) was prepared from chlorotetracycline by catalytic hydrogenolysis of the carbon-chlorine bond, a transformation discovered by Lloyd Conover of Pfizer.⁴ Subsequently, tetracycline was found to be a natural product and,⁵ later still, Lederle researchers isolated 6-demethyltetracyclines (see structures **4** and **5**) from culture broths of a mutant strain of *Streptomyces*.⁶

¹ *Tetracyclines in Biology, Chemistry and Medicine*; Nelson, M.; Hillen, W.; Greenwald, R. A., Eds.; Birkhauser: Boston, **2001**.

² (a) Duggar, B. M. *Ann. N. Y. Acad. Sci.* **1948**, *51*, 177–181. (b) Duggar, B. M. Aureomycin and Preparation of Same. U.S. Patent 2,482,055, Sept 13, 1949.

³ (a) Finlay, A. C.; Hobby, G. L.; P'an, S. Y.; Regna, P. P.; Routien, J. B.; Seeley, D. B.; Shull, G. M.; Sobin, B. A.; Solomons, I. A.; Vinson, J. W.; Kane, J. H. *Science* **1950**, *111*, 85. (b) Sobin, B. A.; Finlay, A. C. Terramycin and its Production. U.S. Patent 2,516,080, July 18, 1950.

⁴ (a) Booth, J. H.; Morton, J.; Petisi, J. P.; Wilkinson, R. G.; Williams, J. H. *J. Am. Chem. Soc.* **1953**, *75*, 4621. (b) Conover, L. H.; Moreland, W. T.; English, A. R.; Stephens, C. R.; Pilgrim, F. J. *J. Am. Chem. Soc.* **1953**, *75*, 4622–4623.

⁵ Minieri, P. P.; Sokol, H.; Firman, M. C. Process for the Preparation of Tetracycline and Chlorotetracycline. U. S. Patent 2,734,018, Feb 7, 1956.

⁶ McCormick, J. R. D.; Sjolander, N. O.; Hirsch, U.; Jensen, E. R.; Doerschuk, A. P. *J. Am. Chem. Soc.* **1957**, *79*, 4561–4563.

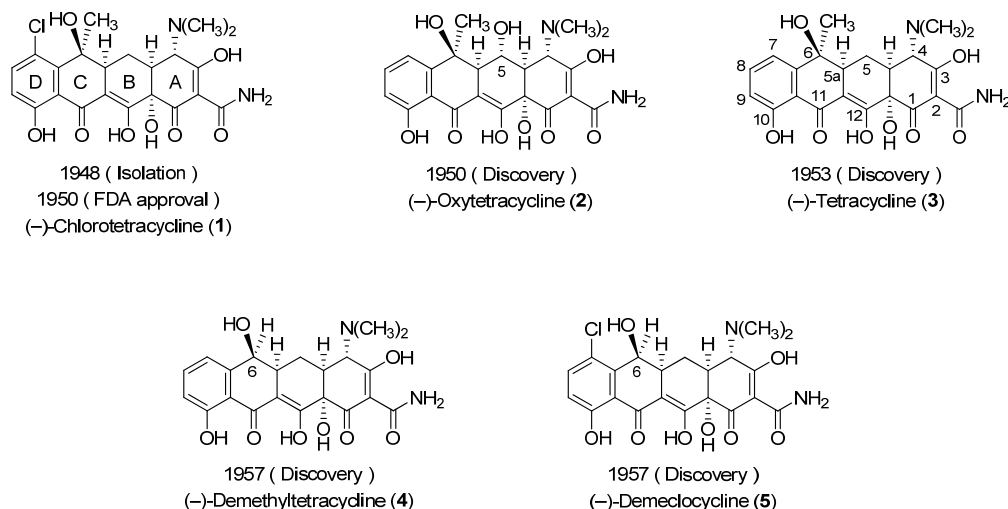


Figure 1.1 Natural tetracycline antibiotics.

All tetracyclines approved for human or veterinary use are fermentation products or are derived from fermentation products by semisynthesis. This is also true of most beta-lactam and all macrolide antibiotics. Tracing the paths of human efforts to produce new antibiotics from natural products not accessible by synthesis reveals an evolutionary process marked by specific, impactful discoveries. In the case of the tetracyclines, Pfizer scientists achieved a major enabling advance approximately 10 years after the class had been identified when they demonstrated that the C6-hydroxyl group of the natural products oxytetracycline (2), tetracycline (3) and 6-demethyltetracycline (4) could be removed reductively.⁷ The 6-deoxytetracyclines produced, including 6-deoxy-6-

⁷ (a) Stephens, C. R.; Murai, K.; Rennhard, H. H.; Conover, L. H.; Brunings, K. J. *J. Am. Chem. Soc.* **1958**, *80*, 5324–5325. (b) McCormick, J. R. D.; Jensen, E. R.; Miller, P. A.; Doerschuk, A. P. *J. Am. Chem. Soc.* **1960**, *82*, 3381–3386. (c) Stephens, C. R.; Beereboom, J. J.; Rennhard, H. H.; Gordon, P. N.; Murai, K.;

demethyltetracycline (sancycline, **6**, Figure 1.2), were found to be more stable than the parent compounds, yet retained broad-spectrum antibacterial activity. The important and now generic antibiotics doxycycline (Pfizer, 1967, **7**) and minocycline (Lederle, 1972, **8**) followed as a consequence, the latter arising from the additional discovery that electrophilic aromatic substitution at C7 becomes possible when the more stable 6-deoxytetracyclines are used as substrates.⁸

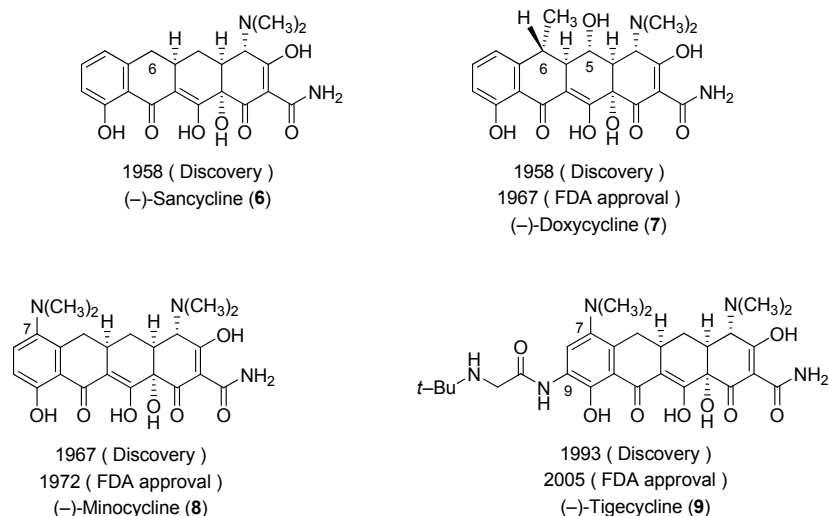


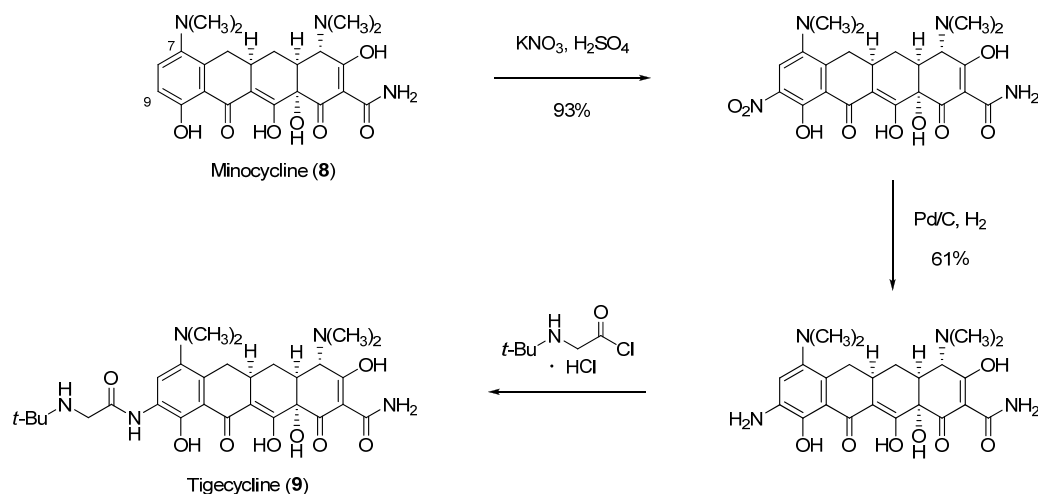
Figure 1.2 Semisynthetic tetracycline antibiotics.

Decades later, a team of Wyeth scientists led by Frank Tally synthesized 7,9-disubstituted tetracycline derivatives, leading to the discovery of the antibiotic tigecycline

Blackwood, R. K.; Schach von Wittenau, M. *J. Am. Chem. Soc.* **1963**, *85*, 2643–2652. (d) Blackwood, R. K.; Stephens, C. R. *J. Am. Chem. Soc.* **1962**, *84*, 4157–4159.

⁸ (a) Martell, M. J.; Boothe, J. H. *J. Med. Chem.* **1967**, *10*, 44–46. (b) Church, R. F. R.; Schaue, R. E.; Weiss, M. J. *J. Org. Chem.* **1971**, *36*, 723–725. (c) Spencer, J. L.; Hlavka, J. J.; Petisi, J.; Krazinski, H. M.; Boothe, J. H. *J. Med. Chem.* **1963**, *6*, 405–407. (d) Zambrano, R. T. U.S. Patent 3,483,251, Dec 9, **1969**.

(Tigacyl®, US approval 2005, **9**).⁹ Tigecycline is the most important member of a class of tetracyclines known as glycylcyclines which retain activity against many tetracycline-resistant bacteria (*vide infra*). As shown in Scheme 1.1 below, tigecycline (**9**) is synthesized from minocycline (**7**) by an efficient three-step sequence comprising: (1) nitration at the C9 position of minocycline upon addition of potassium nitrate to a solution of minocycline in concentrated sulfuric acid, (2) palladium-catalyzed reduction of the nitro group, and (3) acylation of the resulting aniline with 2-(*tert*-butylamino)acetyl chloride hydrochloride.



Scheme 1.1. Synthesis of tigecycline (**9**) from minocycline (**8**).

⁹ (a) Sum, P.-E.; Lee, V. J.; Testa, R. T.; Hlavka, J. J.; Ellestad, G. A.; Bloom, J. D.; Gluzman, Y.; Tally, F. *P. J. Med. Chem.* **1994**, 37, 184–188. (b) Sum, P.-E.; Petersen, P. *Bioorg. Med. Chem. Lett.* **1999**, 9, 1459–1462.

A generalized structure-activity relationship profile of tetracyclines was formulated following extensive semisynthetic investigations (Figure 1.3). Structural modification of the D ring and upper periphery of tetracyclines provided compounds with enhanced, equal or reduced antibacterial activity; this region is therefore considered “variable”. Antibacterial activity was diminished or abolished by modification of the lower periphery and A ring, indicating that the functional groups at these positions are essential for the antibiotic action of tetracyclines. These observations were rationalized by X-ray crystal structures of tetracycline bound to its target, the bacterial ribosome (*vide infra*).¹⁰ The limitations of semisynthesis have meant that relatively few structural variations have been explored along the upper periphery of tetracyclines (C4, C4a, C5, C5a and C6). This region is considered variable largely on the basis that natural tetracyclines have different substitution patterns at C5 and C6. Like many “old” classes of antibiotics, tetracyclines have never been systematically modified by de novo synthesis and knowledge of structure-activity relationships is limited or non-existent at many positions on the scaffold.¹¹

¹⁰ (a) Brodersen, D. E.; Clemons, W. M., Jr.; Carter, A. P.; Morgan-Warren, R. J.; Wimberly, B. T.; Ramakrishnan, V. *Cell* **2000**, *103*, 1143–1154. (b) Pioletti, M.; Schlünzen, F.; Harms, J.; Zarivach, R.; Glühmann, M.; Avila, H.; Bashan, A.; Bartels, H.; Auerbach, T.; Jacobi, C.; Hartsch, T.; Yonath, A.; Franceschi, F. *EMBO J.* **2001**, *20*, 1829–1839.

¹¹ Von Nussbaum, F.; Brands, M.; Hinzen, B.; Weigand, S.; Häbich, D. *Angew. Chem. Int. Ed.* **2006**, *45*, 5072–5129.

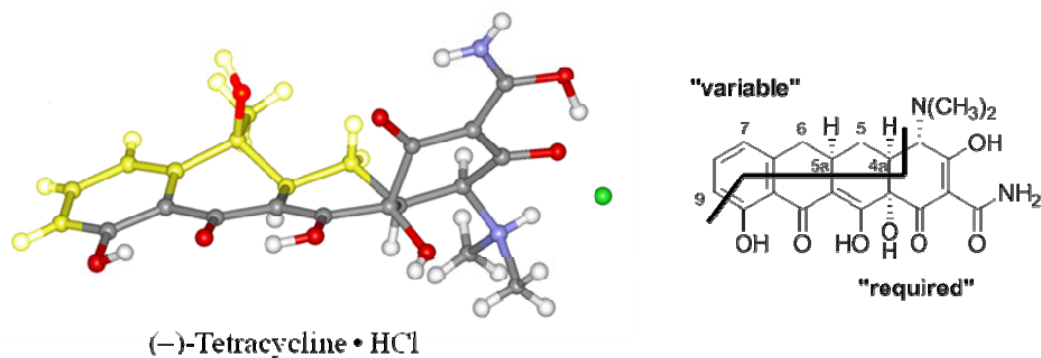


Figure 1.3 Summary of 50 years of structure-activity relationships data.

From the time that the structures of the tetracycline antibiotics were first revealed by Woodward and collaborators,¹² many laboratories have sought to develop a practical route for their synthesis. Strategically, the original route developed by Woodward and collaborators for the synthesis of sancycline employed a "left-to-right" or D→A mode of construction. The Shemyakin and Muxfeldt research groups adopted a similar directionality in their remarkable syntheses of tetracycline (**3**, 1967) and oxytetracycline (**2**, 1968), respectively, using a bicyclic CD-ring precursor as starting material.^{13,14}

¹² (a) Hochstein, F. A.; Stephens, C. R.; Conover, L. H.; Regna, P. P.; Pasternack, R.; Gordon, P. N.; Pilgrim, F. J.; Brunings, K. J.; Woodward, R. B. *J. Am. Chem. Soc.* **1953**, *75*, 5455-5475. (b) Stephens, C. R.; Conover, L. H.; Hochstein, F. A.; Regna, P. P.; Pilgrim, F. J.; Brunings, K. J. *J. Am. Chem. Soc.* **1952**, *74*, 4976-4977.

¹³ (a) Gurevich, A. I.; Karapetyan, M. G.; Kolosov, M. N.; Korobko, V. G.; Onoprienko, V. V.; Popravko, S. A.; Shemyakin, M. M. *Tetrahedron Lett.* **1967**, *8*, 131-134. (b) Kolosov, M. N.; Popravko, S. A.; Shemyakin, M. M. *Lieb. Ann.* **1963**, *668*, 86-91.

¹⁴ (a) Muxfeldt, H.; Hardtmann, G.; Kathawala, F.; Vedejs, E.; Mooberry, J. B. *J. Am. Chem. Soc.* **1968**, *90*, 6534-6536. (b) Muxfeldt, H.; Haas, G.; Hardtmann, G.; Kathawala, F.; Mooberry, J. B.; Vedejs, E. *J. Am. Chem. Soc.* **1979**, *101*, 689-701.

The Myers laboratory adopted a completely different synthetic approach to the tetracyclines, aiming to form the C ring by convergent coupling of D- and AB-ring precursors.^{15,16} This strategy was devised following consideration of structure-activity relationship data and X-ray crystal structures of tetracycline bound to the bacterial ribosome (its putative target).¹⁰ Much of the functionality known to be required for binding to the ribosome was contained (in protected form) in the AB precursor **10** (Scheme 1.2 below). It was intended that structural variation would be permitted in the D-ring portion of tetracyclines, which had emerged as the most promising site for the attachment of new substituents.

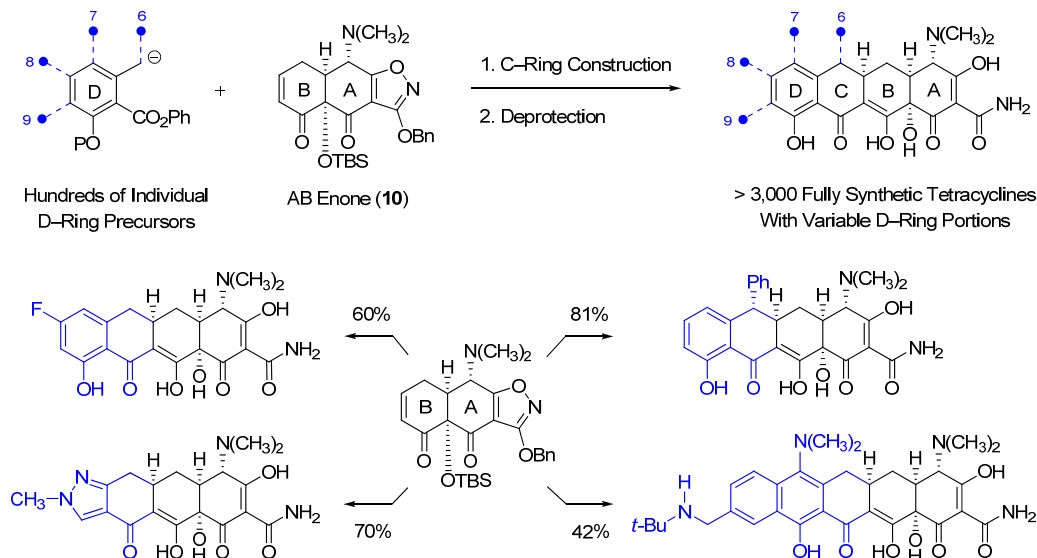
To date more than 3,000 fully synthetic molecules of the tetracycline class, broadly defined, have been prepared by a general and convergent process that involves a Michael–Claisen coupling of the AB enone **10** with structurally diverse D-ring precursors followed by deprotection, a route of typically 3–4 steps (Scheme 1.2).^{17,18} Most of the candidate antibiotics prepared in this way would have been difficult if not impossible to obtain by semisynthesis. Thus, the development of a practical, convergent synthesis of tetracyclines has dramatically expanded the pool of accessible compounds, allowing unprecedented modifications at positions C6, C7, C8, C9 and C10.

¹⁵ Charest, M. G.; Lerner, C. D.; Brubaker, J. D.; Siegel, D. R.; Myers, A. G. *Science* **2005**, *308*, 395–398.

¹⁶ Sun, C.; Wang, Q.; Brubaker, J. D.; Wright, P. M.; Lerner, C. D.; Noson, K.; Charest, M. G.; Siegel, D. R.; Wang, Y.-M.; Myers, A. G. *J. Am. Chem. Soc.* **2008**, *130*, 17913–17927.

¹⁷ Clark, R. B.; He, M.; Fyfe, C.; Lofland, D.; O'Brien, W. J.; Plamondon, L.; Sutcliffe, J. A.; Xiao, X.-Y. *J. Med. Chem.* **2011**, *54*, 1511–1528.

¹⁸ Sun, C.; Hunt, D. K.; Clark, R. B.; Lofland, D.; O'Brien, W. J.; Plamondon, L.; Xiao, X.-Y. *J. Med. Chem.* **2011**, *54*, 3704–3731.



Scheme 1.2. The Myers synthetic approach to tetracyclines.

Three distinct synthetic routes to the AB enone **10** have been reported.^{15,19,20} The convergency and scalability of the second- and third-generation routes have enabled preparation of large quantities of this key intermediate. The third-generation route (see Chapter 4 Introduction for complete discussion) is characterized by a highly diastereoselective A-ring-forming Michael–Claisen coupling reaction, meaning that all four carbon-carbon bonds needed to assemble tetracyclines from three readily available components – a D-ring precursor, B-ring precursor **11** and isoxazole precursor **12** (Figure 1.4) – are formed using this powerful method for bond-pair construction (see Scheme 1.4 for details of these cyclization reactions).

¹⁹ Brubaker, J. D.; Myers, A. G. *Org. Lett.* **2007**, 9, 3523–3526.

²⁰ Kummer, D. A.; Li, D.; Dion, A.; Myers, A. G. *Chem Sci.* **2011**, 2, 1710–1718.

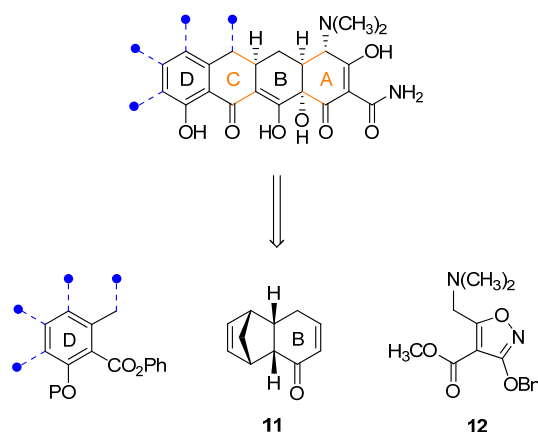


Figure 1.4. Construction of tetracyclines by iterative Michael–Claisen cyclizations; bonds and rings formed by Michael–Claisen reactions are highlighted in orange.

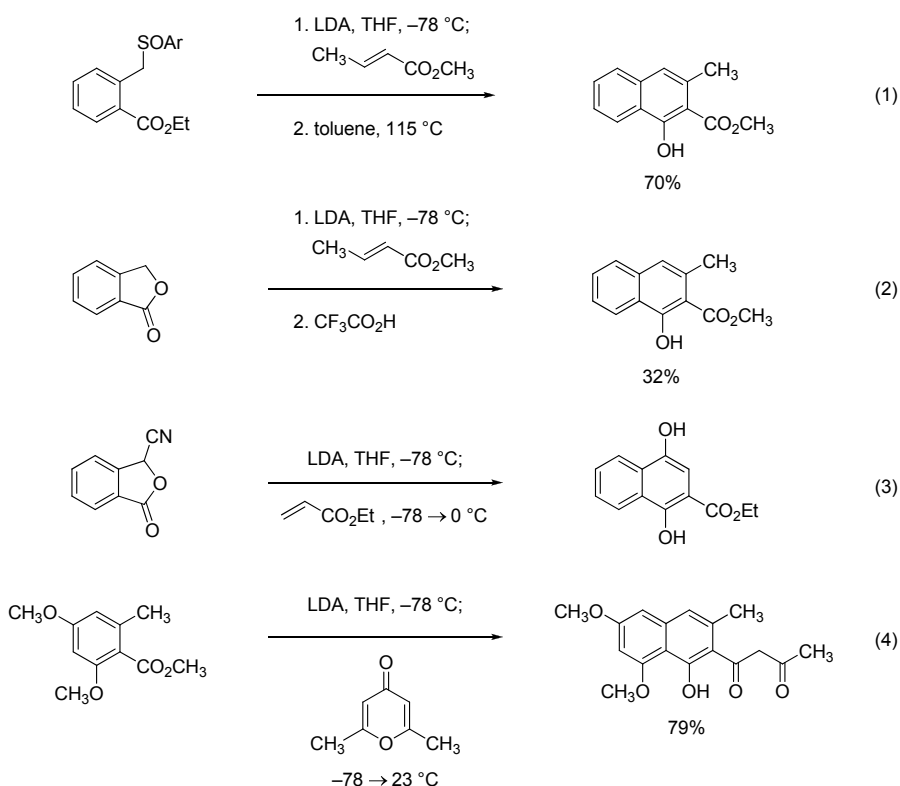
Michael–Claisen Reaction Sequences

Michael–Claisen and Michael–Dieckmann reaction sequences have been widely employed in organic synthesis to construct naphthalene derivatives and non-aromatic six-membered rings.²¹ The origins of this method for bond-pair construction can be traced to 1978, when three different cyclization protocols were introduced by independent research groups. Hauser and Rhee used a sulfoxide-stabilized *o*-toluate ester anion as the nucleophilic component in a Michael–Dieckmann cyclization reaction with methyl crotonate (Scheme 1.3, eq 1). In this case, aromatization occurred upon thermal elimination of phenylsulfenic acid.²² The use of phthalide and cyanophthalide anions as

²¹ (a) Mal, D.; Pahari, P. *Chem. Rev.* **2007**, *107*, 1892–1918. (b) Mitchell, A. S.; Russell, R. A. *Tetrahedron* **1995**, *51*, 5207–5236. (c) Rathwell, K.; Brimble, M. A. *Synthesis* **2007**, *5*, 643–662.

²² Hauser, F. M.; Rhee, R. P. *J. Org. Chem.* **1978**, *43*, 178–180.

nucleophilic components was described by Broom and Sammes (eq 2),²³ and Kraus and Sugimoto (eq 3),²⁴ respectively. Formal loss of water and hydrogen cyanide, respectively, led to naphthoate ester products in these procedures.



Scheme 1.3. Early examples of Michael–Claisen and Michael–Dieckmann cyclizations.

In 1979, the Weinreb and Staunton research groups first reported that simple *o*-toluate ester anions (unsubstituted at the benzylic position) undergo Michael–Claisen

²³ Broom, N. J. P.; Sammes, P. G. *J. Chem. Soc., Chem. Comm.* **1978**, 162–164.

²⁴ Kraus, G. A.; Sugimoto, H. *Tetrahedron Lett.* **1978**, 26, 2263–2266.

cyclization reactions with β -methoxycyclohexenones and γ -pyrones to form naphthyl ketones (eq 4, Scheme 1.3), a sequence sometimes referred to as Staunton–Weinreb annulation.²⁵ Experimental evidence indicates that the mechanism of this reaction sequence involves sequential conjugate addition, β -elimination of alkoxide, re-lithiation at the benzylic position (in the presence of excess base), followed by Claisen cyclization.

There are numerous examples of the formation of non-aromatic 6-membered rings by Michael–Claisen and Michael–Dieckmann reaction sequences.²⁶ However, the stereochemical features of these cyclization reactions have only rarely been discussed,²⁷ frequently because they were of little consequence (aromatization followed cyclization). The Michael–Claisen cyclizations developed as part of Myers’ synthesis of tetracyclines are unusual in their stereochemical complexity, stereocontrol and efficiency. The C-ring-forming cyclizations of D-ring precursors with AB enone **10** appear to proceed with complete stereocontrol at C5a (attack upon a single diastereoface of the enone; see Scheme 1.4 for an example).¹⁶ This selectivity may arise as a consequence of stereoelectronic factors (pseudoaxial addition to the enone) and/or steric effects (addition

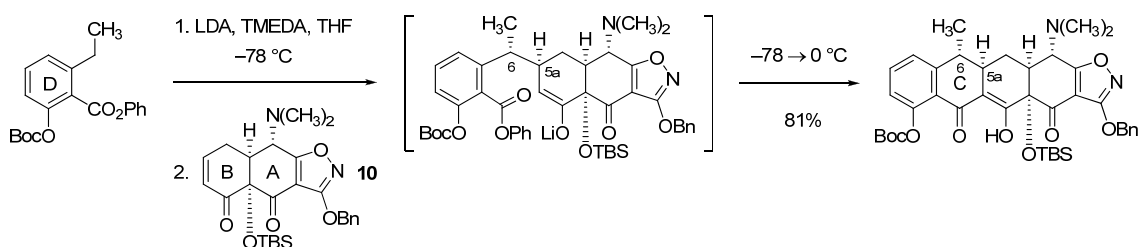
²⁵ (a) Dodd, J. H.; Weinreb, S. M. *Tetrahedron Lett.* **1979**, *38*, 3593–3596. (b) Dodd, J. H.; Starrett, J. E.; Weinreb, S. M. *J. Am. Chem. Soc.* **1984**, *106*, 1811–1812. (c) Leeper, F. J.; Staunton, J. *J. Chem. Soc., Chem. Comm.* **1979**, *5*, 206–207. (d) Leeper, F. J.; Staunton, J. *J. Chem. Soc. Perkin Trans. 1* **1984**, 1053–1059.

²⁶ (a) Tarnchompoo, B.; Thebtaranonth, C.; Thebtaranonth, Y. *Synthesis* **1986**, *9*, 785–786. (b) Boger, D. L.; Zhang, M. *J. Org. Chem.* **1992**, *57*, 3974–3977. (c) Nishizuka, T.; Hirose, S.; Kondo, S.; Ikeda, D.; Takeuchi, T. *J. Antibiotics* **1997**, *50*, 755–764. (d) Hill, B.; Rodrigo, R. *Org. Lett.* **2005**, *7*, 5223–5225. (e) Tatsuta, K.; Yoshimoto, T.; Gunji, H.; Okado, Y.; Takahashi, M. *Chem. Lett.* **2000**, 646–647.

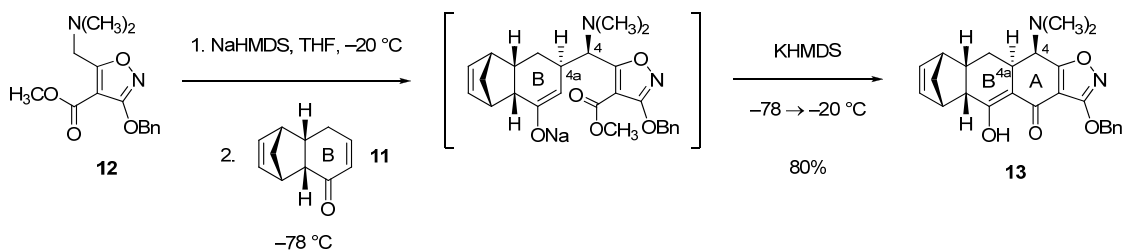
²⁷ For examples of stereocontrol in Michael–Claisen and Michael–Dieckmann cyclization reactions, see: (a) Franck, R. W.; Bhat, V.; Subramaniam, C. S. *J. Am. Chem. Soc.* **1986**, *108*, 2455–2457. (b) Tatsuta, K.; Yamazaki, T.; Mase, T.; Yoshimoto, T. *Tetrahedron Lett.* **1998**, *39*, 1771–1772. (c) White, J. D.; Demnitz, F. W. J.; Qing, X.; Martin, W. H. C. *Org. Lett.* **2008**, *10*, 2833–2836.

of the nucleophile to the π -face opposite the *tert*-butyldimethylsilyloxy substituent, which is also axial; see Figure 1.5 below). The C-ring-forming cyclization depicted in Scheme 1.4 occurs with >20:1 stereoselectivity at C6.

Michael–Claisen cyclization to form the C ring of tetracyclines :



Michael–Claisen cyclization to form the A ring of tetracyclines :



Scheme 1.4. Diastereoselective Michael–Claisen cyclizations to form the C ring and the A ring of tetracyclines.

As noted above, the key step of the third-generation synthesis of the AB enone is another highly diastereoselective Michael–Claisen coupling, in this case forming the A ring of tetracyclines (Scheme 1.4). Conjugate addition of the sodium enolate of isoxazole precursor **12** to the B-ring precursor **11** occurs with complete control of relative stereochemistry at C4 and C4a, affording cycloadduct **13** in 80% yield as a single

diastereomer (following Claisen cyclization). The stereochemistry at C4a is believed to result from approach of the enolate from the less sterically hindered diastereoface of cyclohexenone **11** (opposite the cyclopentene cage).

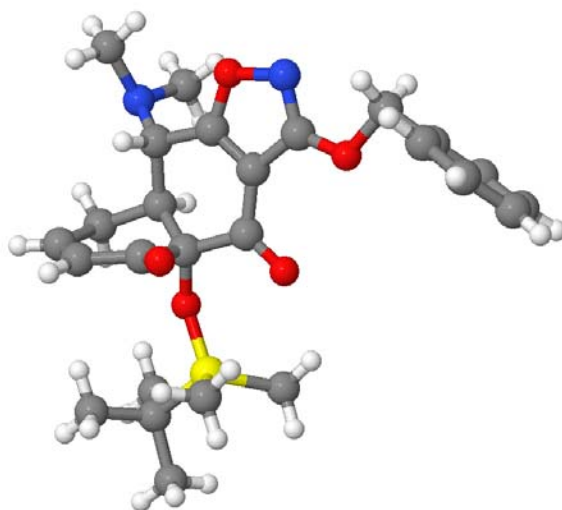


Figure 1.5. X-ray crystal structure of AB enone **10**.

Antibacterial Action of Tetracyclines

The 70S bacterial ribosome is made up of two subunits – the small subunit, 30S, through which mRNA tunnels and which contains on its surface the decoding site where the mRNA sequence is read in blocks of three nucleotides; and the large subunit, 50S, which possesses catalytic ribozyme peptidyltransferase activity and is the site of peptide chain elongation.^{28,29} As mRNA tunnels through the 30S subunit, a short stretch of the

²⁸ *Antibiotics – Actions, Origins, Resistance*; Walsh, C.; ASM Press – Washington, D.C., **2003**.

molecule protrudes through to the interface with the 50S subunit. This stretch consists of six nucleotides which occupy two codon sites: the aminoacyl (A) site, and the peptidyl (P) site. Upstream of the peptidyl site is the exit codon (E) site, where deacylated tRNA moves from the P site following peptidyl transfer.

Aminoacyl-tRNAs arrive at the unoccupied A site in complex with EF-Tu (elongation factor thermo unstable). The existence of Watson-Crick base pairs between the A site mRNA codon and the anti-codon loop of the aminoacyl-tRNA leads to appropriate orientation and complex formation. The P site is occupied by a tRNA molecule carrying the nascent peptide chain. The aminoacylated ends of the tRNA molecules occupying the A and P sites are approximately 75 Å away from the tRNA binding sites, in the catalytic center of the 50S subunit. In each chain elongation step, the aminoacyl moiety of the A site tRNA attacks the adjacent peptide chain of the peptidyl-tRNA. The peptidyl chain (lengthened by one amino acid) is now tethered to the tRNA docked in the A site, and the P site is occupied by a deacylated tRNA molecule. Before the next chain elongation step occurs, the deacylated tRNA moves from the P site to the E site and the peptidyl-tRNA relocates to the P site, opening up the A site for docking of an aminoacyl-tRNA possessing an anticodon loop complementary to the three mRNA nucleotides now being presented in the A site. The translocation process is catalyzed by EF-G (elongation factor G).

²⁹ Wilson, D. N. *Crit. Rev. Biochem. Mol. Biol.* **2009**, *44*, 393-433.

Tetracyclines inhibit bacterial protein synthesis by binding to the 30S subunit near the A site, thereby blocking accommodation of aminoacyl-tRNAs into the A site. Following an initial decoding event involving interaction of the anticodon loop of aminoacyl-tRNA (complexed at this stage with EF-Tu and GTP) with the mRNA codon, the release of aminoacyl-tRNA from EF-Tu is inhibited as the anticodon loop clashes with bound tetracycline during rotation into the A site.^{29,10a} This explanation fits with the observation that tetracycline does not affect the level of ribosomal binding of the ternary complex of aminoacyl-tRNA with EF-Tu and GTP (although binding occurs more slowly). Selective inhibition of bacterial protein synthesis is possible because of structural differences between the ribosomal RNA of bacterial and eukaryotic ribosomes, as well as selective concentration in susceptible bacterial cells.³⁰

Tetracycline binds to the ribosome in complex with Mg^{2+} , as depicted in Figure 1.6 below.^{10a} The C11-C12 keto-enol portion of tetracycline binds to Mg^{2+} , which is then also coordinated by the phosphate oxygens of RNA nucleotides G1197, G1198 and C1054 in helix 34 of the 30S ribosomal subunit. In addition, the phenolic hydroxyl group at C10 and tertiary carbinol at C12a appear to engage in hydrogen bonding interactions with the ribose portion of C1054 and a phosphate oxygen of G1198, respectively. Furthermore, there is an apparent interaction between the A ring of tetracycline and a phosphate oxygen of residue G966 in helix 31, as well as a hydrophobic interaction between the aromatic D ring of tetracycline and the base of C1054 in helix 31.

³⁰ Chopra, I.; Roberts, M. *Microbiol. Mol. Biol. Rev.* **2001**, 65, 232-260.

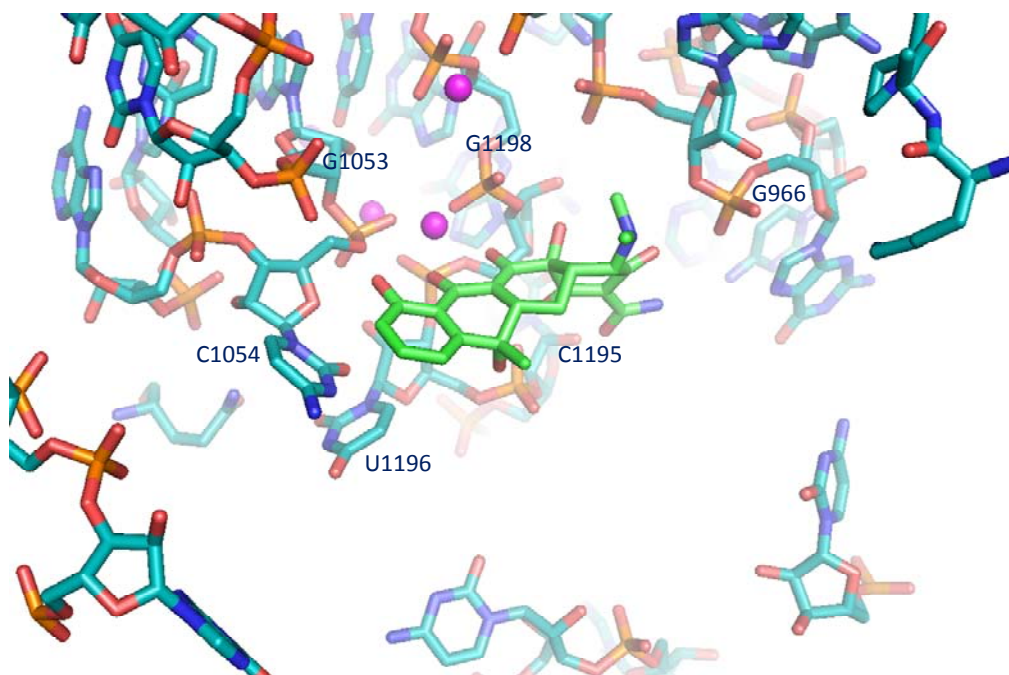


Figure 1.6. Tetracycline bound to its primary binding site in the bacterial ribosome.^{10a}

Tetracycline and glycylcyclines (such as tigecycline, **9**) share a common ribosomal binding site, to which selected glycylcyclines appear to bind five times more efficiently.³¹ It has been proposed that the bulky C9 side-chain of tigecycline either causes the antibiotic to bind to the ribosome in a different orientation to tetracycline, or the ribosomal RNA conformation is altered to accommodate the bulkier drug molecule.³² One (or both) of these effects probably leads to the higher affinity binding of tigecycline

³¹ Bergeron, J.; Ammirati, M.; Danley, D.; James, L.; Norcia, M.; Retsema, J.; Strick, C. A.; Su, W. G.; Sutcliffe, J.; Wondrack, L. *Antimicrob. Agents Chemother.* **1996**, *40*, 2226-2228.

³² Bauer, G.; Berens, C.; Projan, S. J.; Hillen, W. *J. Antimicrob. Chemother.* **2004**, *53*, 592-599.

compared to tetracycline and also helps explain the fact that tigecycline retains activity against many tetracycline-resistant bacteria (*vide infra*).

All bacterial cells are bounded by a cytoplasmic membrane, a symmetric lipid bilayer which is permeable to uncharged, lipophilic molecules. In addition, Gram-negative bacterial cells are also bounded by a second barrier – the outer membrane – which is significantly less permeable to lipophilic molecules than the cytoplasmic membrane. Unlike the cytoplasmic membrane, the bilayer of the outer membrane is asymmetric.³³ The outer leaflet (of the outer membrane) consists of lipopolysaccharides, while the inner leaflet is made up of phospholipids. The “gel-like” nature of the lipopolysaccharide leaflet makes the outer membrane a more effective permeability barrier than the inner membrane.

Donnan potential is the electric potential arising between two solutions of unequal ionic solute concentration separated by a partially permeable membrane. In all mediums containing tetracycline, an equilibrium exists between a net uncharged, metal-free form of tetracycline (denoted “tc” in Figure 1.7 below) and a complex in which deprotonated tetracycline coordinates a magnesium dication, $[M\text{-tc}]^+$.³⁴ The position of the equilibrium in any medium depends on both pH and magnesium ion concentration. The higher the pH and the higher the magnesium concentration, the higher will be the concentration of the

³³ Nikaido, H. *Microbio. Mol. Biol. Rev.* **2003**, 67, 593-656.

³⁴ Key references for bacterial cell penetration of tetracyclines: (a) Yamaguchi, A.; Ohmori, H.; Kaneko-Ohdera, M.; Nomura, T.; Sawai, T. *Antimicrob. Agents Chemother.* **1991**, 35, 53-56. (b) Nikaido, H.; Thanassi, D. G. *Antimicrob. Agents Chemother.* **1993**, 37, 1393-1399. (c) Schnappinger, D.; Hillen, W. *Arch. Microbiol.* **1996**, 165, 359-369.

hydrophilic chelate complex, to which the cytoplasmic membrane is impermeable. In *E. coli*, the cytoplasmic pH is higher than the external pH by about 1.7 pH units, and the cytoplasmic magnesium ion concentration is also higher. Therefore, the proportion of tetracycline in its uncharged (permeable) form is significantly higher in the periplasm than in the cytoplasm. The pH difference is dependent on the proton motive force and explains why tetracycline accumulation is energy dependent.

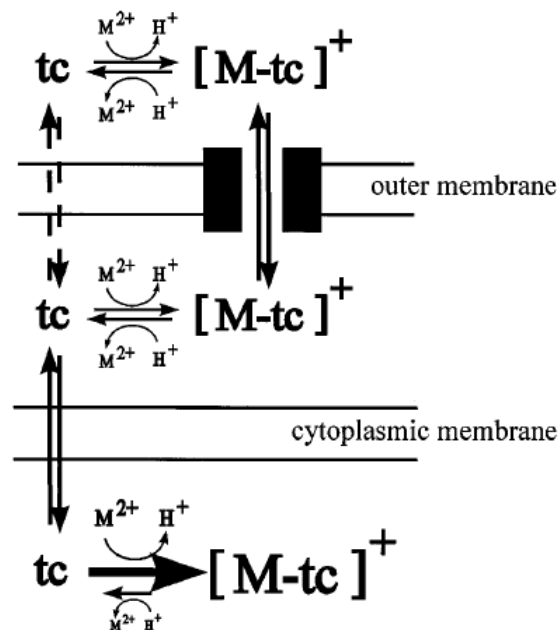


Figure 1.7. Diagrammatic representation of Gram-negative cell penetration by tetracycline (tc).

A high concentration of acidic groups at the surface of the outer membrane means that Mg^{2+} ions are abundant at this location. Tetracyclines, like most antibacterials, are

thought to penetrate the outer membrane of Gram-negative cells predominantly by passing through aqueous channels provided by porin proteins imbedded in the outer membrane. Porin proteins favor passage of charged, hydrophilic solutes, and tetracyclines pass through these channels in complex with Mg^{2+} (denoted $[M-tc]^+$ in the Figure 1.7).^{34,35} The Donnan potential across the outer membrane leads to accumulation of $[M-tc]^+$ in the periplasm (relative to the exterior) and, following equilibration, passage of neutral and metal-free tetracycline across the cytoplasmic membrane, which is permeable to uncharged, lipophilic small molecules. Tetracycline has pKa values of 3.3, 7.7, and 9.7, and at pH 7.4, 7.1% of tetracycline exists in uncharged form. The uncharged form of tetracycline is weakly lipophilic. Although diffusion across the outer membrane is relatively slow, it may still occur at a significant rate with more lipophilic tetracyclines such as minocycline.^{34b}

O'Shea and Moser found that antibacterial agents with activity against Gram-negative bacteria (which, with few exceptions, are a subset of compounds with Gram-positive activity) are significantly more polar (less lipophilic) than "Gram-positive only" agents.³⁶ Antibacterials with Gram-negative activity have a mean relative polar surface area 12% higher than compounds which are only active against Gram-positive bacteria, as well as significantly lower values for $clogD_{7.4}$ (the calculated log of the octanol-water partition coefficient based on the distribution of charged and uncharged forms of the

³⁵ Koebnik, R.; Locher, K. P.; Van Gelder, P. *Mol. Microbiol.* **2000**, 37, 239-253.

³⁶ O'Shea, R.; Moser, H. E. *J. Med. Chem.* **2008**, 51, 2871-2878.

compound at pH 7.4). Furthermore, Gram-negative agents have a smaller mean molecular mass, with a seemingly strict upper limit of 600 Da.

This analysis of physicochemical properties was modified by Silver to differentiate between antibacterials whose targets are located in the cytoplasm (and which reach their targets by diffusion) and those which need not penetrate the inner membrane to exert their antibacterial effect.³⁷ Specifically, antibacterials were divided into two groups: (i) drugs with cytoplasmic targets which enter the cytoplasm by diffusion (including tetracyclines); (ii) drugs with no requirement for diffusion across the lipid bilayer of the cytoplasmic membrane, i.e. antibacterials with extracytoplasmic targets plus those with cytoplasmic targets which are known to move across the cytoplasmic membrane by means other than diffusion (such as the aminoglycosides, whose transport is energy dependent). The difference between these two groups is even more significant than for Gram-positive-only agents versus drugs with Gram-negative activity. “Extracytoplasmic and transported” antibacterials are even more polar (on average) than Gram-negative agents as a whole.

³⁷ Silver, L. L. *Clinical Microbio. Rev.* **2011**, 24, 71–109.

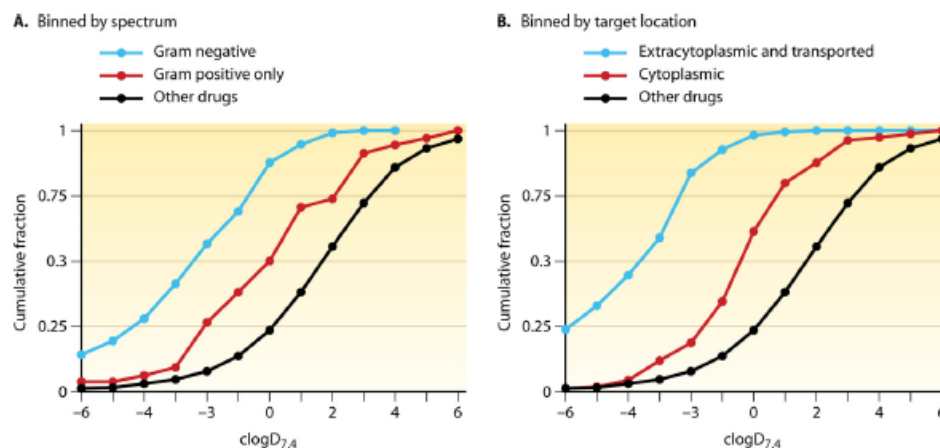


Figure 1.8. Analyses of physicochemical properties of antibacterials (divided into two groups) and drugs in other therapeutic areas; **A:** antibacterials divided into Gram-negative agents and Gram-positive-only agents; **B:** antibacterials divided into those with cytoplasmic targets and those which act extracytoplasmically or are actively transported across the cytoplasmic membrane.

The requirements that Gram-negative antibacterials have higher polarity and lower molecular weight are believed to be driven by the properties of porin proteins. All known porins have a characteristic β -barrel structure and significantly conserved transmembrane β -strands (according to analysis of amino acid sequence and a limited number of crystal structures).³⁸ The presence of charged amino acid side chains on opposite sides of the porin channels leads to highly directional orienting of water

³⁸ (a) Cowan, S. W.; Schirmer, T.; Rummel, G.; Steiert, M.; Ghosh, R.; Pauptit, R. A.; Jansonius, J. N.; Rosenbusch, J. P. *Nature* **1992**, 358, 727–733. (b) Dutzler, R.; Rummel, G.; Alberti, S.; Hernández-Allés, S.; Phale, P. S.; Rosenbusch, J. P.; Benedi, V. J.; Schirmer, T. *Structure* **1999**, 7, 425–434.

molecules, and disruption of this ordered structure is thermodynamically disfavored. Passage of lipophilic molecules is most strongly disfavored because the energy cost for removal of the hydration sphere of channel-lining amino acids and temporary replacement with the small molecule is prohibitively high.³⁹ When hydrophilic solutes come into the channel, the broken hydrogen bonds between water molecules and channel-lining amino acids are temporarily replaced by hydrogen bonds between the hydrophilic solute and polar amino acid side chains. Passage of an antibacterial through these openings requires that the activation energy for removal of the hydration sphere of channel-lining amino acids and temporary replacement with the drug molecule is not prohibitively high. Charged, hydrophilic molecules are therefore more likely to penetrate the outer membrane of Gram-negative cells.

Cell penetration is clearly a crucial factor in determining antibacterial activity of any tetracycline, and the conflict between the broad requirements for passage through the two membranes of Gram-negative bacteria presents a very significant challenge in tetracycline drug discovery. Modified tetracyclines with higher influx rates could hold significant advantages over existing tetracyclines, but as the conditions that mediate compound uptake through the bacterial cell envelope are still incompletely understood, rational design with respect to this feature is extremely difficult.⁴⁰

³⁹ Nikaido, H.; Rosenberg, E. Y.; Foulds, J. J. *Bacteriology* **1983**, 153, 232–240.

⁴⁰ Brotz-Oesterhelt, H.; Sass, P. *Future Microbiology* **2010**, 5, 1553–1579.

Tetracycline Resistance

Decades of clinical and agricultural use have led to widespread bacterial resistance to tetracyclines. The tetracycline “resistome” may be the largest assortment of resistance genes acting against an individual class of antibiotics. A 2010 review stated that there were over 1,189 reported tetracycline genes that had been classified into 41 resistance determinant classes (of which 26 are efflux pumps and 11 are ribosomal protection proteins).⁴¹

The majority of tetracycline efflux proteins are members of the major facilitator superfamily of integral membrane transporters.⁴² Although no crystal structure is currently available, tetracycline efflux proteins are predicted to be water-filled channels surrounded by six transmembrane helices. The flow of protons down a pH gradient provides the energy required to pump tetracycline out of the cytoplasm.⁴³ Export of tetracycline protects ribosomes within the cell by reducing cytoplasmic drug concentration.

Each tetracycline efflux protein has an associated tetracycline repressor protein responsible for regulating expression of the efflux pump. Expression of TetA (a widely distributed and clinically important efflux pump found in Gram-negative bacteria) is regulated by TetR, a protein which forms a dimer and binds to DNA operator sequences

⁴¹ Thaker, M.; Spanogiannopoulos; Wright, G. D. *Cell. Mol. Life Sci.* **2010**, *67*, 419–431.

⁴² Paulsen, I. T.; Brown, M. H.; Skurray, R. A. *Microbiol. Rev.* **1996**, *60*, 575–608.

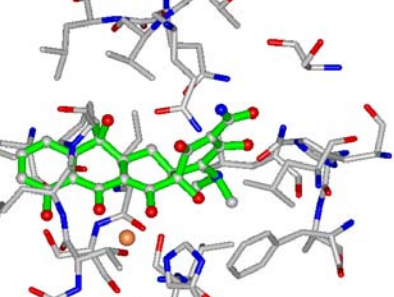
⁴³ Yamaguchi, A.; Ono, N.; Akasaka, T.; Noumi, T.; Sawai, T. *J. Biol. Chem.* **1990**, *265*, 15525–15530.

tetO1 and *tetO2*. Upon entering the cytoplasm, tetracycline forms a complex with Mg^{2+} and the complex in turn binds to the TetR–DNA complex, leading to a conformational change within the TetR dimer which dramatically reduces its affinity for the DNA operator sequences, leading to dissociation of the protein–DNA complex and transcription of both TetA and TetR.

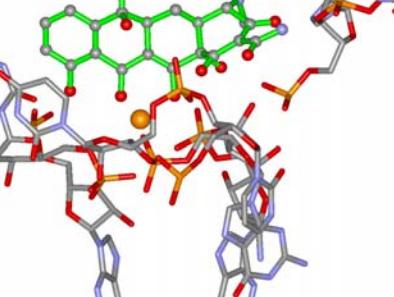
A crystal structure of the complex formed between TetR and tetracycline– Mg^{2+} provided a detailed view of the binding interactions between the antibiotic and the repressor protein (Figure 1.9A below).⁴⁴ Although there is significant sequence variation amongst the repressor proteins responsible for regulating the expression of different efflux proteins, the amino acid residues involved in hydrogen bonding to tetracycline and Mg^{2+} coordination are largely conserved. The crystal structure of the complex formed between tetracycline and TetR revealed that the repressor protein completely surrounds the antibiotic, forming an extensive network of contacts around the tetracycline scaffold (tetracycline has a K_d of ~ 1 nM for Tet(R), compared with ~ 1 μ M for the bacterial ribosome). In contrast, the interactions between tetracycline and its primary binding site in the 30S ribosomal subunit are largely confined to the highly oxygenated “lower” periphery of the molecule, while the upper periphery of the antibiotic projects away from the binding site into free aqueous solution (see Figure 1.9B). As a result of this difference, it is conceivable that the attachment of new substituents in this region (C4a, C5, C5a and C6) could disrupt the interaction with TetR (and potentially combat

⁴⁴ (a) Hinrichs, W.; Kisker, C.; Duvel, M.; Saenger, W. *Science* **1994**, 264, 418–420. (b) Kisker, C.; Hinrichs, W.; Tovar, K.; Hillen, W.; Saenger, W. *J. Mol. Biol.* **1995**, 247, 260–280. (c) Orth, P.; Schnappinger, D.; Hillen, W.; Saenger, W.; Hinrichs, W. *Nature Struct. Biol.* **2000**, 7, 215–219.

A.



B.



C.

⁴⁵ Degenkolb, J.; Takahashi, M.; Ellestad, G. A.; Hillen, W. *Antimicrob. Agents Chemother.* **1991**, *35*, 1591-1595.

Multi-drug efflux pumps expel a range of structurally dissimilar compounds from bacterial cells, including antibiotics of many different classes.⁴⁶ The non-selective export of multiple antibacterial agents means that these pumps are often associated with multi-drug resistance. Any given bacterial species may express a number of different multi-drug efflux pumps; some are constitutively expressed (conferring intrinsic multi-drug resistance) while the expression of others may be induced by the presence of certain substrates. Across different species of bacteria there is significant variation in the structure and substrate scope of efflux pumps, so the impact of multi-drug efflux systems on antibacterial susceptibility is highly species-dependent. Multi-drug efflux pumps can be either single component or multi-component systems. Those expressed in some Gram-negative bacteria are tripartite systems, with a constituent inner membrane transporter protein, periplasmic accessory protein (or membrane-fusion protein) and outer membrane protein channel.⁴⁶

Tetracyclines are substrates for some multi-drug efflux pumps, including those expressed in *Pseudomonas aeruginosa*, a particularly problematic pathogen. Resistance of *Pseudomonas* strains to multiple classes of otherwise effective antibiotics is a result of both slow permeation (poor influx) and highly efficient efflux of drug molecules.⁴⁷ Tigecycline is exported from *Pseudomonas* by multi-drug pumps less efficiently than

⁴⁶ (a) Piddock, L. J. V. *Clin. Microbiol. Rev.* **2006**, *19*, 382-402. (b) Piddock, L. J. V. *Nature Rev. Microbiol.* **2006**, *4*, 629-636.

⁴⁷ Li, X. Z.; Livermore, D. M.; Nikaido, H. *Antimicrob. Agents Chemother.* **1994**, *38*, 1732-1741.

older tetracyclines, but efflux is still sufficient to confer resistance.⁴⁸ Given that glycylicyclines are exported less efficiently and that the relative contributions of different multi-drug pumps to net efflux varies significantly between different tetracyclines, it is possible that efflux pump-mediated drug resistance could be overcome through chemical modification of existing, otherwise effective drugs.

Ribosomal protection proteins (RPPs) are thought to give rise to tetracycline resistance by binding to tetracycline–ribosome complex at a distinct site (i.e. away from the primary tetracycline binding site), causing a ribosomal conformation change which weakens the interaction between tetracycline and the ribosome.⁴⁹ Tetracycline is thus “dislodged” from its primary binding site (Figure 1.10 below). Upon tetracycline release, GTP is hydrolyzed and the RPP dissociates from the ribosome.⁵⁰ RPPs have significant sequence homology with elongation factors EF-Tu and EF-G, both of which are also GTPases.⁵¹ The mechanism by which RPPs “recognize” ribosomes bound by tetracycline has not been conclusively established. It is possible that tetracycline binding induces a conformational change which promotes RPP binding. Alternatively, since Tet(O) (a prevalent and well-studied RPP) cannot bind to a ribosome with an occupied A site, the ability of tetracycline to block the ribosome in a state with an open A site may explain the

⁴⁸ Dean, C. R.; Visalli, M. A.; Projan, S. J.; Sum, P.-E.; Bradford, P. A. *Antimicrob. Agents Chemother.* **2003**, *47*, 972-978.

⁴⁹ Connell, S. R.; Tracz, D. M.; Nierhaus, K. H.; Taylor, D. E. *Antimicrob. Agents Chemother.* **2003**, *47*, 3675-3681.

⁵⁰ Burdett, V. *J. Bacteriol.* **1996**, *178*, 3246-3251.

⁵¹ (a) Taylor, D. E.; Chau, A. *Antimicrob. Agents Chemother.* **1996**, *40*, 1-5. (b) Kobayashi, T.; Nonaka, L.; Maruyama, F.; Suzuki, S. *J. Mol. Evol.* **2007**, *65*, 228-235.

binding preference of RPPs.⁵² It is not known whether RPPs prevent rebinding of tetracycline after causing tetracycline release.

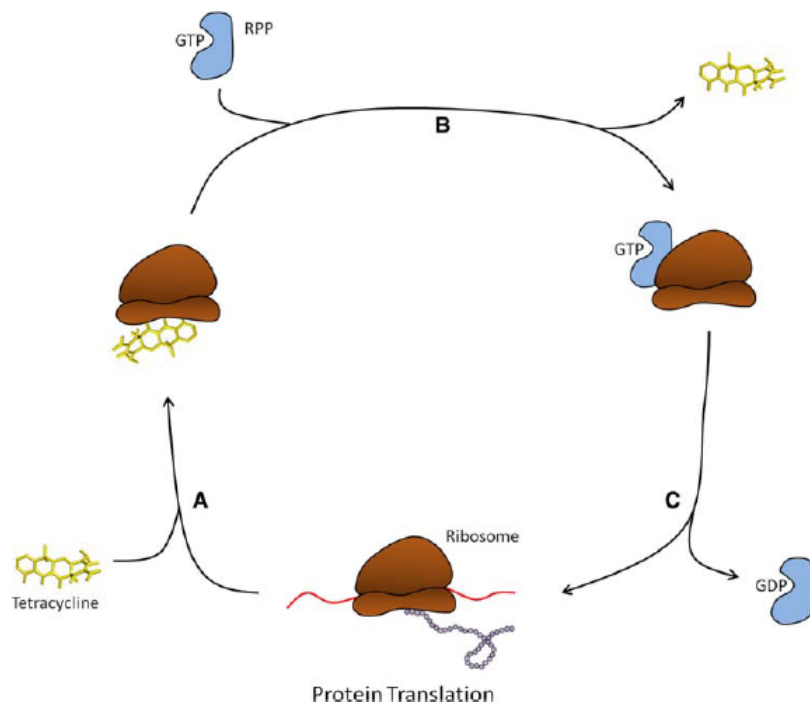


Figure 1.10. Ribosomal protection resistance mechanism.⁴¹

Glycylcycline antibiotics such as tigecycline retain activity against bacteria expressing ribosomal protection proteins. Tigecycline and older tetracyclines all bind to the same primary binding site in the ribosome, but tigecycline binds more strongly and in a slightly different orientation. It is possible that RPPs bind less strongly to the tigecycline–ribosome complex than to the tetracycline–ribosome complex, or that RPP

⁵² Connell, S. R.; Trieber, C. A.; Einfeldt, E.; Dinos, G. P.; Taylor, D. E.; Nierhaus, K. *EMBO J.* **2003**, *22*, 945-953.

binding to the tigecycline–ribosome complex causes little or no conformational change (i.e. tigecycline is simply harder to dislodge).

Glycylcyclines also show a high level of activity against organisms carrying tetracycline efflux resistance determinants. Someya and co-workers studied the glycylcycline antibiotic 9-(*N,N*-dimethylaminoglycylamido)-6-demethyl-6-deoxy-tetracycline (DMG-DMDOT) and found that it does induce expression of the TetA efflux protein, indicating that this glycylcycline is a substrate for TetR.⁵³ There are therefore two possible explanations for the potent activity of this glycylcycline in the presence of tetracycline efflux determinants: (1) the efflux protein is not able to recognize the glycylcycline, or (2) the efflux protein–glycylcycline complex cannot be translocated across the bacterial membrane. Indirect results suggest that the glycylcycline does not bind to the efflux protein TetA (at least not to the tetracycline binding site), thus explaining the ability of this antibiotic to overcome resistance caused by tetracycline-specific efflux.

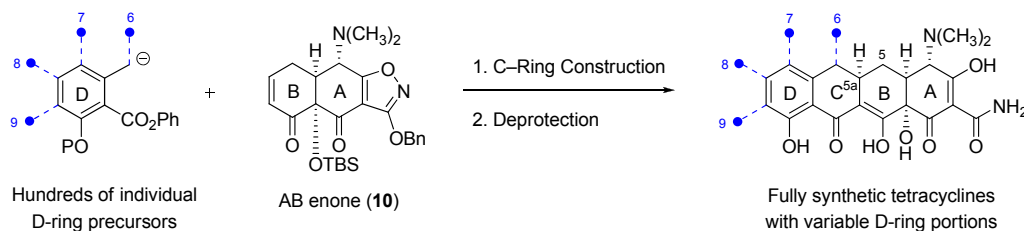
⁵³ Someya, Y.; Yamaguchi, A.; Sawai, T. *Antimicrobial Agents and Chemotherapy* **1995**, 39, 247-249.

Chapter 2

Synthesis of C5a-Substituted Tetracyclines

Introduction

Previous work has demonstrated that our fully synthetic approach to tetracyclines allows modifications at positions C6, C7, C8, C9 and C10 that are not feasible by semisynthesis (Scheme 2.1).^{54,55} Given that the AB plus D strategy for tetracycline synthesis had proven to be robust across a range of different carbocyclic and heterocyclic D-ring precursors, we questioned whether the key C-ring-forming coupling reaction would still be effective with new AB precursors of wide structural variability, potentially enabling modifications at positions on the A and B rings of tetracycline that have never previously been modified. The development of chemical pathways that expand our synthetic platform to allow efficient preparation of tetracyclines of variable composition at positions C5 and C5a is the subject of this thesis.



Scheme 2.1. Synthesis of tetracyclines by coupling of AB enone **10** with D-ring precursors of wide structural variability followed by deprotection.

⁵⁴ (a) Charest, M. G.; Lerner, C. D.; Brubaker, J. D.; Siegel, D. R.; Myers, A. G. *Science* **2005**, *308*, 395–398. (b) Sun, C.; Wang, Q.; Brubaker, J. D.; Wright, P. M.; Lerner, C. D.; Noson, K.; Charest, M. G.; Siegel, D. R.; Wang, Y.-M.; Myers, A. G. *J. Am. Chem. Soc.* **2008**, *130*, 17913–17927.

⁵⁵ (a) Clark, R. B.; He, M.; Fyfe, C.; Lofland, D.; O'Brien, W. J.; Plamondon, L.; Sutcliffe, J. A.; Xiao, X.-Y. *J. Med. Chem.* **2011**, *54*, 1511–1528. (b) Sun, C.; Hunt, D. K.; Clark, R. B.; Lofland, D.; O'Brien, W. J.; Plamondon, L.; Xiao, X.-Y. *J. Med. Chem.* **2011**, *54*, 3704–3731.

Position C5a is one of two points of fusion of the B and C rings of tetracyclines and, as such, substitution of this position gives rise to a quaternary carbon center. Inspection of X-ray crystallographic data of tetracycline bound to the 30S subunit of the ribosome of *Thermus Thermophilus* suggests that substitution of position C5a (situated in the “variable” or hydrophobic region of the tetracycline skeleton, away from the functionality required for binding to the bacterial ribosome) would not obviously impede ribosome binding and thus could present an interesting and unexplored avenue for the discovery of potential new antibiotics to address problems such as bacterial resistance (Figure 2.1).⁵⁶

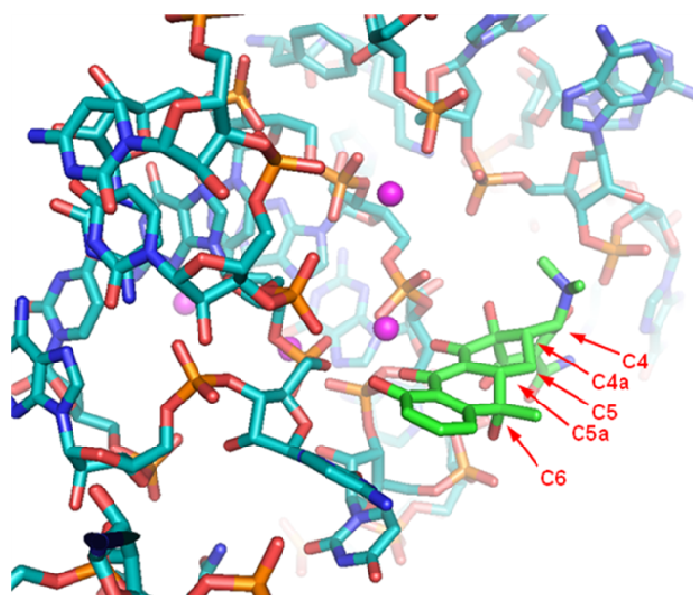


Figure 2.1. Tetracycline bound to the 30S subunit of the bacterial ribosome.^{56a}

⁵⁶ (a) Brodersen, D. E.; Clemons, W. M., Jr.; Carter, A. P.; Morgan-Warren, R. J.; Wimberly, B. T.; Ramakrishnan, V. *Cell* **2000**, *103*, 1143–1154. (b) Pioletti, M.; Schlünzen, F.; Harms, J.; Zarivach, R.; Glühmann, M.; Avila, H.; Bashan, A.; Bartels, H.; Auerbach, T.; Jacobi, C.; Hartsch, T.; Yonath, A.; Franceschi, F. *EMBO J.* **2001**, *20*, 1829–1839.

The limitations of semisynthesis have meant that modification of C5a has not previously been viable. Unpublished research by W. Rogalski and R. Kirchlechner led to the synthesis of analogs such as racemic 6-demethyl-6-deoxy-7-chloro-5a-methyltetracyclines, with both the natural and unnatural stereochemistry at C5a (compounds **14** and **15**, Figure 2.2 below).⁵⁷ The racemic stereoisomer with natural C5a stereochemistry (**14**) showed good activity against Gram-positive bacteria (including some tetracycline-resistant strains of *S. aureus*, in which it was more active than minocycline) but was completely inactive against Gram-negative organisms tested. The corresponding C5a-epimer **15** was less active across all strains tested but did retain poor activity against tetracycline-resistant Gram-positive organisms. 6-Demethyl-6-deoxy-7-methoxy-epi-5a-methyltetracycline (compound **16**, unnatural stereochemistry at C5a) was found to be completely inactive.

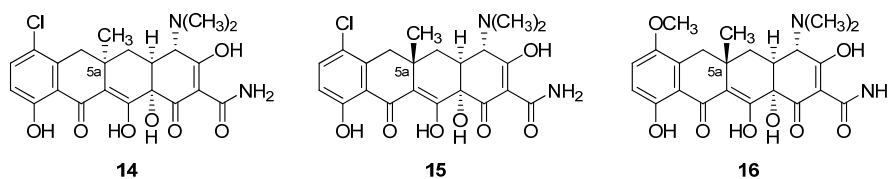
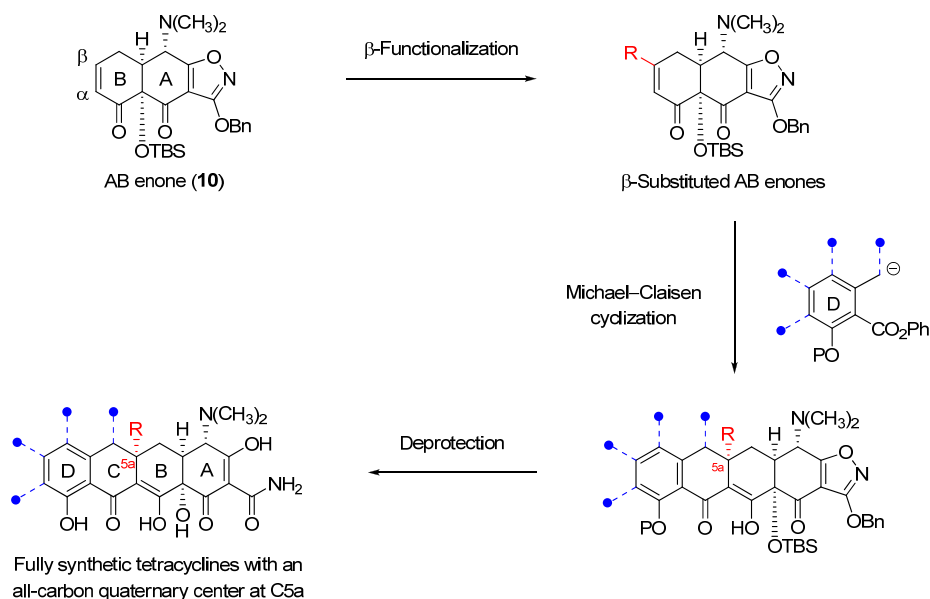


Figure 2.2. Racemic, fully synthetic tetracyclines possessing methyl substituents at C5a, prepared by W. Rogalski and R. Kirchlechner.⁵⁷

To apply our general route for tetracycline synthesis to C5a-substituted analogs it was first necessary to develop methodology to prepare AB enones containing different β -substituents, and then to determine if these modified AB enones would successfully

⁵⁷ Cunha, B. A. Clinical Uses of Tetracyclines. In *Handbook of Experimental Pharmacology*; Hlavka, J. J. and Boothe, J. H., Eds.; Springer-Verlag: New York, 1985; pp 393–403.

undergo Michael–Claisen cyclization reactions with D-ring precursors, transformations that would give rise to a quaternary, stereogenic center at position C5a (Scheme 2.2).



Scheme 2.2. Synthesis of fully synthetic tetracyclines with an all-carbon quaternary center at C5a from β -substituted AB enones.

The most rapid and straightforward approach to the synthesis of β -substituted AB enones appeared to be the direct functionalization of the AB enone **10**. While introduction of simple alkyl groups such as β -methyl proved to be relatively straightforward (though low-yielding), introduction of more highly oxidized β -substituents was less so, and provided us with the opportunity to pursue a number of chemical innovations. The subsequent stereocontrolled construction of the C ring, comprising an all-carbon quaternary center at position C5a, was viewed to be a challenging transformation, and its successful implementation we view to be a significant

advance. During the course of our investigations we also serendipitously discovered a C5a–C11a-bridged cyclopropane-containing tetracycline intermediate that has proven to be an extraordinarily versatile precursor to a diverse array of C5a-substituted tetracyclines, providing another avenue for the synthesis of this novel class of substituted tetracycline antibiotics.

Results

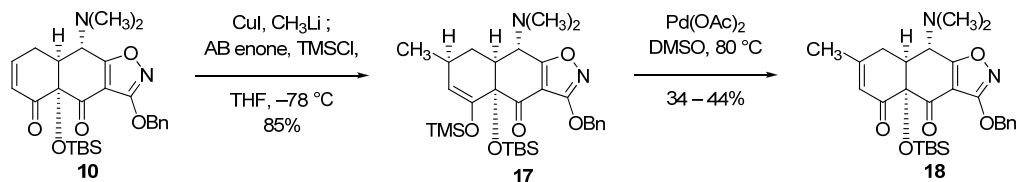
As a first step toward the stereocontrolled construction of all-carbon quaternary, C5a-substituted tetracyclines we first sought to develop methods to transform the AB enone **10** into β -substituted AB enones as novel cyclization substrates. A conventional reaction sequence served for the synthesis of the simple β -methyl-substituted AB enone **18** (Scheme 2.3). Specifically, conjugate addition of lithium dimethylcuprate to the AB enone **10** in the presence of trimethylsilylchloride⁵⁸ afforded the corresponding β -methyl-substituted trimethylsilyl enol ether **17** in 85% yield (1D-NOESY experiments support the 5a-*S*-stereochemistry depicted, in accord with all precedent in this system);^{54b} oxidation of this intermediate with palladium acetate in dimethyl sulfoxide (DMSO) at 80 °C then afforded the β -methyl-substituted AB enone **18** in modest yield (44% yield on 160-mg scale, and 34% yield on 2.8-g scale).^{59,60} Attempted oxidation of the intermediate

⁵⁸ Corey, E. J.; Boaz, N. W. *Tetrahedron Lett.* **1985**, 26, 6019–6022.

⁵⁹ Ito, Y.; Hirao, T.; Saegusa, T. *J. Org. Chem.* **1978**, 43, 1011–1013.

⁶⁰ The highest yield of the β -methyl-substituted enone **18** was obtained when the oxidation was performed on a small scale (160 mg, 1.15 equiv Pd(OAc)₂, DMSO, 80 °C, 16 h) and the work-up was carried out before the starting material had been completely consumed. Mass recovery from this reaction was consistently poor.

trimethylsilyl enol ether **17** with the alternative oxidant *o*-iodoxybenzoic acid (IBX) was not successful.⁶¹



Scheme 2.3. Synthesis of β -methyl-substituted AB enone **18** from the β -unsubstituted AB enone **10**.

To transform the AB enone **10** into β -substituted AB enones with more highly oxidized β -substituents we were led to explore novel chemistry, as precededent methods were deemed to be too indirect or were impracticable in the present application.^{62,63,64} First, we developed a versatile sequence for β -functionalization of the AB enone **10**

⁶¹ Nicolaou, K. C.; Gray, D. L. F.; Montagnon, T.; Harrison, S. T. *Angew. Chem. Int. Ed.* **2002**, *41*, 996–1000.

⁶² Enones with ester, aldehyde and alkoxymethyl substituents at the β -position can be prepared indirectly from unsubstituted enone starting materials via β -cyano-substituted enones: (a) Fukuta, Y.; Mita, T.; Fukuda, N.; Kanai, M.; Shibasaki, M. *J. Am. Chem. Soc.* **2006**, *128*, 6312–6313. (b) Nicolaou, K. C.; Li, A. *Angew. Chem. Int. Ed.* **2008**, *47*, 6579–6582. (c) Isobe, M.; Nishikawa, T.; Pikul, S.; Goto, T. *Tetrahedron Lett.* **1987**, *28*, 6485–6488.

⁶³ Though not successful in the current application (using the AB enone **10** as substrate), phosphoniosilylation methodology has been used to introduce β -alkoxycarbonyl substituents in enone substrates: (a) Kim, S.; Lee, P. H.; Kim, S. S. *Bull. Korean Chem Soc.* **1989**, *10*, 218–219. (b) Kim, J. H.; Jung, H. K. *Bull. Korean Chem Soc.* **2004**, *25*, 1729–1732.

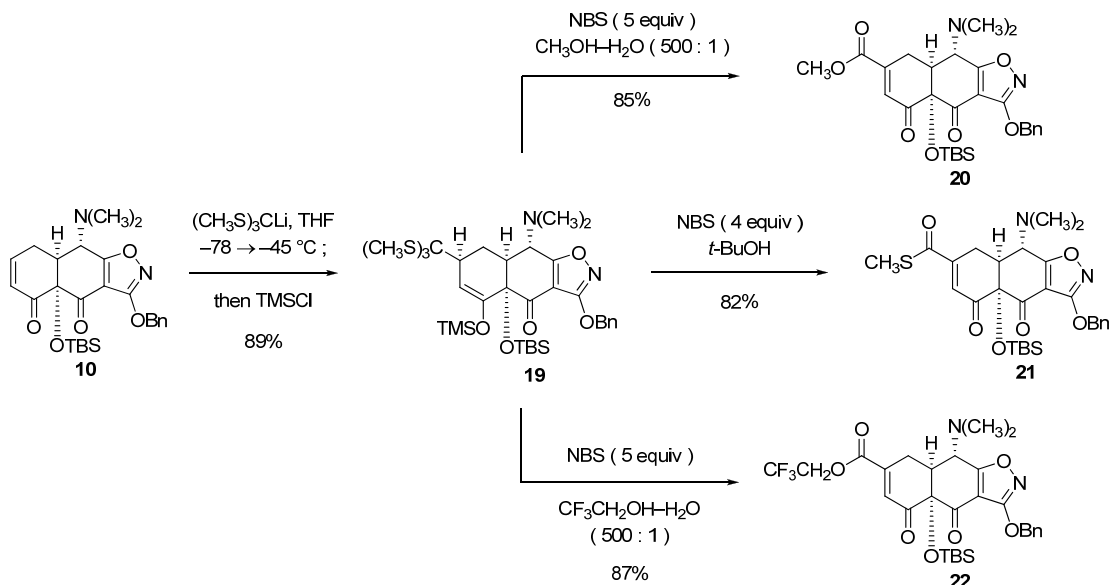
⁶⁴ Alternative synthetic sequences for the preparation of enones with β -alkoxymethyl and β -aldehyde substituents from unsubstituted enone starting materials: (a) Kienzle, F.; Minder, R. E. *Helv. Chim. Acta* **1976**, *59*, 439–452. (b) Heguaburu, V.; Schapiro, V.; Pandolfi, E. *Tetrahedron Lett.* **2010**, *51*, 6921–6923.

initiated by conjugate addition of the Seebach reagent tris(methylthio)methylolithium⁶⁵ (THF, $-78 \rightarrow -45$ °C) followed by trapping of the resulting enolate at -45 °C with chlorotrimethylsilane (Scheme 2.4 below).^{66,67} The corresponding β -tris(methylthio)methyl trimethylsilyl enol ether (**19**) was isolated as a single stereoisomer (stereochemistry not determined) in 89% yield after purification by flash-column chromatography. We found that oxidation of the trimethylsilyl enol ether function and transformation of the tris(methylthio)methyl group occurred simultaneously upon treatment of a solution of **19** in the solvent mixture 500:1 methanol–water with an excess of *N*-bromosuccinimide (NBS, 5 equiv) at 23 °C, affording the AB enone containing a β -methyl ester substituent (**20**) in 85% yield. The detailed mechanism of the transformation of the intermediate **19** into the β -substituted AB enone **20** is not known, but presumably involves some variation of a sequence involving α -bromination of the trimethylsilyl enol ether, bromonium-induced conversion of the tris(methylthio)methyl substituent into the corresponding methyl ester (with incorporation of one molar equivalent each of methanol and water), and elimination of hydrogen bromide.

⁶⁵ (a) Seebach, D. *Angew. Chem. Int. Ed.* **1967**, *6*, 442–443. (b) Bürstinghaus, R.; Seebach, D. *Chem. Ber.* **1977**, *110*, 841–851. (c) Gröbel, B.-T.; Seebach, D. *Synthesis* **1977**, 357–402. (d) “Tris(methylthio)methane” *Electronic Encyclopedia of Reagents for Organic Synthesis* **2007**.

⁶⁶ Other examples of conjugate addition–enolate trapping reactions of tris(methylthio)methylolithium with α,β -unsaturated carbonyl compounds: (a) Damon, R. E.; Schlessinger, R. H. *Tetrahedron Lett.* **1976**, *19*, 1561–1564. (b) Mikołajczyk, M.; Kielbasiński, P.; Wiczorek, M. W.; Blaszczyk, J.; Kolbe, A. *J. Org. Chem.* **1990**, *55*, 1198–1203.

⁶⁷ The regioselectivity observed upon reaction of tris(methylthio)methylolithium with α,β -unsaturated carbonyl compounds is substrate-dependent. For an example of a 1,2-addition reaction, see: Dailey, O. D., Jr.; Fuchs, P. L. *J. Org. Chem.* **1980**, *45*, 216–236.

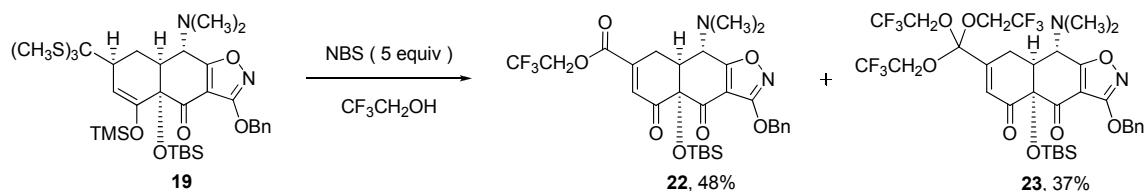


Scheme 2.4. Two-step syntheses of modified AB enones with methyl ester, thioester and trifluoroethyl ester groups at the β -position, starting from the β -unsubstituted AB enone **10**.

By modification of the reaction solvent we found that different esters could be synthesized, including active esters. For example, treatment of a solution of the trimethylsilyl enol ether **19** in *tert*-butanol with NBS (4 equiv) at 23°C afforded the AB enone **21** bearing an *S*-methyl thioester at the β -position in 82% yield (Scheme 2.4 above).⁶⁸ Alternatively, addition of NBS (5 equiv) to a solution of substrate **19** in 2,2,2-trifluoroethanol and water (500:1 mixture) at 23°C afforded the corresponding β -trifluoroethyl ester-substituted AB enone **22** in 87% yield. Interestingly, treatment of a solution of **19** in 2,2,2-trifluoroethanol (no added water) with NBS (5 equiv) afforded β -

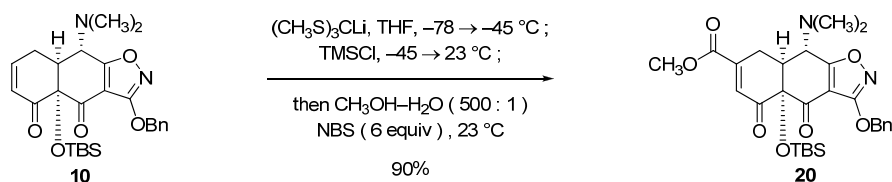
⁶⁸ Degani, I.; Dughera, S.; Fochi, R.; Gatti, A. *Synthesis* **1996**, 4, 467–469.

trifluoroethyl ortho ester-substituted enone **23** as a major by-product (37% yield, Scheme 2.5).



Scheme 2.5. Formation of a β-trifluoroethyl ortho ester-substituted AB enone (**23**).

In a further optimization, we found that transformation of the β-unsubstituted AB enone **10** to the β-methyl ester-substituted AB enone **20** could be achieved directly, and most efficiently (90% yield), in a single operation (Scheme 2.6 below).



Scheme 2.6. Synthesis of the β-methyl ester-substituted AB enone **20** from the β-unsubstituted AB enone **10** in a single operation.

The transformations of Schemes 2.4–2.6 represent novel, direct and highly efficient β-functionalization reactions of an enone substrate. Important foundational precedents include the conversion of a β-cyano-substituted trimethylsilyl enol ether to the corresponding β-cyano enone upon sequential treatment with NBS and triethylamine^{62a} as

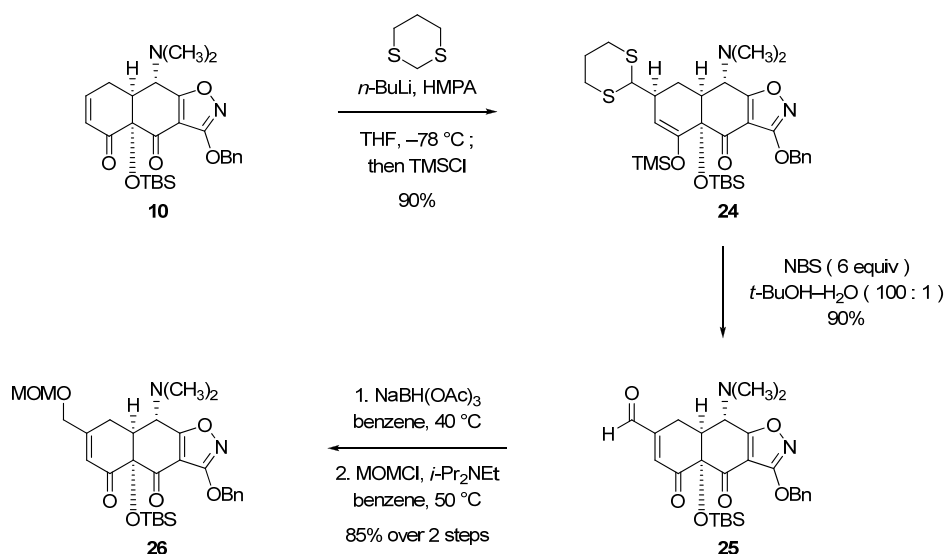
well as the original discovery that dithianes undergo oxidative hydrolysis in the presence of *N*-halosuccinimides.⁶⁹

A related strategy was effective for the synthesis of the AB enone **25** bearing a β -carbaldehyde substituent, which in turn provided an expedient route to AB enones with β -alkoxymethyl substituents (Scheme 2.7). Thus, conjugate addition of the Corey–Seebach reagent 2-lithio-1,3-dithiane⁷⁰ to the AB enone **10** in the presence of hexamethylphosphoramide (HMPA)⁷¹ at $-78\text{ }^{\circ}\text{C}$ followed by quenching of the resulting enolate intermediate with chlorotrimethylsilane provided the β -(1,3-dithian-2-yl) trimethylsilyl enol ether **24** as a single stereoisomer (90% yield; stereochemistry not determined). Treatment of the latter product with NBS (6 equiv) in the solvent mixture 100:1 *tert*-butanol–water at $23\text{ }^{\circ}\text{C}$ afforded the β -carbaldehyde AB enone **25** in 90% yield. Selective reduction of the aldehyde group occurred upon warming a solution of **25** and sodium triacetoxyborohydride in benzene at $40\text{ }^{\circ}\text{C}$. The resulting primary alcohol was then protected as a methoxymethyl ether in the presence of chloromethyl methyl ether and *N,N*-diisopropylethylamine in benzene at $50\text{ }^{\circ}\text{C}$ to afford the β -methoxymethoxymethyl AB enone **26** (85% yield over two steps).

⁶⁹ Corey, E. J.; Erickson, B. W. *J. Org. Chem.* **1971**, *36*, 3553–3560.

⁷⁰ (a) Corey, E. J.; Seebach, D. *Angew. Chem. Int. Ed.* **1965**, *4*, 1075–1077. (b) Seebach, D.; Corey, E. J. *J. Org. Chem.* **1975**, *40*, 231–237. (c) Page, P. C. B.; van Niel, M. B.; Prodger, J. C. *Tetrahedron* **1989**, *45*, 7643–7677.

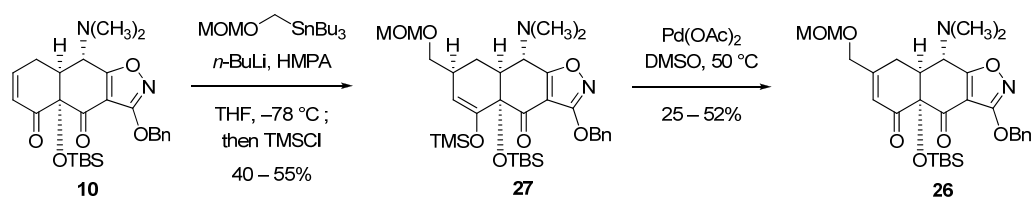
⁷¹ (a) Brown, C. A.; Yamaichi, A. *J. Chem. Soc., Chem Commun.* **1979**, 100–101. (b) Lucchetti, J.; Dumont, W.; Krief, A. *Tetrahedron Lett.* **1979**, *20*, 2695–2696. (c) Mukhopadhyay, T.; Seebach, D. *Helv. Chim. Acta* **1982**, *65*, 385–391.



Scheme 2.7. Synthesis of the β -methoxymethoxymethyl AB enone **26** from the AB enone **10** via the β -carbaldehyde AB enone **25**.

β -Methoxymethoxymethyl AB enone **26** could also be prepared in fewer steps but much lower (and highly variable) yield by reaction of the AB enone **10** with (methoxymethoxy)methyl lithium (prepared *in situ* from tri-*n*-butyl[(methoxymethoxy)methyl]stannane⁷² and *n*-butyllithium) in the presence of HMPA at -78 °C, trapping of the resulting enolate with chlorotrimethylsilane (affording the β -methoxymethoxymethyl trimethylsilyl enol ether **27** in 40–55% yield), and then oxidation of the intermediate **27** with palladium acetate in DMSO at 50 °C (providing AB enone **26** in 25–52% yield; Scheme 2.8).

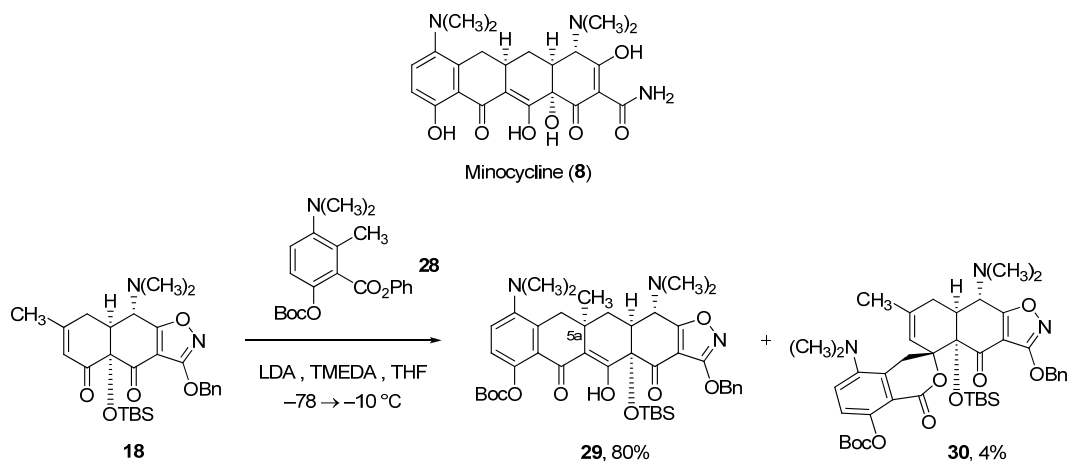
⁷² For preparation of tri-*n*-butyl[(methoxymethoxy)methyl]stannane, see: Danheiser, R. L.; Romines, K. R.; Koyama, H.; Gee, S. K.; Johnson, C. R.; Medich, J. R. *Org. Synth.* **1993**, *71*, 133; *Org. Synth.* **1998**, *Coll. Vol.* *9*, 704.



Scheme 2.8. Alternative synthesis of the β -methoxymethoxymethyl AB enone **26** from the AB enone **10**.

Having established versatile methodology for the synthesis of β -substituted AB enone substrates, we next investigated the feasibility of constructing the C ring of tetracyclines with an all-carbon quaternary C5a stereocenter by a Michael–Claisen cyclization reaction (Schemes 2.9 and 2.10). The D-ring precursor **28** was chosen for initial cyclization experiments. This precursor comprises the D-ring functionality of minocycline (**8**) and was known from prior research to be an effective substrate in Michael–Claisen cyclization reactions.^{54b} Addition of the β -methyl-substituted AB enone **18** (1 equiv) to a bright red solution of the *o*-toluate ester anion formed by deprotonation of the minocycline D-ring precursor **28** (3 equiv) with lithium diisopropylamide (LDA, 3 equiv) in the presence of *N,N,N',N'*-tetramethylethylenediamine (TMEDA, 6 equiv) at $-78\text{ }^{\circ}\text{C}$, followed by warming to $-10\text{ }^{\circ}\text{C}$, provided the Michael–Claisen cyclization product **29** in 80% yield as a single stereoisomer after purification by flash-column chromatography. A minor by-product (compound **30**, 4%), thought to be the product of 1,2-addition-cyclization (by lactonization), was isolated separately.⁷³

⁷³ Michael–Claisen cyclization product **29** was obtained in 60% yield and 1,2-addition-cyclization product **30** was not observed when the cyclization reaction was performed without TMEDA as an additive.

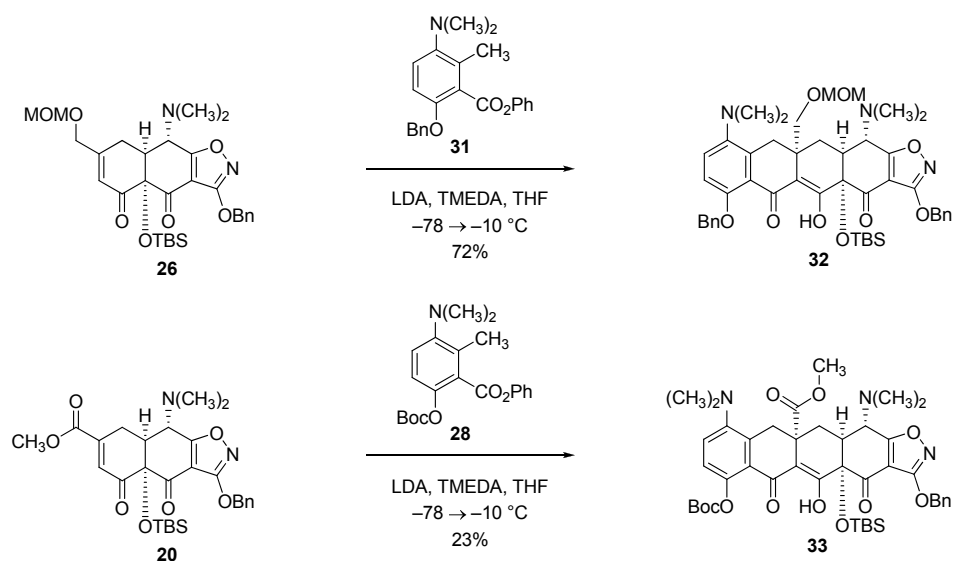


Scheme 2.9. Stereocontrolled formation of an all-carbon quaternary center by Michael–Claisen cyclization of an *o*-toluate ester anion with β -methyl-substituted AB enone **18**.

The stereochemical assignment of the Michael–Claisen cyclization product (**29**), with C5a-*R* configuration, is supported by nOe studies; this stereochemistry is homologous with that of Michael–Claisen cyclization products derived from the non-substituted AB enone **10**.^{54b} In both cases, addition appears to occur from a single diastereoface of the enone, that opposite the C12a *tert*-butyldimethylsilyloxy substituent. There are two examples in the literature of Michael–Claisen cyclization reactions of achiral β -methyl cyclohexenones with *o*-toluate ester anions,⁷⁴ but we are unaware of any examples beyond those described in this thesis of the stereocontrolled construction of a six-membered ring containing a quaternary center by a Michael–Claisen cyclization reaction.

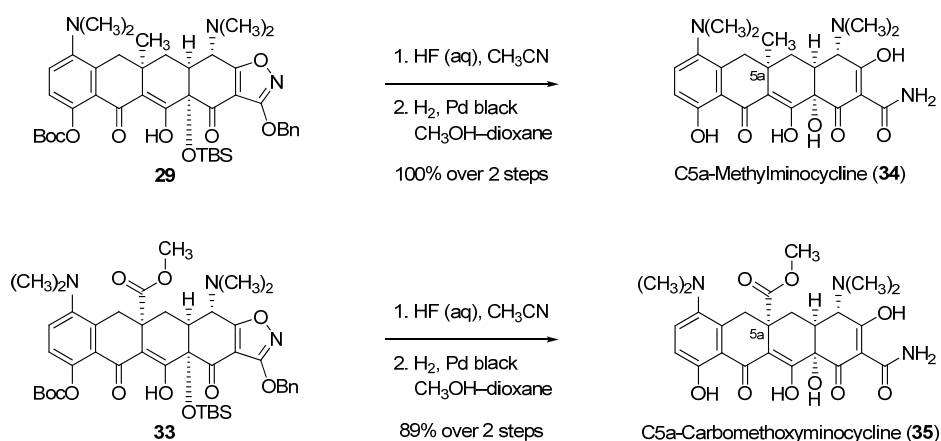
⁷⁴ Hill, B.; Rodrigo, R. *Org. Lett.* **2005**, 7, 5223–5225.

Michael–Claisen reaction of the β -methoxymethoxymethyl AB enone **26** and the minocycline D-ring precursor **31** (with OBn protection at C10, chosen so as to allow later deprotection of the methoxymethyl ether at C5a without concomitant cleavage of the C10 phenoxy protective group) was also efficient, affording the cyclization product **32**, with a protected C5a-hydroxymethyl-substituted quaternary center, in 72% yield (Scheme 2.10). Reaction of the β -methyl ester AB enone **20** with the anion formed from the minocycline D-ring precursor **28** afforded a complex mixture of products containing the desired Michael–Claisen cyclization product **33** as one component. Cycloadduct **33** was isolated in 23% yield after purification by sequential flash-column chromatography and reverse-phase high-performance liquid chromatography (rp-HPLC).



Scheme 2.10. Stereocontrolled formation of an all-carbon quaternary center by Michael–Claisen cyclization reactions of *o*-toluate ester anions with β -substituted AB enones.

Two-step deprotection of cyclization products **29** and **33** under typical conditions^{54b,75} provided C5a-methyliminocycline (**34**, 100% yield, Scheme 2.11) and C5a-carbomethoxyiminocycline (**35**, 89% yield), respectively, after purification by rp-HPLC.



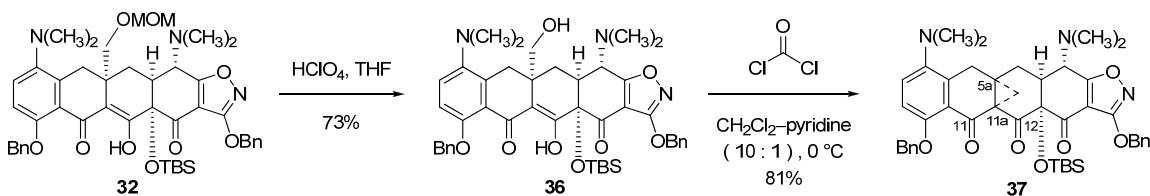
Scheme 2.11. Synthesis of C5a-methyliminocycline (**34**) and C5a-carbomethoxyiminocycline (**35**) by two-step deprotection of cyclization products **29** and **33**, respectively.

In a search for a versatile branch point for the synthesis of various C5a-substituted tetracyclines we were led to a serendipitous but highly effective solution (Scheme 2.12). Removal of the methoxymethyl ether protective group within the Michael–Claisen cyclization product **32** was achieved by treatment with perchloric acid⁷⁶ providing the substituted neopentyl alcohol **36** (73% yield). Addition of phosgene to a solution of **36** in

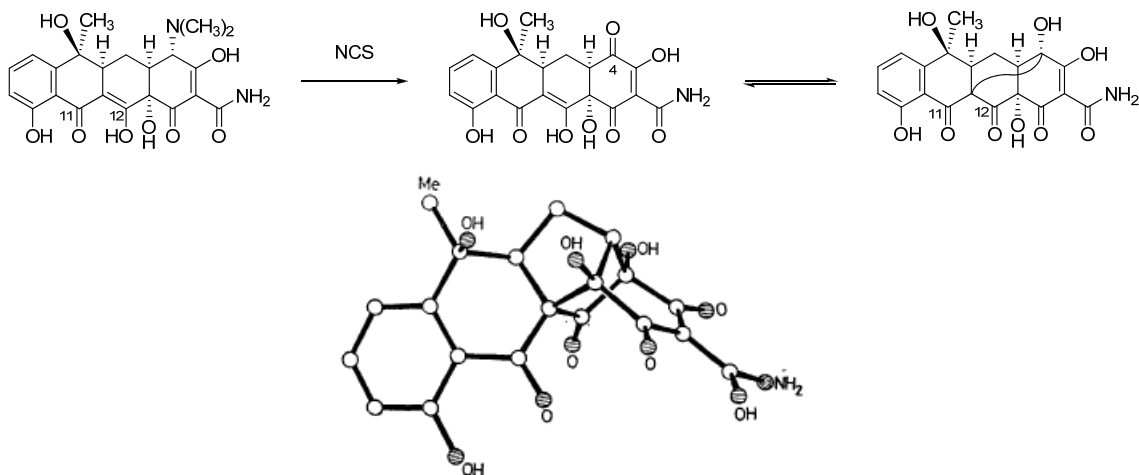
⁷⁵ Stork, G.; Hagedorn, A. A. III. *J. Am. Chem. Soc.* **1978**, *100*, 3609–3611.

⁷⁶ Perchloric acid is a strong oxidizing agent and can form explosive mixtures. For safety information, see: (a) Wolsey, W. C. *J. Chem. Educ.* **1973**, *50*, A335–A337. (b) Muse, L. A. *J. Chem. Educ.* **1972**, *49*, A463–A466.

dichloromethane–pyridine (10:1) at 0 °C unexpectedly afforded the C5a–C11a-bridged cyclopropane tetracycline precursor **37** in 81% yield.



Scheme 2.12. Discovery of a C5a–C11a-bridged cyclopropane tetracycline precursor (**37**).



Scheme 2.13. Bridged tetracycline product formed by an internal nucleophilic addition involving the (C11–C12) 1,3-diketone of tetracycline.⁷⁷

After the fact, the formation of cyclopropane **37** is easily rationalized. In this context it is interesting to note that Barton and co-workers had previously reported that the (C11–C12) 1,3-diketone of tetracycline can participate in an internal nucleophilic

addition, albeit in that case with addition to an electrophilic carbonyl group that had been introduced at position C4 (Scheme 2.13 above).⁷⁷

Cyclopropanes with geminal electron-withdrawing substituents are known to undergo nucleophilic ring-opening,⁷⁸ a transformation often enhanced in the presence of Lewis acids.⁷⁹ We were led to explore the use of magnesium salts as Lewis acid activators in this system in view of the well documented affinity of Mg^{2+} for binding to the (C11–C12) 1,3-diketone function of tetracyclines, complexation which is critical for inhibition of the ribosome.⁵⁶ We observed that the bridged cyclopropane intermediate **37** underwent regioselective ring-opening at the bridging carbon atom in the presence of various nucleophiles and magnesium bromide as Lewis acid (Chart 2.1). The ring-opened products were readily deprotected in the typical two-step sequence to furnish the corresponding C5a-substituted tetracyclines. For example, reaction of the C5a–C11a-bridged cyclopropane tetracycline precursor **37** with pyrrolidine (10 equiv) in the presence of a stoichiometric amount of anhydrous magnesium bromide in THF at 23 °C, followed by direct deprotection of the crude ring-opened product (**38**), provided C5a-pyrrolidinomethylminocycline (**39**) in 74% yield over the three steps after purification by rp-HPLC.

⁷⁷ Barton, D. H. R.; Ley, S. V.; Meguro, K.; Williams, D. J. *J. Chem. Soc., Chem. Commun.* **1977**, 790–791.

⁷⁸ For an overview, see: “Electrophilic Cyclopropanes in Organic Synthesis” Danishefsky, S. *Acc. Chem. Res.* **1979**, *12*, 66–72.

⁷⁹ Examples of Lewis acid-promoted ring-opening of activated cyclopropanes: (a) Swain, N. A.; Brown, R. C. D.; Bruton, G. *J. Org. Chem.* **2004**, *69*, 122–129. (b) Tanimori, S.; He, M.; Nakayama, M. *Synth. Commun.* **1993**, *23*, 2861–2868. (c) Lifchits, O.; Charette, A. B. *Org. Lett.* **2008**, *10*, 2809–2812.

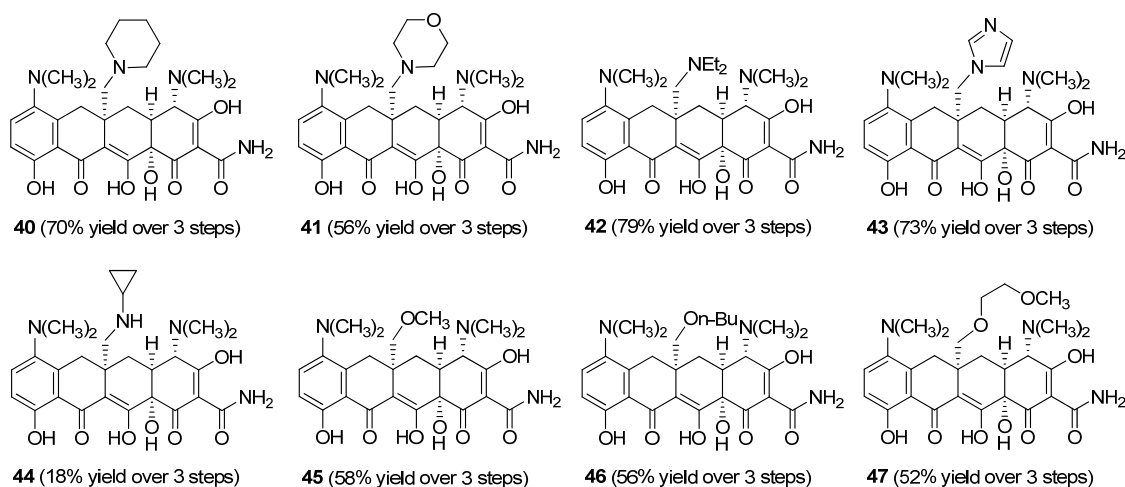
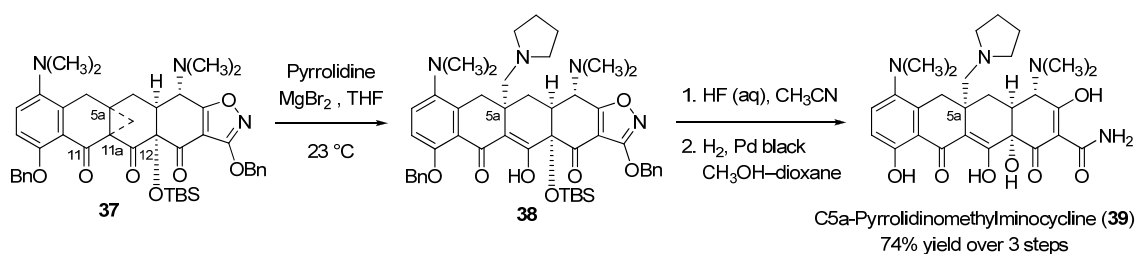


Chart 2.1. Fully synthetic tetracyclines prepared from the C5a–C11a-bridged cyclopropane intermediate **37** by magnesium bromide-promoted ring-opening followed by two-step deprotection.

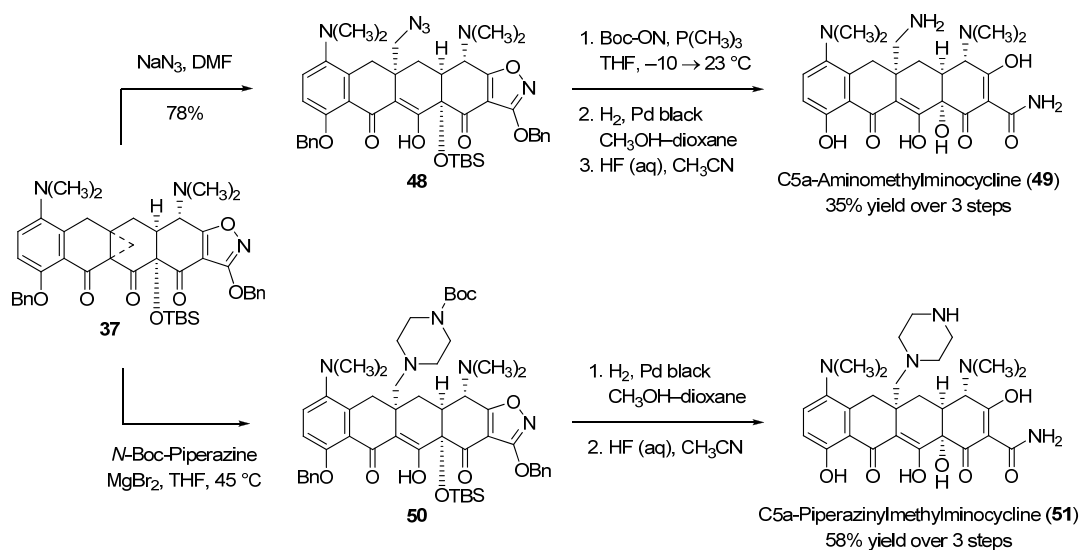
A number of different amines and alcohols were found to function effectively as nucleophiles in the magnesium bromide-promoted cyclopropane ring-opening reaction (Chart 2.1). Ring-opening reactions were typically performed with a large excess of nucleophile (≥ 7 equiv) and stoichiometric or superstoichiometric quantities of anhydrous magnesium bromide in THF (in the cases of low molecular weight alcohols as nucleophiles, the alcohol was used as solvent) at a range of temperatures (23–75 °C, see experimental section for details). Partial (and inconsequential) loss of the benzyl ether

phenolic protective group was observed to occur in the cyclopropane ring-opening reaction in some instances.

The C5a–C11a-bridged cyclopropane intermediate **37** also served as a precursor to tetracyclines with aminomethyl (**49**) and piperazinylmethyl (**51**) substituents at position C5a (Scheme 2.14), highly versatile compounds which functioned as further branch-points for the synthesis of C5a-substituted tetracyclines (Figures 2.3 and 2.4). Thus, treatment of cyclopropane **37** with sodium azide in dimethylformamide at 23 °C afforded the azido-substituted ring-opened product **48** in 78% yield after purification by flash-column chromatography. Addition of trimethylphosphine (2 equiv) to a solution of the azide **48** and 2-(*tert*-butoxycarbonyloxyimino)-2-phenylacetonitrile (Boc-ON, 2 equiv) in THF at –10 °C followed by warming to 23 °C afforded the corresponding *tert*-butyl carbamate (51% yield).⁸⁰ Two-step deprotection of the *tert*-butyl carbamate intermediate was best achieved by an inverted deprotection sequence (hydrogenolysis followed by treatment with hydrofluoric acid),⁸¹ providing C5a-aminomethylminocycline **49** after purification by rp-HPLC (69% yield over two steps). In addition, magnesium bromide-promoted ring-opening of cyclopropane **37** with *N*-*tert*-butoxycarbonyl-piperazine followed by deprotection of the ring-opened product **50** provided C5a-piperazinylmethylminocycline (**51**, 58% yield over three steps).

⁸⁰ Ariza, X.; Urpí, F.; Viladomat, C.; Vilarrasa, J. *Tetrahedron Lett.* **1998**, 39, 9101–9102.

⁸¹ The hydrogenolysis deprotection step (typically the final step) was slow and low-yielding in the presence of primary and secondary amines. To synthesize the amines **49** and **51** most efficiently the usual order of deprotection steps was reversed and the hydrogenolysis reaction was performed on substrates in which primary or secondary amines were protected as *tert*-butyl carbamates. For discussion of the inhibitory effects of amines on Pd-catalyzed hydrogenolysis, see: Sajiki, H.; Hirota, K. *Tetrahedron* **1998**, 54, 13981–13996.



Scheme 2.14. Synthesis of substrates for final-step diversification from cyclopropane **37**.

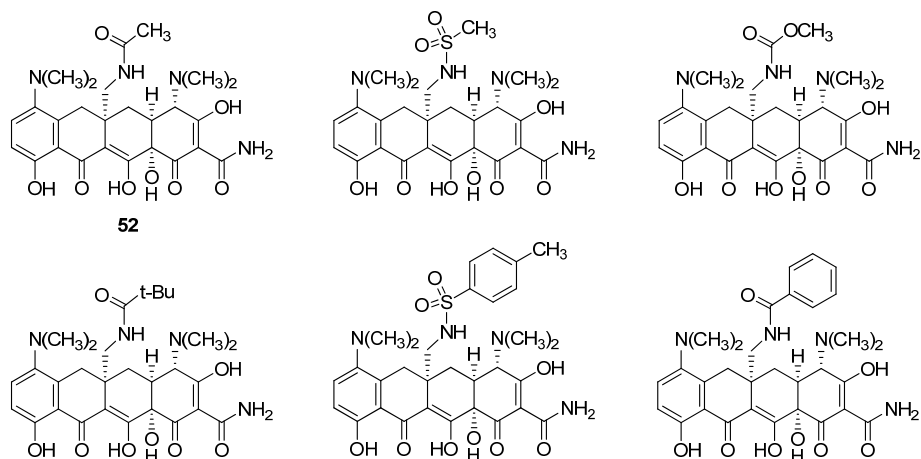


Figure 2.3. Selected fully synthetic tetracyclines prepared by final-step diversification of C5a-aminomethyliminocycline (**49**).

Final-step diversification of **49** and **51** was readily achieved, affording a range of novel tetracyclines with C5a substituents incorporating amides, sulfonamides and amines

(Figures 2.3 and 2.4). In this manner the C5a–C11a-bridged cyclopropane **37** served as a common precursor for the synthesis of more than 25 structural variants of minocycline with a diverse range of substituents at C5a.

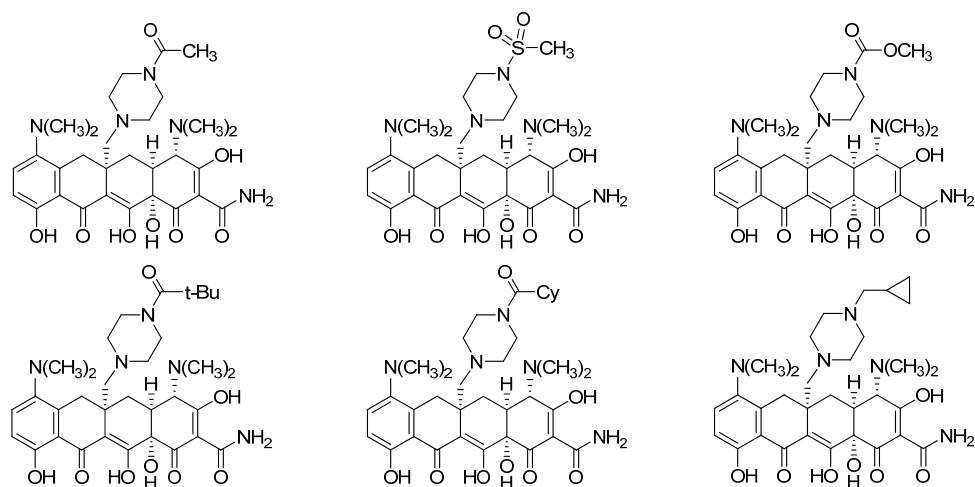


Figure 2.4. Fully synthetic tetracyclines prepared by final-step diversification of C5a-piperazinylmethylminocycline (**51**).

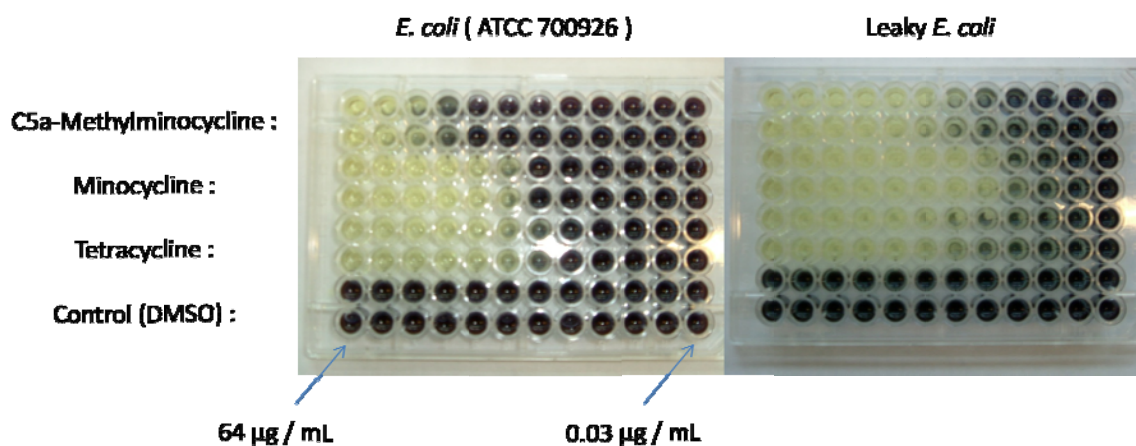
Antibacterial Activities

Minimum inhibitory concentrations (MICs) were determined in whole-cell antibacterial assays using a panel of tetracycline-sensitive and tetracycline-resistant Gram-positive and Gram-negative bacteria. Initial experiments were performed with assistance from members of the Kahne research group, and more thorough analyses of antibacterial activity were conducted at Tetraphase Pharmaceuticals. In summary, analogs of minocycline possessing angular substituents at C5a were found to be significantly less active than the parent compound against both Gram-positive and Gram-negative bacteria.

MIC assays for C5a-methylminocycline (**34**), minocycline (**8**) and tetracycline (**3**) against tetracycline-susceptible *E. coli* and leaky *E. coli* strains are depicted in Figure 2.5 below. Leaky *E. coli* has a less asymmetric and more permeable outer membrane than the corresponding *E. coli* strain due to knockout of a lipopolysaccharide gene. As discussed in Chapter 1, the outer membrane of Gram-negative bacteria is asymmetric and consists of both lipopolysaccharides and phospholipids.⁸² The “gel-like” nature of the lipopolysaccharide component makes the outer membrane a more effective permeability barrier than the inner membrane, and most antibacterials (including tetracyclines) penetrate the outer membrane predominantly by passing through aqueous channels provided by porin proteins.

To determine MIC values, 96-well plates containing the bacterial strain and an appropriate medium were treated with different concentrations of drug molecules. Each pair of rows corresponds to a different small molecule and the drug concentration decreases uniformly across each plate (from left to right, as depicted). Following incubation, the wells were treated with a stain which (in the examples shown in Figure 2.5 below) turned black in the presence of bacteria, indicating that the drug concentration was insufficient to prevent bacterial growth.

⁸² Nikaido, H. *Microbio. Mol. Biol. Rev.* **2003**, 67, 593-656.



	<i>E. coli</i>	Leaky <i>E. coli</i>
C5a-Methylminocycline (Rows 1 & 2)	16	1
Minocycline (Rows 3 & 4)	2	0.5
Tetracycline (Rows 5 & 6)	2	0.5

Figure 2.5. Minimum inhibitory concentration (MIC) assays and values in $\mu\text{g} / \text{mL}$ for C5a-methylminocycline (**34**), minocycline (**8**) and tetracycline (**3**) against *E. coli* and leaky *E. coli* strains.

The results of these MIC assays revealed that C5a-methylminocycline possesses antibacterial activity but is 8-fold less active than minocycline against the *E. coli* strain and 2-fold less active in leaky *E. coli*. Since there is a smaller difference in potency in leaky *E. coli* where the drug molecules are better able to penetrate the outer membrane by diffusion (as well as by passage through porin channels), the reduced activity of C5a-methylminocycline relative to minocycline in *E. coli* could be partly due to reduced outer membrane permeability.

Complete antibacterial activity data for C5a-substituted analogs is presented in the tables at the end of this chapter (pages 57–62). The C5a-modified compounds synthesized in this study were found to be significantly less active than minocycline (the parent compound) against both Gram-positive and Gram-negative bacteria. Analogs with smaller substituents (e.g. methyl) at C5a exhibited modest activity against some bacterial strains, while most of the compounds with larger substituents appended at C5a were almost completely inactive as antibiotics. The detrimental effect of C5a-substitution on activity did not seem to be dependent on the tetracycline resistance determinants possessed by a given bacterial strain.

β -Methyl-substituted AB enone **18** was also transformed into C5a-methyltigecycline (**54**) via the four-step synthetic sequence presented in Scheme 2.15 below. 5a-Methyltigecycline was found to have greatly reduced potency relative to tigecycline. Indeed, the detrimental effect on activity (C5a-methyl vs. C5a-unsubstituted) was even more pronounced for tigecycline than for minocycline, indicating that the introduction of substituents at this position diminishes (or eliminates) antibiotic activity regardless of the D-ring substitution pattern.

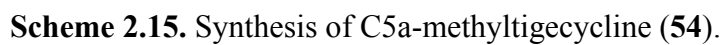
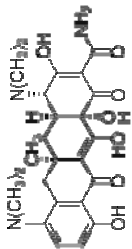
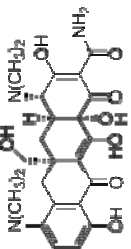


Table 2.1. Minimum inhibitory concentration (MIC) values for minocycline and minocycline analogs (µg/mL)

	GP										GN									
	SA101					SA159					SA161					SA164				
	µM	µM	µM	µM	µM	µM	µM	µM	µM	µM	µM	µM	µM	µM	µM	µM	µM	µM	µM	µM
<div> <div>Minocycline</div>  </div>	0.03	8	8	8	≤0.016	0.125	16	≤0.016	4	16										
	1	32	32	0.25	1	>32	0.125	>32	>32	>32										
	1	>32	>32	0.5	4	>32	0.25	>32	>32	>32										
<div> <div>Minocycline</div>  </div>	2	≤0.016	0.25	8	8	8	8	8	8	8	8	8	8	8	8	8	8	8	8	8
	4	0.5	4	>32	>32	>32	>32	>32	>32	>32	>32	>32	>32	>32	>32	>32	>32	>32	>32	>32
	8	0.5	2	>32	>32	>32	>32	>32	>32	>32	>32	>32	>32	>32	>32	>32	>32	>32	>32	>32

Abbreviations: GP, Gram-positive; GN, Gram-negative; organisms – S.A. *Staphylococcus aureus*; EF, *Enterococcus faecalis*; SP, *Streptococcus pneumoniae*; EC, *Escherichia coli*; KP, *Klebsiella pneumoniae*; PM, *Proteus mirabilis*; PA, *Pseudomonas aeruginosa*; AB, *Acinetobacter baumannii*; SM, *Stenotrophomonas maltophilia*; BC, *Burkholderia cenocepacia*; resistance determinants – tetM, ribosomal protection proteins; tetA, tetB, tetracycline efflux proteins; KO, multiple efflux pump knockout; ESBL, extended-spectrum beta-lactamase; tolC, multiple efflux pump knockout.

Table 2.2. Minimum inhibitory concentration (MIC) values for C-5a-substituted minocycline analogs ($\mu\text{g/mL}$)

	GP										GM												
	SA101	SA19T	SA161	SA158	SE164	EF159	SP106	SP160	SP312		H1262	MC205	EC107	EC155	KP153	KP457	PM112	PA555	PA566	KO	tetB		
	4	>32	>32	1	2	>32	0.5	>32	>32	>32	4	1	8	>32	>32	>32	>32	>32	>32	4	16	8	>32
	2	4	4	2	2	4	0.5	4	4	4	32	2	>32	>32	>32	>32	>32	>32	>32	>32	>32	>32	>32
	1	32	>32	0.25	0.5	>32	0.25	>32	>32	>32	8	0.25	4	>32	>32	>32	>32	>32	>32	2	16	8	>32
	2	>32	>32	0.5	4	>32	0.125	>32	>32	>32	1	1	4	>32	>32	>32	>32	>32	>32	2	16	8	>32

Table 2.3. Minimum inhibitory concentration (MIC) values for C5a-substituted ninocycline analogs (µg/mL)

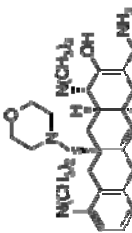
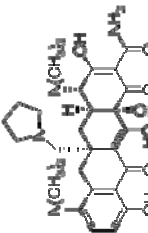
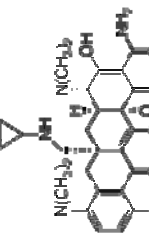

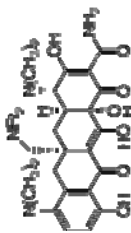
	GP										CN												
	SA10 ⁺	SA10 ⁺	SA10 ⁺	SA10 ⁺	SE10 ⁺	LI 130	SP100	SP100	SP100	SP312	H1222	M2203	EC107	EC150	NP153	NP457	PI112	PA555	PA555	AB250	SB268	BC240	
	testM	testM	testK	testK	testM	testM	testM	testM	testM	testM	testB	testA	testA	testA	testM	testM	testM	testM	testM	testB	testB	testB	
	8	16	16	4	4	32	4	>32	>32	32	>32	4	32	>32	>32	>32	>32	>32	>32	16	32	32	>32
	16	32	>32	4	4	>32	4	>32	>32	>32	>32	4	8	32	16	32	32	>32	4	16	8	>32	
	32	>32	>32	8	>8	>32	8	>32	>32	>32	>32	8	32	>32	>32	>32	>32	>32	8	>32	32	>32	
	16	32	>32	8	8	>32	4	>32	>32	>32	>32	4	8	>32	32	>32	>32	>32	32	32	>8	>32	
	32	>32	>32	8	8	>32	8	>32	>32	>32	>32	8	>8	>32	32	>32	>32	>32	>8	32	>8	>32	

Table 2.5. Minimum inhibitory concentration (MIC) values for C5a-substituted minocycline analogs (µg/mL)

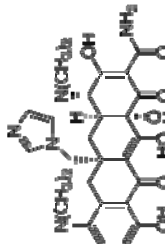
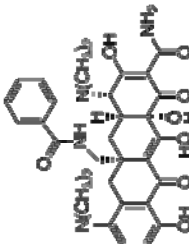
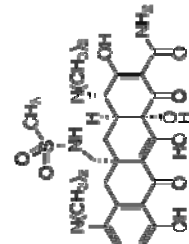
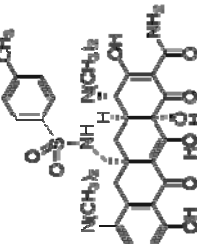
	GP										GN										
	SA-0*	SA158	EF327	EF404	SP-60	SP312	EC107	EC155	EC378	EC380	EC382	KF457	PM385	PA555	PA556	PA564	PA569	EC303	AG250	SM258	BC240
	16	>32	4	>32	>32	>32	8	>32	2	4	2	32	>32	>32	2	1	32	>32	>32	>32	>32
	8	8	2	>32	32	2	32	>32	32	2	2	>32	>32	>32	32	8	>32	>32	>32	>32	>32
	>32	>32	2	>32	>32	>32	>32	>32	8	>32	4	>32	>32	>32	2	2	>32	>32	>32	>32	>32
	16	32	4	32	32	32	>32	>32	>32	4	4	>32	>32	>32	>32	8	>32	>32	>32	>32	>32

Table 2.6. Minimum inhibitory concentration (MIC) values for C-5a-substituted minocycline analogs (µg/mL)

	GP										GN												
	SA101	SA191	SA161	SA168	SE104	EF109	SP108	SP108	SP108	SP108	HI232	MC235	EC107	EC155	4P133	SP437	PM112	PA555	PA555	AB250	SP425	BC240	
	101M	101M	101M	101K	101K	101M	101M	101M	101M	101M	101M	101M	101M	101A	101A	101A	101M	101M	101M	101M	101M	101M	101M
	32	>32	>32	4	8	>32	2	>32	32	32	8	4	>32	>32	>32	>32	>32	>32	2	>32	>32	>32	
	16	>32	>32	4	8	>32	2	>32	>32	>32	>32	8	>32	>32	>32	>32	>32	>32	32	>32	>32	>32	
	16	16	16	8	8	32	4	>32	32	32	>32	8	>32	32	>32	>32	>32	>32	>32	>32	>32	>32	
	16	16	16	8	8	16	4	32	16	16	>32	8	>32	>32	>32	>32	>32	>32	>32	>32	>32	>32	

Conclusion

Synthetic methodological advances have permitted efficient and stereocontrolled construction of fully synthetic tetracyclines containing an all-carbon quaternary, stereogenic center at position C5a, a structurally novel class of compounds in this important family of therapeutic agents. We anticipate that the new strategies presented herein for the introduction of ester, thioester and aldehyde substituents at the β -position of cyclohexenones will be of value in many contexts. The discovery of a highly diversifiable bridged cyclopropane-containing tetracycline intermediate enabled efficient synthesis of numerous C5a-substituted tetracyclines. Although it is conceivable that many of these structures could also have been accessed by Michael–Claisen cyclization reactions of individually prepared β -substituted AB enones, the discovery of a diversifiable late-stage intermediate greatly expedited the process of synthesis, in that a single Michael–Claisen cycloadduct served as a precursor to large numbers of C5a-substituted tetracyclines. The C5a-modified analogs synthesized in this study were found to be significantly less active than the corresponding C5a-unsubstituted tetracyclines against both Gram-positive and Gram-negative bacteria.

Experimental Section

General experimental procedures: All reactions were performed in round-bottom flasks fitted with rubber septa under a positive pressure of argon, unless otherwise noted. Air- and moisture-sensitive liquids were transferred via syringe or stainless steel cannula. Organic solutions were concentrated by rotary evaporation (house vacuum, ca. 25–40 Torr) at ambient temperature, unless otherwise noted. Analytical thin-layer chromatography (TLC) was performed using glass plates pre-coated with silica gel (0.25 mm, 60 Å pore-size, 230–400 mesh, Merck KGA) impregnated with a fluorescent indicator (254 nm). TLC plates were visualized by exposure to ultraviolet light, then were stained with either an aqueous sulfuric acid solution of ceric ammonium molybdate (CAM) or an aqueous sodium carbonate solution of potassium permanganate (KMnO₄) followed by brief heating on a hot plate. Flash-column chromatography was performed as described by Still *et al.*,⁸³ employing silica gel (60 Å, 32–63 µM, standard grade, Dynamic Adsorbents, Inc.).

Materials: Commercial solvents and reagents were used as received with the following exceptions. Diisopropylamine, trimethylsilyl chloride, and hexamethylphosphoramide were distilled from calcium hydride under an atmosphere of argon or dinitrogen. Tetrahydrofuran was purified by the method of Pangborn *et al.*⁸⁴ The molarity of *n*-

⁸³ W. C. Still, M. Khan, A. Mitra, *J. Org. Chem.* **1978**, *43*, 2923–2925.

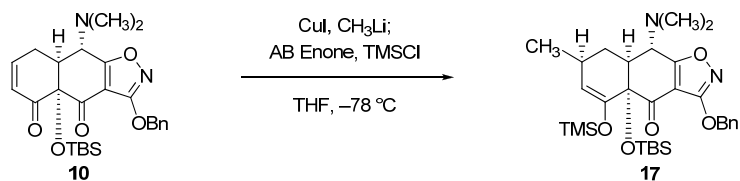
⁸⁴ A. B. Pangborn, M. A. Giardello, R. H. Grubbs, R. K. Rosen, F. J. Timmers, *Organometallics* **1996**, *15*, 1518–1520.

butyllithium solutions was determined by titration against a standard solution of diphenylacetic acid in tetrahydrofuran (average of three determinations).⁸⁵

Instrumentation: Proton magnetic resonance (^1H NMR) spectra were recorded on Varian INOVA 500 (500 MHz) or 600 (600 MHz) NMR spectrometers at 23 °C. Proton chemical shifts are expressed in parts per million (ppm, δ scale) and are referenced to residual protium in the NMR solvent (CHCl_3 , δ 7.26). Data are represented as follows: chemical shift, multiplicity (s = singlet, d = doublet, t = triplet, q = quartet, m = multiplet and/or multiple resonances, br = broad, app = apparent), integration, and coupling constant (J) in Hertz. Carbon nuclear magnetic resonance spectra (^{13}C NMR) were recorded on Varian INOVA 500 (125 MHz) NMR spectrometers at 23 °C. Carbon chemical shifts are expressed in parts per million (ppm, δ scale) and are referenced to the carbon resonances of the NMR solvent (CDCl_3 , δ 77.0). Fluorine nuclear magnetic resonance spectra (^{19}F NMR) were recorded on a Varian INOVA 400 NMR spectrometer at 23 °C. Infrared (IR) spectra were obtained using a Shimadzu 8400S FT-IR spectrometer and were referenced to a polystyrene standard. Data are represented as follows: frequency of absorption (cm^{-1}), intensity of absorption (s = strong, m = medium, w = weak, br = broad). High-resolution mass spectra were obtained at the Harvard University Mass Spectrometry Facility. X-ray crystallographic analyses were performed at the Harvard University X-ray Crystallographic Laboratory by Dr. Shao-Liang Zheng.

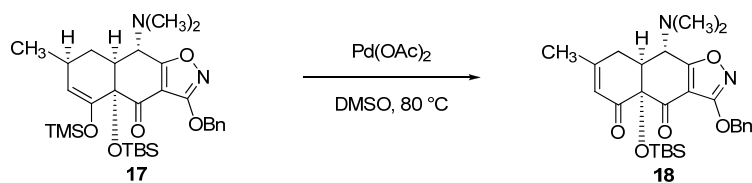
⁸⁵ W. G. Kofron, L. M. Baclawski, *J. Org. Chem.* **1976**, *41*, 1879–1880.

Minimum Inhibitory Concentration (MIC) Values. MIC values were used to determine the efficacy of a particular antibiotic by measuring its ability to inhibit growth at a range of different concentrations. A 96-well plate (Corning Costar 3596) was prepared by adding 100 μ L of media to all wells and an additional 87.2 μ L of media to the first column of wells. 12.8 μ L of drug solution in dimethyl sulfoxide (DMSO) was then added to the first well of each row (2.0 mg/mL drug solution provides final concentration of 64 μ g/mL in the first column of wells). A serial dilution was performed across the plate, discarding the final 100 μ L of media. Cells were prepared by reinoculating an overnight culture into fresh lysogeny broth (LB) until they reached an $OD_{600} = \sim 0.6$, then by diluting the cells 100-fold in fresh LB in a media reservoir. 100 μ L of cells from the media reservoir were then added to each row of the plate. Cells were incubated for 24 h at 37 °C. A 1 mg/mL aqueous solution of thiazolyl blue tetrazolium bromide (MTT) was prepared and 50 μ L of this solution was added to each well. Following incubation for a further 1 h, MICs were determined by measuring the first well that stained successfully (indicating respiration by the organism). The drug concentration present in the last well in which the stain did not appear provided the MIC value for a particular drug molecule in this bacterial strain. The MIC value for each drug was verified by a duplicate (two rows for each small molecule) and the growth of bacteria in the absence of small molecule was confirmed using a DMSO control.



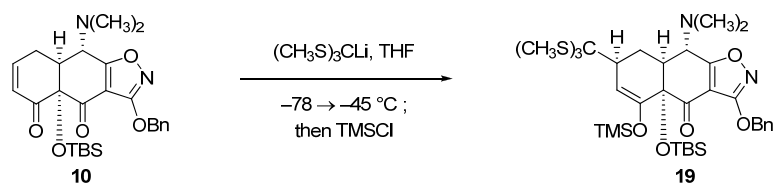
β -Methyl-substituted trimethylsilyl enol ether 17. A round-bottomed flask charged with copper (I) iodide (1.89 g, 9.95 mmol, 1.6 equiv) was flame-dried under high vacuum. After cooling to room temperature, the flask was blanketed with dry argon. Tetrahydrofuran (50 mL) was added and the resulting suspension was cooled to 0 °C. A solution of methyllithium in ethyl ether (1.6 M, 12.2 mL, 19.6 mmol, 3.15 equiv) was added dropwise via syringe over 5 min. The resulting solution was stirred at 0 °C for 20 min, then was cooled to –78 °C. A solution of the AB enone **10** (3.0 g, 6.22 mmol, 1 equiv) and chlorotrimethylsilane (1.25 mL, 9.95 mmol, 1.6 equiv) in tetrahydrofuran (10 mL) was added to the cuprate solution dropwise via syringe at –78 °C. After stirring at –78 °C for 90 min, the cooling bath was removed and the product solution was diluted with ethyl acetate (100 mL) and hexanes (100 mL). A mixture of saturated aqueous ammonium chloride solution and saturated aqueous ammonium hydroxide solution (19:1, 100 mL) was then added carefully. The phases were separated and the organic phase was washed sequentially with saturated aqueous ammonium chloride solution (100 mL) and saturated aqueous sodium chloride solution (2 x 100 mL). The organic phase was dried over anhydrous sodium sulfate. The dried solution was filtered and the filtrate was concentrated. The product was purified by flash-column chromatography (7% ethyl acetate-hexanes), providing β -methyl-substituted trimethylsilyl enol ether **17** as a white solid (3.01 g, 85%).

$R_f = 0.57$ (15% ethyl acetate-hexanes); ^1H NMR (500 MHz, CDCl_3) δ 7.48 (dd, 2H, $J = 8.0, 1.5$ Hz), 7.36-7.31 (m, 3H), 5.36 (AB quartet, 2H), 4.69 (d, 1H, $J = 3.0$ Hz), 3.76 (d, 1H, $J = 10.0$ Hz), 2.55-2.52 (m, 1H), 2.44 (s, 6H), 2.32-2.25 (m, 2H), 1.84 (d, 1H, $J = 13.5$ Hz), 1.18 (d, 3H, $J = 7.5$ Hz), 0.87 (s, 9H), 0.22 (s, 3H), 0.11 (s, 3H), -0.04 (s, 9H); ^{13}C NMR (125 MHz, CDCl_3) δ 189.7, 181.5, 167.4, 147.2, 135.2, 128.6, 128.5, 128.4, 110.7, 108.3, 80.7, 72.2, 61.1, 46.3, 41.9, 26.2, 26.0, 25.1, 24.0, 18.8, -0.5 , -2.8 , -3.6 ; FTIR (neat film), 2955 (w), 1721 (m), 1653 (w), 1614 (w), 1510 (m), 1471 (w), 1250 (m), 1198 (m), 1148 (m), 936 (m), 833 (s) cm^{-1} ; HRMS-ESI (m/z): $[\text{M}+\text{H}]^+$ calcd for $\text{C}_{30}\text{H}_{47}\text{N}_2\text{O}_5\text{Si}_2$, 571.3018; found, 571.3041.



β-Methyl-substituted AB enone 18.⁶⁰ Palladium (II) acetate (75 mg, 0.329 mmol, 1.15 equiv) was added to a solution of β-methyl-substituted trimethylsilyl enol ether **17** (163 mg, 0.286 mmol, 1 equiv) in anhydrous dimethyl sulfoxide (3.0 mL) at 23 °C. The resulting mixture was heated to 80 °C. After stirring at this temperature for 16 h, the reaction mixture was allowed to cool to 23 °C. The cooled suspension was diluted with ethyl acetate (20 mL) and the whole was filtered through a pad of Celite. Hexanes (20 mL) were added to the filtrate and the resulting solution was washed sequentially with saturated aqueous sodium bicarbonate solution (20 mL) and saturated aqueous sodium chloride solution (2 x 20 mL). The organic phase was dried over anhydrous sodium sulfate. The dried solution was filtered and the filtrate was concentrated. The product was purified by flash-column chromatography (10% ethyl acetate-hexanes), affording the β-methyl-substituted AB enone **18** as a pale yellow solid (63 mg, 44%).

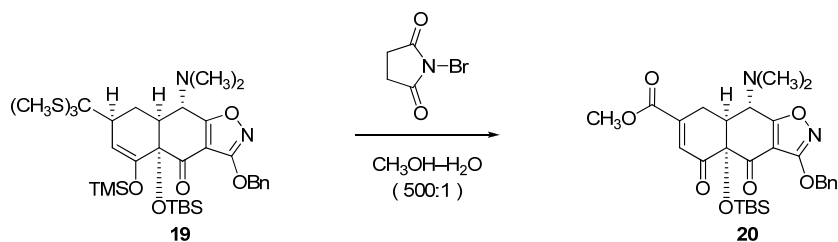
R_f = 0.26 (15% ethyl acetate-hexanes); ^1H NMR (500 MHz, CDCl_3) δ 7.50 (d, 2H, J = 7.0 Hz), 7.40-7.32 (m, 3H), 5.93 (s, 1H), 5.35 (AB quartet, 2H), 3.74 (d, 1H, J = 11.0 Hz), 2.81-2.70 (m, 3H), 2.46 (s, 6H), 2.01 (s, 3H), 0.82 (s, 9H), 0.26 (s, 3H), 0.05 (s, 3H); ^{13}C NMR (125 MHz, CDCl_3) δ 193.1, 188.1, 181.2, 167.5, 161.2, 135.0, 128.5, 128.5, 124.7, 108.4, 82.5, 72.5, 59.8, 47.5, 42.0, 30.4, 25.9, 24.4, 19.0, -2.5, -4.2; FTIR (neat film), 2930 (w), 1719 (s), 1672 (m), 1510 (m), 1472 (w), 1175 (m), 1045 (m), 936 (s), 829 (m) cm^{-1} ; HRMS-ESI (m/z): $[\text{M}+\text{H}]^+$ calcd for $\text{C}_{27}\text{H}_{37}\text{N}_2\text{O}_5\text{Si}$, 497.2466; found, 497.2494.



β -Tris(methylthio)methyl trimethylsilyl enol ether **19.** A solution of *n*-butyllithium in hexanes (2.5 M, 518 μ L, 1.30 mmol, 1.25 equiv) was added dropwise via syringe to a solution of tris(methylthio)methane (176 μ L, 1.30 mmol, 1.25 equiv) in tetrahydrofuran (11 mL) at -78 $^{\circ}\text{C}$. The resulting colorless solution was stirred at this temperature for 20 min, whereupon a solution of the AB enone **10** (500 mg, 1.04 equiv, 1 equiv) in tetrahydrofuran (3.0 mL) was added dropwise via syringe, forming a bright orange-yellow solution. The reaction solution was allowed to warm slowly to -45 $^{\circ}\text{C}$ over 60 min, then chlorotrimethylsilane (199 μ L, 1.55 mmol, 1.5 equiv) was added. The (yellow) reaction mixture was stirred at -45 $^{\circ}\text{C}$ for 30 min, then was partitioned between aqueous potassium phosphate buffer solution (pH 7.0, 0.2 M, 20 mL) and dichloromethane (30 mL). The phases were separated and the aqueous phase was extracted with dichloromethane (20 mL). The organic extracts were combined and the combined solution was dried over anhydrous sodium sulfate. The dried solution was filtered and the filtrate was concentrated, affording an orange-yellow oil. The crude product was purified by flash-column chromatography (6% ethyl acetate–hexanes), providing β -tris(methylthio)methyl trimethylsilyl enol ether **19** as a pale yellow foam (654 mg, 89%).

R_f = 0.69 (20% ethyl acetate–hexanes); ^1H NMR (500 MHz, CDCl_3) δ 7.49–7.47 (m, 2H), 7.37–7.32 (m, 3H), 5.37 (AB quartet, 2H), 5.36 (d, 1H, J = 2.0 Hz), 4.00 (d, 1H, J = 9.3 Hz), 3.15–3.12 (m, 1H), 2.52 (dd, 1H, J = 14.4, 4.2 Hz), 2.45 (s, 6H), 2.42–2.39 (m, 1H), 2.18 (s, 9H), 2.14–2.06 (m, 1H), 0.86 (s, 9H), 0.22 (s, 3H), 0.12 (s, 3H), -0.01 (s, 9H); ^{13}C

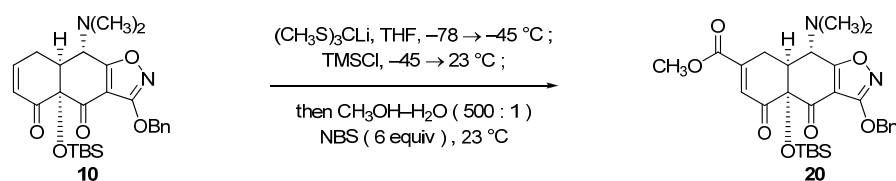
NMR (125 MHz, CDCl₃) δ 189.6, 181.6, 167.2, 150.5, 135.2, 128.6, 128.5, 128.4, 108.7, 103.8, 81.6, 75.1, 72.2, 61.7, 46.6, 42.1, 41.7, 26.1, 21.2, 19.0, 14.1, -0.3, -2.6, -3.3; FTIR (neat film), 1722 (m), 1651 (w), 1614 (w), 1510 (m), 1472 (w), 1254 (m), 1206 (w), 903 (m), 839 (s) cm⁻¹; HRMS-ESI (m/z): [M+H]⁺ calcd for C₃₃H₅₃N₂O₅S₃Si₂, 709.2650; found, 709.2617.



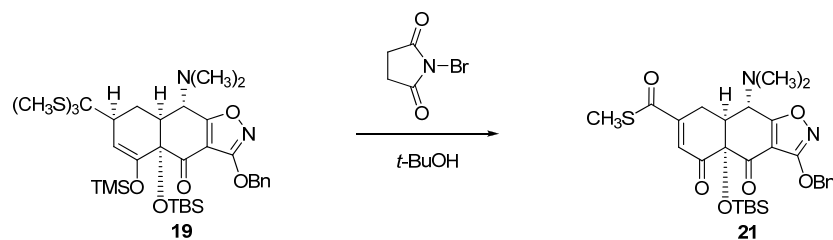
β -Methyl ester-substituted AB enone 20. *N*-Bromosuccinimide (151 mg, 0.846 mmol, 5.0 equiv) was added in one portion to a stirring solution of β -tris(methylthio)methyl trimethylsilyl enol ether **19** (120 mg, 0.169 mmol, 1 equiv) in methanol (4.5 mL) and water (9.0 μ L, 3.0 equiv, 500:1 mixture of methanol and water) at 23 °C. The pale yellow reaction solution was allowed to stir at 23 °C for 30 min, then was concentrated. The resulting yellow oil was dissolved in dichloromethane (20 mL) and the resulting solution was washed with saturated aqueous sodium bicarbonate solution (20 mL). The phases were separated and the aqueous phase was extracted with dichloromethane (20 mL). The organic extracts were combined and the combined solution was dried over anhydrous sodium sulfate. The dried solution was filtered and the filtrate was concentrated. The crude product was purified by flash-column chromatography (11% ethyl acetate-hexanes, grading to 15%), providing the β -methyl ester-substituted AB enone **20** as a yellow solid (78 mg, 85%).

R_f = 0.26 (15% ethyl acetate-hexanes); ^1H NMR (500 MHz, CDCl_3) δ 7.50 (d, 2H, J = 6.9 Hz), 7.40-7.33 (m, 3H), 6.82 (d, 1H, J = 1.8 Hz), 5.36 (AB quartet, 2H), 3.87 (s, 3H), 3.65 (d, 1H, J = 10.5 Hz), 3.21 (d, 1H, J = 18.8 Hz), 2.91-2.84 (m, 2H), 2.46 (s, 6H), 0.80 (s, 9H), 0.26 (s, 3H), 0.03 (s, 3H); ^{13}C NMR (125 MHz, CDCl_3) δ 194.2, 187.0, 181.1, 167.4, 166.1, 147.1, 134.9, 131.4, 128.6, 128.5, 128.5, 108.3, 82.5, 72.6, 59.3, 52.9, 47.2, 41.9, 25.9, 24.6, 19.0, -2.5, -4.1; FTIR (neat film), 1721 (s), 1684 (m), 1609 (w), 1510

(m), 1252 (m), 1173 (m), 1030 (m), 831 (m), 737 (m) cm^{-1} ; HRMS-ESI (m/z): $[\text{M}+\text{H}]^+$
calcd for $\text{C}_{28}\text{H}_{37}\text{N}_2\text{O}_7\text{Si}$, 541.2365; found, 541.2368.



Single-operation synthesis of β -methyl ester-substituted AB enone **20.** A solution of *n*-butyllithium in hexanes (2.5 M, 104 μ L, 0.259 mmol, 1.25 equiv) was added dropwise via syringe to a solution of tris(methylthio)methane (35.2 μ L, 0.259 mmol, 1.25 equiv) in tetrahydrofuran (2.0 mL) at -78 $^\circ\text{C}$. The resulting colorless solution was stirred at this temperature for 20 min, whereupon a solution of the AB enone **10** (100 mg, 0.207 mmol, 1 equiv) in tetrahydrofuran (0.4 mL) was added dropwise via syringe, forming a bright orange-yellow solution. The reaction solution was allowed to warm slowly to -45 $^\circ\text{C}$ over 30 min, then chlorotrimethylsilane (39.7 μ L, 0.311 mmol, 1.5 equiv) was added. The resulting (yellow) mixture was allowed to warm to 23 $^\circ\text{C}$ over 30 min, whereupon methanol (4.0 mL), water (8.0 μ L, 2.1 equiv, 500:1 mixture of methanol and water) and *N*-bromosuccinimide (221 mg, 1.24 mmol, 6.0 equiv) were added in sequence. The reaction mixture was allowed to stir at 23 $^\circ\text{C}$ for 30 min, then was concentrated. The resulting oily (yellow) suspension was dissolved in dichloromethane (15 mL) and the resulting solution was washed with saturated aqueous sodium bicarbonate solution (15 mL). The phases were separated and the aqueous phase was extracted with dichloromethane (15 mL). The organic extracts were combined and the combined solution was dried over anhydrous sodium sulfate. The dried solution was filtered and the filtrate was concentrated. The crude product was purified by flash-column chromatography (7% acetone-hexanes), providing the β -methyl ester-substituted AB enone **20** as a yellow solid (101 mg, 90%).

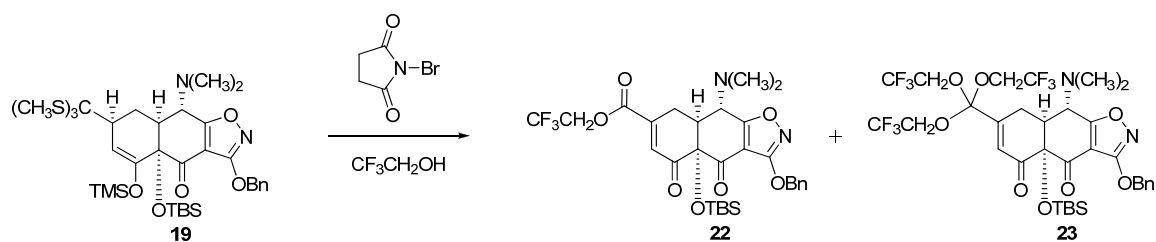


β -S-Methyl thioester-substituted AB enone 21. *N*-Bromosuccinimide (48 mg, 0.271 mmol, 4.0 equiv) was added in one portion to a stirring solution of β -tris(methylthio)methyl trimethylsilyl enol ether **19** (48 mg, 0.068 mmol, 1 equiv) in *tert*-butanol (3.0 mL) at 23 °C. The resulting bright yellow suspension was allowed to stir at 23 °C for 45 min (slowly clearing to give a yellow solution). The reaction mixture was diluted with dichloromethane (20 mL) and the resulting solution was washed with saturated aqueous sodium bicarbonate solution (20 mL). The phases were separated and the aqueous phase was extracted with dichloromethane (20 mL). The organic extracts were combined and the combined solution was dried over anhydrous sodium sulfate. The dried solution was filtered and the filtrate was concentrated. The crude product was purified by flash-column chromatography (8% ethyl acetate-hexanes), providing the β -S-methyl thioester-substituted AB enone **19** as a pale yellow solid (31 mg, 82%).

R_f = 0.51 (20% ethyl acetate-hexanes); ^1H NMR (500 MHz, CDCl_3) δ 7.51-7.50 (m, 2H), 7.41-7.35 (m, 3H), 6.72 (d, 1H, J = 2.4 Hz), 5.36 (AB quartet, 2H), 3.70 (d, 1H, J = 10.7 Hz), 3.30 (d, 1H, J = 19.5 Hz), 2.98-2.93 (m, 1H), 2.89 (dd, 1H, J = 10.5, 3.7 Hz), 2.49 (s, 6H), 2.45 (s, 3H), 0.82 (s, 9H), 0.26 (s, 3H), 0.05 (s, 3H); ^{13}C NMR (125 MHz, CDCl_3) δ 194.2, 192.9, 186.8, 181.0, 167.4, 153.2, 134.9, 128.6, 128.5, 128.5, 127.8, 108.3, 82.6, 72.6, 59.3, 47.3, 41.9, 25.9, 25.9, 24.4, 19.0, 11.9, -2.5, -4.0; FTIR (neat

film), 1721 (m), 1684 (w), 1661 (w), 1510 (m), 1136 (w), 1040 (m), 937 (s), 735 (s) cm^{-1} ; HRMS–ESI (m/z): $[\text{M}+\text{H}]^+$ calcd for $\text{C}_{28}\text{H}_{37}\text{N}_2\text{O}_6\text{SSi}$, 557.2136; found, 557.2109.

FTIR (neat film), 1742 (m), 1721 (s), 1688 (m), 1607 (w), 1510 (m), 1167 (s), 936 (s) cm^{-1} ; HRMS–ESI (m/z): $[\text{M}+\text{H}]^+$ calcd for $\text{C}_{29}\text{H}_{36}\text{F}_3\text{N}_2\text{O}_7\text{Si}$, 609.2238; found, 609.2299.

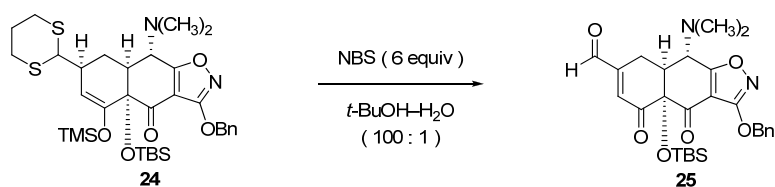


β -Trifluoroethyl ortho ester-substituted enone 23. *N*-Bromosuccinimide (100 mg, 0.564 mmol, 5.0 equiv) was added in one portion to a stirring solution of β -tris(methylthio)methyl trimethylsilyl enol ether **19** (80 mg, 0.113 mmol, 1 equiv) in 2,2,2-trifluoroethanol (3.0 mL) at 23 °C. The bright orange reaction solution was allowed to stir at 23 °C for 45 min, then was concentrated. The resulting yellow oil was dissolved in dichloromethane (20 mL) and the resulting solution was washed with saturated aqueous sodium bicarbonate solution (20 mL). The phases were separated and the aqueous phase was extracted with dichloromethane (20 mL). The organic extracts were combined and the combined solution was dried over anhydrous sodium sulfate. The dried solution was filtered and the filtrate was concentrated. The crude product was purified by flash-column chromatography (4% acetone-hexanes, grading to 6%), affording the β -trifluoroethyl ester-substituted AB enone **22** as a yellow solid (33 mg, 48%). Further purification by preparative HPLC on an Agilent Prep C18 column [10 μ m, 250 x 21.2 mm, UV detection at 250 nm, Solvent A: water, Solvent B: methanol, injection volume: 10.0 mL (8.5 mL water, 1.5 mL methanol), gradient elution with 85 \rightarrow 100% B over 40 min, flow rate: 15.0 mL/min, fractions eluting at 27-29 min collected and concentrated] provided the β -trifluoroethyl ortho ester-substituted enone **23** as a white solid (33 mg, 37%).

$R_f = 0.48$ (15% ethyl acetate-hexanes); ^1H NMR (500 MHz, CDCl_3) δ 7.50 (d, 2H, $J = 7.3$ Hz), 7.41-7.35 (m, 3H), 6.31 (d, 1H, $J = 2.3$ Hz), 5.37 (s, 2H), 4.04-3.97 (m, 6H), 3.61 (d, 1H, $J = 10.5$ Hz), 2.93 (d, 1H, $J = 17.4$ Hz), 2.87-2.82 (m, 2H), 2.46 (s, 6H), 0.84 (s, 9H), 0.25 (s, 3H), 0.11 (s, 3H); ^{13}C NMR (125 MHz, CDCl_3) δ 192.5, 186.4, 180.9, 167.4, 151.9, 134.9, 128.6, 128.6, 128.5, 126.8, 122.9 (q, $J = 277.4$ Hz), 112.0, 108.3, 82.3, 72.7, 61.3 (q, $J = 36.6$ Hz), 59.4, 47.4, 41.7, 25.9, 23.8, 18.9, -2.4, -3.7; FTIR (neat film), 1724 (m), 1688 (w), 1611 (w), 1514 (m), 1288 (s), 1175 (s) cm^{-1} ; HRMS–ESI (m/z): $[\text{M}+\text{H}]^+$ calcd for $\text{C}_{33}\text{H}_{40}\text{F}_9\text{N}_2\text{O}_8\text{Si}$, 791.2405; found, 791.2459.

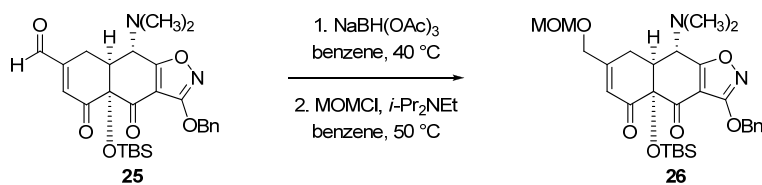


2.28-2.23 (m, 2H), 2.15-2.09 (m, 1H), 1.90-1.80 (m, 1H), 0.86 (s, 9H), 0.21 (s, 3H), 0.10 (s, 3H), -0.01 (s, 9H); ^{13}C NMR (125 MHz, CDCl_3) δ 189.4, 181.5, 167.3, 149.5, 135.1, 128.7, 128.5, 128.4, 108.5, 104.8, 81.0, 72.3, 61.3, 54.9, 46.1, 41.9, 37.1, 31.1, 30.8, 26.1, 25.7, 21.8, 18.9, -0.4, -2.7, -3.6; FTIR (neat film), cm^{-1} 2953 (w), 1721 (s), 1653 (w), 1614 (w), 1510 (s), 1472 (w), 1454 (w), 1254 (s), 1204 (w), 1150 (w), 1024 (w), 934 (s), 901 (s), 835 (s); HRMS-ESI (m/z): $[\text{M}+\text{H}]^+$ calcd for $\text{C}_{33}\text{H}_{51}\text{N}_2\text{O}_5\text{S}_2\text{Si}_2$, 675.2772; found, 675.2783.



β -Carbaldehyde AB enone **25.** *N*-Bromosuccinimide (158 mg, 0.889 mmol, 6.0 equiv) was added in one portion to a stirring solution of β -(1,3-dithian-2-yl) trimethylsilyl enol ether **24** (100 mg, 0.148 mmol, 1 equiv) in *tert*-butanol (4.0 mL) and water (40 μ L) at 23 $^{\circ}$ C. The reaction mixture was stirred at this temperature for 1 h, then was partitioned between dichloromethane (20 mL) and saturated aqueous sodium bicarbonate solution (20 mL). The phases were separated and the aqueous phase was extracted with dichloromethane (20 mL). The organic extracts were combined and the combined solution was dried over anhydrous sodium sulfate. The dried solution was filtered and the filtrate was concentrated. The crude product was purified by flash-column chromatography (12% ethyl acetate-hexanes), affording the β -carbaldehyde AB enone **25** as a yellow solid (68 mg, 90%).

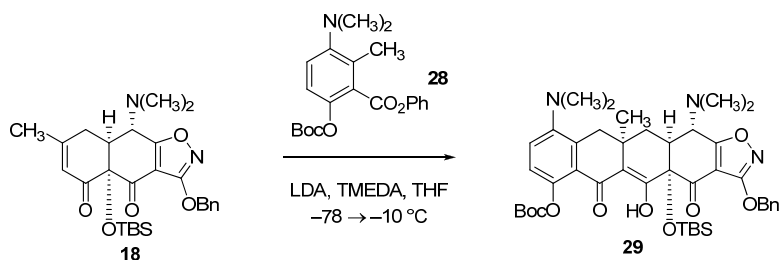
R_f = 0.18 (15% ethyl acetate-hexanes); ^1H NMR (500 MHz, CDCl_3) δ 9.82, (s, 1H), 7.50 (d, 2H, J = 6.9 Hz), 7.41-7.35 (m, 3H), 6.66 (d, 1H, J = 2.7 Hz), 5.36 (AB quartet, 2H), 3.58 (d, 1H, J = 11.0 Hz), 3.17 (d, 1H, J = 19.7 Hz), 2.90 (dd, 1H, J = 10.8, 4.8 Hz), 2.77-2.71 (m, 1H), 2.44 (s, 6H), 0.78 (s, 9H), 0.27 (s, 3H), 0.05 (s, 3H); ^{13}C NMR (125 MHz, CDCl_3) δ 194.6, 193.4, 186.5, 181.2, 167.4, 152.5, 137.2, 134.9, 128.6, 128.5, 128.5, 108.3, 83.2, 72.7, 59.4, 47.0, 41.8, 25.9, 21.5, 19.0, -2.5, -4.0; FTIR (neat film), 1721 (m), 1694 (m), 1607 (w), 1510 (m), 1173 (w), 1036 (m), 937 (s), 737 (s) cm^{-1} ; HRMS-ESI (m/z): $[\text{M}+\text{H}]^+$ calcd for $\text{C}_{27}\text{H}_{35}\text{N}_2\text{O}_6\text{Si}$, 511.2259; found, 511.2286.



β -Methoxymethoxymethyl AB enone 26. Sodium triacetoxyborohydride (205 mg, 0.918 mmol, 3.5 equiv) was added in one portion to a solution of the β -carbaldehyde AB enone **25** (134 mg, 0.262 mmol, 1 equiv) in benzene (2.0 mL) at 23 °C. The resulting solution was heated to 40 °C. After stirring at 40 °C for 5 ½ h, the reaction mixture was allowed to cool to 23 °C. The cooled solution was diluted with dichloromethane (30 mL), and the resulting solution was added slowly and carefully to saturated aqueous sodium bicarbonate solution (30 mL). The phases were separated and the aqueous phase was extracted with dichloromethane (30 mL). The organic extracts were combined and the combined solution was dried over anhydrous sodium sulfate. The dried solution was filtered and the filtrate was concentrated. *N,N*-Diisopropylethylamine (229 μ L, 1.31 mmol, 5.0 equiv) and chloromethyl methyl ether (59.8 μ L, 0.787 mmol, 3.0 equiv) were added sequentially to a solution of the crude reduction product in benzene (1.5 mL) at 23 °C. The reaction flask was sealed and the solution was heated to 50 °C. After stirring at 50 °C for 24 h, the reaction mixture was allowed to cool to 23 °C. The cooled solution was partitioned between dichloromethane (30 mL) and saturated aqueous sodium bicarbonate solution (30 mL). The layers were separated and the aqueous phase was extracted with dichloromethane (30 mL). The organic extracts were combined and the combined solution was dried over anhydrous sodium sulfate. The dried solution was filtered and the filtrate was concentrated, affording an orange oil. The product was purified by flash-column chromatography (15% ethyl acetate-hexanes, grading to 17%

ethyl acetate-hexanes), providing the β -methoxymethoxymethyl AB enone **26** as a pale yellow solid (124 mg, 85% yield, two steps).

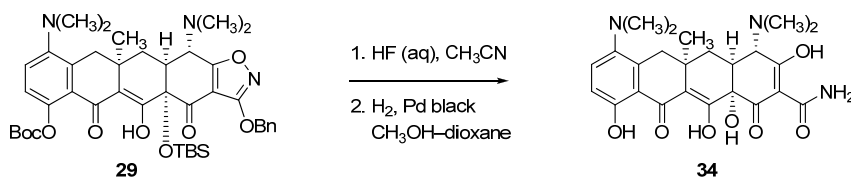
R_f = 0.40 (30% ethyl acetate-hexanes); ^1H NMR (500 MHz, CDCl_3) δ 7.50 (d, 2H, J = 7.0 Hz), 7.40-7.32 (m, 3H), 6.21 (s, 1H), 5.35 (AB quartet, 2H), 4.67 (AB quartet, 2H), 4.16 (m, 2H), 3.74 (d, 1H, J = 10.0 Hz), 3.38 (s, 3H), 2.80-2.74 (m, 3H), 2.45 (s, 6H), 0.82 (s, 9H), 0.26 (s, 3H), 0.05 (s, 3H); ^{13}C NMR (125 MHz, CDCl_3) δ 193.1, 187.7, 181.1, 167.5, 159.7, 135.0, 128.5, 128.5, 128.5, 122.4, 108.4, 96.0, 83.0, 72.6, 68.4, 59.6, 55.5, 47.5, 41.9, 25.9, 25.8, 19.0, -2.5, -4.1; FTIR (neat film), cm^{-1} 2951 (w), 2930 (w), 1719 (s), 1674 (m), 1510 (s), 1175 (m), 1152 (m), 1038 (s), 934 (s), 829 (s), 735 (s); HRMS-ESI (m/z): $[\text{M}+\text{H}]^+$ calcd for $\text{C}_{29}\text{H}_{41}\text{N}_2\text{O}_7\text{Si}$, 557.2678; found, 557.2690.



Michael–Claisen cyclization product 29. A freshly prepared solution of lithium diisopropylamide in tetrahydrofuran (1.0 M, 1.21 mL, 1.21 mmol, 3.0 equiv) was added dropwise via syringe to a solution of phenyl ester **28** (449 mg, 1.21 mmol, 3.0 equiv) and TMEDA (365 μ L, 2.42 mmol, 6.0 equiv) in tetrahydrofuran (15 mL) at -78 $^{\circ}$ C, forming a bright red solution. After stirring at -78 $^{\circ}$ C for 40 min, a solution of the β -methyl-substituted AB enone **18** (200 mg, 0.403 mmol, 1 equiv) in tetrahydrofuran (3.0 mL) was added to the reaction solution dropwise via syringe. The resulting mixture was allowed to warm slowly to -10 $^{\circ}$ C over 80 min, then was partitioned between aqueous potassium phosphate buffer solution (pH 7.0, 0.2 M, 60 mL) and dichloromethane (60 mL). The phases were separated and the aqueous phase was extracted with dichloromethane (2×40 mL). The organic extracts were combined and the combined solution was dried over anhydrous sodium sulfate. The dried solution was filtered and the filtrate was concentrated, affording an orange-yellow oil. The product was purified by flash-column chromatography (15% ethyl acetate-hexanes, grading to 20%), providing the Michael–Claisen cyclization product **29** as a yellow solid (249 mg, 80%).

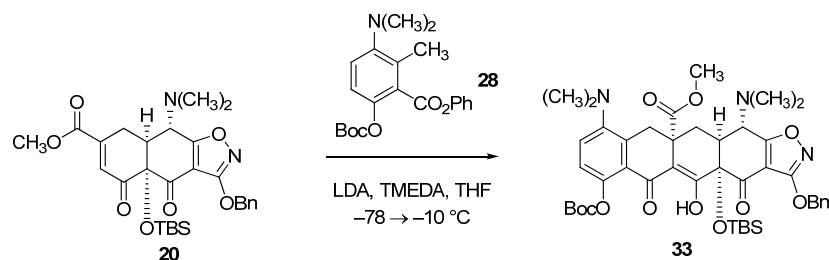
R_f = 0.28 (20% ethyl acetate-hexanes); ^1H NMR (600 MHz, CDCl_3) δ 15.96 (s, 1H), 7.49 (d, 2H, J = 7.8 Hz), 7.39–7.33 (m, 3H), 7.26–7.24 (m, 1H), 7.04 (d, 1H, J = 8.5 Hz), 5.36 (s, 2H), 4.16 (d, 1H, J = 10.0 Hz), 3.20 (d, 1H, J = 16.1 Hz), 2.75 (d, 1H, J = 16.1 Hz), 2.66 (s, 6H), 2.54–2.50 (m, 7H), 2.37 (d, 1H, J = 14.4 Hz), 2.16 (dd, 1H, J = 14.8, 4.5

Hz), 1.56 (s, 9H), 1.12 (s, 3H), 0.90 (s, 9H), 0.25 (s, 3H), 0.21 (s, 3H); ^{13}C NMR (125 MHz, CDCl_3) δ 186.8, 185.6, 181.7, 178.3, 167.6, 152.3, 150.4, 145.4, 136.4, 135.1, 128.5, 128.4, 128.3, 124.2, 123.9, 122.3, 112.0, 108.1, 83.8, 81.7, 72.4, 60.7, 47.0, 44.2, 41.9, 40.6, 32.4, 32.1, 29.8, 27.7, 26.4, 19.2, -1.9, -2.3; FTIR (neat film), 1759 (w), 1721 (m), 1613 (w), 1510 (m), 1456 (w), 1265 (m), 1152 (m), 737 (s) cm^{-1} ; HRMS-ESI (m/z): $[\text{M}+\text{H}]^+$ calcd for $\text{C}_{42}\text{H}_{55}\text{N}_3\text{O}_9\text{Si}$, 774.3780; found, 774.3796.



C5a-Methylminocycline (34). Concentrated aqueous hydrofluoric acid solution (48 wt%, 2.0 mL) was added to a solution of the Michael–Claisen cyclization product **14** (249 mg, 0.322 mmol, 1 equiv) in acetonitrile (3.0 mL) in a polypropylene reaction vessel at 23 °C. The reaction solution was stirred vigorously at 23 °C for 17 h, then was poured into water (100 mL) containing dipotassium hydrogenphosphate trihydrate (20.0 g). The resulting mixture was extracted with ethyl acetate (100 mL, then 2 x 50 mL). The organic extracts were combined and the combined solution was dried over anhydrous sodium sulfate. The dried solution was filtered and the filtrate was concentrated, affording an orange-brown solid. Methanol (3.0 mL) and dioxane (3.0 mL) were added to the crude product, forming an orange-brown solution. Palladium black (13.7 mg, 0.129 mmol, 0.4 equiv) was added in one portion at 23 °C. An atmosphere of hydrogen was introduced by briefly evacuating the flask, then flushing with pure hydrogen (1 atm). The reaction mixture was stirred at 23 °C for 1 h, then was filtered through a plug of Celite. The filtrate was concentrated, affording a brownish yellow solid. The product was purified by preparative HPLC on an Agilent Prep C18 column [10 µm, 250 x 21.2 mm, UV detection at 350 nm, Solvent A: 0.1% trifluoroacetic acid in water, Solvent B: acetonitrile, 2 batches, injection volume: 5.0 mL (4.0 mL 0.1% trifluoroacetic acid in water, 1.0 mL acetonitrile), gradient elution with 5→40% B over 50 min, flow rate: 7.5 mL/min]. Fractions eluting at 24-31 min were collected and concentrated, affording C5a-methylminocycline trifluoroacetate **17** as a yellow solid (188 mg, 100%, two steps).

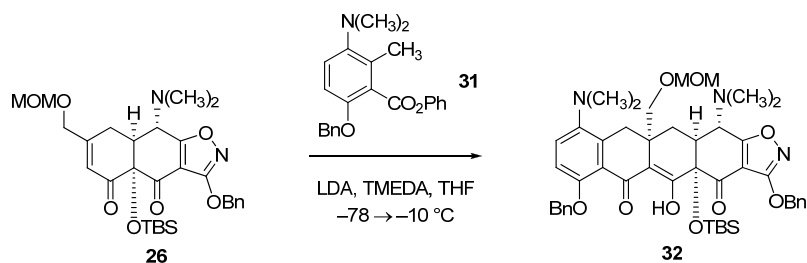
^1H NMR (600 MHz, CD_3OD , trifluoroacetate) δ 7.90 (d, 1H, $J = 9.4$ Hz), 7.07 (d, 1H, $J = 9.4$ Hz), 4.13 (d, 1H, $J = 1.0$ Hz), 3.25 (s, 6H), 3.17 (d, 1H, $J = 15.8$ Hz), 3.07-3.02 (m, 1H), 3.04 (s, 6H), 2.80 (d, 1H, $J = 15.7$ Hz), 2.05 (dd, 1H, $J = 13.8, 2.9$ Hz), 1.93 (dd, 1H, $J = 14.1, 13.9$ Hz), 1.26 (s, 3H); HRMS–ESI (m/z): $[\text{M}+\text{H}]^+$ calcd for $\text{C}_{24}\text{H}_{29}\text{N}_3\text{O}_7$, 472.2078; found, 472.2087.



Michael–Claisen cyclization product 33. A freshly prepared solution of lithium diisopropylamide in tetrahydrofuran (1.0 M, 0.416 mL, 0.416 mmol, 3.0 equiv) was added dropwise via syringe to a solution of phenyl ester **28** (155 mg, 0.416 mmol, 3.0 equiv) and TMEDA (126 μ L, 0.832 mmol, 6.0 equiv) in tetrahydrofuran (6 mL) at -78°C , forming a bright red solution. After stirring at -78°C for 40 min, a solution of the β -methyl ester-substituted AB enone **20** (75 mg, 0.139 mmol, 1 equiv) in tetrahydrofuran (1.5 mL) was added to the reaction solution dropwise via syringe. The resulting mixture was allowed to warm slowly to -10°C over 75 min, then was partitioned between aqueous potassium phosphate buffer solution (pH 7.0, 0.2 M, 25 mL) and dichloromethane (25 mL). The phases were separated and the aqueous phase was further extracted with dichloromethane (2×20 mL). The organic extracts were combined and the combined solution was dried over anhydrous sodium sulfate. The dried solution was filtered and the filtrate was concentrated, affording a yellow solid. The crude product was purified first by flash-column chromatography (15% acetone-hexanes), then by preparative HPLC on an Agilent Prep C18 column [10 μ m, 250 x 21.2 mm, UV detection at 350 nm, Solvent A: water, Solvent B: methanol, injection volume: 6.0 mL (5.0 mL methanol, 1.0 mL water), gradient elution with 85 \rightarrow 100% B over 40 min, flow rate: 15 mL/min]. Fractions eluting at 25–28 min were collected and concentrated, providing the Michael–Claisen cyclization product **33** as a yellow solid (26 mg, 23%).

$R_f = 0.34$ (25% ethyl acetate-hexanes); ^1H NMR (500 MHz, CDCl_3) δ 15.97 (s, 1H), 7.49 (d, 2H, $J = 7.3$ Hz), 7.39-7.33 (m, 3H), 7.24 (d, 1H, $J = 8.3$ Hz), 7.03 (d, 1H, $J = 8.3$ Hz), 5.37 (s, 2H), 4.11 (d, 1H, $J = 9.3$ Hz), 3.84 (d, 1H, $J = 16.1$ Hz), 3.36 (s, 3H), 2.80 (d, 1H, $J = 16.1$ Hz), 2.67-2.64 (m, 1H), 2.64 (s, 6H), 2.57-2.53 (m, 2H), 2.51 (s, 6H), 1.57 (s, 9H), 0.82 (s, 9H), 0.23 (s, 3H), 0.17 (s, 3H); ^{13}C NMR (125 MHz, CDCl_3) δ 187.6, 186.2, 181.5, 176.3, 175.2, 167.6, 152.4, 150.0, 145.4, 135.0, 134.2, 128.5, 128.5, 128.3, 124.6, 124.4, 123.1, 108.0, 106.8, 83.8, 80.9, 72.5, 60.6, 52.4, 46.6, 44.2, 44.1, 41.9, 38.2, 27.7, 26.2, 19.1, -2.1, -2.9; FTIR (neat film), 1761 (w), 1722 (m), 1512 (m), 1234 (s), 1150 (s), 833 (m), 733 (s) cm^{-1} ; HRMS-ESI (m/z): $[\text{M}+\text{H}]^+$ calcd for $\text{C}_{43}\text{H}_{56}\text{N}_3\text{O}_{11}\text{Si}$, 818.3679; found, 818.3760.

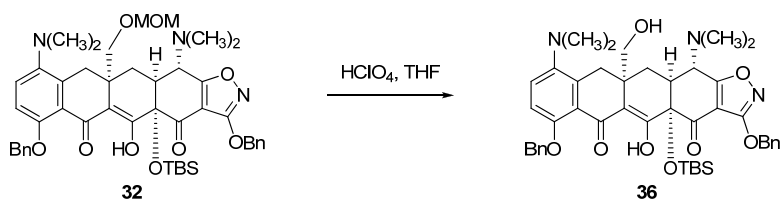
^1H NMR (600 MHz, CD_3OD) δ 7.81 (d, 1H, $J = 9.2$ Hz), 7.03 (d, 1H, $J = 9.2$ Hz), 4.14 (s, 1H), 3.66 (d, 1H, $J = 15.7$ Hz), 3.61 (s, 3H), 3.14 (s, 6H), 2.97 (s, 6H), 2.87-2.83 (m, 2H), 2.53 (dd, 1H, $J = 14.3, 2.6$ Hz), 2.04 (dd, 1H, $J = 14.2, 14.1$ Hz); HRMS-ESI (m/z): $[\text{M}+\text{H}]^+$ calcd for $\text{C}_{26}\text{H}_{30}\text{N}_3\text{O}_9$, 516.1977; found, 516.2011.



Michael–Claisen cyclization product 32. A freshly prepared solution of lithium diisopropylamide (1.0 M, 7.86 mL, 7.86 mmol, 3.6 equiv) was added dropwise via syringe to a solution of phenyl ester **31** (2.84 g, 7.86 mmol, 3.6 equiv) and TMEDA (2.27 mL, 15.1 mmol, 7.0 equiv) in tetrahydrofuran (60 mL) at $-78\text{ }^{\circ}\text{C}$, forming a bright red solution. After stirring at $-78\text{ }^{\circ}\text{C}$ for 40 min, a solution of the β -methoxymethoxymethyl AB enone **26** (1.20 g, 2.16 mmol, 1 equiv) in tetrahydrofuran (15 mL) was added to the reaction solution dropwise via syringe. The resulting mixture was allowed to warm slowly to $-10\text{ }^{\circ}\text{C}$ over 80 min, then was partitioned between aqueous potassium phosphate buffer solution (pH 7.0, 0.2 M, 100 mL) and dichloromethane (100 mL). The phases were separated and the aqueous phase was further extracted with dichloromethane (2 x 75 mL). The organic extracts were combined and the combined solution was dried over anhydrous sodium sulfate. The dried solution was filtered and the filtrate was concentrated, affording an orange-yellow oil. The product was purified by flash-column chromatography (3.5% ethyl acetate-dichloromethane), providing the Michael–Claisen cyclization product **32** as a yellow solid (1.29 g, 72%).

$R_f = 0.31$ (30% ethyl acetate-hexanes); $^1\text{H NMR}$ (500 MHz, CDCl_3) δ 16.77 (s, 1H), 7.51 (d, 4H, $J = 8.0\text{ Hz}$), 7.41–7.28 (m, 6H), 7.21 (d, 1H, $J = 9.0\text{ Hz}$), 6.90 (d, 1H, $J = 9.0\text{ Hz}$), 5.38 (s, 2H), 5.17 (AB quartet, 2H), 4.47 (d, 1H, $J = 6.5\text{ Hz}$), 4.34 (d, 1H, $J = 6.5\text{ Hz}$), 4.15 (d, 1H, $J = 9.5\text{ Hz}$), 3.78 (d, 1H, $J = 16.5\text{ Hz}$), 3.38 (d, 1H, $J = 9.0\text{ Hz}$), 3.27 (d, 1H,

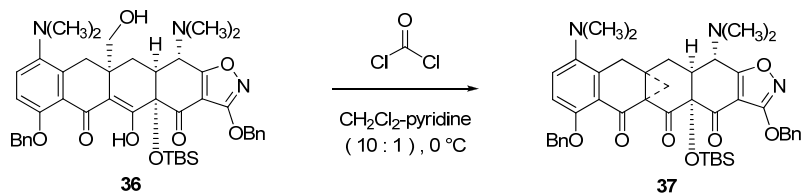
$J = 9.5$ Hz), 3.12 (s, 3H), 2.63 (s, 6H), 2.65-2.58 (m, 1H), 2.51 (s, 6H), 2.51-2.41 (m, 2H), 2.32 (dd, 1H, $J = 14.5, 2.0$ Hz), 0.93 (s, 9H), 0.29 (s, 3H), 0.20 (s, 3H); ^{13}C NMR (125 MHz, CDCl_3) δ 186.9, 184.6, 183.0, 181.6, 167.7, 154.7, 145.7, 136.8, 136.1, 135.1, 128.5, 128.4, 128.4, 128.3, 127.7, 127.0, 125.0, 120.7, 113.7, 108.1, 107.2, 96.1, 82.3, 72.9, 72.4, 71.4, 61.1, 54.6, 46.4, 44.4, 41.9, 35.8, 34.7, 28.4, 26.5, 19.3, -2.0, -2.1; FTIR (neat film), 2932 (w), 1721 (s), 1611 (w), 1510 (m), 1472 (m), 1452 (m), 1269 (w), 1148 (w), 1107 (w), 1040 (s), 1020 (s), 922 (w), 831 (s), 733 (s) cm^{-1} ; HRMS-ESI (m/z): $[\text{M}+\text{H}]^+$ calcd for $\text{C}_{46}\text{H}_{58}\text{N}_3\text{O}_9\text{Si}$, 824.3937; found, 824.3885.



Substituted neopentyl alcohol 36. Perchloric acid⁷⁶ (13.0 mL, 70% solution) was added dropwise over 5 min to a solution of the Michael–Claisen cyclization product **32** (1.04 g, 1.26 mmol, 1 equiv) in tetrahydrofuran (130 mL) at 23 °C. After stirring at this temperature for 10 min, the reaction solution was slowly and carefully poured into ice-cold saturated aqueous sodium bicarbonate solution (300 mL). The resulting mixture was extracted with dichloromethane (2 x 250 mL, then 50 mL). The organic extracts were combined and the combined solution was dried over anhydrous sodium sulfate. The dried solution was filtered and the filtrate was concentrated, providing an orange-yellow oil. The product was purified by flash-column chromatography (55% ethyl acetate-hexanes, grading to 75% ethyl acetate-hexanes), affording the substituted neopentyl alcohol **36** as a yellow solid (720 mg, 73%).

R_f = 0.26 (65% ethyl acetate-hexanes); ^1H NMR (500 MHz, CDCl_3) δ 16.76 (s, 1H), 7.53-7.49 (m, 4H), 7.41-7.28 (m, 6H), 7.22 (d, 1H, J = 9.0 Hz), 6.90 (d, 1H, J = 9.0 Hz), 5.38 (s, 2H), 5.17 (AB quartet, 2H), 4.11 (d, 1H, J = 9.5 Hz), 3.66 (d, 1H, J = 16.0 Hz), 3.48 (d, 1H, J = 11.0 Hz), 3.32 (d, 1H, J = 11.0 Hz), 2.64 (s, 6H), 2.68-2.59 (m, 1H), 2.56-2.48 (m, 1H), 2.51 (s, 6H), 2.38 (dd, 1H, J = 14.5, 4.5 Hz), 2.23 (brd, 1H, J = 14.0 Hz), 0.92 (s, 9H), 0.25 (s, 3H), 0.18 (s, 3H); ^{13}C NMR (125 MHz, CDCl_3) δ 186.7, 184.7, 182.7, 181.4, 167.7, 154.9, 145.7, 136.8, 135.9, 135.1, 128.5, 128.5, 128.5, 128.3, 127.8, 126.9, 125.3, 120.7, 113.7, 108.2, 107.3, 82.3, 72.4, 71.4, 68.2, 61.3, 46.2, 44.7, 42.0, 36.8, 34.5, 28.2, 26.5, 19.3, -1.8, -2.0; FTIR (neat film), 2938 (w), 1719 (m), 1609 (w),

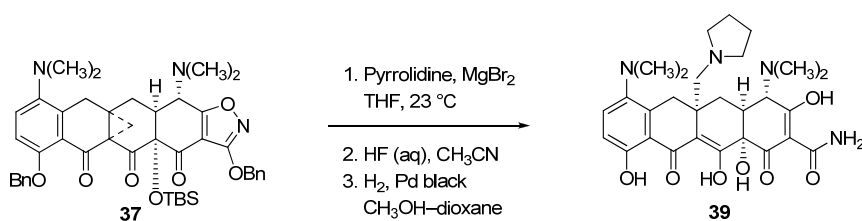
1510 (s), 1452 (s), 1265 (m), 1020 (m), 829 (s), 733 (s) cm^{-1} ; HRMS-ESI (m/z): $[\text{M}+\text{H}]^+$
calcd for $\text{C}_{44}\text{H}_{54}\text{N}_3\text{O}_8\text{Si}$, 780.3675; found, 780.3654.



C5a–C11a-Bridged cyclopropane tetracycline precursor 37. 4Å molecular sieves (2.4 g, small chunks) were added to a solution of the substituted neopentyl alcohol **36** (720 mg, 0.923 mmol, 1 equiv) in dichloromethane (72 mL) and pyridine (7.2 mL) at 23 °C. The resulting mixture was stirred at 23 °C for 1 h, then was cooled to 0 °C. A solution of phosgene in toluene (20 wt%, 537 µL, 1.02 mmol, 1.1 equiv) was added dropwise to the cooled mixture. The resulting solution was stirred at 0 °C for 1 h, whereupon aqueous potassium phosphate buffer solution (pH 7.0, 0.2 M, 20 mL) was added. The resulting mixture was allowed to warm to 23 °C, then was filtered to remove the molecular sieves. Dichloromethane (60 mL) and aqueous potassium phosphate buffer solution (pH 7.0, 0.2M, 60 mL) were added and the phases were separated. The aqueous phase was further extracted with dichloromethane (2 x 60 mL). The organic extracts were combined and the combined solution was dried over anhydrous sodium sulfate. The dried solution was filtered and the filtrate was concentrated, providing an orange-yellow oil. The product was purified by flash-column chromatography (20% ethyl acetate-hexanes, grading to 30% ethyl acetate-hexanes), affording the C5a–C11a-bridged cyclopropane tetracycline precursor **37** as a white solid (572 mg, 81%).

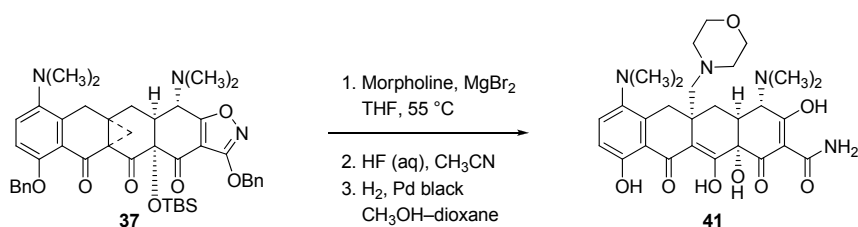
R_f = 0.25 (30% ethyl acetate-hexanes); ^1H NMR (500 MHz, CDCl_3) δ 7.52 (d, 2H, J = 7.3 Hz), 7.44-7.24 (m, 8H), 7.13 (d, 1H, J = 9.0 Hz), 6.86 (d, 1H, J = 9.0 Hz), 5.35 (s, 2H), 5.05 (AB quartet, 2H), 4.01 (d, 1H, J = 10.5 Hz), 3.85 (d, 1H, J = 17.4 Hz), 2.77 (d, 1H, J = 17.4 Hz), 2.68-2.57 (m, 3H), 2.62 (s, 6H), 2.49 (s, 6H), 2.25 (d, 1H, J = 5.0 Hz),

1.71 (d, 1H, $J = 5.0$ Hz), 0.89 (s, 9H), 0.28, (s, 3H), 0.12 (s, 3H); ^{13}C NMR (125 MHz, CDCl_3) δ 194.4, 191.8, 185.3, 180.9, 167.6, 152.6, 144.8, 136.7, 135.0, 132.2, 128.6, 128.5, 128.5, 128.4, 127.6, 127.1, 123.3, 123.2, 113.5, 107.9, 84.0, 72.6, 71.2, 58.8, 49.0, 44.8, 43.1, 41.8, 32.1, 31.1, 30.9, 26.6, 26.3, 19.5, -2.0 , -2.6 ; FTIR (neat film), 2938 (w), 1728 (s), 1711 (m), 1670 (w), 1510 (m), 1474 (m), 1452 (m), 1362 (w), 1258 (m), 916 (m), 827 (s), 733 (s) cm^{-1} ; HRMS–ESI (m/z): $[\text{M}+\text{H}]^+$ calcd for $\text{C}_{44}\text{H}_{52}\text{N}_3\text{O}_7\text{Si}$, 762.3569; found, 762.3569.



concentrated. The product was purified by preparative HPLC on an Agilent Prep C18 column [10 μ m, 250 x 21.2 mm, UV detection at 350 nm, Solvent A: 0.1% trifluoroacetic acid in water, Solvent B: acetonitrile, injection volume: 5.0 mL (4.0 mL 0.1% trifluoroacetic acid in water, 1.0 mL acetonitrile), gradient elution with 5 \rightarrow 35% B over 50 min, flow rate: 7.5 mL/min]. Fractions eluting at 39-43 min were collected and concentrated, affording C5a-pyrrolidinomethylminocycline bistrifluoroacetate **39** as a yellow solid (12.5 mg, 74%, three steps).

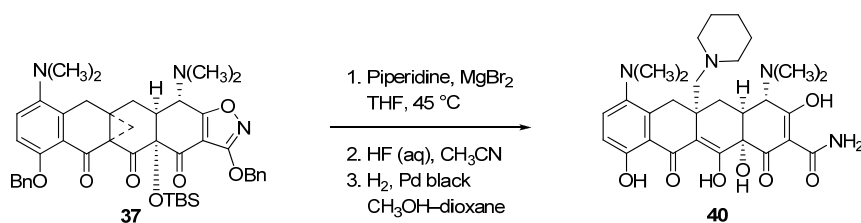
^1H NMR (600 MHz, CD_3OD , bistrifluoroacetate) δ 7.55 (d, 1H, J = 9.0 Hz), 6.95 (d, 1H, J = 9.0 Hz), 4.05 (s, 1H), 3.84 (brs, 1H), 3.75-3.71 (brs, 1H), 3.73 (d, 1H, J = 14.4 Hz), 3.62 (d, 1H, J = 16.8 Hz), 3.20 (d, 1H, J = 13.2 Hz), 3.14 (d, 1H, J = 15.0 Hz), 3.13-3.03 (brs, 1H), 3.10 (s, 6H), 2.70 (s, 6H), 2.67 (d, 1H, J = 16.8 Hz), 2.59 (dd, 1H, J = 15.0, 3.0 Hz), 2.50 (brs, 1H), 2.02-1.90 (m, 5H); HRMS–ESI (m/z): $[\text{M}+\text{H}]^+$ calcd for $\text{C}_{28}\text{H}_{37}\text{N}_4\text{O}_7$, 541.2657; found, 541.2684.



C5a-Morpholinomethyliminocycline (41). Anhydrous magnesium bromide (6.3 mg, 0.034 mmol, 2.0 equiv) was added to a solution of the C5a-C11a-bridged cyclopropane **37** (13.0 mg, 0.017 mmol, 1 equiv) and morpholine (15 μ L, 0.17 mmol, 10 equiv) in tetrahydrofuran (0.5 mL) at 23 $^{\circ}$ C. The reaction flask was sealed and the reaction mixture was heated to 55 $^{\circ}$ C. After stirring at 55 $^{\circ}$ C for 14 h, the reaction mixture was allowed to cool to 23 $^{\circ}$ C. The cooled mixture was partitioned between dichloromethane and saturated aqueous sodium bicarbonate solution (10 mL each). The phases were separated and the aqueous phase was further extracted with dichloromethane (10 mL). The organic extracts were combined and the combined solution was dried over anhydrous sodium sulfate. The dried solution was filtered and the filtrate was concentrated. The crude ring-opened product was dissolved in acetonitrile (1.2 mL). The resulting solution was transferred to a polypropylene reaction vessel and concentrated aqueous hydrofluoric acid solution (48 wt%, 0.8 mL) was added. The reaction mixture was stirred vigorously at 23 $^{\circ}$ C for 16 $\frac{1}{2}$ h, then was poured into water (30 mL) containing dipotassium hydrogenphosphate (8.0 g). The resulting mixture was extracted with ethyl acetate (3 x 40 mL). The organic extracts were combined and the combined solution was dried over anhydrous sodium sulfate. The dried solution was filtered and the filtrate was concentrated. Palladium black (5.0 mg, 0.047 mmol, 2.8 equiv) was added in one portion to a solution of the crude product in methanol (1.0 mL) and dioxane (1.0 mL) at 23 $^{\circ}$ C. An atmosphere of hydrogen was introduced by briefly evacuating the flask, then flushing

with pure hydrogen (1 atm). The reaction mixture was stirred at 23 °C for 1 ¾ h, then was filtered through a plug of Celite. The filtrate was concentrated. The product was purified by preparative HPLC on an Agilent Prep C18 column [10 µm, 250 x 21.2 mm, UV detection at 350 nm, Solvent A: 0.1% trifluoroacetic acid in water, Solvent B: acetonitrile, injection volume: 5.0 mL (4.0 mL 0.1% trifluoroacetic acid in water, 1.0 mL acetonitrile), gradient elution with 5→25% B over 50 min, then 25→100% B over 20 min, flow rate: 7.5 mL/min]. Fractions eluting at 49-52 min were collected and concentrated, affording C5a-morpholinomethylminocycline bistrifluoroacetate **41** as an orange-yellow solid (7.5 mg, 56%, three steps).

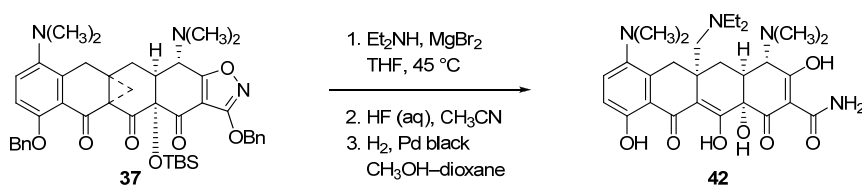
¹H NMR (600 MHz, CD₃OD, bistrifluoroacetate) δ 7.56 (d, 1H, *J* = 9.0 Hz), 6.95 (d, 1H, *J* = 9.0 Hz), 4.04 (s, 1H), 3.77-3.69 (m, 4H), 3.53 (d, 1H, *J* = 16.8 Hz), 3.24 (d, 1H, *J* = 13.2 Hz), 3.18-3.14 (m, 1H), 3.08 (s, 6H), 2.99-2.94 (m, 2H), 2.88 (d, 1H, *J* = 15.0 Hz), 2.81-2.72 (m, 2H), 2.74 (s, 6H), 2.62 (d, 1H, *J* = 16.8 Hz), 2.53 (brd, 1H, *J* = 14.4 Hz), 1.92 (dd, 1H, *J* = 14.2, 14.0 Hz); HRMS–ESI (*m/z*): [M+H]⁺ calcd for C₂₈H₃₇N₄O₈, 557.2606; found, 557.2611.



C5a-Piperidinylmethylminocycline (40). Anhydrous magnesium bromide (8.2 mg, 0.045 mmol, 2.0 equiv) was added to a solution of the C5a–C11a-bridged cyclopropane **37** (17.0 mg, 0.022 mmol, 1 equiv) and piperidine (22 μ L, 0.223 mmol, 10 equiv) in tetrahydrofuran (0.5 mL) at 23 °C. The reaction mixture was stirred at 23 °C for 21 h, then was heated to 45 °C. After stirring at this temperature for 14 h, the reaction mixture was allowed to cool to 23 °C. The cooled mixture was partitioned between dichloromethane (15 mL) and saturated aqueous sodium bicarbonate solution (10 mL). The phases were separated and the aqueous phase was extracted with dichloromethane (10 mL). The organic extracts were combined and the combined solution was dried over anhydrous sodium sulfate. The dried solution was filtered and the filtrate was concentrated. The crude ring-opened product was dissolved in acetonitrile (1.2 mL). The resulting solution was transferred to a polypropylene reaction vessel and concentrated aqueous hydrofluoric acid solution (48 wt%, 0.8 mL) was added. The reaction mixture was stirred vigorously at 23 °C for 13 h, then was poured into water (30 mL) containing dipotassium hydrogenphosphate (8.0 g). The resulting mixture was extracted with ethyl acetate (3 x 40 mL). The organic extracts were combined and the combined solution was dried over anhydrous sodium sulfate. The dried solution was filtered and the filtrate was concentrated. Palladium black (5.0 mg, 0.047 mmol, 2.8 equiv) was added in one portion to a solution of the crude product in methanol (1.0 mL) and dioxane (1.0 mL) at 23 °C. An atmosphere of hydrogen was introduced by briefly evacuating the flask, then flushing

with pure hydrogen (1 atm). The reaction mixture was stirred at 23 °C for 1 ½ h, then was filtered through a plug of Celite. The filtrate was concentrated. The product was purified by preparative HPLC on an Agilent Prep C18 column [10 µm, 250 x 21.2 mm, UV detection at 350 nm, Solvent A: 0.1% trifluoroacetic acid in water, Solvent B: acetonitrile, injection volume: 5.0 mL (4.0 mL 0.1% trifluoroacetic acid in water, 1.0 mL acetonitrile), gradient elution with 5→35% B over 50 min, flow rate: 7.5 mL/min]. Fractions eluting at 40-44 min were collected and concentrated, affording C5a-piperidinylmethyliminocycline bistrifluoroacetate **40** as a yellow solid (12.0 mg, 70%, three steps).

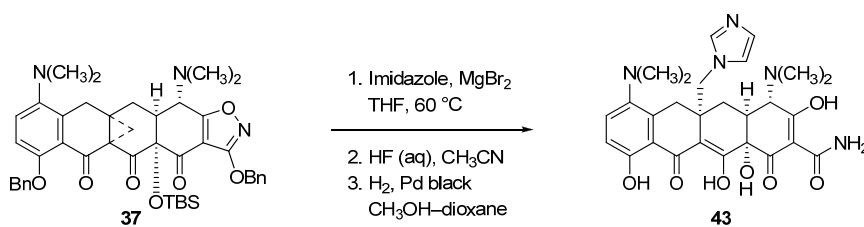
¹H NMR (600 MHz, CD₃OD, bistrifluoroacetate) δ 7.56 (d, 1H, *J* = 9.0 Hz), 6.96 (d, 1H, *J* = 9.0 Hz), 4.10 (d, 1H, *J* = 2.4 Hz), 3.66 (d, 1H, *J* = 16.8 Hz), 3.46 (d, 1H, *J* = 14.4 Hz), 3.40-3.35 (brm, 1H), 3.27-3.23 (m, 1H), 3.23-3.18 (m, 1H), 3.10 (s, 6H), 3.10-3.00 (m, 2H), 2.71 (s, 6H), 2.71-2.62 (m, 2H), 2.59 (dd, 1H, *J* = 15.0, 3.0 Hz), 2.02 (dd, 1H, *J* = 15.1, 12.7 Hz), 1.95-1.88 (brm, 1H), 1.85-1.78 (brm, 2H), 1.72-1.61 (brm, 2H), 1.43-1.36 (brm, 1H); HRMS–ESI (*m/z*): [M+H]⁺ calcd for C₂₉H₃₉N₄O₇, 555.2813; found, 555.2788.



C5a-Diethylaminomethylminocycline (42). Anhydrous magnesium bromide (7.2 mg, 0.039 mmol, 2.0 equiv) was added to a solution of the C5a-C11a-bridged cyclopropane **37** (15.0 mg, 0.020 mmol, 1 equiv) and diethylamine (102 μL , 0.987 mmol, 50 equiv) in tetrahydrofuran (0.5 mL) at $23\text{ }^\circ\text{C}$. The reaction flask was sealed and the reaction mixture was heated to $45\text{ }^\circ\text{C}$. After stirring at this temperature for 20 h, the reaction mixture was allowed to cool to room temperature. The reaction flask was opened briefly and a second portion of diethylamine (204 μL , 1.97 mmol, 100 equiv) was added. The flask was resealed and the reaction mixture was heated to $45\text{ }^\circ\text{C}$. After stirring at this temperature for a further 55 h, the reaction mixture was allowed to cool to $23\text{ }^\circ\text{C}$. The cooled mixture was partitioned between dichloromethane and saturated aqueous sodium bicarbonate solution (10 mL each). The phases were separated and the aqueous phase was extracted with dichloromethane (10 mL). The organic extracts were combined and the combined solution was dried over anhydrous sodium sulfate. The dried solution was filtered and the filtrate was concentrated. The crude ring-opened product was dissolved in acetonitrile (1.2 mL). The resulting solution was transferred to a polypropylene reaction vessel and concentrated aqueous hydrofluoric acid solution (48 wt%, 0.8 mL) was added. The reaction mixture was stirred vigorously at $23\text{ }^\circ\text{C}$ for $10\frac{1}{2}$ h, then was poured into water (30 mL) containing dipotassium hydrogenphosphate (8.0 g). The resulting mixture was extracted with ethyl acetate (3 x 40 mL). The organic extracts were combined and the combined solution was dried over anhydrous sodium sulfate. The dried solution was

filtered and the filtrate was concentrated. Palladium black (5.0 mg, 0.047 mmol, 2.8 equiv) was added in one portion to a solution of the crude product in methanol (1.0 mL) and dioxane (1.0 mL) at 23 °C. An atmosphere of hydrogen was introduced by briefly evacuating the flask, then flushing with pure hydrogen (1 atm). The reaction mixture was stirred at 23 °C for 1 ¾ h, then was filtered through a plug of Celite. The filtrate was concentrated. The product was purified by preparative HPLC on an Agilent Prep C18 column [10 µm, 250 x 21.2 mm, UV detection at 350 nm, Solvent A: 0.1% trifluoroacetic acid in water, Solvent B: acetonitrile, injection volume: 5.0 mL (4.0 mL 0.1% trifluoroacetic acid in water, 1.0 mL acetonitrile), gradient elution with 5→40% B over 50 min, flow rate: 7.5 mL/min]. Fractions eluting at 36-39 min were collected and concentrated, affording C5a-diethylaminomethylminocycline bistrifluoroacetate **42** as a yellow solid (12.0 mg, 79%, three steps).

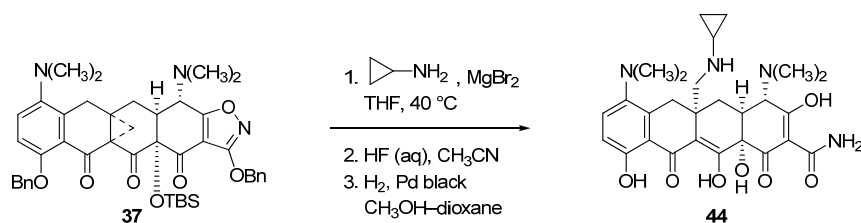
¹H NMR (600 MHz, CD₃OD, bistrifluoroacetate) δ 7.54 (d, 1H, *J* = 9.0 Hz), 6.95 (d, 1H, *J* = 9.0 Hz), 4.10 (d, 1H, *J* = 3.0 Hz), 3.61 (d, 1H, *J* = 16.8 Hz), 3.42 (d, 1H, *J* = 15.0 Hz), 3.25-3.20 (m, 2H), 3.16-3.02 (brm, 3H), 3.10 (s, 6H), 2.93 (brs, 1H), 2.73-2.69 (m, 1H), 2.70 (s, 6H), 2.52 (dd, 1H, *J* = 15.0, 3.0 Hz), 2.07 (dd, 1H, *J* = 14.1, 13.3 Hz), 1.28 (brs, 3H), 1.04 (brs, 3H); HRMS–ESI (*m/z*): [M+H]⁺ calcd for C₂₈H₃₉N₄O₇, 543.2813; found, 543.2821.



C5a-*N*-Imidazolymethyliminocycline (43). Anhydrous magnesium bromide (7.2 mg, 0.039 mmol, 3.0 equiv) was added to a solution of the C5a-C11a-bridged cyclopropane **37** (10.0 mg, 0.013 mmol, 1 equiv) and imidazole (6.2 mg, 0.091 mmol, 7.0 equiv) in tetrahydrofuran (0.5 mL) at 23 °C. The reaction flask was sealed and the reaction mixture was heated to 60 °C. After stirring at this temperature for 60 h, the reaction mixture was allowed to cool to 23 °C. The cooled mixture was partitioned between dichloromethane and saturated aqueous sodium bicarbonate solution (15 mL each). The phases were separated and the aqueous phase was extracted with dichloromethane (15 mL). The organic extracts were combined and the combined solution was dried over anhydrous sodium sulfate. The dried solution was filtered and the filtrate was concentrated. The crude ring-opened product was dissolved in acetonitrile (1.2 mL). The resulting solution was transferred to a polypropylene reaction vessel and concentrated aqueous hydrofluoric acid solution (48 wt%, 0.8 mL) was added. The reaction mixture was stirred vigorously at 23 °C for 18 h, then was poured into water (30 mL) containing dipotassium hydrogenphosphate (8.0 g). The resulting mixture was extracted with ethyl acetate (3 x 40 mL). The organic extracts were combined and the combined solution was dried over anhydrous sodium sulfate. The dried solution was filtered and the filtrate was concentrated. Palladium black (5.0 mg, 0.047 mmol, 3.6 equiv) was added in one portion to a solution of the crude product in methanol (1.0 mL) and dioxane (1.0 mL) at 23 °C. An atmosphere of hydrogen was introduced by briefly evacuating the flask, then flushing

with pure hydrogen (1 atm). The reaction mixture was stirred at 23 °C for 1 ¼ h, then was filtered through a plug of Celite. The filtrate was concentrated. The product was purified by preparative HPLC on an Agilent Prep C18 column [10 µm, 250 x 21.2 mm, UV detection at 350 nm, Solvent A: 0.1% trifluoroacetic acid in water, Solvent B: acetonitrile, injection volume: 5.0 mL (4.0 mL 0.1% trifluoroacetic acid in water, 1.0 mL acetonitrile), gradient elution with 5→40% B over 50 min, flow rate: 7.5 mL/min]. Fractions eluting at 25-27 min were collected and concentrated, affording C5a-imidazolylmethylminocycline bistrifluoroacetate **43** as a yellow solid (7.3 mg, 73%, three steps).

¹H NMR (600 MHz, CD₃OD, bistrifluoroacetate) δ 8.42 (t, 1H, *J* = 1.3 Hz), 7.51 (d, 1H, *J* = 9.0 Hz), 7.40 (dd, 1H, *J* = 1.8, 1.5 Hz), 7.23 (dd, 1H, *J* = 1.8, 1.6 Hz), 6.86 (d, 1H, *J* = 9.0 Hz), 4.48 (AB quartet, 2H), 4.13 (s, 1H), 3.42 (d, 1H, *J* = 16.8 Hz), 3.25 (dd, 1H, *J* = 13.8, 1.2 Hz), 3.11 (s, 6H), 2.73 (s, 6H), 2.69 (d, 1H, *J* = 16.2 Hz), 2.14 (dd, 1H, *J* = 15.0, 3.0 Hz), 1.98 (dd, 1H, *J* = 14.5, 14.2 Hz); HRMS–ESI (*m/z*): [M+H]⁺ calcd for C₂₇H₃₂N₅O₇, 538.2296; found, 538.2285.



C5a-Cyclopropylaminomethylminocycline (44). Anhydrous magnesium bromide (8.2 mg, 0.045 mmol, 2.0 equiv) was added to a solution of the C5a-C11a-bridged cyclopropane **37** (17.0 mg, 0.022 mmol, 1 equiv) and cyclopropylamine (15 μ L, 0.223 mmol, 10 equiv) in tetrahydrofuran (0.5 mL) at 23 $^{\circ}$ C. The reaction mixture was stirred at 23 $^{\circ}$ C for 16 h, then was heated to 40 $^{\circ}$ C. After stirring at this temperature for 22 h, the reaction mixture was allowed to cool to room temperature. The reaction flask was opened briefly and a second portion of cyclopropylamine (15 μ L, 0.223 mmol, 10 equiv) was added. The flask was sealed and the reaction mixture was heated to 40 $^{\circ}$ C. After stirring at this temperature for a further 13 h, the reaction mixture was allowed to cool to 23 $^{\circ}$ C. The cooled mixture was partitioned between dichloromethane (15 mL) and saturated aqueous sodium bicarbonate solution (10 mL). The phases were separated and the aqueous phase was extracted with dichloromethane (10 mL). The organic extracts were combined and the combined solution was dried over anhydrous sodium sulfate. The dried solution was filtered and the filtrate was concentrated. The crude ring-opened product was dissolved in acetonitrile (1.2 mL). The resulting solution was transferred to a polypropylene reaction vessel and concentrated aqueous hydrofluoric acid solution (48 wt%, 0.8 mL) was added. The reaction mixture was stirred vigorously at 23 $^{\circ}$ C for 12 h, then was poured into water (30 mL) containing dipotassium hydrogenphosphate (8.0 g). The resulting mixture was extracted with ethyl acetate (3 x 40 mL). The organic extracts were combined and the combined solution was dried over anhydrous sodium sulfate. The

dried solution was filtered and the filtrate was concentrated. Palladium black (5.0 mg, 0.047 mmol, 2.8 equiv) was added in one portion to a solution of the crude product in methanol (1.0 mL) and dioxane (1.0 mL) at 23 °C. An atmosphere of hydrogen was introduced by briefly evacuating the flask, then flushing with pure hydrogen (1 atm). The reaction mixture was stirred at 23 °C for 3 ½ h, then was filtered through a plug of Celite. The filtrate was concentrated. The product was purified by preparative HPLC on an Agilent Prep C18 column [10 µm, 250 x 21.2 mm, UV detection at 350 nm, Solvent A: 0.1% trifluoroacetic acid in water, Solvent B: acetonitrile, injection volume: 5.0 mL (4.0 mL 0.1% trifluoroacetic acid in water, 1.0 mL acetonitrile), gradient elution with 5→35% B over 50 min, flow rate: 7.5 mL/min]. Fractions eluting at 35-36 min were collected and concentrated, affording C5a-cyclopropylaminomethylminocycline bistrifluoroacetate **44** as a yellow solid (3.0 mg, 18%, three steps).

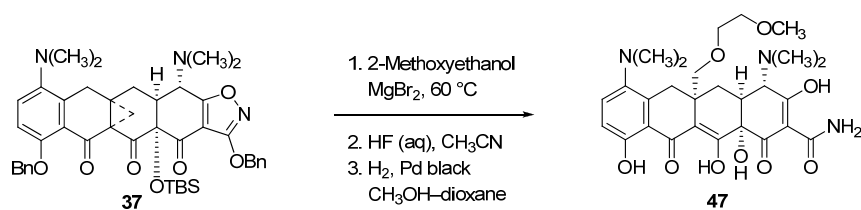
¹H NMR (600 MHz, CD₃OD, bistrifluoroacetate) δ 7.58 (d, 1H, *J* = 9.0 Hz), 6.96 (d, 1H, *J* = 9.0 Hz), 4.00 (d, 1H, *J* = 2.4 Hz), 3.60 (d, 1H, *J* = 14.4 Hz), 3.55 (d, 1H, *J* = 16.8 Hz), 3.19-3.10 (m, 1H), 3.13 (s, 6H), 3.03 (d, 1H, *J* = 14.4 Hz), 2.76 (s, 6H), 2.76-2.70 (m, 1H), 2.62-2.58 (m, 1H), 2.25 (dd, 1H, *J* = 14.8, 2.8 Hz), 1.98 (dd, 1H, *J* = 14.2, 13.8 Hz), 0.89-0.82 (m, 1H), 0.77-0.69 (m, 3H); HRMS–ESI (*m/z*): [M+H]⁺ calcd for C₂₇H₃₅N₄O₇, 527.2500; found, 527.2502.

mixture was stirred at 23 °C for 2 ½ h, then was filtered through a plug of Celite. The filtrate was concentrated. The product was purified by preparative HPLC on an Agilent Prep C18 column [10 µm, 250 x 21.2 mm, UV detection at 350 nm, Solvent A: 0.1% trifluoroacetic acid in water, Solvent B: acetonitrile, injection volume: 7.0 mL (6.0 mL 0.1% trifluoroacetic acid in water, 1.0 mL acetonitrile), gradient elution with 5→40% B over 50 min, flow rate: 7.5 mL/min]. Fractions eluting at 29-33 min were collected and concentrated, affording C5a-methoxymethylminocycline trifluoroacetate **45** as a yellow solid (7.1 mg, 58%, three steps).

¹H NMR (600 MHz, CD₃OD, hydrochloride) δ 7.82 (d, 1H, *J* = 9.4 Hz), 7.05 (d, 1H, *J* = 9.2 Hz), 4.15 (s, 1H), 3.49 (d, 1H, *J* = 10.3 Hz), 3.36 (d, 1H, *J* = 15.6 Hz), 3.25 (s, 3H), 3.14 (s, 6H), 3.12 (d, 1H, *J* = 10.3 Hz), 3.08-3.04 (m, 1H), 2.99 (s, 6H), 2.56 (d, 1H, *J* = 15.6 Hz), 2.41 (dd, 1H, *J* = 14.1, 2.9 Hz), 1.69 (dd, 1H, *J* = 14.1, 13.9 Hz); HRMS–ESI (*m/z*): [M+H]⁺ calcd for C₂₅H₃₂N₃O₈, 502.2184; found, 502.2186.

filtered through a plug of Celite. The filtrate was concentrated. The product was purified by preparative HPLC on an Agilent Prep C18 column [10 μ m, 250 x 21.2 mm, UV detection at 350 nm, Solvent A: 0.1% trifluoroacetic acid in water, Solvent B: acetonitrile, injection volume: 5.0 mL (4.0 mL 0.1% trifluoroacetic acid in water, 1.0 mL acetonitrile), gradient elution with 5 \rightarrow 40% B over 50 min, flow rate: 7.5 mL/min]. Fractions eluting at 41-44 min were collected and concentrated, affording C5a-*n*-butoxymethylminocycline trifluoroacetate **46** as a yellow solid (7.3 mg, 56%, three steps).

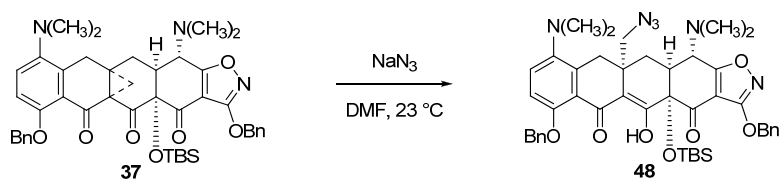
^1H NMR (600 MHz, CD_3OD , trifluoroacetate) δ 7.81 (d, 1H, J = 9.0 Hz), 7.04 (d, 1H, J = 9.6 Hz), 4.16 (s, 1H), 3.50 (d, 1H, J = 10.2 Hz), 3.38-3.30 (m, 3H), 3.21 (d, 1H, J = 9.6 Hz), 3.13 (s, 6H), 3.11-3.06 (m, 1H), 2.98 (s, 6H), 2.58 (d, 1H, J = 15.6 Hz), 2.42 (dd, 1H, J = 13.8, 3.0 Hz), 1.71 (dd, 1H, J = 13.9, 13.8 Hz), 1.50-1.39 (m, 2H), 1.34-1.24 (m, 2H), 0.87 (t, 3H, J = 7.2 Hz); HRMS–ESI (m/z): $[\text{M}+\text{H}]^+$ calcd for $\text{C}_{28}\text{H}_{38}\text{N}_3\text{O}_8$, 544.2653; found, 544.2655.



C5a-Methoxyethoxymethylminocycline (47). Anhydrous magnesium bromide (6.2 mg, 0.034 mmol, 2.0 equiv) was added to a solution of the C5a-C11a-bridged cyclopropane **37** (13.0 mg, 0.017 mmol, 1 equiv) in 2-methoxyethanol (0.5 mL) at 23 °C. The resulting mixture was heated to 60 °C. After stirring at 60 °C for 26 h, the reaction mixture was allowed to cool to 23 °C. The cooled mixture was partitioned between aqueous potassium phosphate buffer solution (pH 7.0, 0.2 M, 10 mL) and dichloromethane (10 mL). The phases were separated and the aqueous phase was further extracted with dichloromethane (10 mL). The organic extracts were combined and the combined solution was dried over anhydrous sodium sulfate. The dried solution was filtered and the filtrate was concentrated. The crude ring-opened product was dissolved in acetonitrile (1.2 mL). The resulting solution was transferred to a polypropylene reaction vessel and concentrated. Aqueous hydrofluoric acid solution (48 wt%, 0.8 mL) was added. The reaction mixture was stirred vigorously at 23 °C for 10 ½ h, then was poured into water (30 mL) containing dipotassium hydrogenphosphate (8.0 g). The resulting mixture was extracted with ethyl acetate (3 x 40 mL). The organic extracts were combined and the combined solution was dried over anhydrous sodium sulfate. The dried solution was filtered and the filtrate was concentrated. Palladium black (5.0 mg, 0.047 mmol, 2.8 equiv) was added in one portion to a solution of the crude product in methanol (1.0 mL) and dioxane (1.0 mL) at 23 °C. An atmosphere of hydrogen was introduced by briefly evacuating the flask, then flushing with pure hydrogen (1 atm). The reaction mixture was stirred at 23 °C for 1 ¾ h,

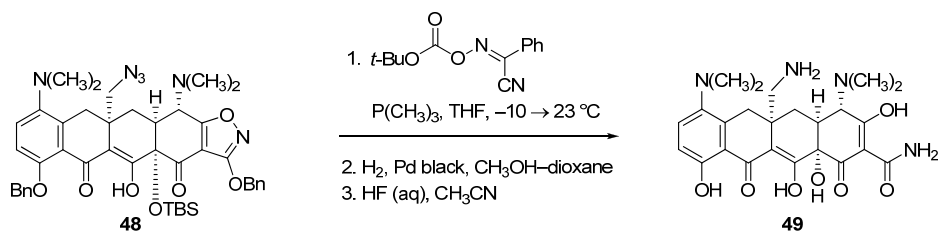
then was filtered through a plug of Celite. The filtrate was concentrated. The product was purified by preparative HPLC on an Agilent Prep C18 column [10 μ m, 250 x 21.2 mm, UV detection at 350 nm, Solvent A: 0.1% trifluoroacetic acid in water, Solvent B: acetonitrile, injection volume: 5.0 mL (4.0 mL 0.1% trifluoroacetic acid in water, 1.0 mL acetonitrile), gradient elution with 5 \rightarrow 40% B over 50 min, flow rate: 7.5 mL/min]. Fractions eluting at 32-34 min were collected and concentrated, affording C5a-methoxyethoxymethylminocycline trifluoroacetate **47** as a yellow solid (5.8 mg, 52%, three steps).

^1H NMR (600 MHz, CD_3OD , trifluoroacetate) δ 7.83 (d, 1H, J = 9.0 Hz), 7.05 (d, 1H, J = 9.0 Hz), 4.13 (s, 1H), 3.54-3.45 (m, 4H), 3.44-3.40 (m, 1H), 3.34 (d, 1H, J = 15.6 Hz), 3.27-3.25 (m, 1H), 3.26 (s, 3H), 3.18 (s, 6H), 3.11 (brd, 1H, J = 14.4 Hz), 2.99 (s, 6H), 2.61 (d, 1H, J = 16.2 Hz), 2.45 (dd, 1H, J = 14.4, 3.0 Hz), 1.71 (t, 1H, J = 14.4 Hz); HRMS–ESI (m/z): $[\text{M}+\text{H}]^+$ calcd for $\text{C}_{27}\text{H}_{36}\text{N}_3\text{O}_9$, 546.2446; found, 546.2459.



Azido ring-opened product 48. Sodium azide (50.0 mg, 0.763 mmol, 3.0 equiv) was added to a solution of the C5a-C11a-bridged cyclopropane **37** (194 mg, 0.255 mmol, 1 equiv) in dimethylformamide (7.5 mL) at 23 °C. The resulting solution was stirred at this temperature for 14 h, then was partitioned between saturated aqueous sodium chloride solution and diethyl ether (60 mL each). The phases were separated and the aqueous phase was further extracted with diethyl ether (60 mL). The organic extracts were combined and the combined solution was dried over anhydrous sodium sulfate. The dried solution was filtered and the filtrate was concentrated. The product was purified by flash-column chromatography (12% ethyl acetate-hexanes), providing the azido-substituted ring-opened product **48** as a yellow solid (160 mg, 78%).

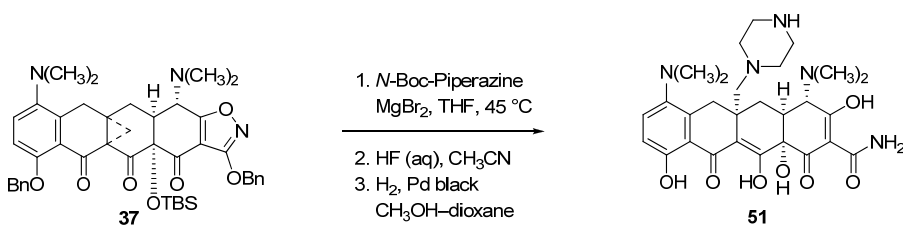
= 0.41 (30% ethyl acetate-hexanes); ^1H NMR (500 MHz, CDCl_3) δ 16.72 (s, 1H), 7.51 (brd, 4H, $J = 8.0$ Hz), 7.41-7.26 (m, 7H), 6.95 (d, 1H, 8.5 Hz), 5.38 (s, 2H), 5.18 (AB quartet, 2H), 4.11 (d, 1H, $J = 10.5$ Hz), 3.72 (d, 1H, $J = 16.5$ Hz), 3.30 (d, 1H, $J = 11.5$ Hz), 3.13 (d, 1H, $J = 11.5$ Hz), 2.65 (s, 6H), 2.65-2.45 (m, 2H), 2.51 (s, 6H), 2.35-2.25 (m, 2H), 0.92 (s, 9H), 0.27 (s, 3H), 0.19 (s, 3H); ^{13}C NMR (125 MHz, CDCl_3) δ 186.5, 184.0, 183.6, 181.5, 167.7, 154.9, 145.9, 136.7, 135.3, 135.0, 128.5, 128.5, 128.5, 128.4, 127.9, 127.0, 125.8, 120.2, 114.0, 108.3, 107.3, 82.3, 72.5, 71.5, 61.1, 59.1, 46.6, 44.6, 41.9, 36.4, 35.2, 28.3, 26.5, 19.3, -1.9, -2.1; FTIR (neat film), 2099 (s), 1721 (s), 1609 (m), 1510 (s), 1258 (m), 829 (s) cm^{-1} ; HRMS-ESI (m/z): $[\text{M}+\text{H}]^+$ calcd for $\text{C}_{44}\text{H}_{53}\text{N}_6\text{O}_7\text{Si}$, 805.3740; found, 805.3722.



C5a-Aminomethylminocycline (49).⁸⁰ A solution of trimethylphosphine in tetrahydrofuran (1.0 M, 398 μL , 0.398 mmol, 2.0 equiv) was added dropwise via syringe to a solution of the azido-substituted ring-opened product **48** (160 mg, 0.199 mmol, 1 equiv) and 2-(*tert*-butoxycarbonyloxymino)-2-phenylacetonitrile (98.0 mg, 0.398 mmol, 2.0 equiv) in tetrahydrofuran at $-10\text{ }^\circ\text{C}$. The reaction mixture was allowed to warm to $23\text{ }^\circ\text{C}$ over 15 min. After stirring at this temperature for 15 h, the product solution was partitioned between dichloromethane and water (60 mL each). The phases were separated and the organic phase was washed sequentially with water (60 mL) and saturated aqueous sodium chloride solution (2 x 60 mL). The organic solution was then dried over anhydrous sodium sulfate. The dried solution was filtered and the filtrate was concentrated. The product was purified by flash-column chromatography (25% ethyl acetate-hexanes), providing the desired *tert*-butyl carbamate as a yellow solid (90 mg, 51%). Methanol (2.5 mL) and dioxane (2.5 mL) were added to this product, forming a yellow solution. Palladium black (25 mg, 0.235 mmol, 2.3 equiv) was added in one portion at $23\text{ }^\circ\text{C}$. An atmosphere of hydrogen was introduced by briefly evacuating the flask, then flushing with pure hydrogen (1 atm). The reaction mixture was stirred at $23\text{ }^\circ\text{C}$ for 1 h, whereupon more palladium black (25 mg) was added. The resulting mixture was stirred at $23\text{ }^\circ\text{C}$ for a further 2 h, then was filtered through a plug of Celite. The filtrate was concentrated, providing an orange solid. Concentrated aqueous hydrofluoric acid (48

wt%, 1.4 mL) was added to a solution of the crude product in acetonitrile (2.0 mL) in a polypropylene reaction vessel at 23 °C. The reaction mixture was stirred vigorously at 23 °C for 15 h. Excess hydrofluoric acid was quenched by the careful addition of methoxytrimethylsilane (9.0 mL). The resulting mixture was concentrated. The product was purified by preparative HPLC on an Agilent Prep C18 column [10 µm, 250 x 21.2 mm, UV detection at 350 nm, Solvent A: 0.1% trifluoroacetic acid in water, Solvent B: acetonitrile, injection volume: 5.0 mL (4.0 mL 0.1% trifluoroacetic acid in water, 1.0 mL acetonitrile), gradient elution with 5→40% B over 50 min, flow rate: 7.5 mL/min]. Fractions eluting at 22-27 min were collected and concentrated, affording C5a-aminomethylminocycline bistrifluoroacetate **49** as a yellow solid (50 mg, 69%, two steps).

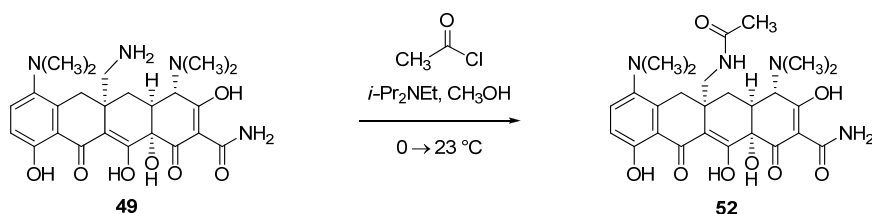
¹H NMR (500 MHz, CD₃OD, bistrifluoroacetate) δ 7.88 (d, 1H, *J* = 9.0 Hz), 7.10 (d, 1H, *J* = 9.0 Hz), 4.09 (d, 1H, *J* = 2.5 Hz), 3.60 (d, 1H, *J* = 17.0 Hz), 3.34 (d, 1H, *J* = 14.5 Hz), 3.18 (s, 6H), 3.16 (s, 6H), 3.20-3.14 (m, 1H), 3.02 (d, 1H, *J* = 14.5 Hz), 2.95 (d, 1H, *J* = 17.0 Hz), 2.33 (dd, 1H, *J* = 15.0, 3.0 Hz), 1.96 (dd, 1H, *J* = 14.6, 13.7 Hz); HRMS–ESI (*m/z*): [M+H]⁺ calcd for C₂₄H₃₁N₄O₇, 487.2187; found 487.2181.



C5a-Piperazinylmethylminocycline (51). Anhydrous magnesium bromide (51.0 mg, 0.276 mmol, 2.0 equiv) was added to a solution of the C5a-C11a-bridged cyclopropane **37** (105 mg, 0.138 mmol, 1 equiv) and *tert*-butyl 1-piperazine carboxylate (186 mg, 1.00 mmol, 7.2 equiv) in tetrahydrofuran (2.0 mL) at 23 °C. The reaction flask was sealed and the reaction mixture was heated to 45°C. After stirring at 45 °C for 36 h, the reaction mixture was allowed to cool to 23 °C. The cooled mixture was partitioned between dichloromethane and saturated aqueous sodium bicarbonate solution (25 mL each). The phases were separated and the aqueous phase was extracted with dichloromethane (25 mL). The organic extracts were combined and the combined solution was dried over anhydrous sodium sulfate. The dried solution was filtered and the filtrate was concentrated. The product mixture was filtered through a short pad of silica gel (eluting with 40% ethyl acetate-hexanes) and the filtrate was concentrated, affording an orange-yellow oil. Methanol (2.5 mL) and dioxane (2.5 mL) were added to the crude ring-opened product (**50**), forming an orange-yellow solution. Palladium black (25 mg, 0.235 mmol, 1.7 equiv) was added in one portion at 23 °C. An atmosphere of hydrogen was introduced by briefly evacuating the flask, then flushing with pure hydrogen (1 atm). The reaction mixture was stirred at 23 °C for 2 h, then was filtered through a plug of Celite. The filtrate was concentrated, providing an orange solid. Concentrated aqueous hydrofluoric acid (48 wt%, 1.5 mL) was added to a solution of the crude product in acetonitrile (2.0 mL) in a polypropylene reaction vessel at 23 °C. The reaction mixture was stirred

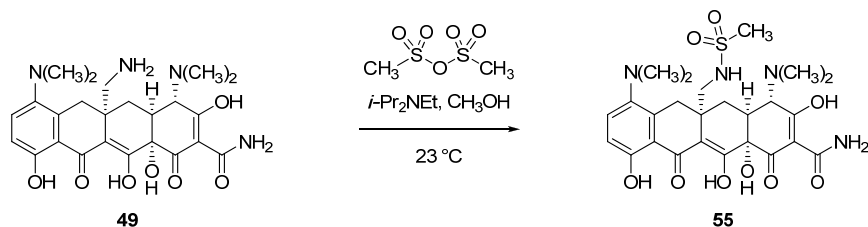
vigorously at 23 °C for 14 h. Excess hydrofluoric acid was quenched by the careful addition of methoxytrimethylsilane (10.0 mL). The resulting mixture was concentrated. The product was purified by preparative HPLC on an Agilent Prep C18 column [10 µm, 250 x 21.2 mm, UV detection at 350 nm, Solvent A: 0.1% trifluoroacetic acid in water, Solvent B: acetonitrile, 2 batches, injection volume (for each batch): 5.0 mL (4.0 mL 0.1% trifluoroacetic acid in water, 1.0 mL acetonitrile), gradient elution with 5→35% B over 50 min, flow rate: 7.5 mL/min]. Fractions eluting at 22-29 min were collected and concentrated, affording C5a-piperazinylmethylminocycline bistrifluoroacetate **51** as a yellow solid (63 mg, 58%, three steps).

¹H NMR (600 MHz, CD₃OD, bistrifluoroacetate) δ 7.58 (d, 1H, *J* = 9.6 Hz), 6.93 (d, 1H, *J* = 9.0 Hz), 4.06 (s, 1H), 3.44 (d, 1H, *J* = 16.2 Hz), 3.11 (brd, 1H, *J* = 12.6 Hz), 3.08-3.02 (m, 2H), 3.05 (s, 6H), 3.01-2.95 (m, 2H), 2.82 (s, 6H), 2.61-2.56 (m, 3H), 2.50 (d, 1H, *J* = 16.2 Hz), 2.48-2.42 (m, 3H), 2.20 (dd, 1H, *J* = 13.8, 3.0 Hz), 1.74 (dd, 1H, *J* = 14.1, 13.9 Hz); HRMS–ESI (*m/z*): [M+H]⁺ calcd for C₂₈H₃₈N₅O₇, 556.2766; found, 556.2771.



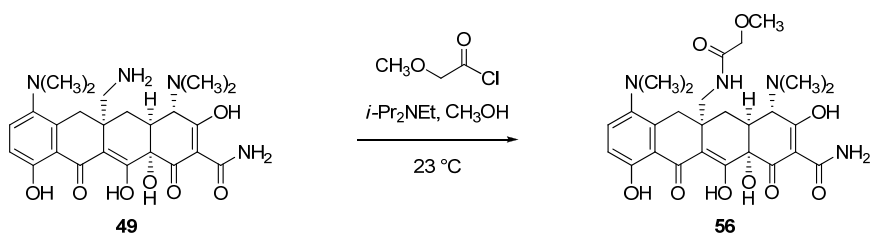
C5a-*N*-Acetylaminomethyliminocycline (52). Acetyl chloride (0.9 μ L, 0.013 mmol, 2.3 equiv) was added to a solution of C5a-aminomethyliminocycline bistrifluoroacetate (**49**, 4.0 mg, 0.0056 mmol, 1 equiv) and *N,N*-diisopropylethylamine (4.6 μ L, 0.027 mmol, 4.8 equiv) in methanol (200 μ L) at 0 °C. The resulting solution was allowed to warm to 23 °C over 5 min. The reaction mixture was stirred at this temperature for 1 h, then was concentrated. The product was purified by preparative HPLC on an Agilent Prep C18 column [10 μ m, 250 x 21.2 mm, UV detection at 350 nm, Solvent A: 0.1% trifluoroacetic acid in water, Solvent B: acetonitrile, injection volume: 5.0 mL (4.0 mL 0.1% trifluoroacetic acid in water, 1.0 mL acetonitrile), gradient elution with 5→40% B over 50 min, flow rate: 7.5 mL/min]. Fractions eluting at 25-28 min were collected and concentrated, affording C5a-*N*-acetylaminomethyliminocycline trifluoroacetate **52** as a yellow solid (3.2 mg, 89%).

¹H NMR (600 MHz, CD₃OD, trifluoroacetate) δ 7.80 (d, 1H, J = 9.0 Hz), 7.03 (d, 1H, J = 9.0 Hz), 3.89 (s, 1H), 3.46 (d, 1H, J = 14.4 Hz), 3.27 (d, 1H, J = 13.8 Hz), 3.23 (d, 1H, J = 16.8 Hz), 3.15-3.08 (m, 13H), 2.63 (d, 1H, J = 16.2 Hz), 2.11 (dd, 1H, J = 14.4, 2.4 Hz), 1.91 (s, 3H), 1.69 (t, 1H, J = 14.4 Hz); HRMS–ESI (m/z): [M+H]⁺ calcd for C₂₆H₃₃N₄O₈, 529.2293; found 529.2299.



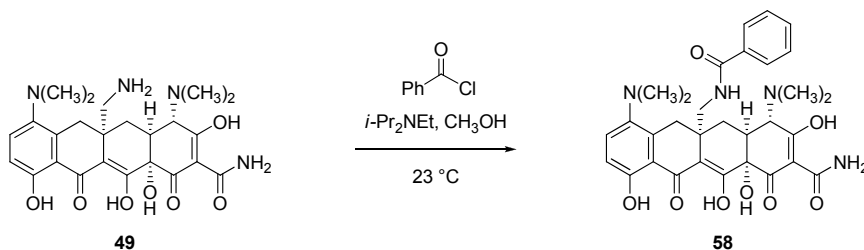
C5a-*N*-Methanesulfonylaminomethylminocycline (55). Methanesulfonic anhydride (2.3 mg, 0.013 mmol, 2.3 equiv) was added to a solution of C5a-aminomethylminocycline bistrifluoroacetate (**49**, 4.0 mg, 0.0056 mmol, 1 equiv) and *N,N*-diisopropylethylamine (4.6 μ L, 0.027 mmol, 4.8 equiv) in methanol (200 μ L) at 23 °C. The reaction mixture was stirred at this temperature for 2 h, then was concentrated. The product was purified by preparative HPLC on an Agilent Prep C18 column [10 μ m, 250 x 21.2 mm, UV detection at 350 nm, Solvent A: 0.1% trifluoroacetic acid in water, Solvent B: acetonitrile, injection volume: 5.0 mL (4.0 mL 0.1% trifluoroacetic acid in water, 1.0 mL acetonitrile), gradient elution with 5 \rightarrow 40% B over 50 min, flow rate: 7.5 mL/min]. Fractions eluting at 28-30 min were collected and concentrated, affording C5a-*N*-methanesulfonylaminomethyl-minocycline trifluoroacetate **55** as a yellow solid (1.5 mg, 39%).

^1H NMR (600 MHz, CD_3OD , trifluoroacetate) δ 7.77 (d, 1H, J = 9.0 Hz), 7.01 (d, 1H, J = 9.0 Hz), 3.91 (s, 1H), 3.34 (d, 1H, J = 16.2 Hz), 3.26-3.21 (m, 2H), 3.08 (s, 6H), 3.03 (s, 6H), 2.99 (d, 1H, J = 13.8 Hz), 2.86 (s, 3H), 2.60 (d, 1H, J = 16.2 Hz), 2.35 (dd, 1H, J = 14.4, 3.0 Hz), 1.70 (t, 1H, J = 14.4 Hz); HRMS-ESI (m/z): $[\text{M}+\text{H}]^+$ calcd for $\text{C}_{25}\text{H}_{32}\text{N}_4\text{O}_9\text{S}$, 565.1963; found 565.1973.



C5a-*N*-Methoxyacetylaminomethyliminocycline (56). Methoxyacetyl chloride (1.2 μ L, 0.013 mmol, 2.3 equiv) was added to a solution of C5a-aminomethyliminocycline bistrifluoroacetate (**49**, 4.0 mg, 0.0056 mmol, 1 equiv) and *N,N*-diisopropylethylamine (4.6 μ L, 0.027 mmol, 4.8 equiv) in methanol (200 μ L) at 23 °C. The reaction mixture was stirred at this temperature for 2 h, then was concentrated. The product was purified by preparative HPLC on an Agilent Prep C18 column [10 μ m, 250 x 21.2 mm, UV detection at 350 nm, Solvent A: 0.1% trifluoroacetic acid in water, Solvent B: acetonitrile, injection volume: 5.0 mL (4.0 mL 0.1% trifluoroacetic acid in water, 1.0 mL acetonitrile), gradient elution with 5 \rightarrow 40% B over 50 min, flow rate: 7.5 mL/min]. Fractions eluting at 28-30 min were collected and concentrated, affording C5a-*N*-methoxyacetylaminomethyliminocycline trifluoroacetate **56** as a yellow solid (2.0 mg, 53%).

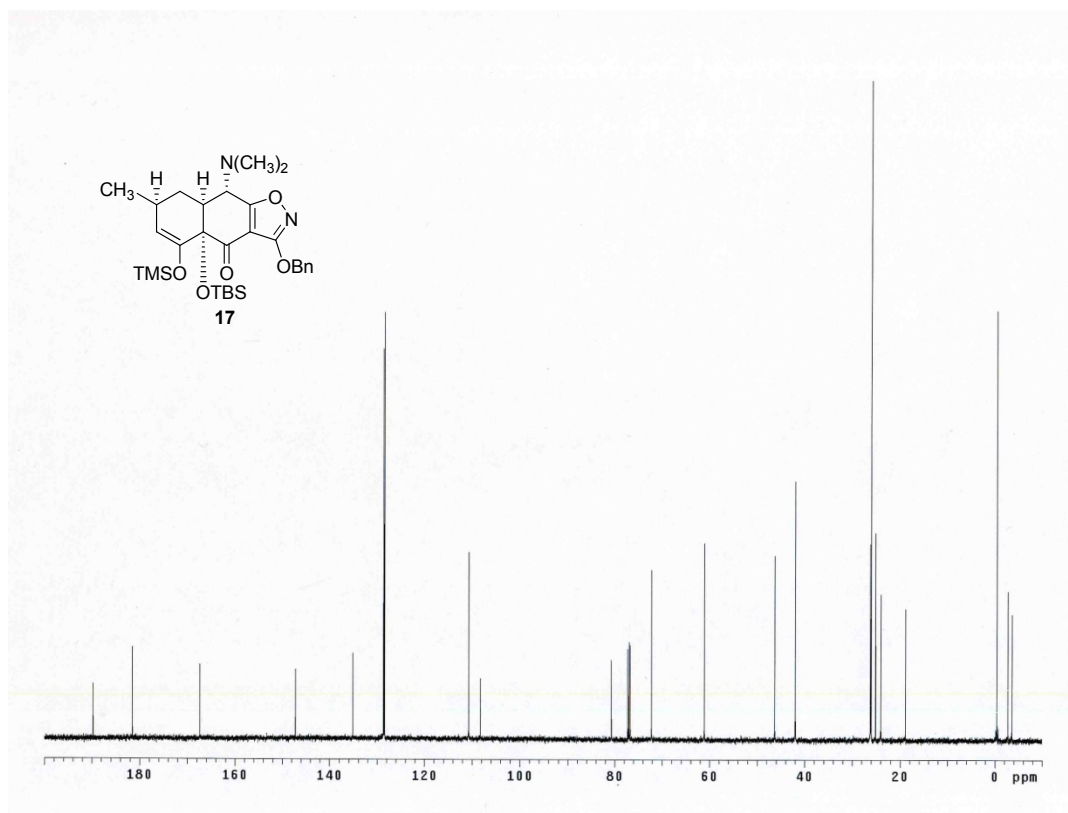
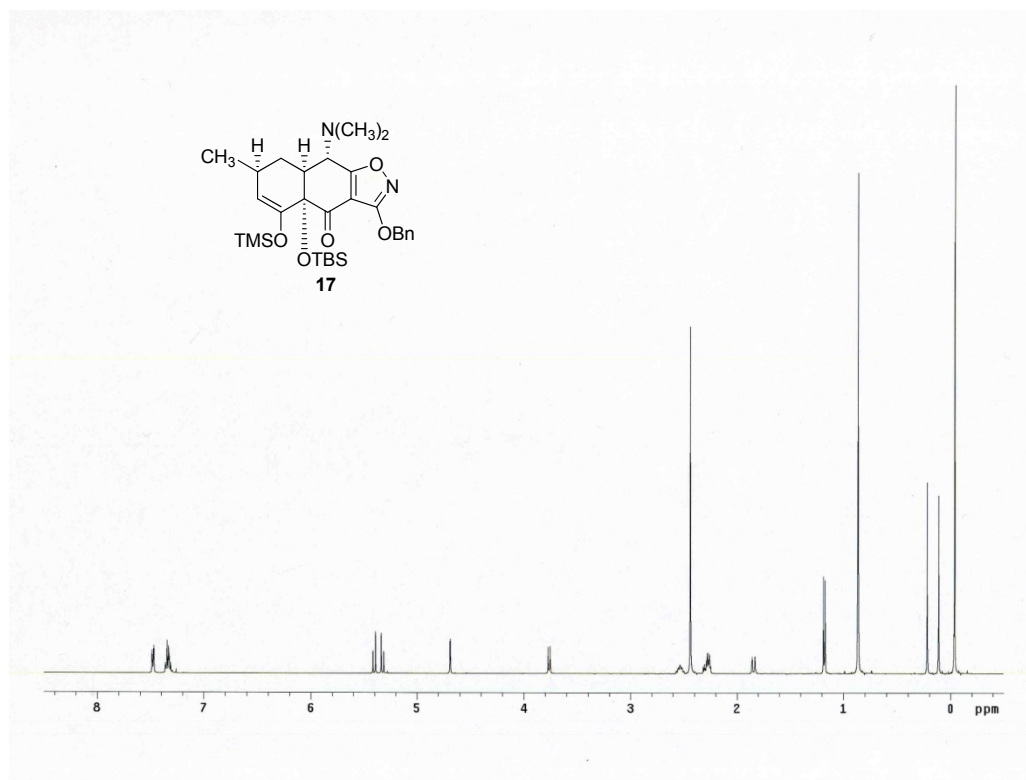
^1H NMR (600 MHz, CD_3OD , trifluoroacetate) δ 7.75 (d, 1H, J = 9.0 Hz), 7.00 (d, 1H, J = 9.0 Hz), 3.92 (s, 1H), 3.84 (AB quartet, 2H, J = 15.0 Hz, $\Delta\nu$ = 10.2 Hz), 3.59 (d, 1H, J = 14.4 Hz), 3.40 (s, 3H), 3.32-3.28 (m, 1H), 3.27 (d, 1H, J = 15.6 Hz), 3.10 (s, 6H), 3.10-3.07 (m, 1H), 3.03 (s, 6H), 2.58 (d, 1H, J = 16.2 Hz), 2.09 (dd, 1H, J = 14.4, 3.0 Hz), 1.69 (t, 1H, J = 13.8 Hz); HRMS-ESI (m/z): $[\text{M}+\text{H}]^+$ calcd for $\text{C}_{27}\text{H}_{34}\text{N}_4\text{O}_9$, 559.2399; found 559.2435.

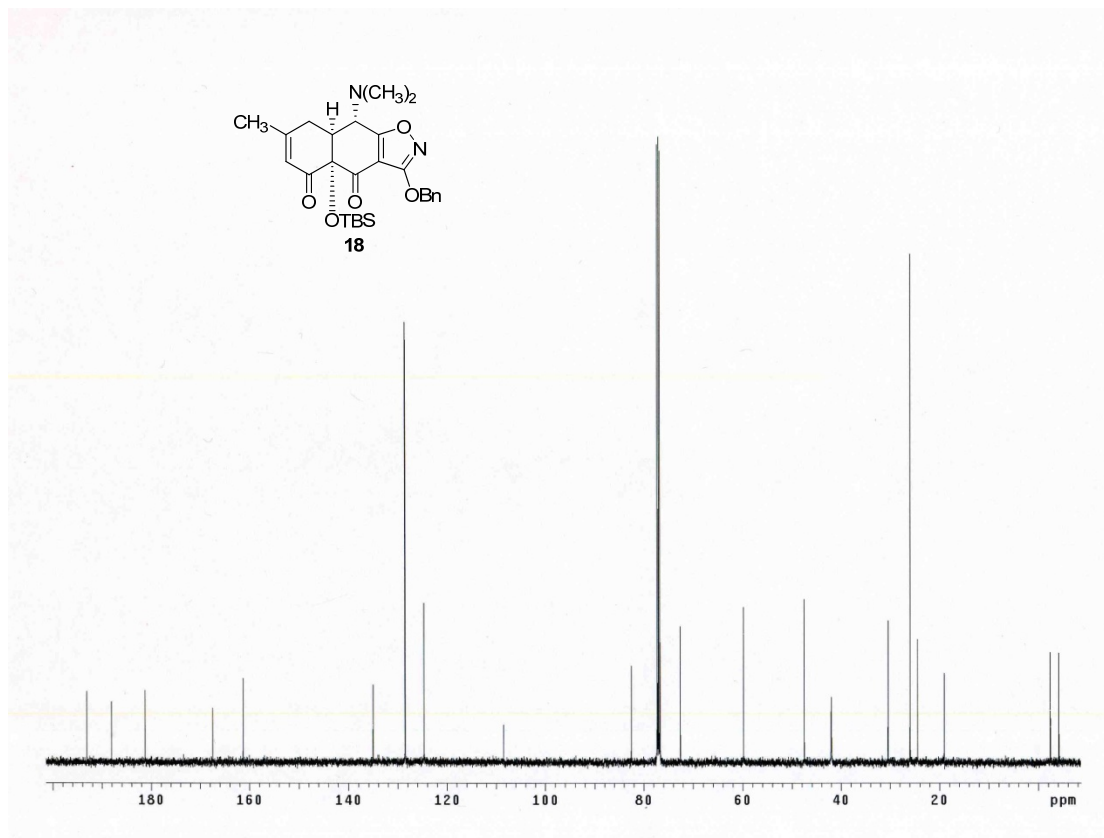
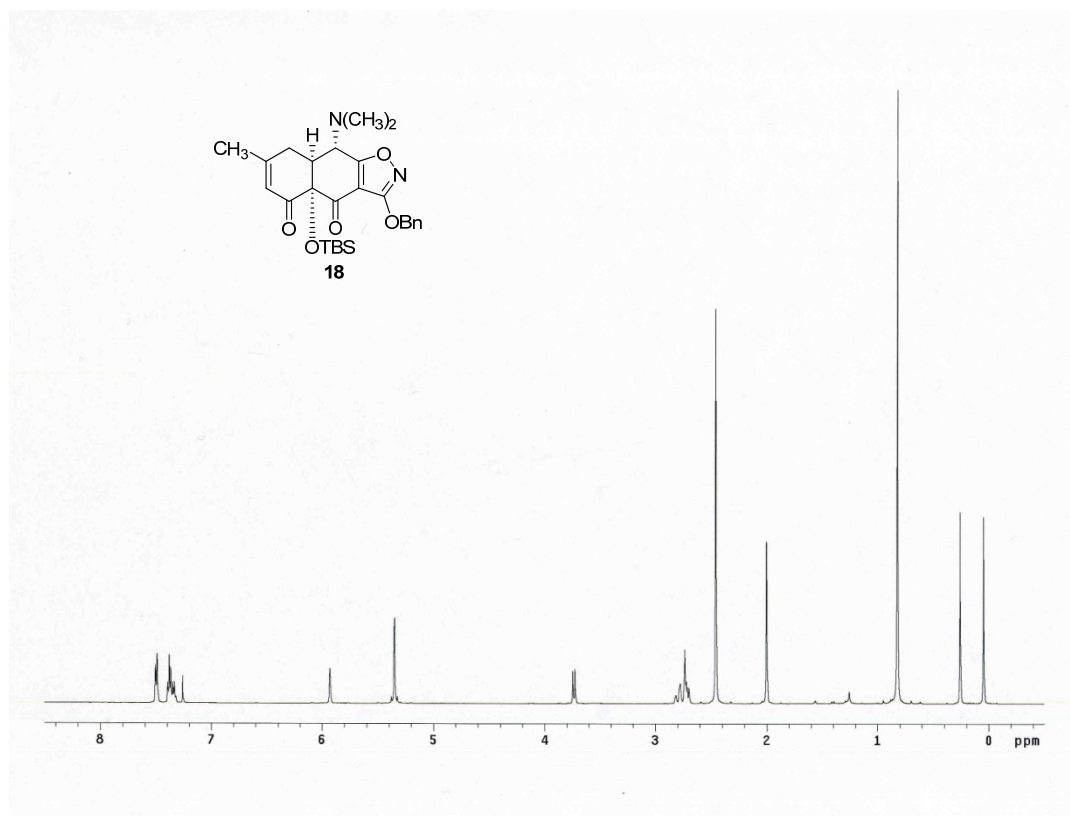


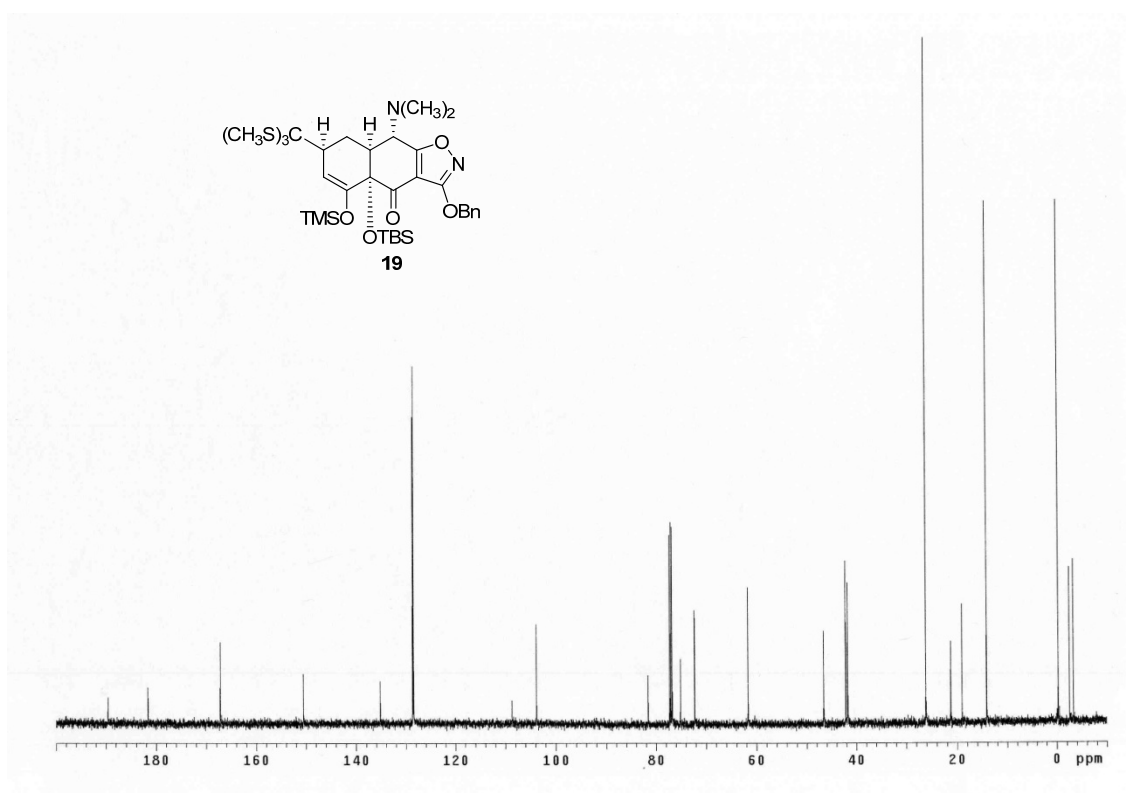
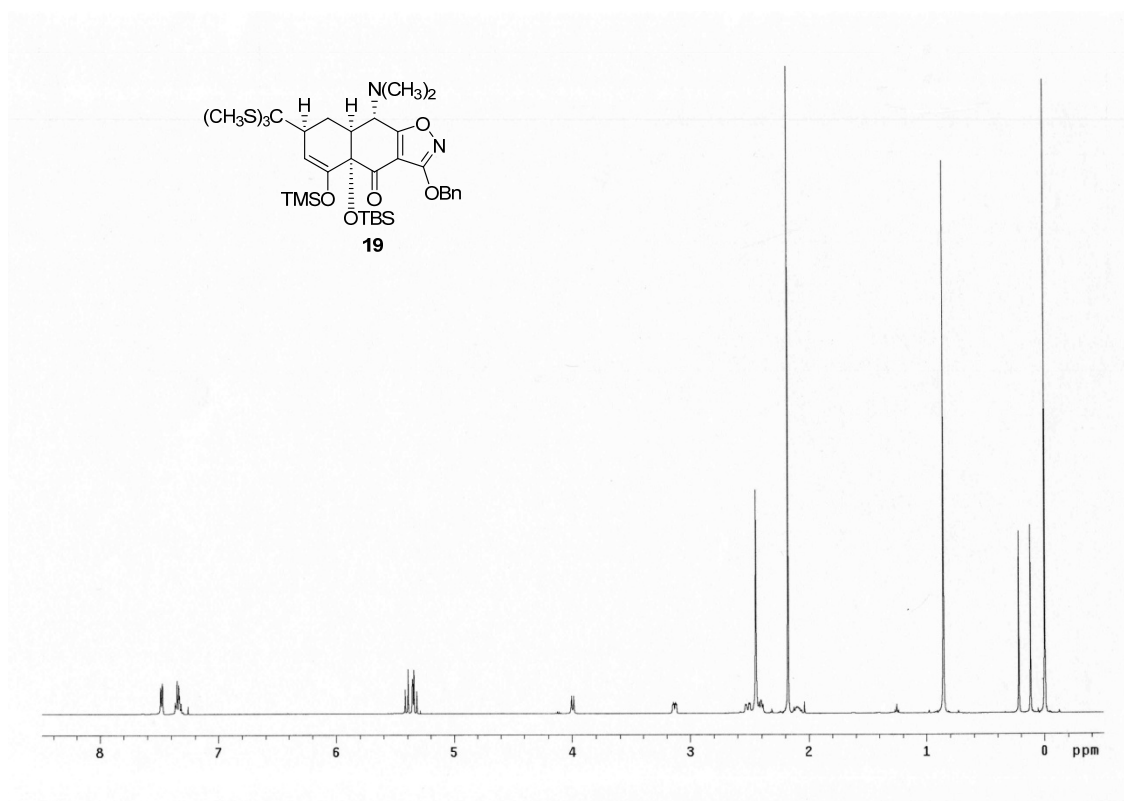
C5a-*N*-Benzoylaminomethyliminocycline (58). Benzoyl chloride (1.5 μL , 0.013 mmol, 2.3 equiv) was added to a solution of C5a-aminomethyliminocycline bistrifluoroacetate (**49**, 4.0 mg, 0.0056 mmol, 1 equiv) and *N,N*-diisopropylethylamine (4.6 μL , 0.027 mmol, 4.8 equiv) in methanol (200 μL) at 23 $^{\circ}\text{C}$. The reaction mixture was stirred at this temperature for 1 $\frac{1}{2}$ h, then was concentrated. The product was purified by preparative HPLC on an Agilent Prep C18 column [10 μm , 250 x 21.2 mm, UV detection at 350 nm, Solvent A: 0.1% trifluoroacetic acid in water, Solvent B: acetonitrile, injection volume: 5.0 mL (4.0 mL 0.1% trifluoroacetic acid in water, 1.0 mL acetonitrile), gradient elution with 5 \rightarrow 40% B over 50 min, flow rate: 7.5 mL/min]. Fractions eluting at 38-40 min were collected and concentrated, affording C5a-*N*-benzoylaminomethyliminocycline trifluoroacetate **58** as a yellow solid (1.6 mg, 41%).

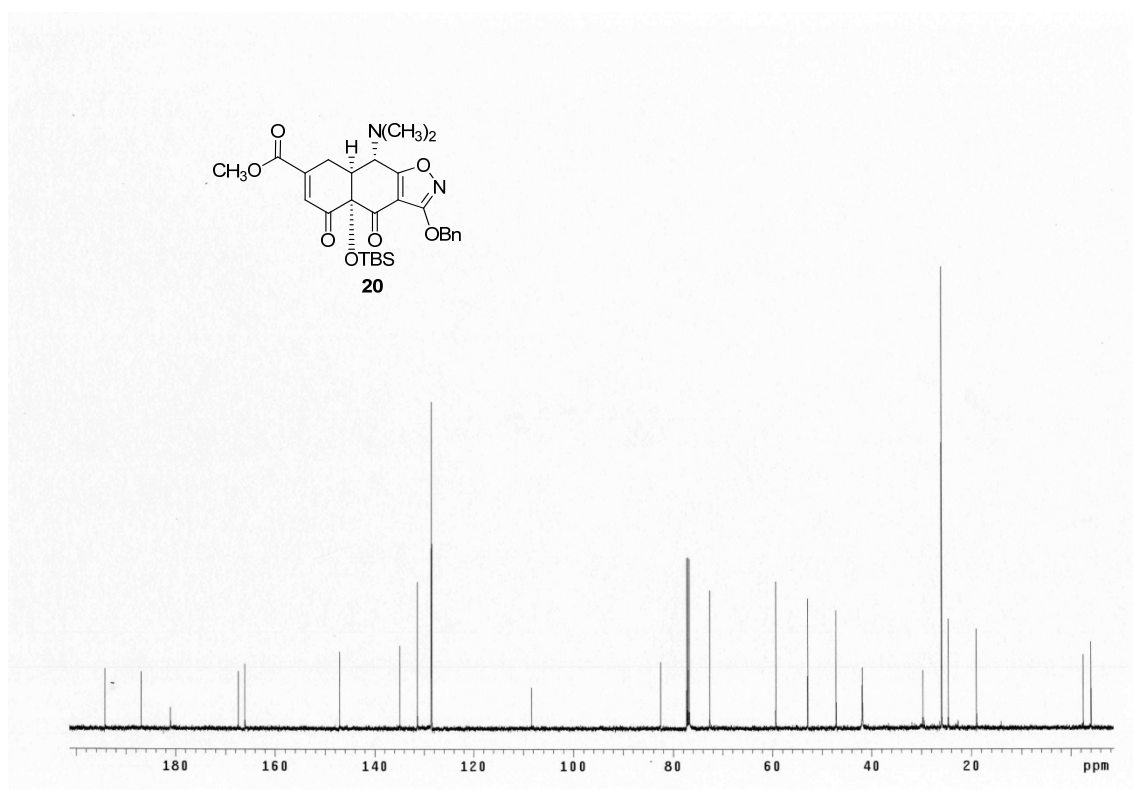
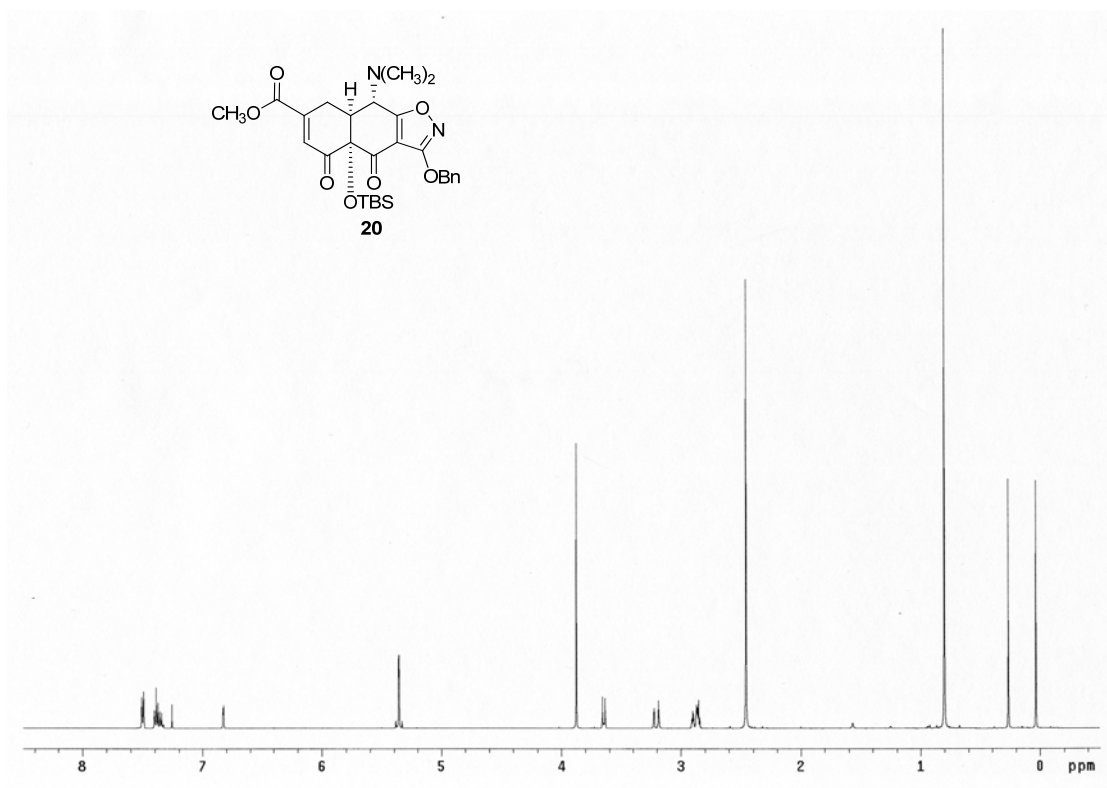
^1H NMR (600 MHz, CD_3OD , trifluoroacetate) δ 7.75 (d, 2H, $J = 7.2$ Hz), 7.70 (d, 1H, $J = 9.6$ Hz), 7.54 (t, 1H, $J = 7.8$ Hz), 7.45 (t, 2H, $J = 7.8$ Hz), 6.95 (d, 1H, $J = 9.0$ Hz), 3.94 (s, 1H), 3.74 (d, 1H, $J = 14.4$ Hz), 3.37 (d, 1H, $J = 15.6$ Hz), 3.36-3.27 (m, 2H), 3.13 (s, 6H), 3.02 (s, 6H), 2.63 (d, 1H, $J = 16.2$ Hz), 2.21 (dd, 1H, $J = 14.4, 2.4$ Hz), 1.76 (t, 1H, $J = 14.4$ Hz); HRMS-ESI (m/z): $[\text{M}+\text{H}]^+$ calcd for $\text{C}_{31}\text{H}_{35}\text{N}_4\text{O}_8$, 591.2449; found 591.2459.

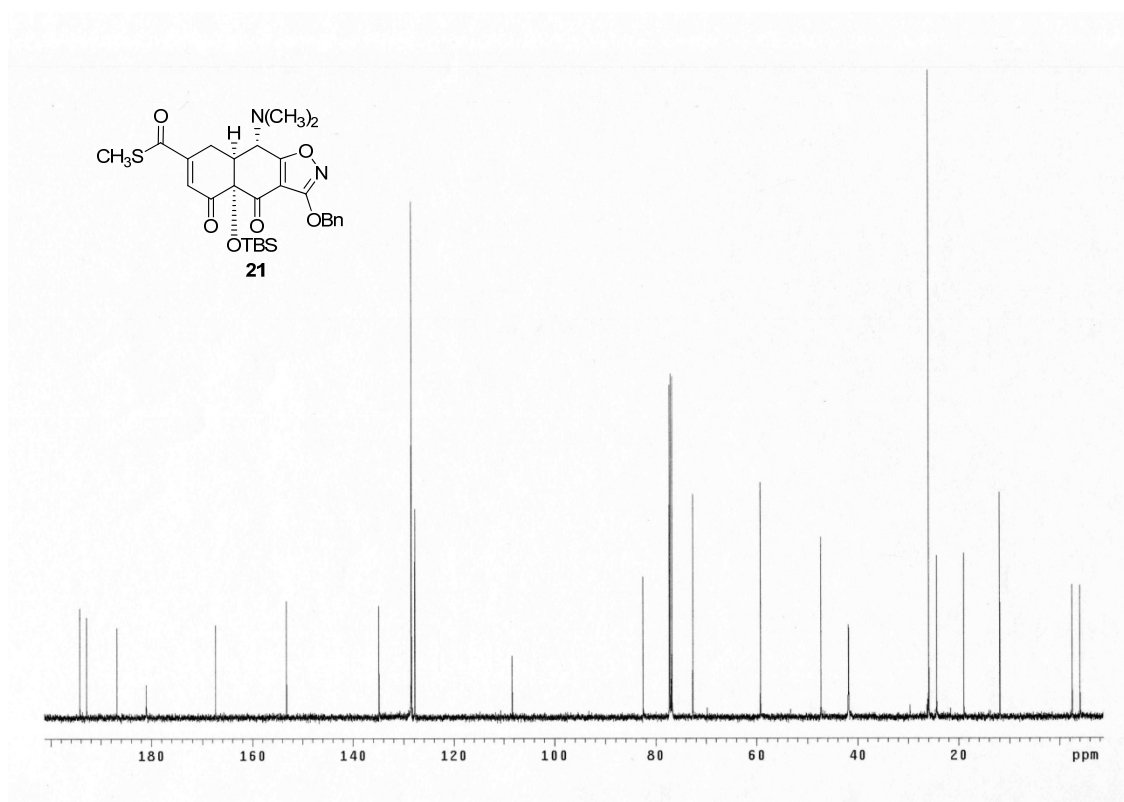
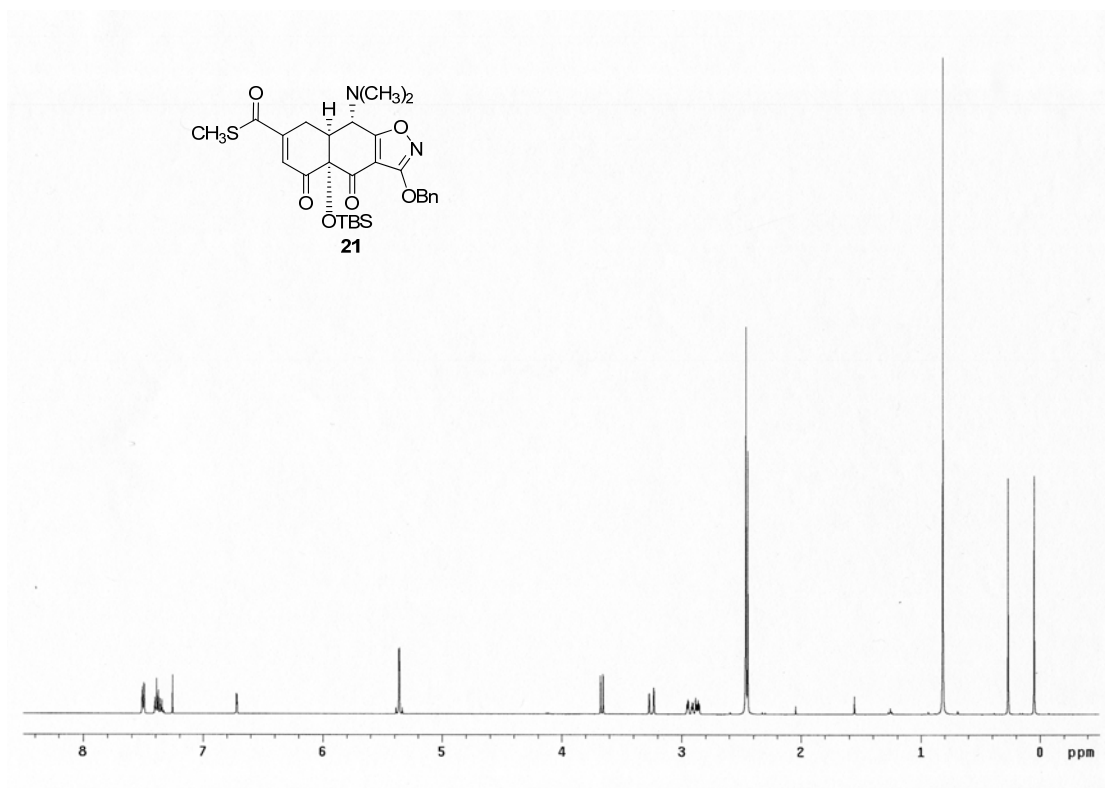
Catalog of spectra

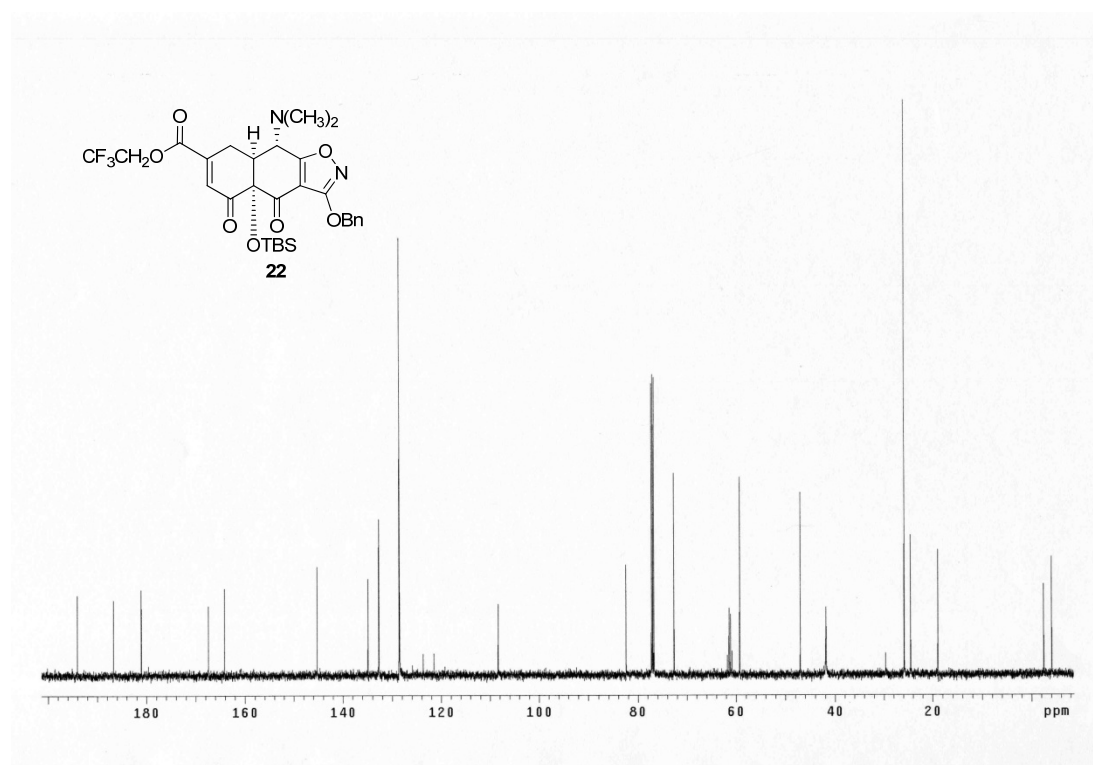
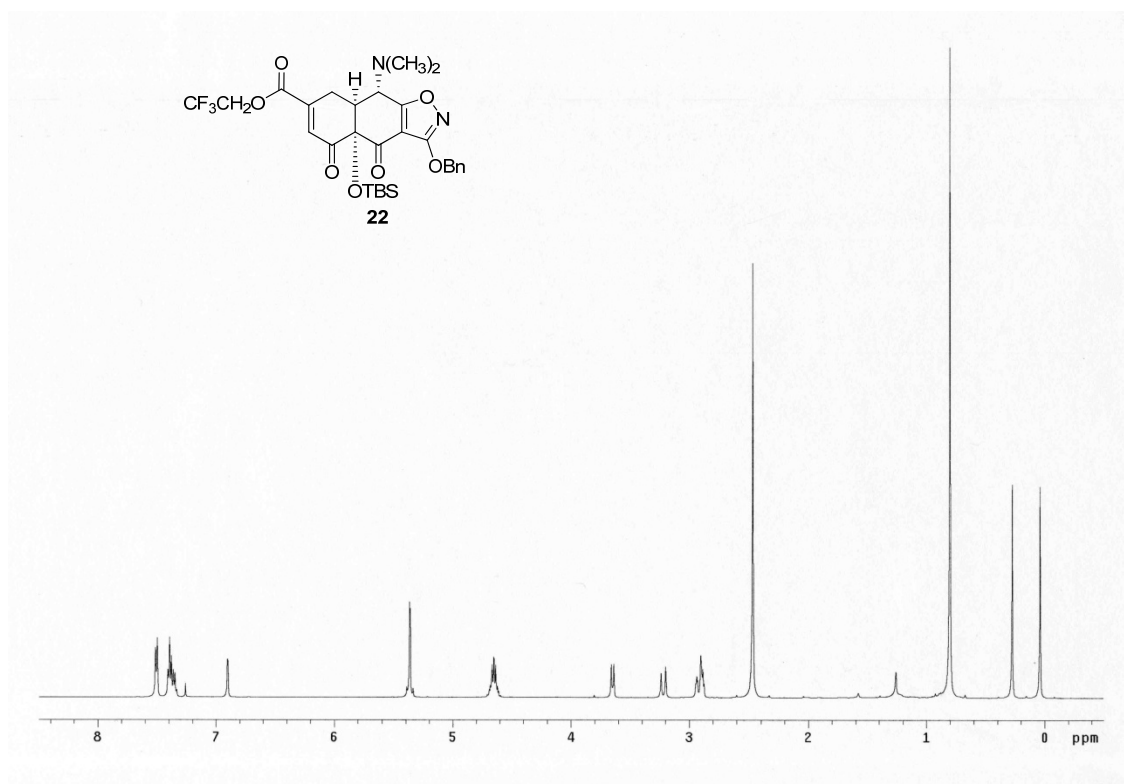


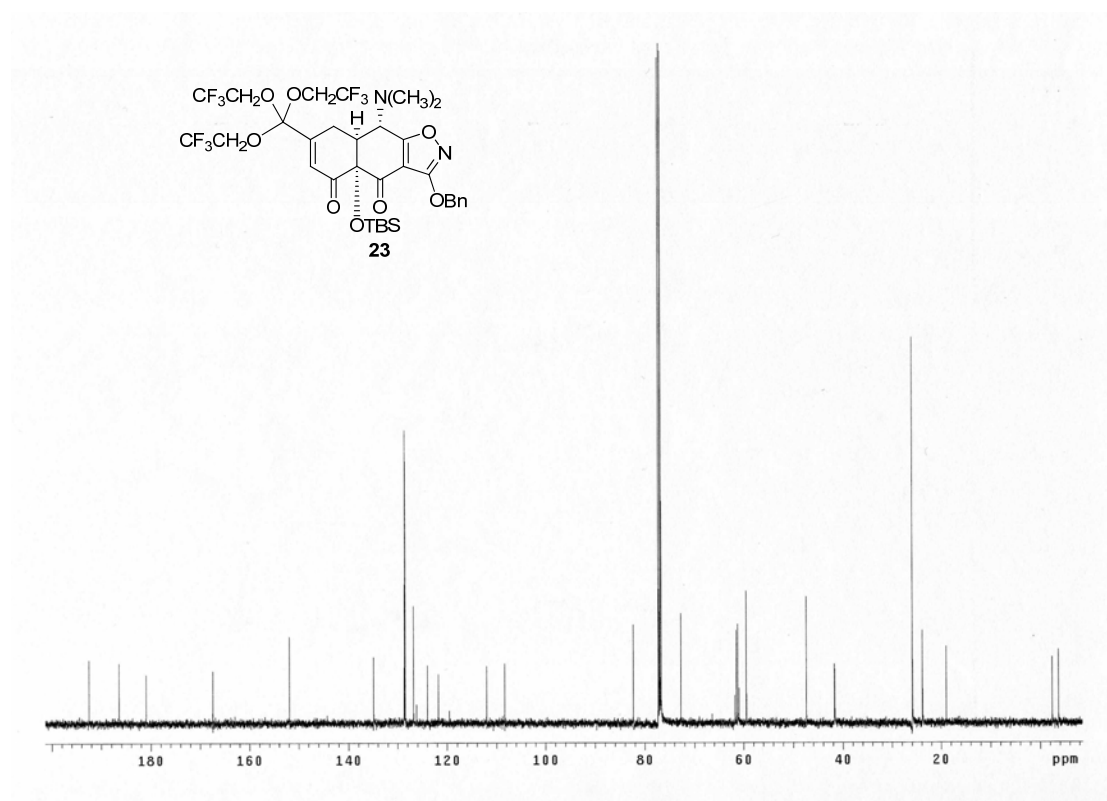
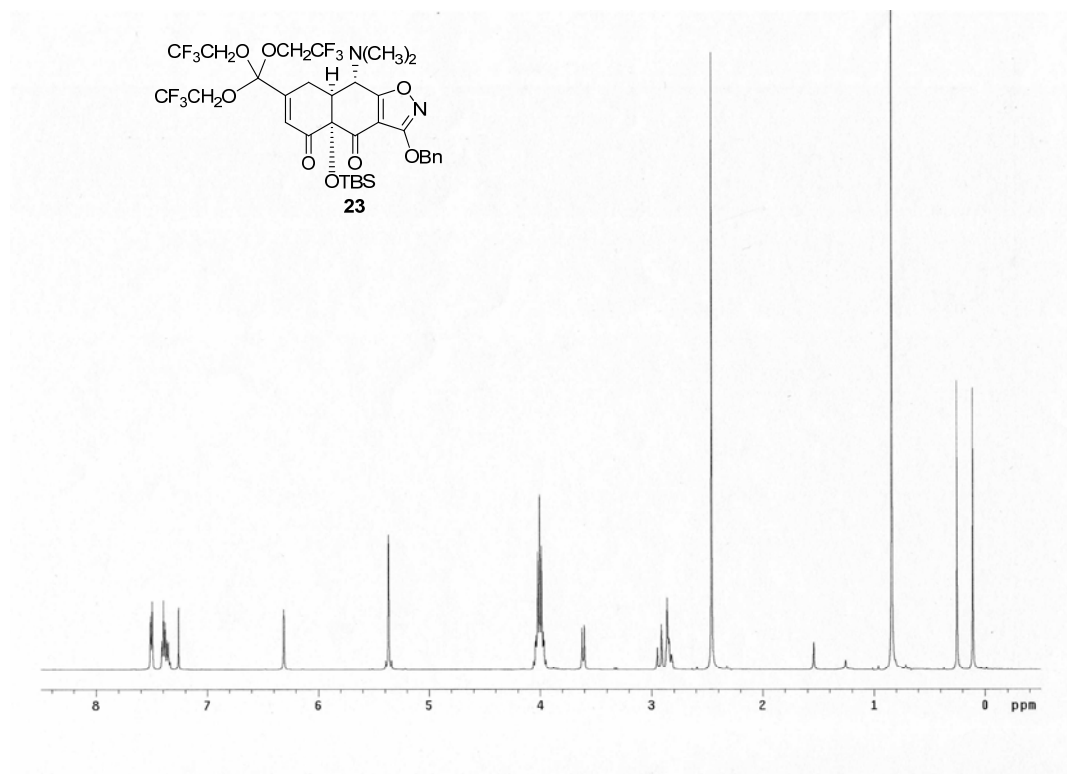


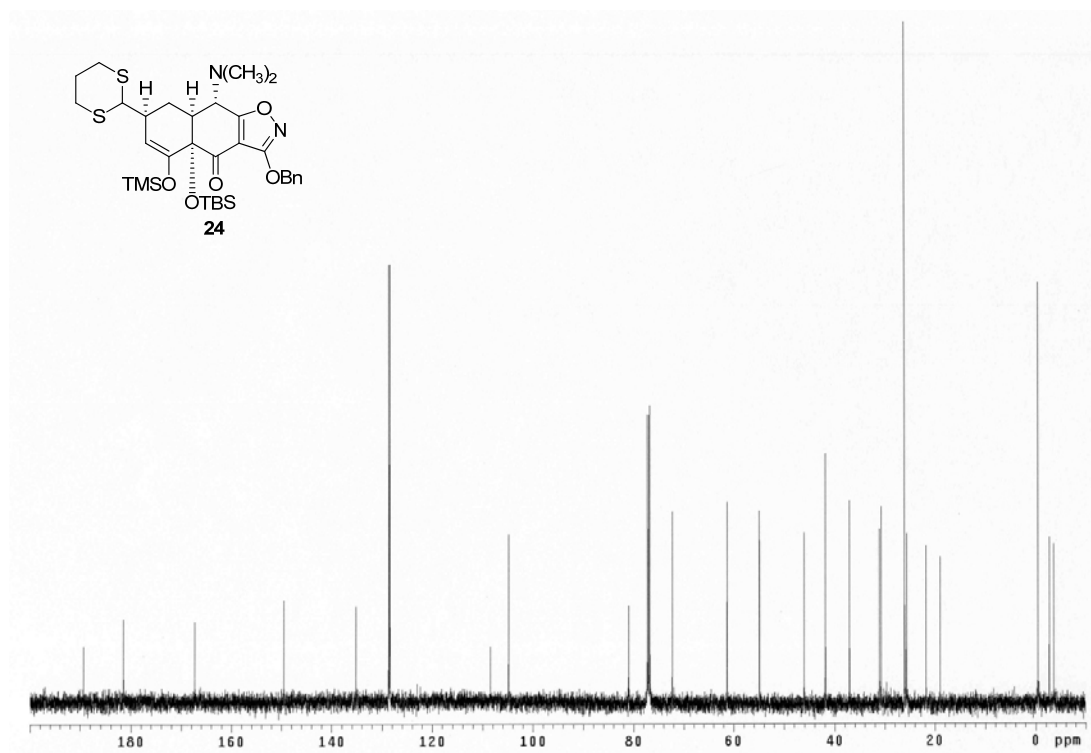
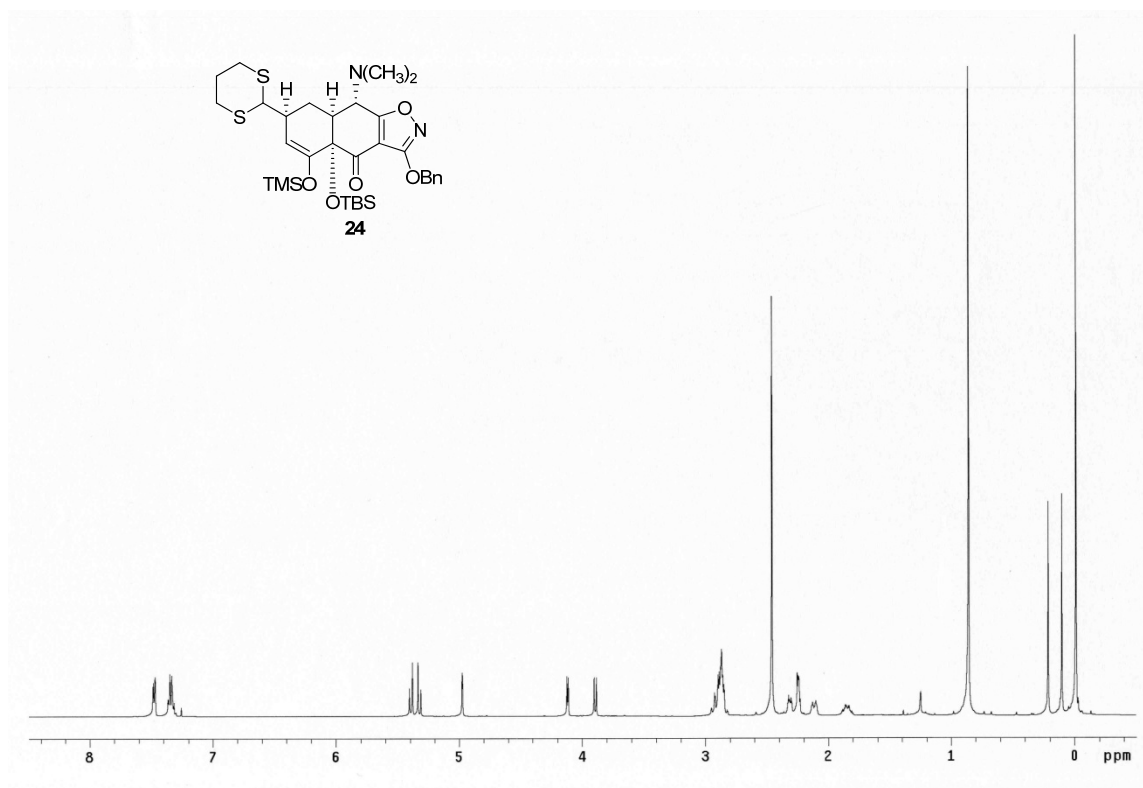


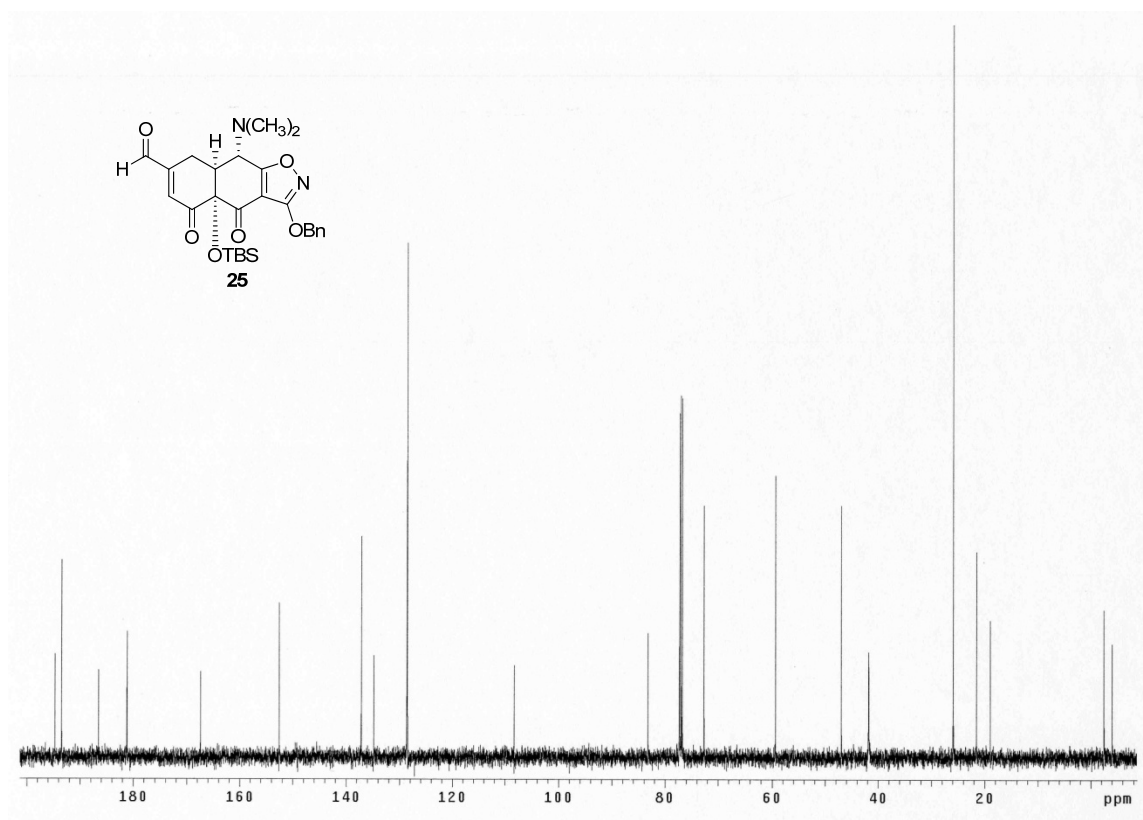
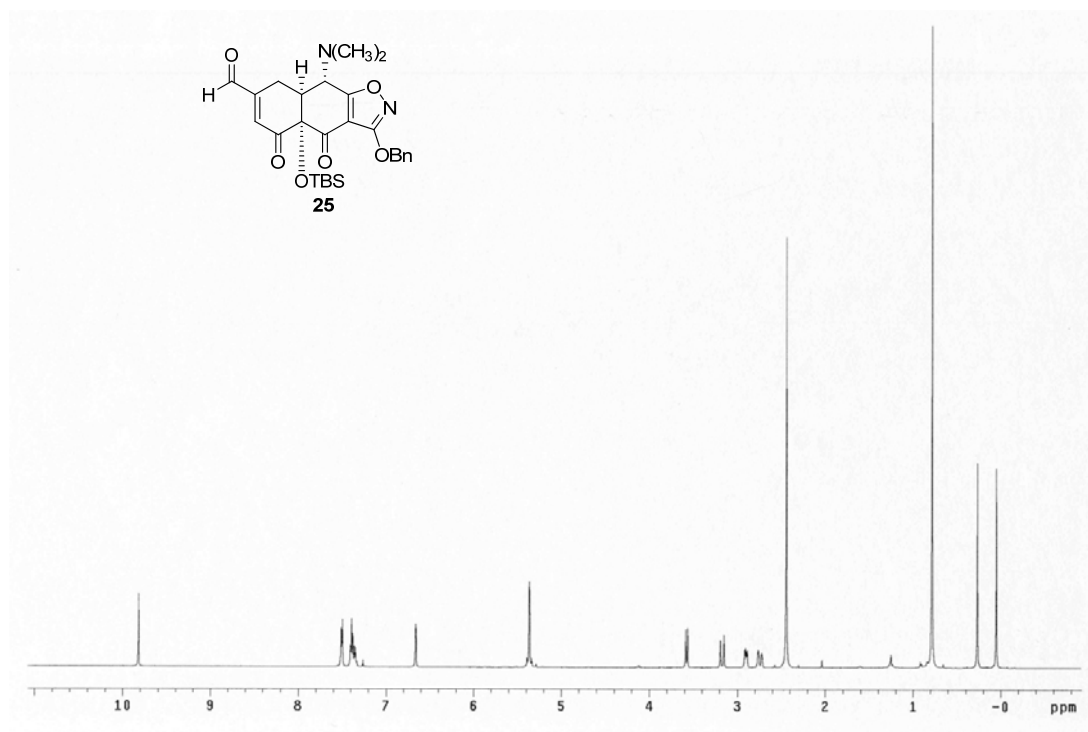


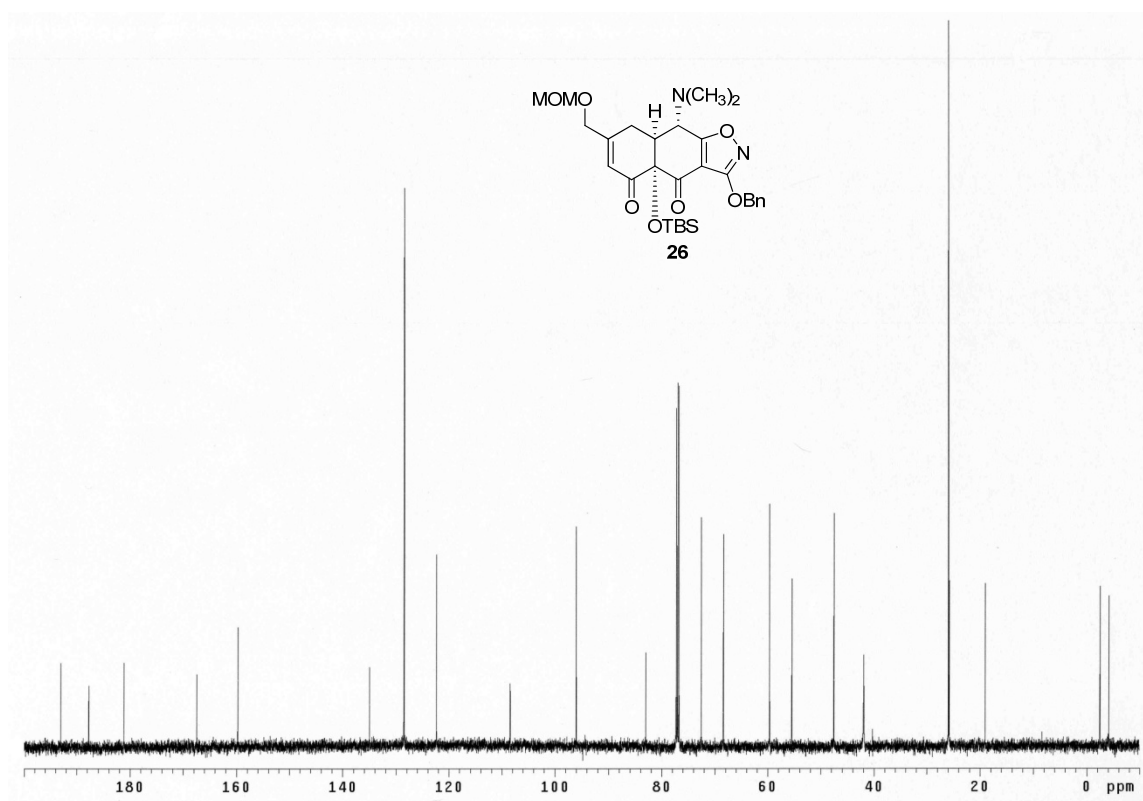
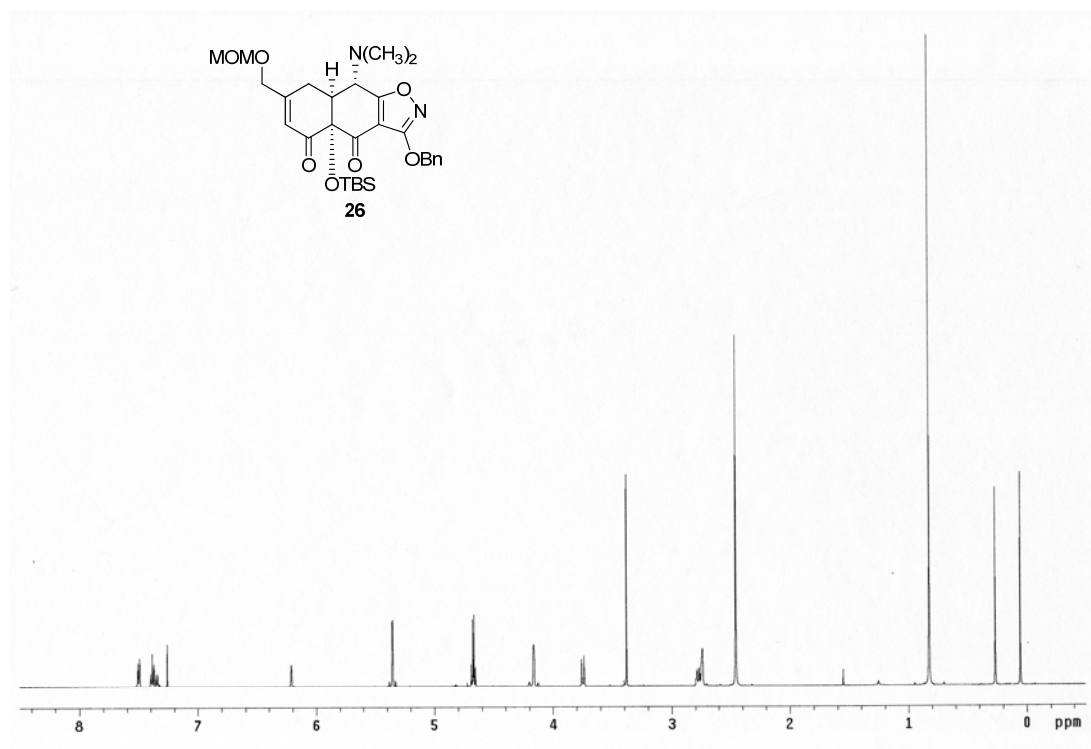


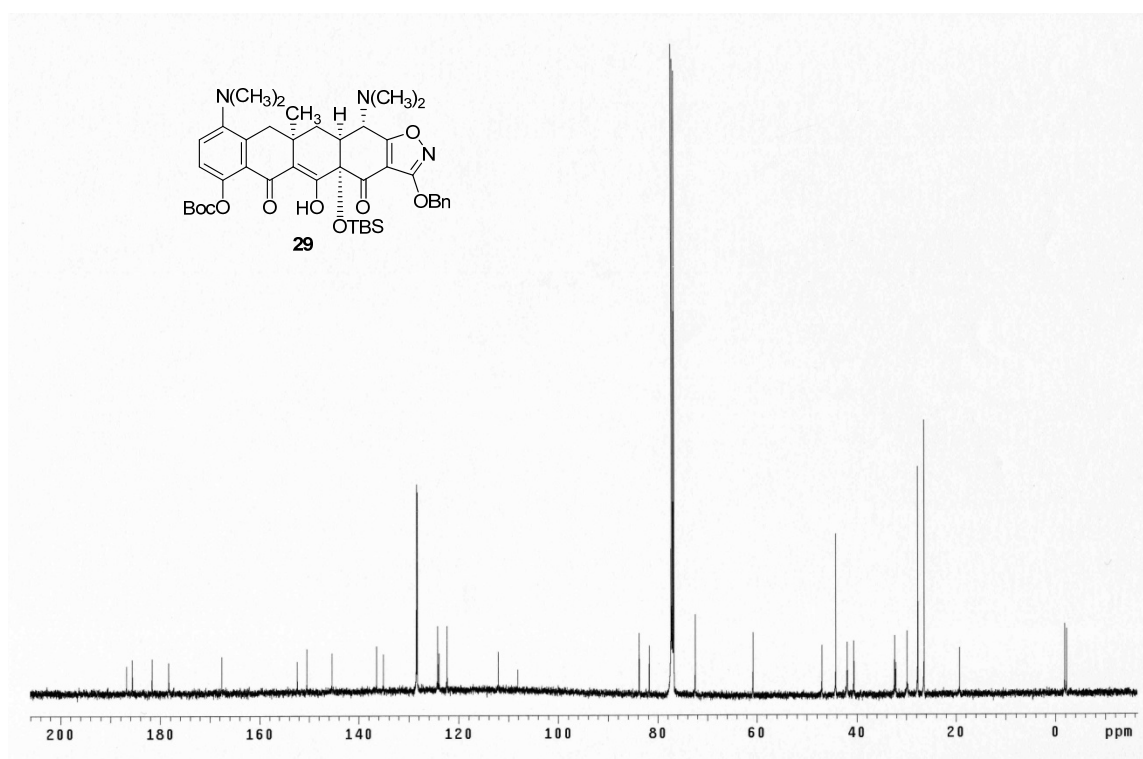
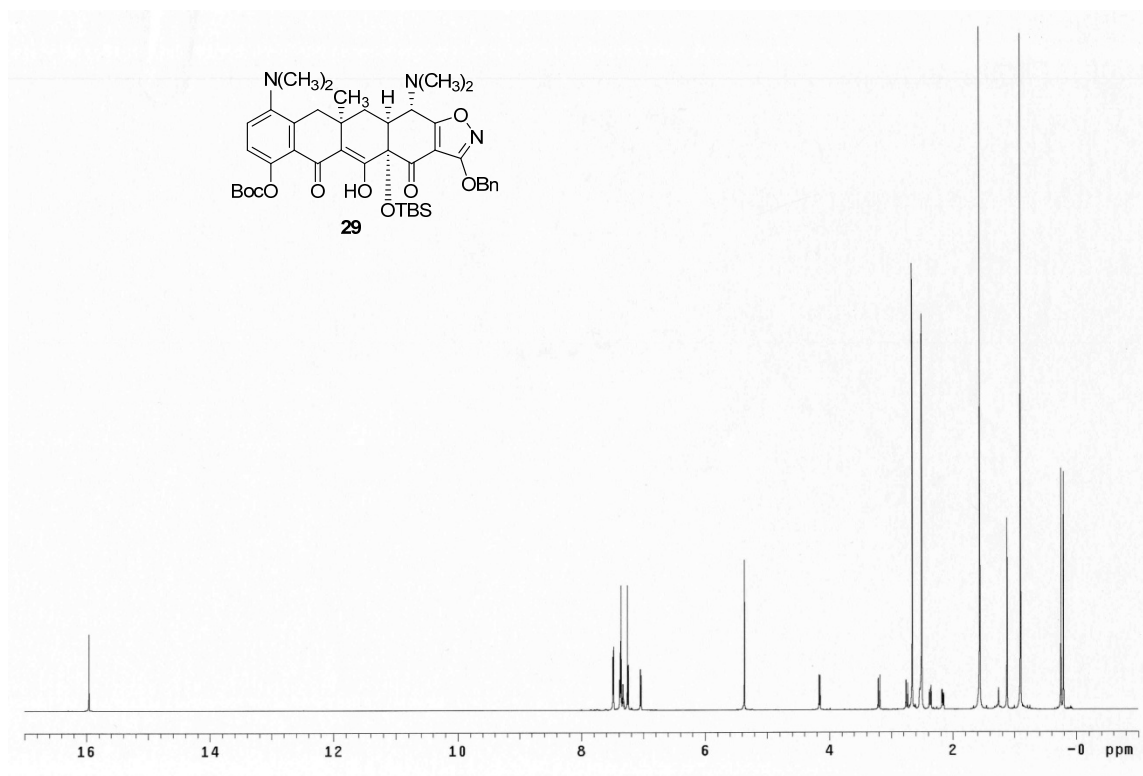


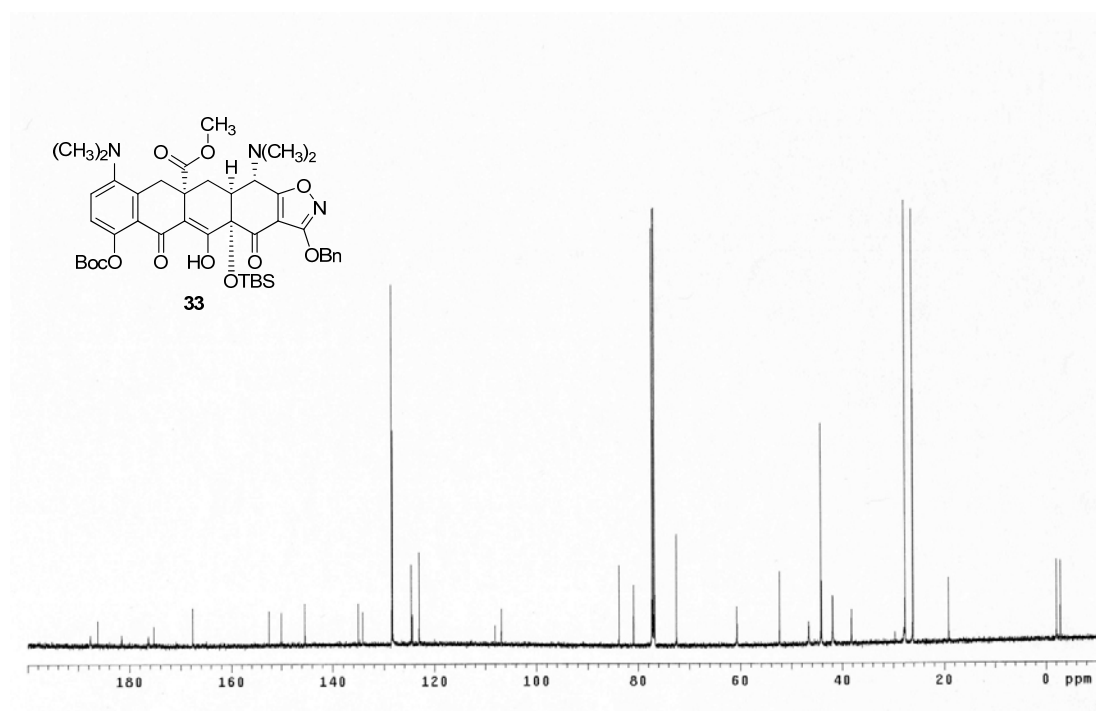
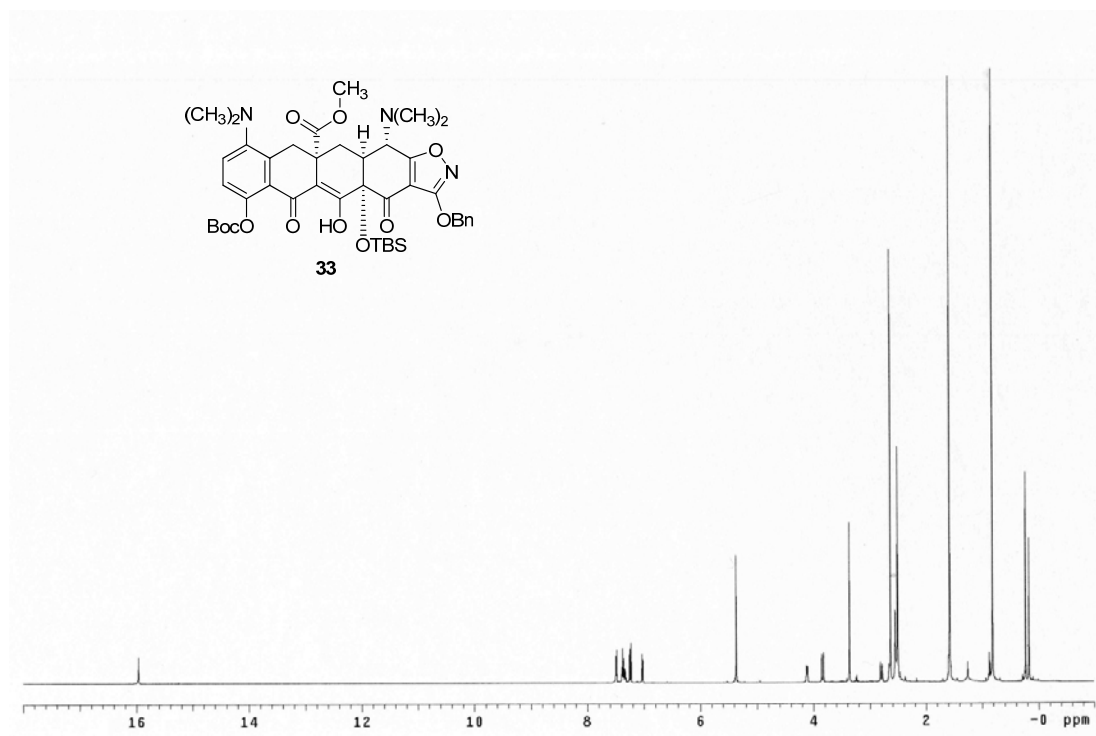


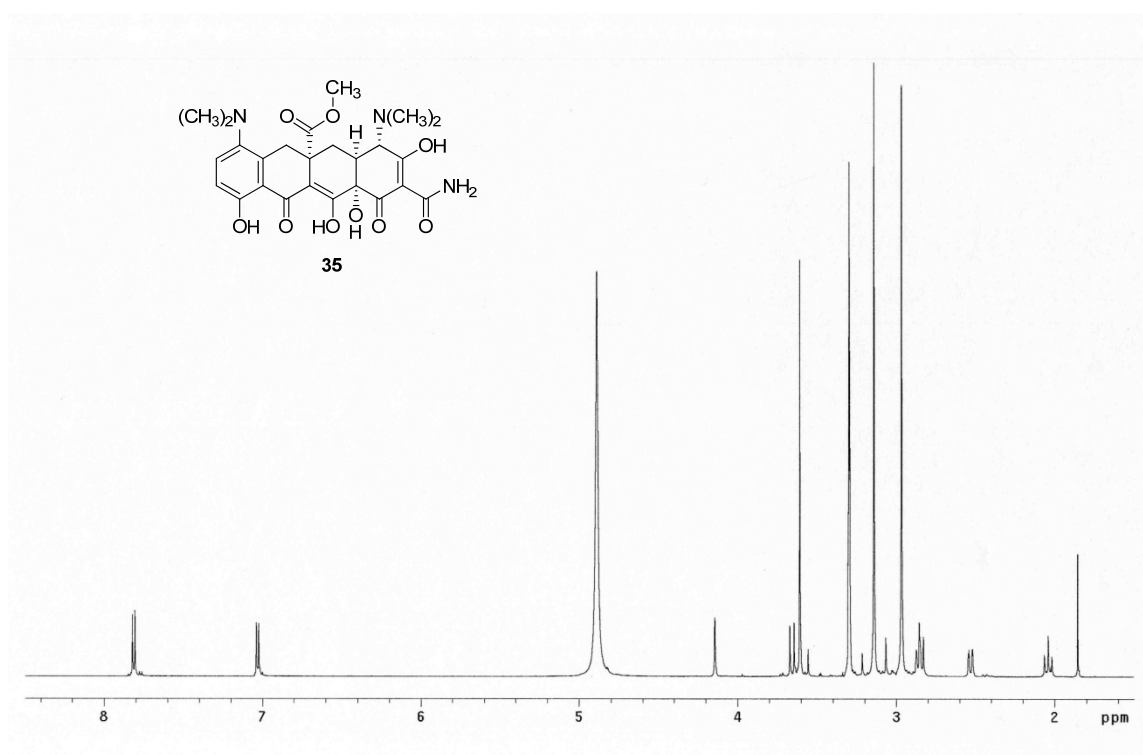
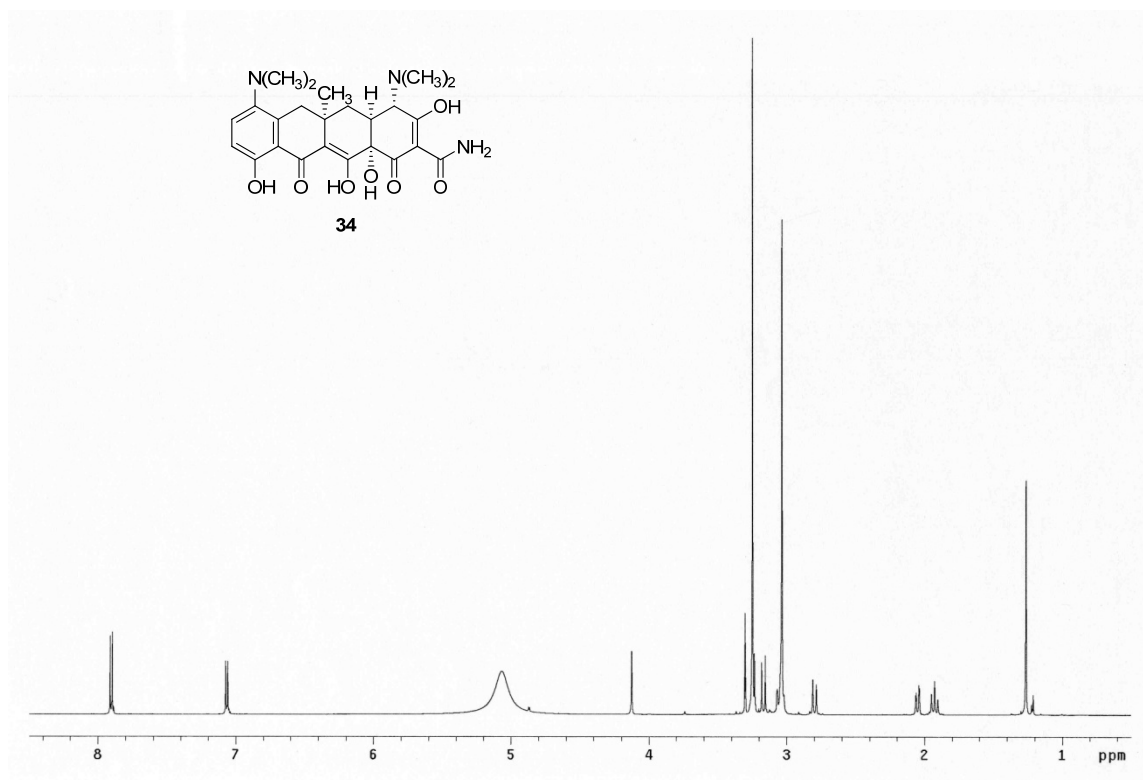


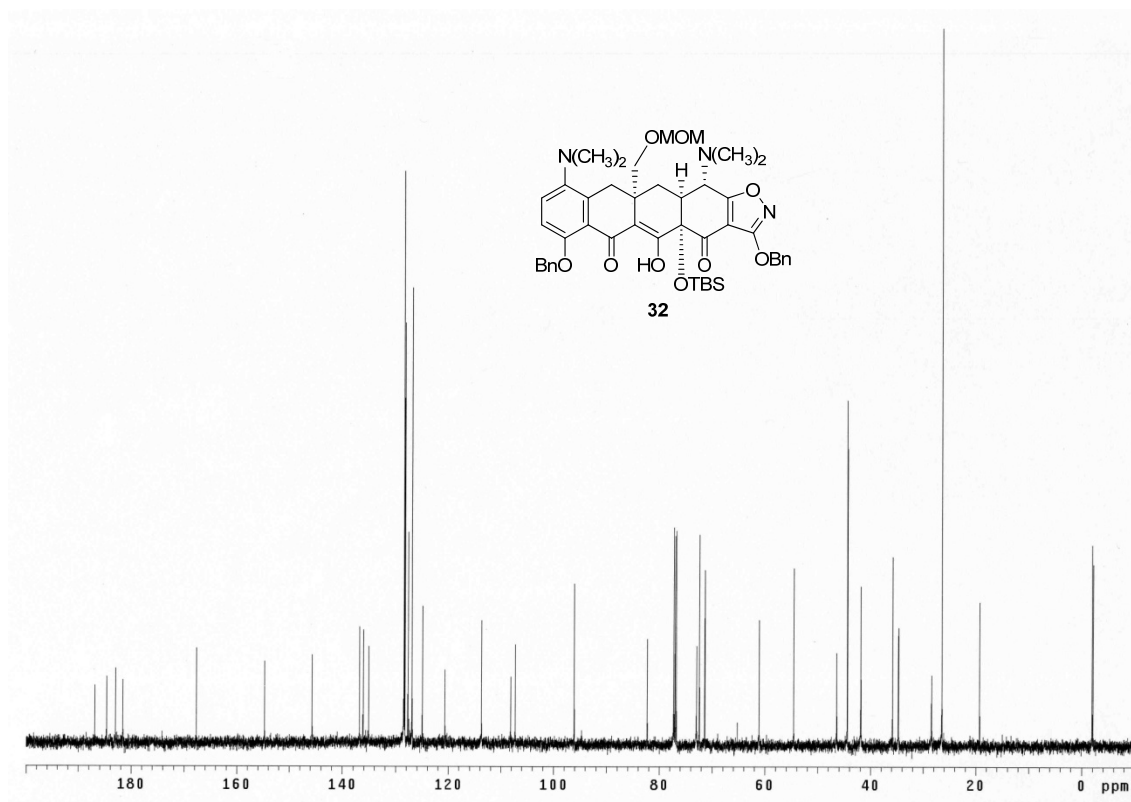
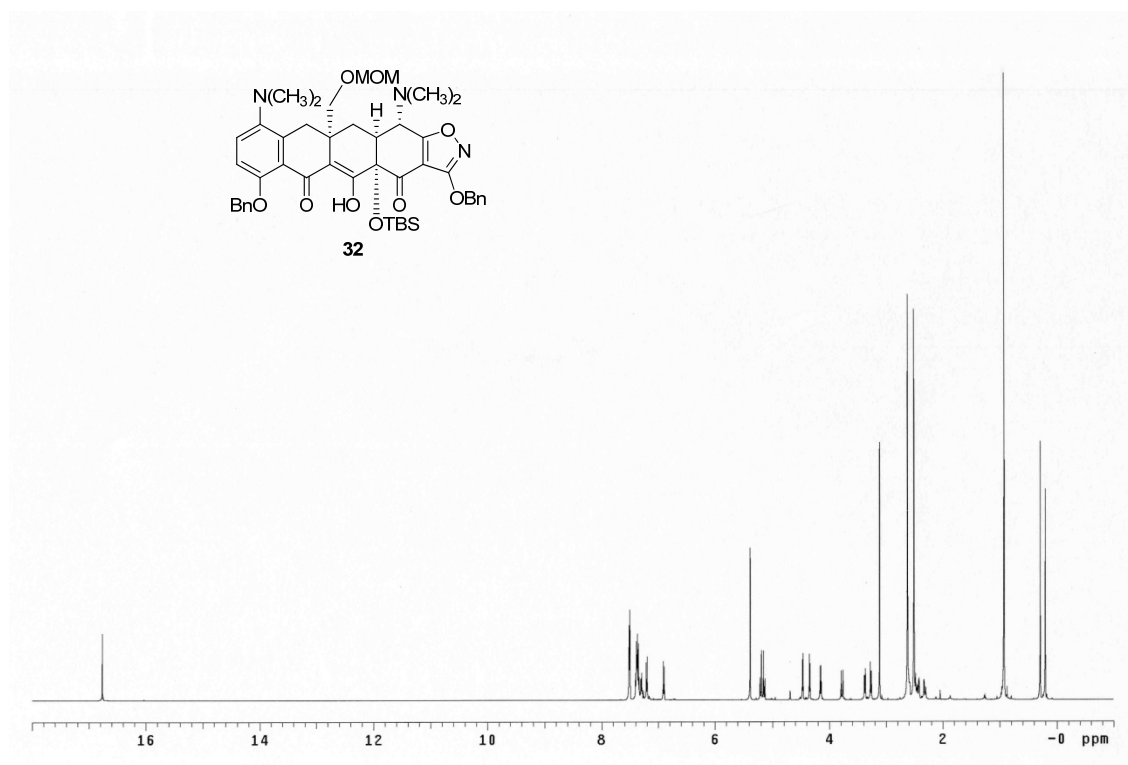


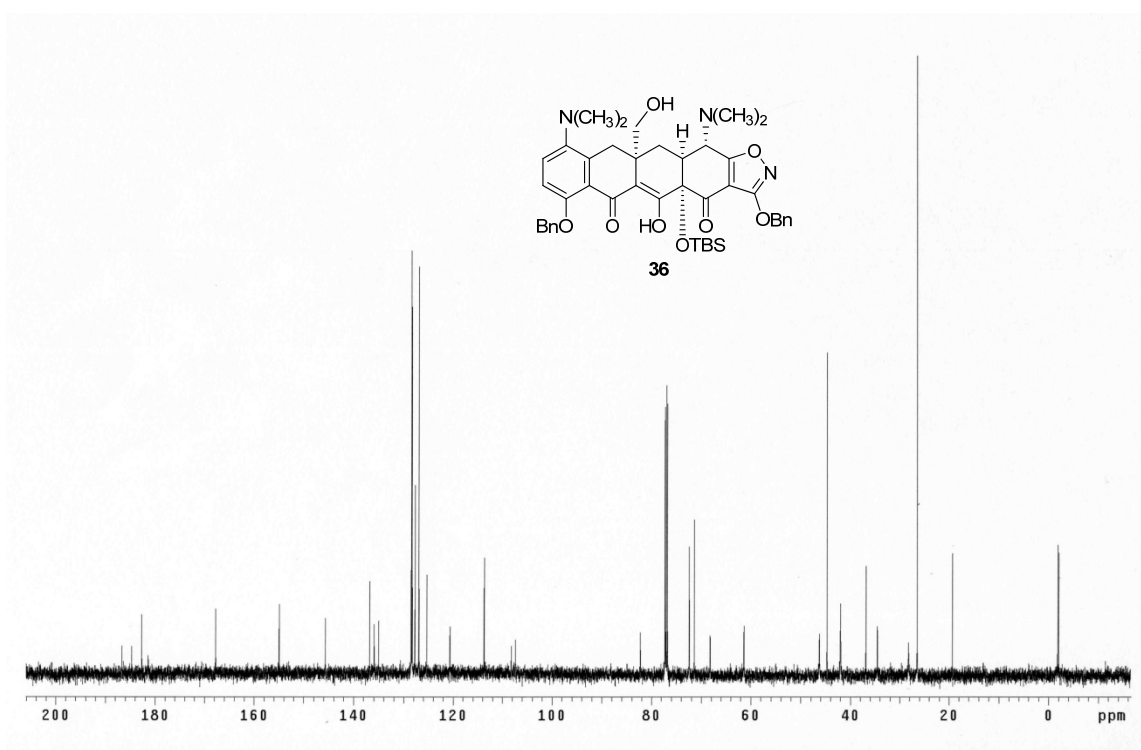
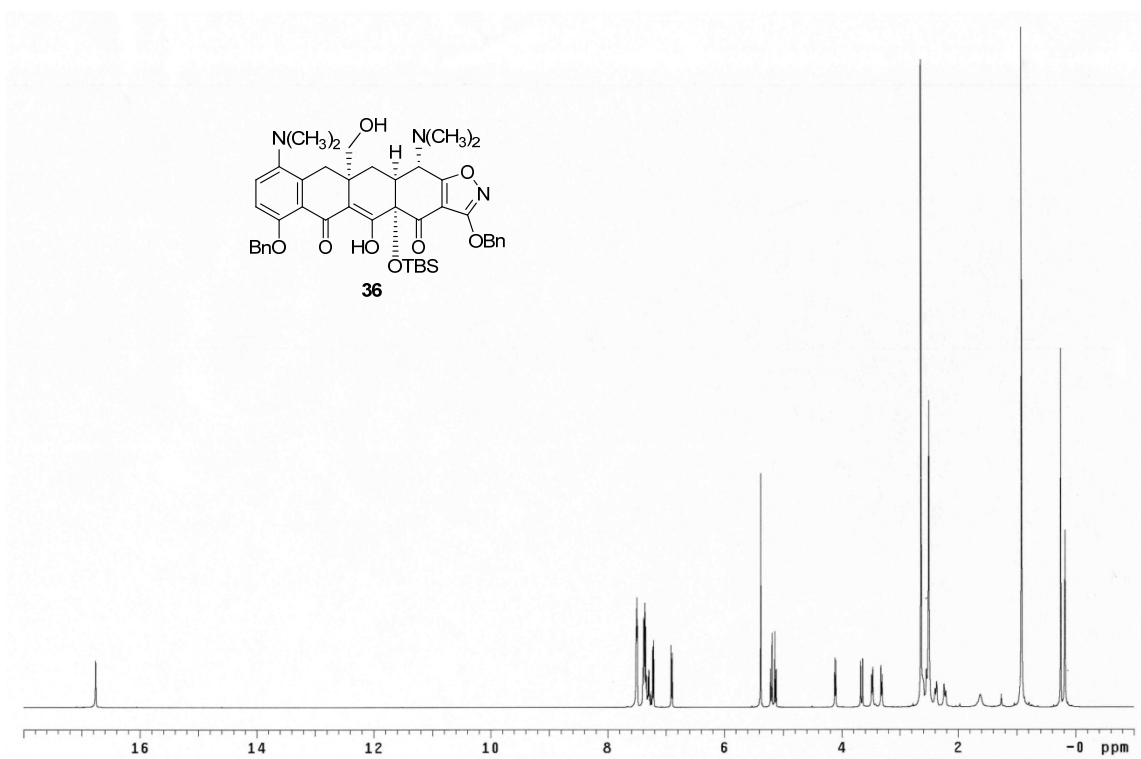


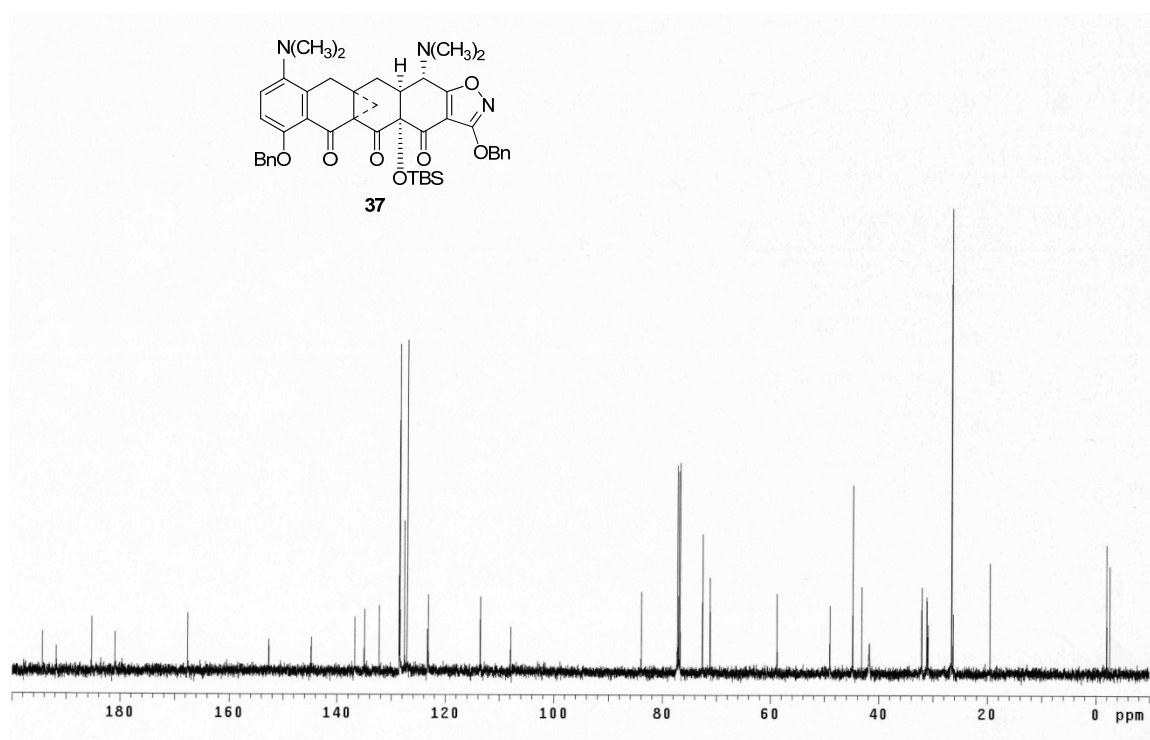
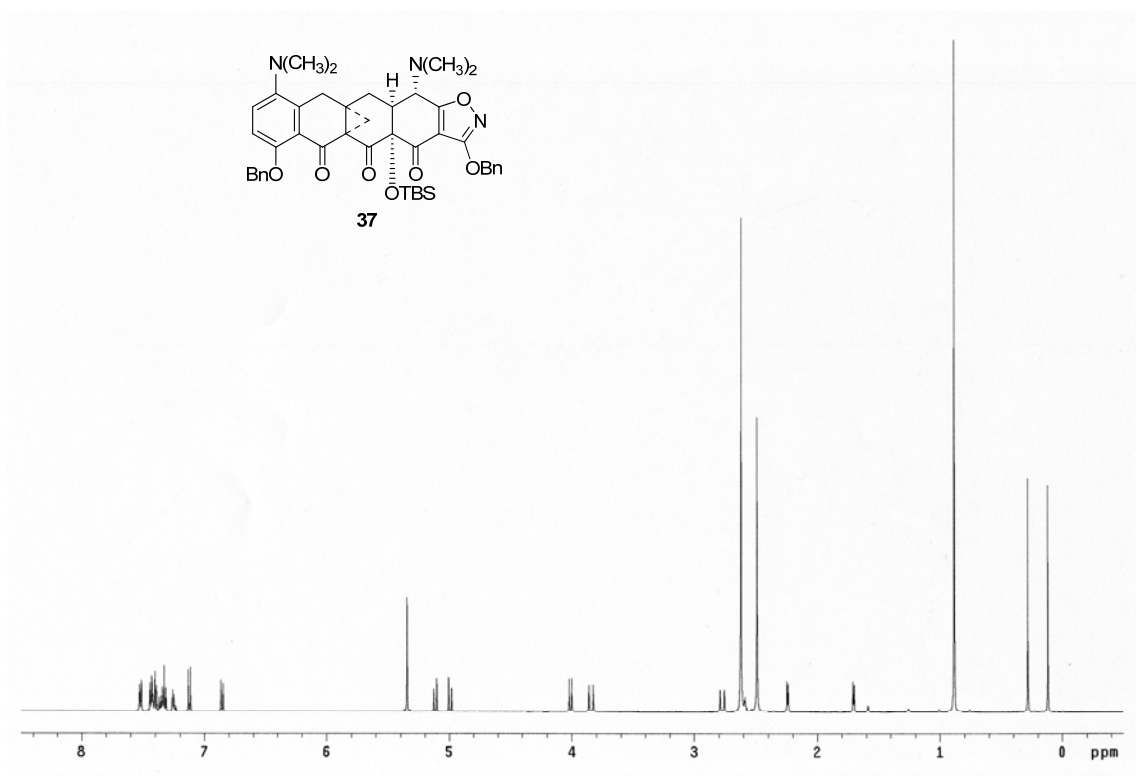


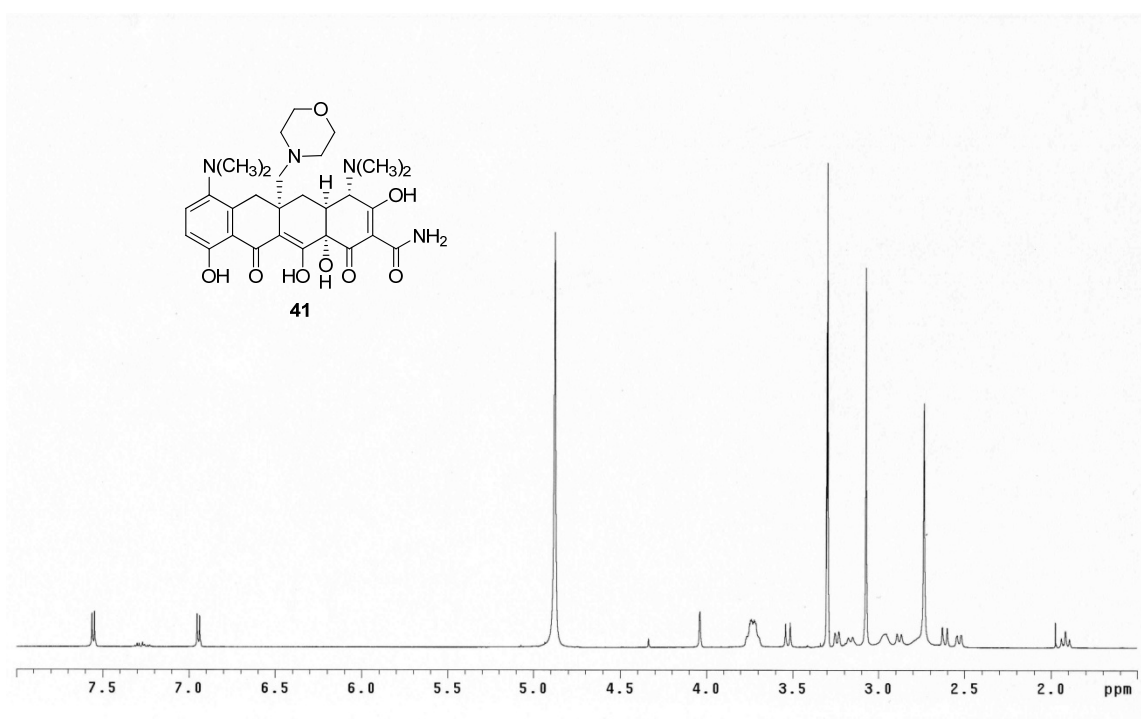
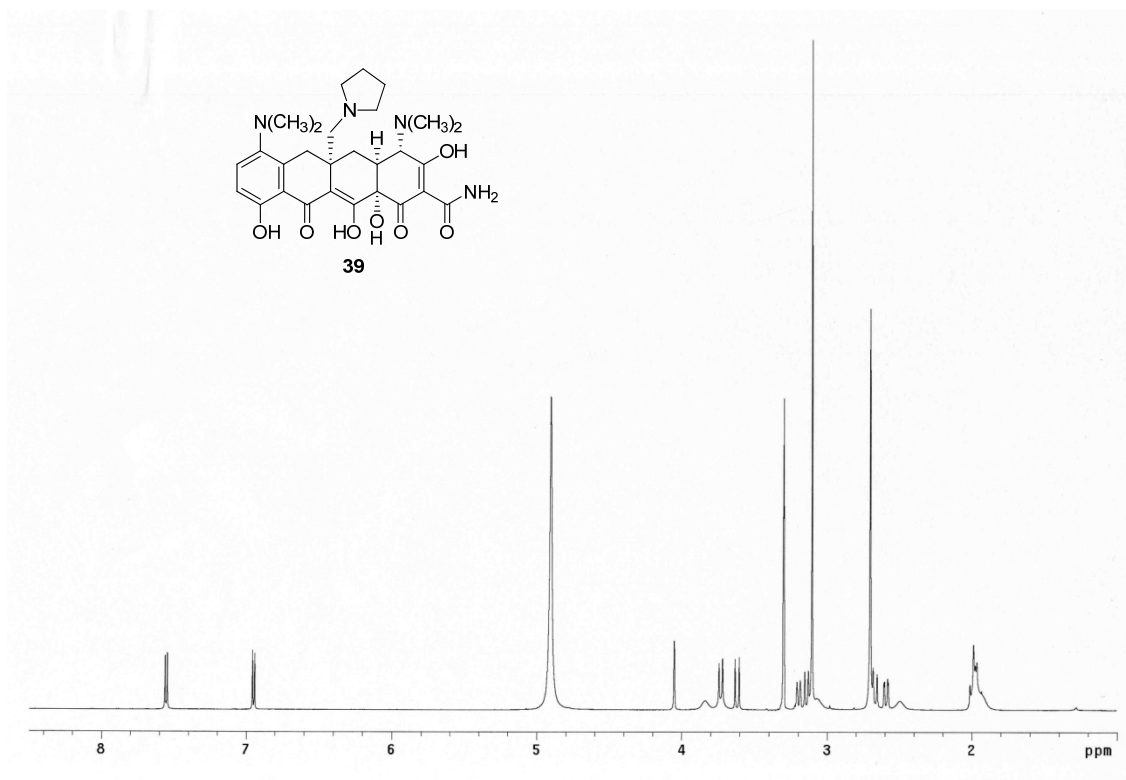


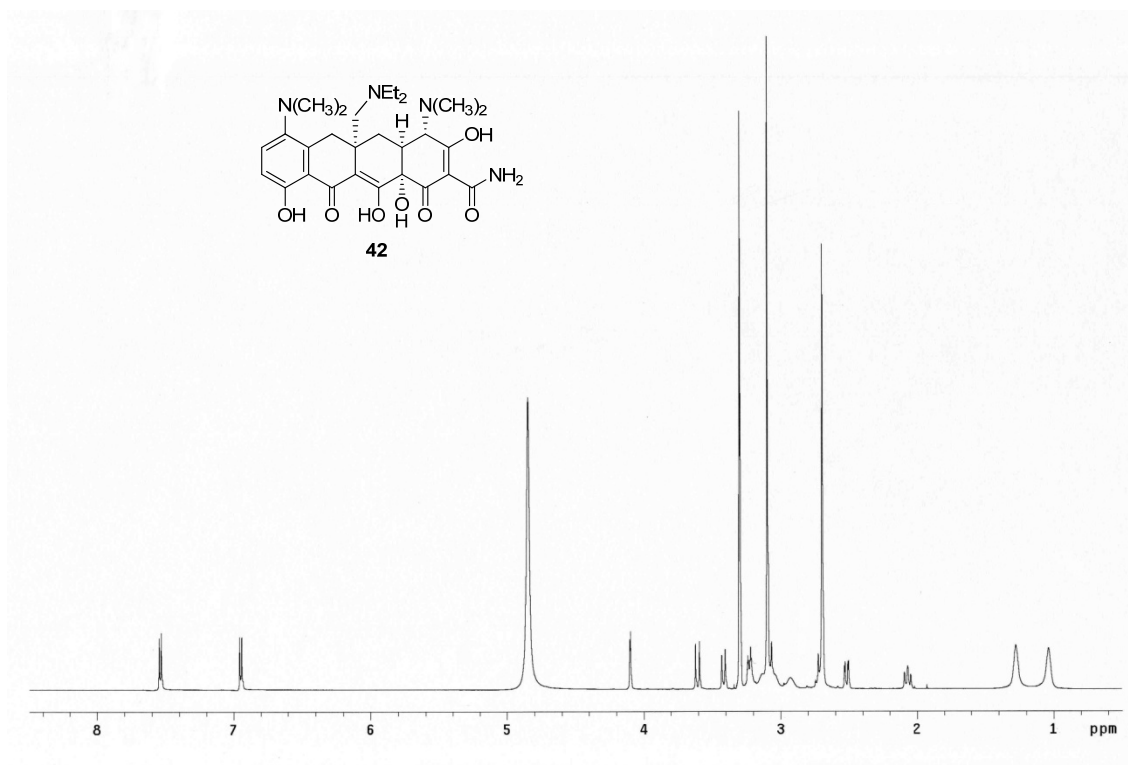
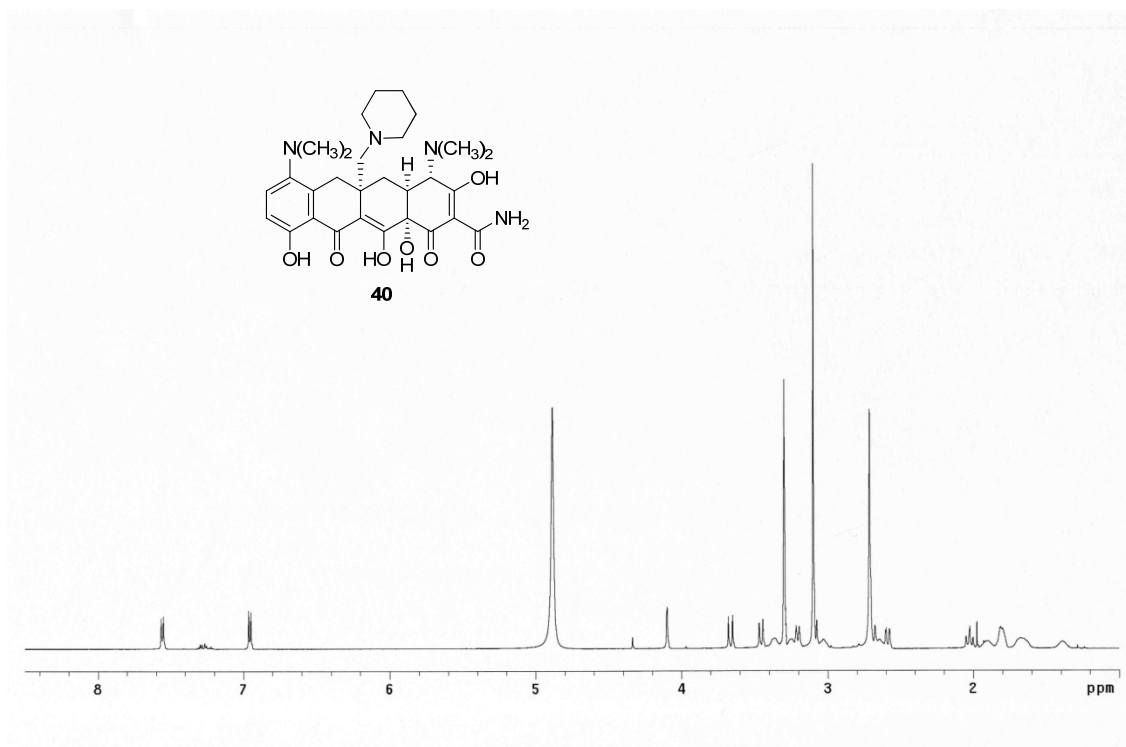


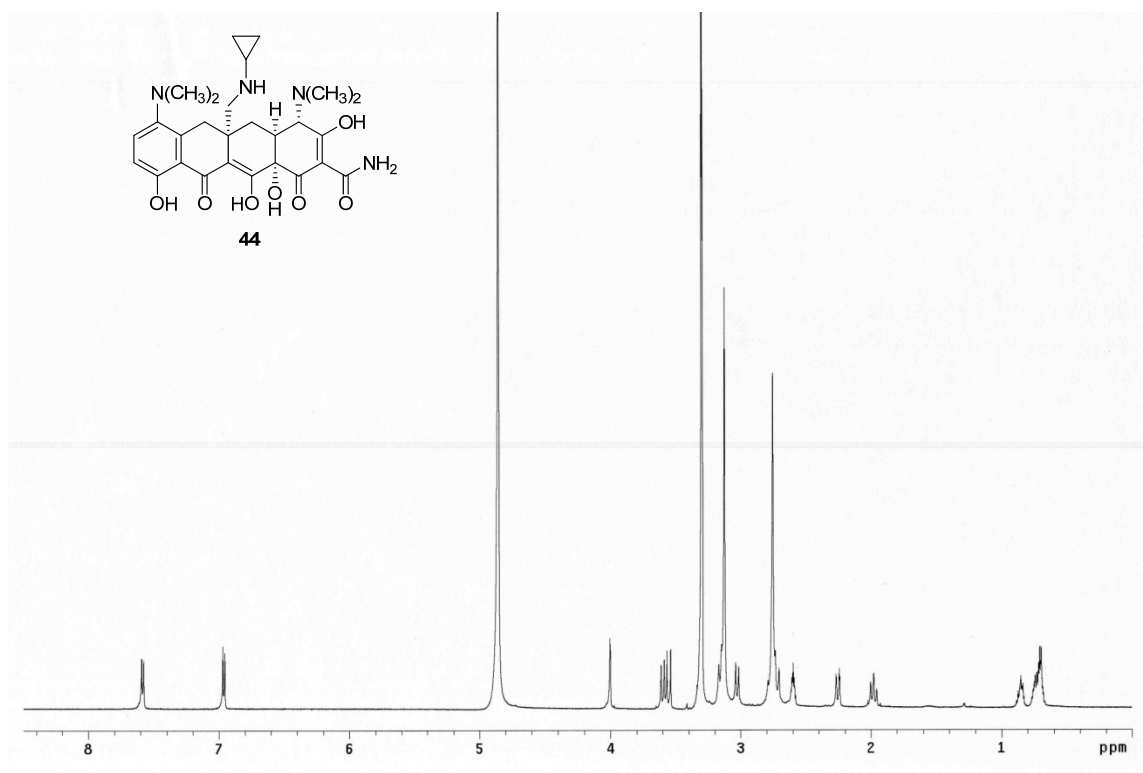
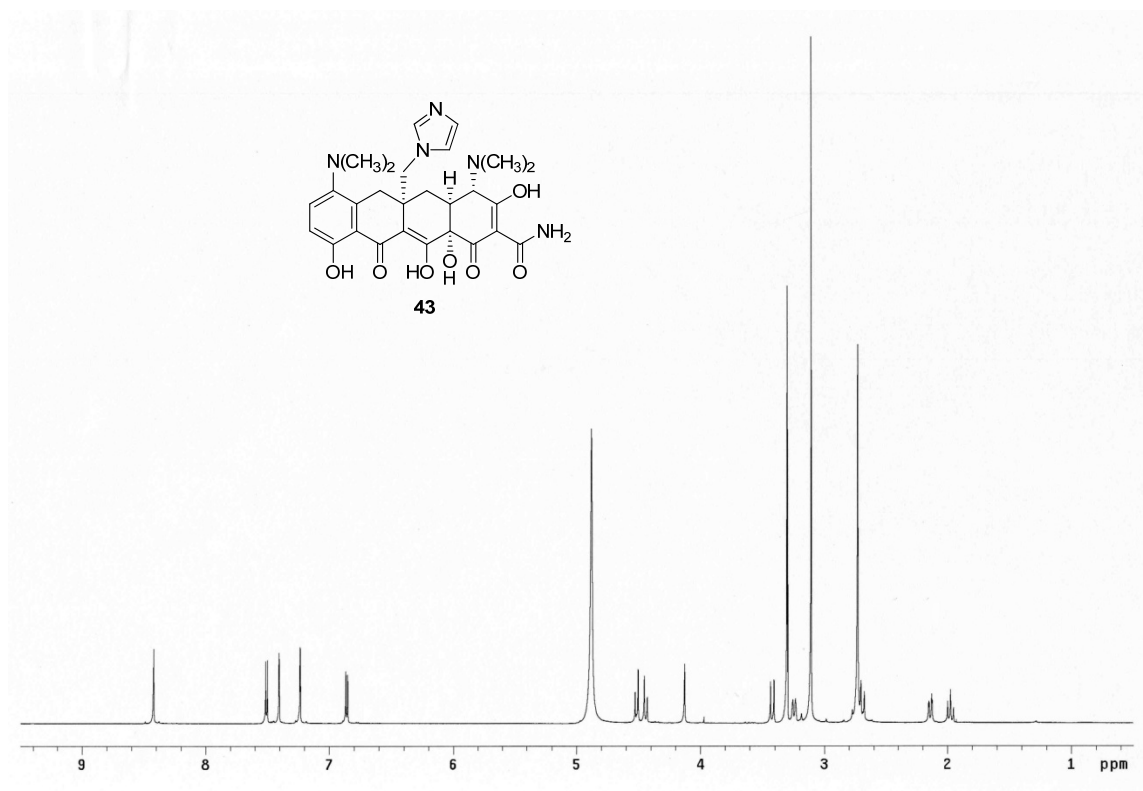


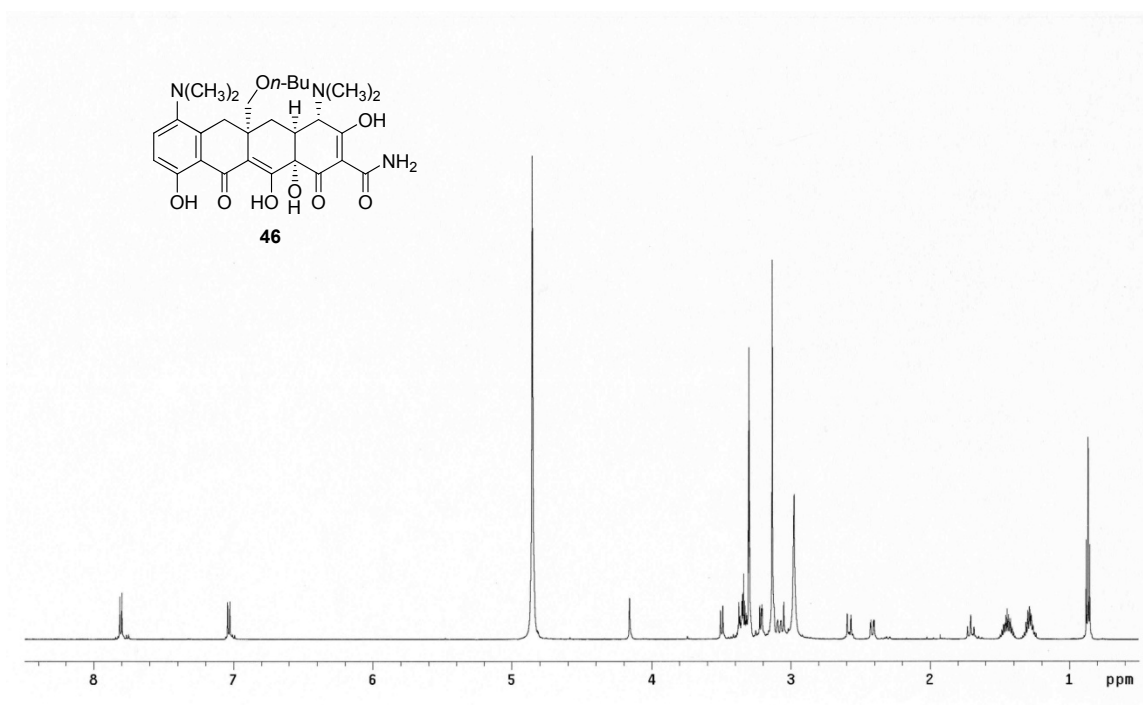
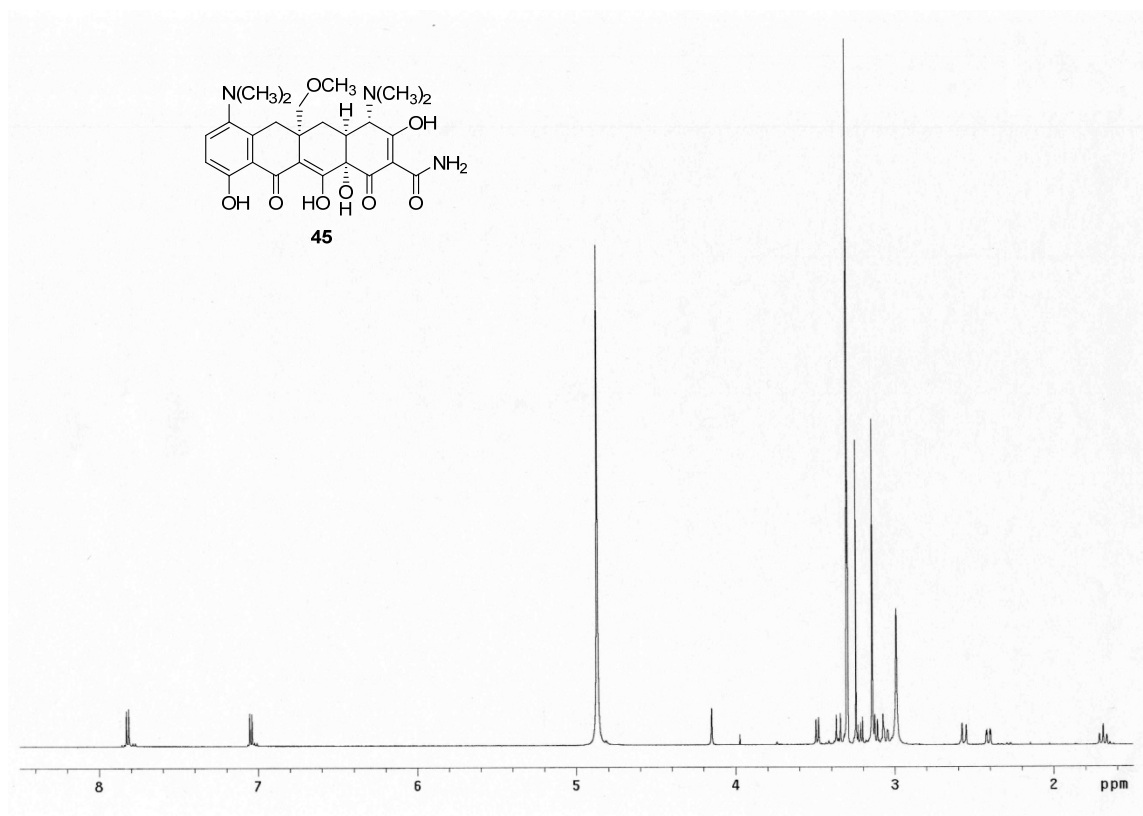


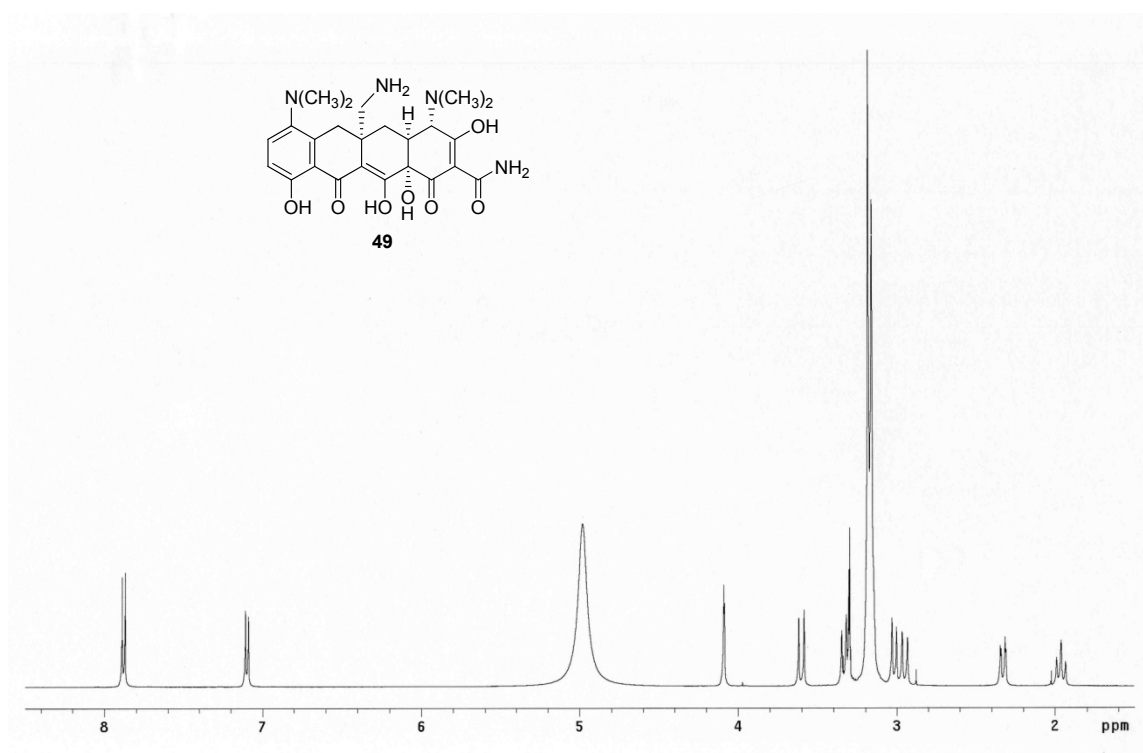
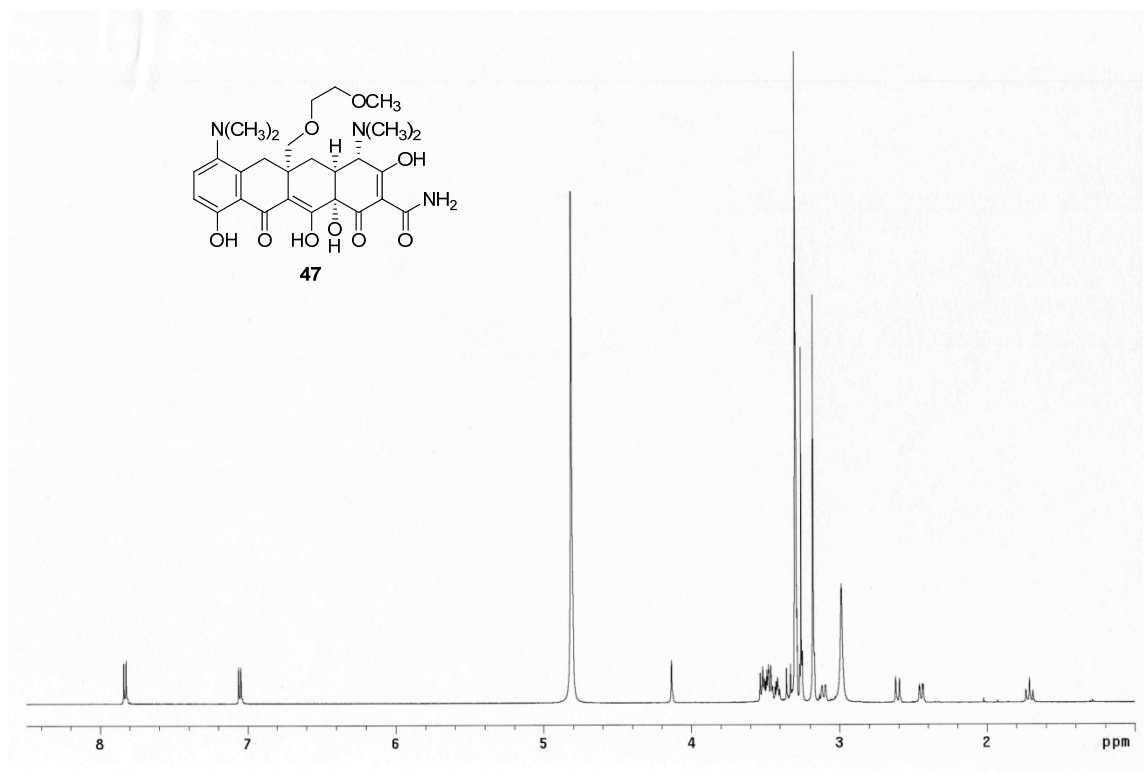


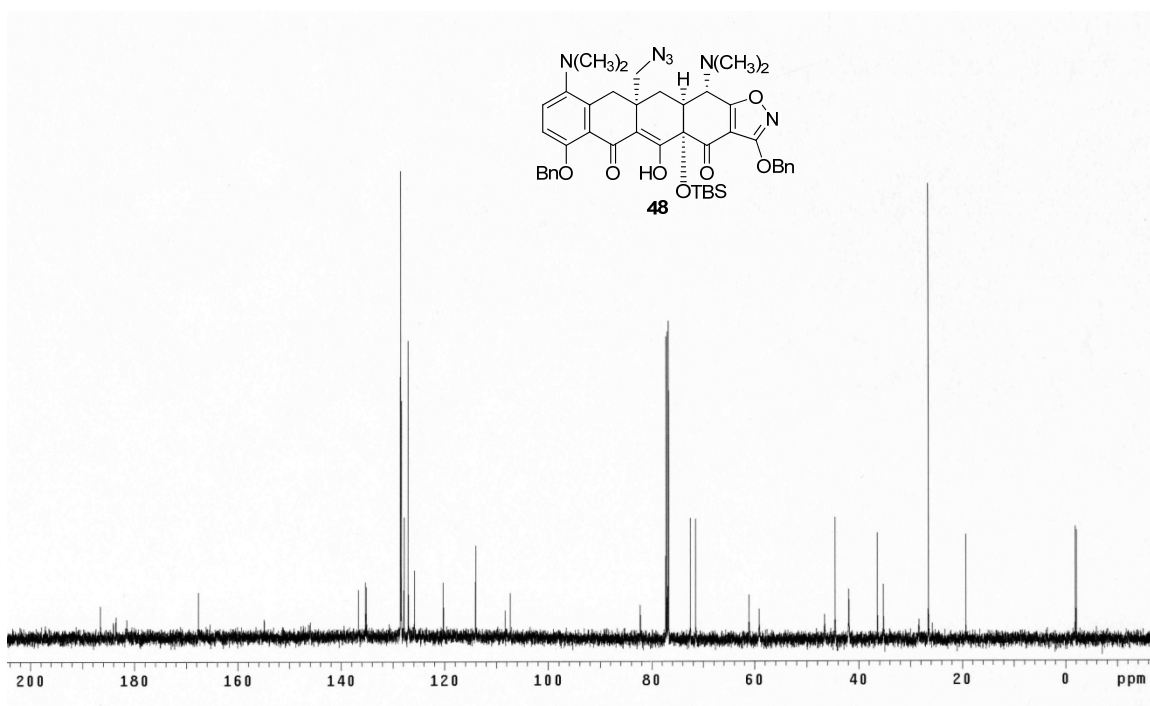
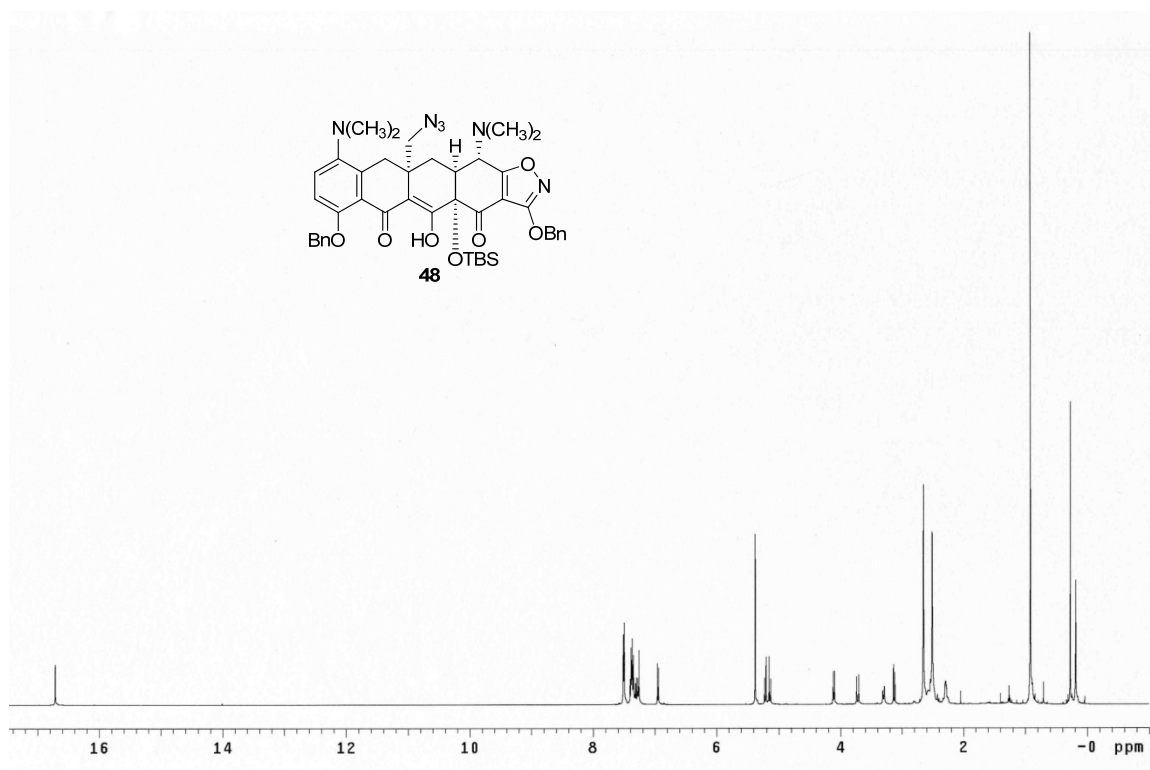


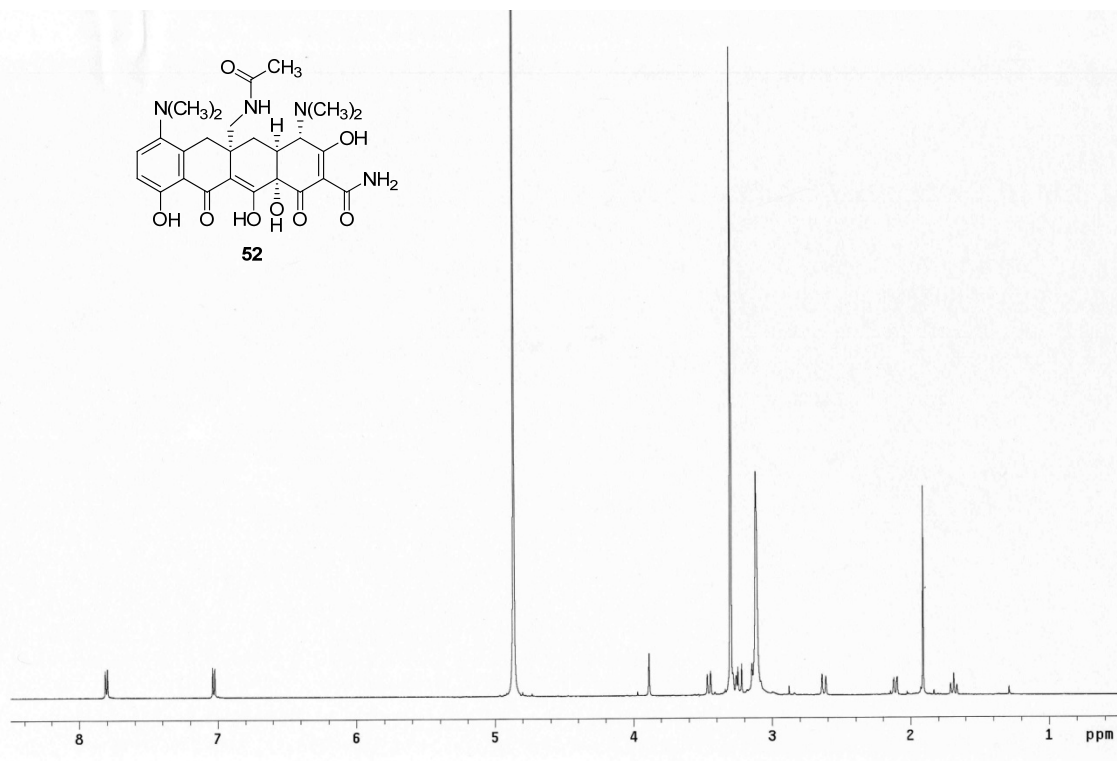
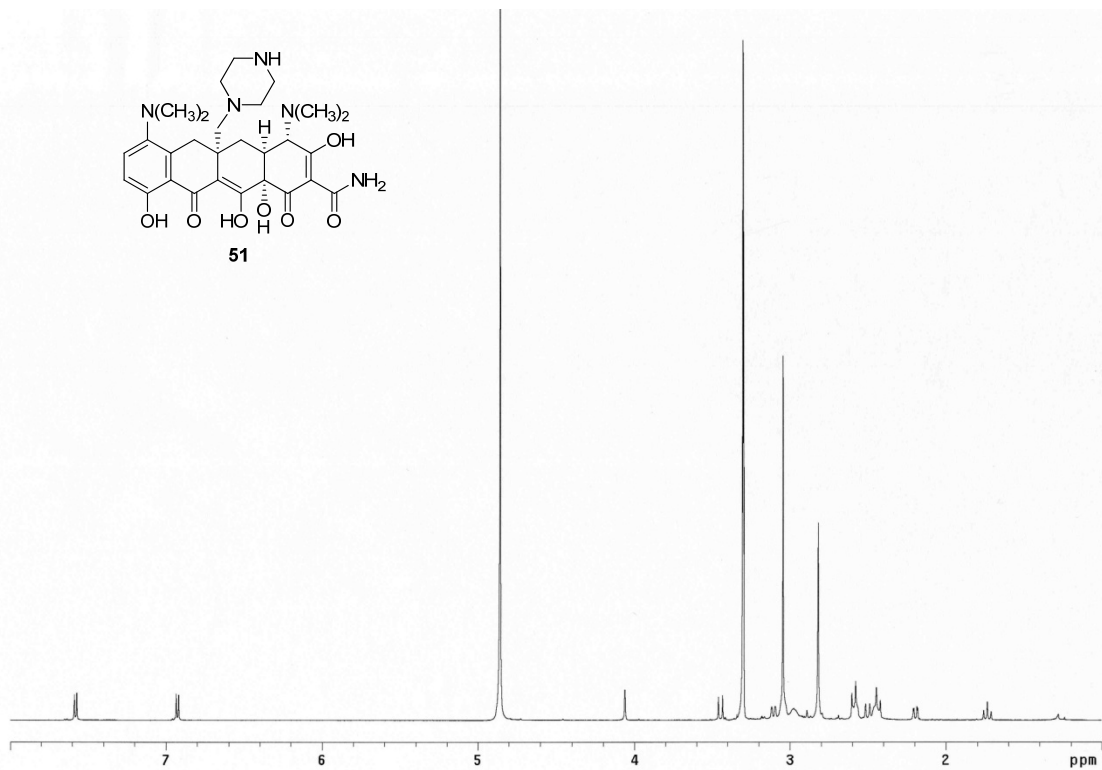


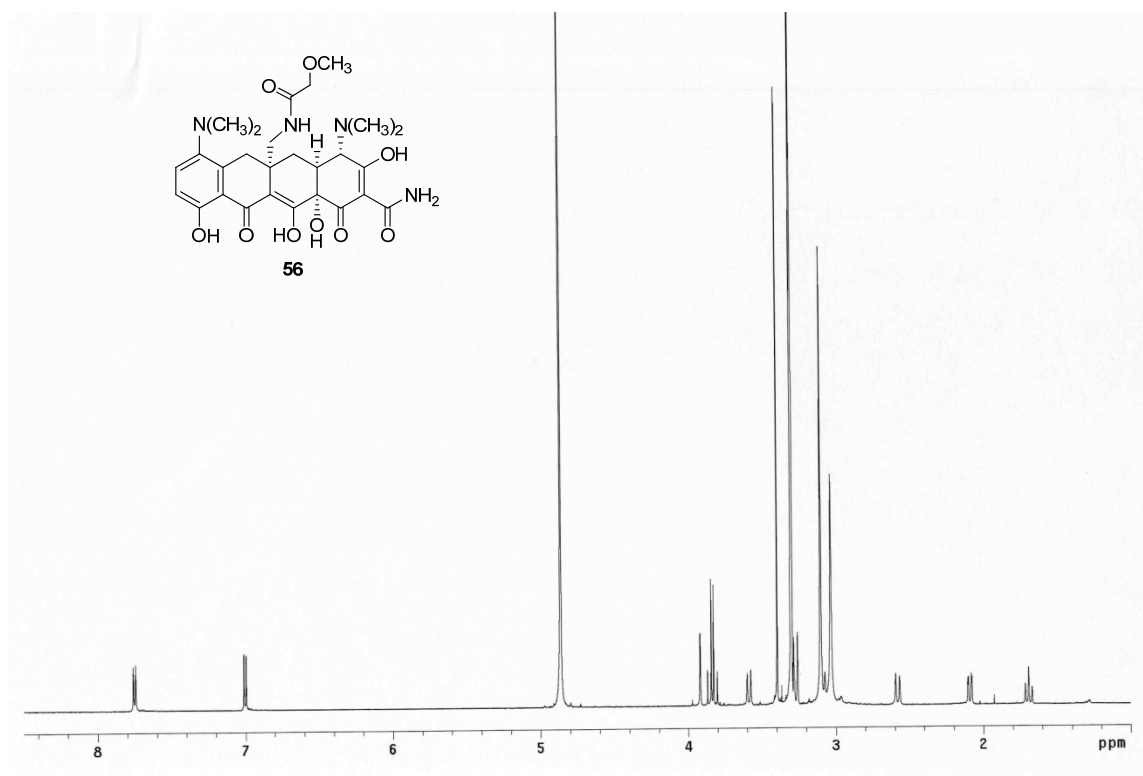
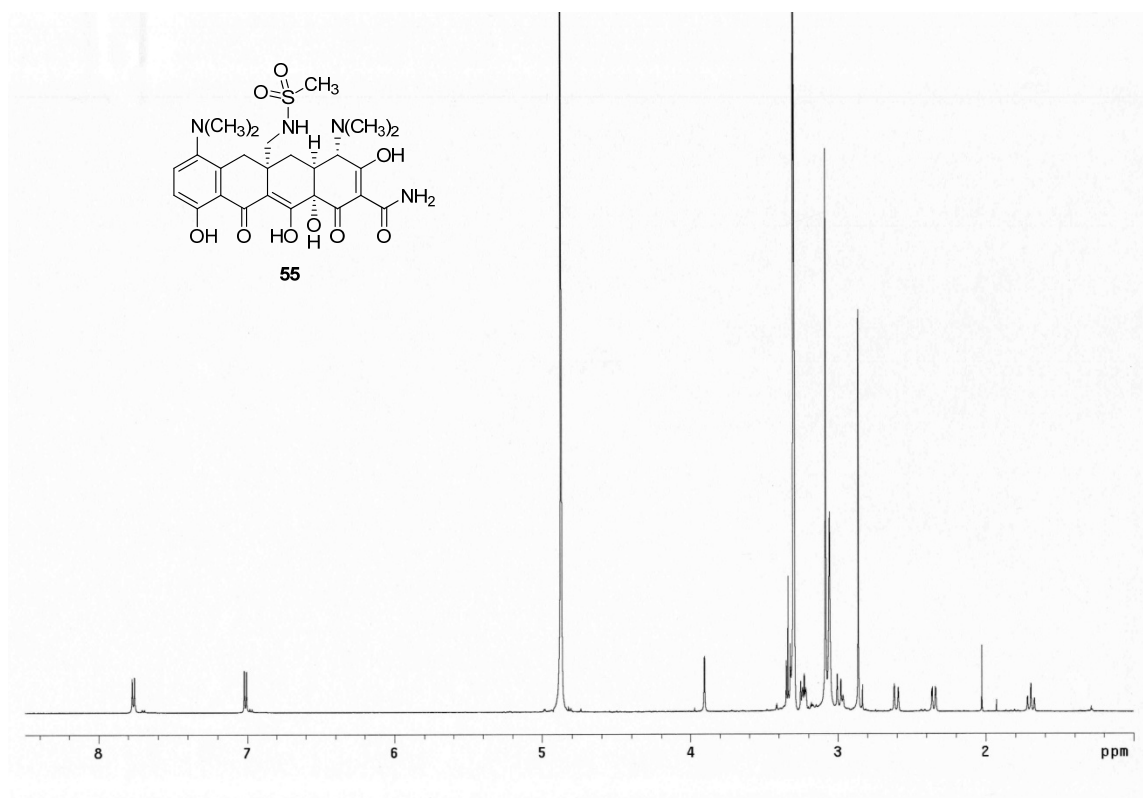


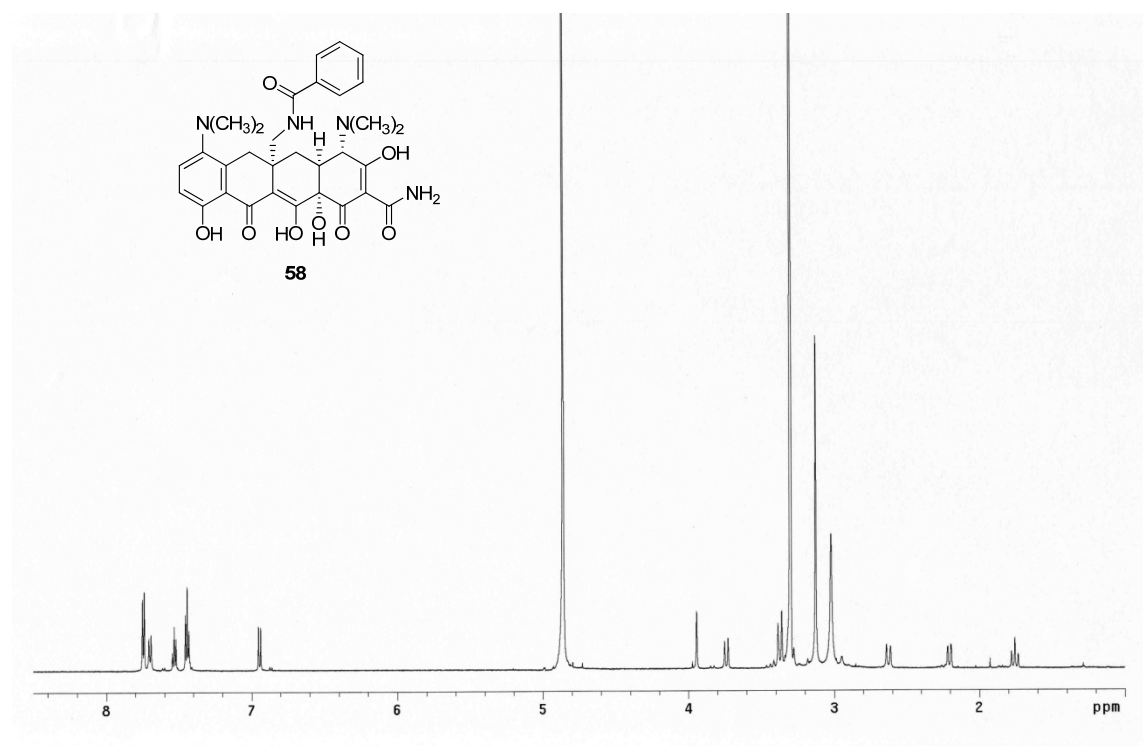
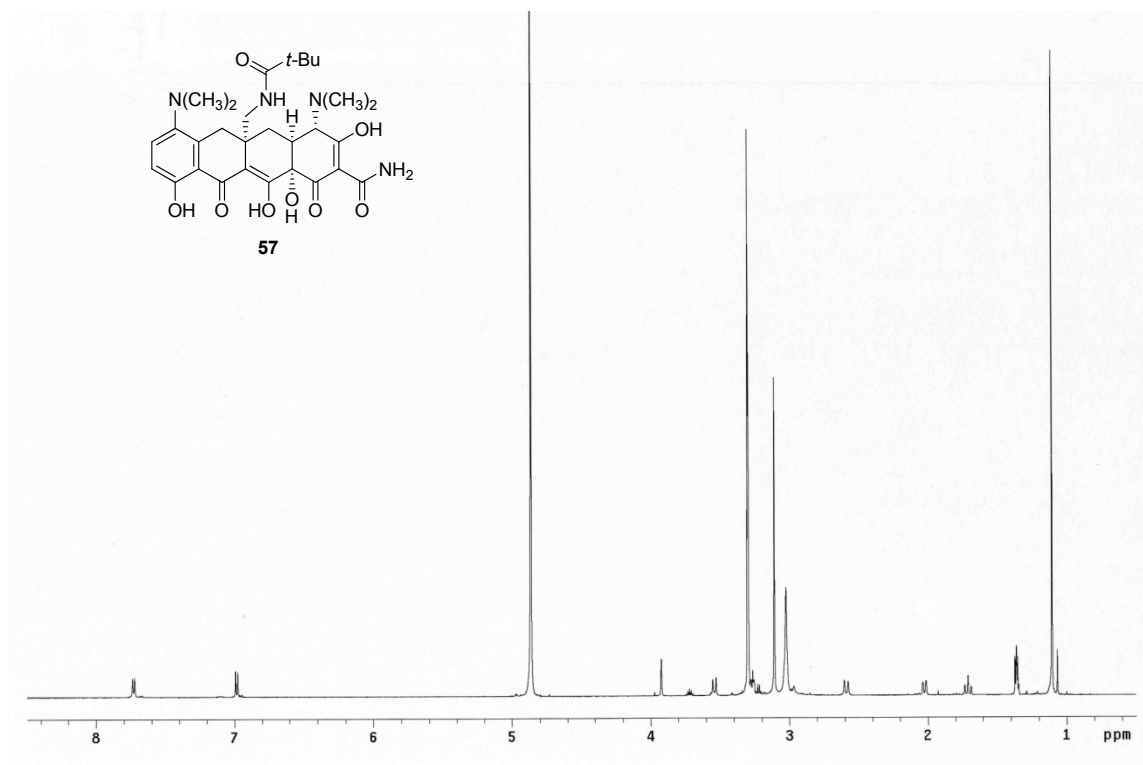












Chapter 3

Synthesis of C5-Substituted Tetracyclines

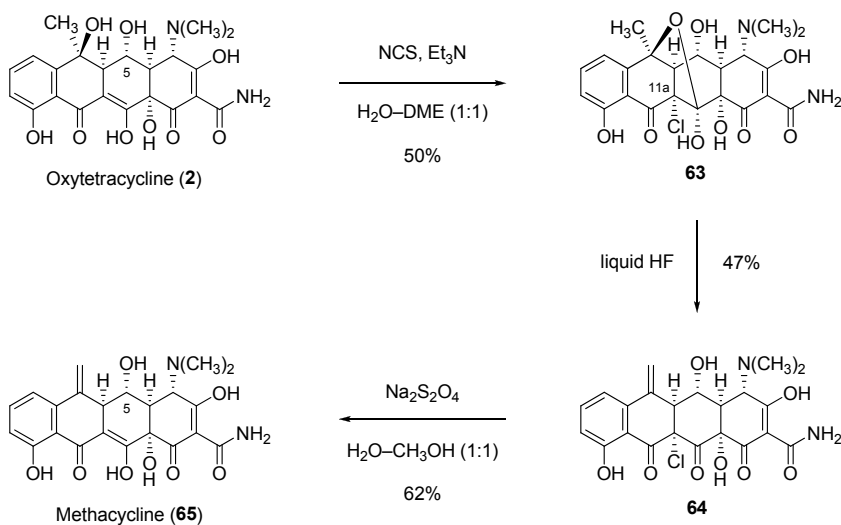
Introduction

Oxytetracycline (**2**, Scheme 3.1) is the only naturally-occurring tetracycline with substitution at C5.⁸⁶ Methacycline (**65**) and doxycycline (**7**), semisynthetic tetracycline antibiotics which are derived from oxytetracycline, retain the C5 hydroxyl substituent found in the natural product. The synthesis of methacycline is presented in Scheme 3.1 below. Treatment of oxytetracycline with *N*-chlorosuccinimide (NCS) in 50% aqueous 1,2-dimethoxyethane in the presence of triethylamine affords chlorinated product **63**.⁸⁷ The 11a-chloro substituent prevents formation of anhydrotetracyclines (which contain an aromatic C ring) in subsequent steps. Exocyclic dehydration of **63** in the presence of anhydrous hydrogen fluoride provides exo-methylene **64**, which is then converted into methacycline (**65**) upon reductive removal of the 11a-chloro substituent with sodium hydrosulfite. Doxycycline (**7**) was originally isolated from the mixture of products obtained by palladium-catalyzed hydrogenolysis of oxytetracycline. It is now prepared on an industrial scale by hydrogenation of methacycline (**65**) in the presence of a rhodium metal complex (Scheme 3.2 below).⁸⁸ Following its approval in 1967, doxycycline became Pfizer's first once-a-day, broad-spectrum antibiotic. The utility of doxycycline has declined due to increasingly widespread bacterial resistance, but it is still used frequently to treat acne, rosacea, chlamydia, syphilis and rickettsial infections.

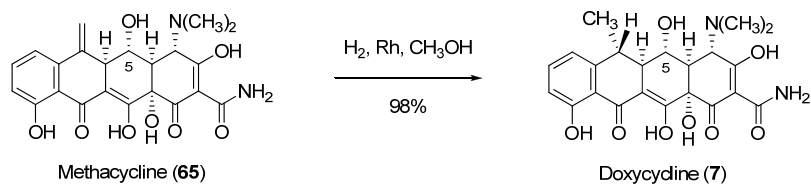
⁸⁶ *Tetracyclines in Biology, Chemistry and Medicine*; Nelson, M., Hillen, W., Greenwald, R. A., Eds.; Birkhauser: Boston, 2001.

⁸⁷ (a) Blackwood, R. K.; Beereboom, J. J.; Rennhard, H. H.; Schach Von Wittenau, M.; Stephen, C. R. *J. Am. Chem. Soc.* **1961**, 83, 2773–2775. (b) Blackwood, R. K.; Beereboom, J. J.; Rennhard, H. H.; Schach Von Wittenau, M.; Stephen, C. R. *J. Am. Chem. Soc.* **1963**, 85, 3943–3953.

⁸⁸ Villax, I.; Page, P. U.S. Patent 4,500,458, **1985**.



Scheme 3.1. Synthesis of methacycline (65) from oxytetracycline (2).



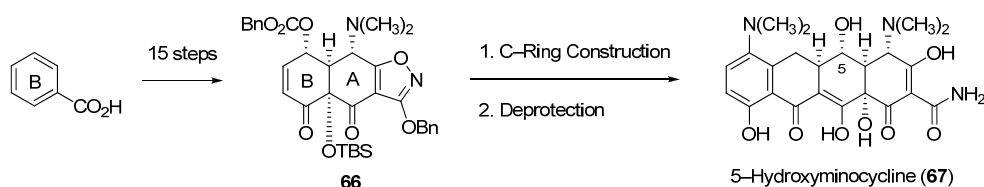
Scheme 3.2. Synthesis of doxycycline (7) from methacycline (65).

A limited range of tetracyclines with modified C5 substituents has been prepared by semisynthesis.⁸⁹ The C5 hydroxyl group of doxycycline can be oxidized using dimethyl sulfoxide and acetic anhydride to provide the corresponding ketone (5-deoxy-5-oxo-doxycycline), which was found to be inactive. In addition, selective esterification of

⁸⁹ Cunha, B. A. Clinical Uses of Tetracyclines. In *Handbook of Experimental Pharmacology*; Hlavka, J. J. and Boothe, J. H., Eds.; Springer-Verlag: New York, 1985; pp 393–403.

the C5 secondary carbinol can be achieved by treatment of tetracyclines with carboxylic acids in the presence of strong acids such as HF and CH₃SO₃H (esterification of the C12a tertiary carbinol does not occur under these conditions). Tetracyclines with ester substituents at C5 were generally found to be less active than the corresponding C5-hydroxy compounds, although certain C5-esters exhibited notable activity against tetracycline-resistant Gram-positive organisms. The 5-formyl derivatives of methacycline and doxycycline were reported to be more active than their parent compounds.

The first-generation synthesis of the AB enone **10** also provided access to an AB precursor with a protected hydroxyl group at the γ -position (enone **66**, Scheme 3.3).⁹⁰ Dr. Qui Wang, a postdoctoral researcher in the Myers laboratory, converted oxygenated AB enone **66** to 5-hydroxyminocycline (**67**). This fully synthetic tetracycline was found to be 2- to 4-fold less active than minocycline against most bacterial strains tested (and significantly less active against others).

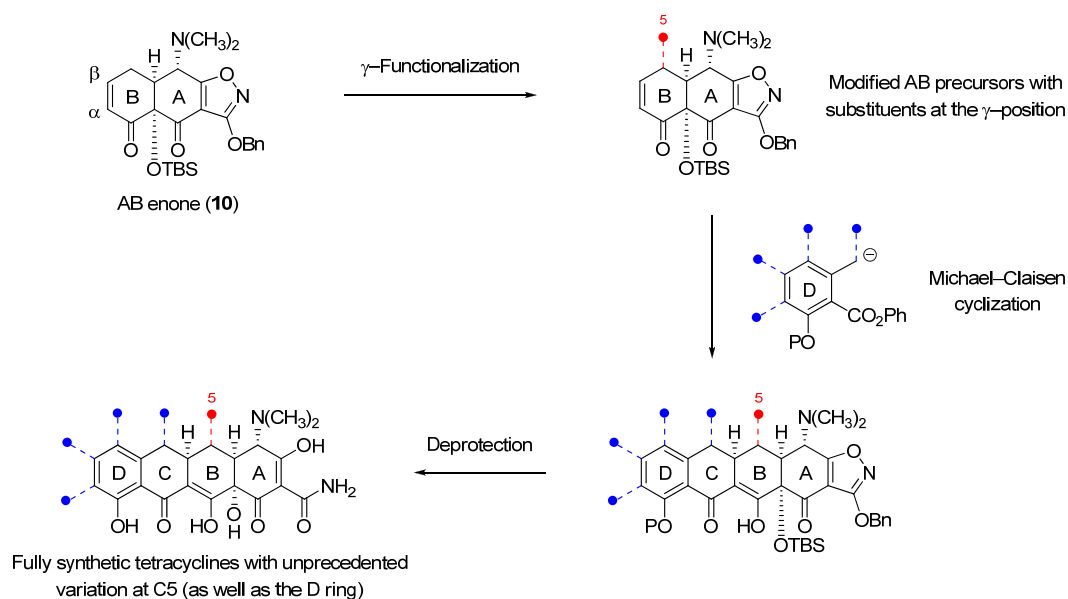


Scheme 3.3. Synthesis of 5-hydroxyminocycline (**67**) from oxygenated AB enone **66**.

The lack of knowledge of structure-activity relationships at position C5 led us to consider expansion of our fully synthetic platform to enable a thorough analysis of this

⁹⁰ Charest, M. G.; Lerner, C. D.; Brubaker, J. D.; Siegel, D. R.; Myers, A. G. *Science* **2005**, *308*, 395–398.

chemical space. The availability of large quantities of the AB enone **10** meant that this compound could be used as starting material for these investigations. We envisioned preparing fully synthetic tetracyclines with unprecedented modifications at C5 by Michael–Claisen cyclizations of diverse γ -substituted AB precursors with D-ring precursors, followed by deprotection (Scheme 3.4). In this chapter, the development of chemical pathways for transformation of the AB enone **10** into a range of γ -substituted AB enones and then C5-substituted tetracyclines will be described.

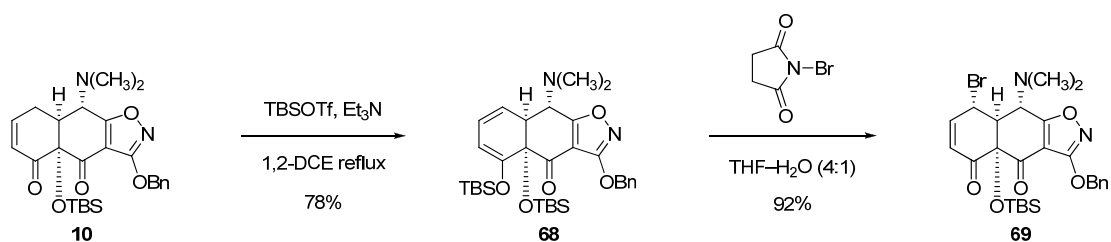


Scheme 3.4. Synthesis of fully synthetic C5-substituted tetracyclines from γ -substituted AB enones.

Results

The chemical reactivity that has formed the foundation of our efforts to prepare γ -substituted AB precursors was discovered by Dr. Evan Hecker, a post-doctoral researcher in the Myers laboratory. The AB enone **10** was first converted to *tert*-butyldimethylsilyl dienol ether **68** in 78% yield by heating a solution of **10**, *tert*-butyldimethylsilyl trifluoromethanesulfonate (1.5 equiv) and triethylamine (3 equiv) in 1,2-dichloroethane at reflux for 18 h (Scheme 3.5). Treatment of a solution of *tert*-butyldimethylsilyl dienol ether **68** in the solvent mixture 4:1 tetrahydrofuran–water with *N*-bromosuccinimide (NBS) at 23 °C then afforded γ -(α)-bromo AB precursor **69** as a single diastereomer in 92% yield. This stereochemical assignment was supported by NOE studies and confirmed by X-ray crystallography (Figure 3.1). The regio- and stereo-selectivity of this bromination reaction are striking. The γ -selectivity of electrophilic addition may be governed by electronic effects,⁹¹ but could also be augmented by significant steric hindrance on both faces of the silyl dienol ether **68** at the α -position (presumably **68** adopts a similar conformation to the AB enone **10**). The (α)-stereochemistry of the bromo substituent results from selective electrophilic addition to the “lower” convex face of silyl dienol ether **68**.

⁹¹ For a discussion of the factors governing the regioselectivity of vinylogous aldol reactions of silyl dienol ether nucleophiles, see: Denmark, S. E.; Heemstra Jr., J. R.; Beutner, G. L. *Angew. Chem. Int. Ed.* **2005**, *44*, 4682–4698.



Scheme 3.5. Two-step synthesis of γ -(α)-bromo AB precursor **69** from the AB enone **10**.

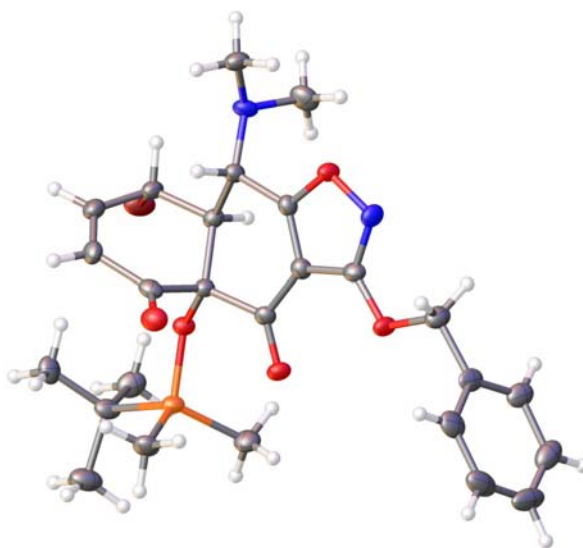
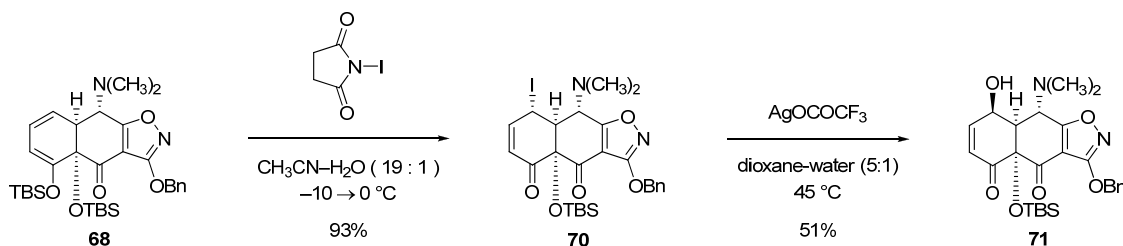


Figure 3.1. X-ray crystal structure of γ -(α)-bromo AB precursor **69**.

Building upon this result, I chose to pursue the synthesis of an intermediate which could be more easily diversified than γ -bromo enone **69**. Addition of *N*-iodosuccinimide to a solution of silyl dienol ether **68** in acetonitrile and water (19:1 mixture) at $-10\text{ }^{\circ}\text{C}$, followed by warming to $0\text{ }^{\circ}\text{C}$ afforded γ -(α)-iodo AB enone **70** (Scheme 3.6). Exclusion of light during reaction, work-up and purification enabled isolation of γ -iodo enone **70** in

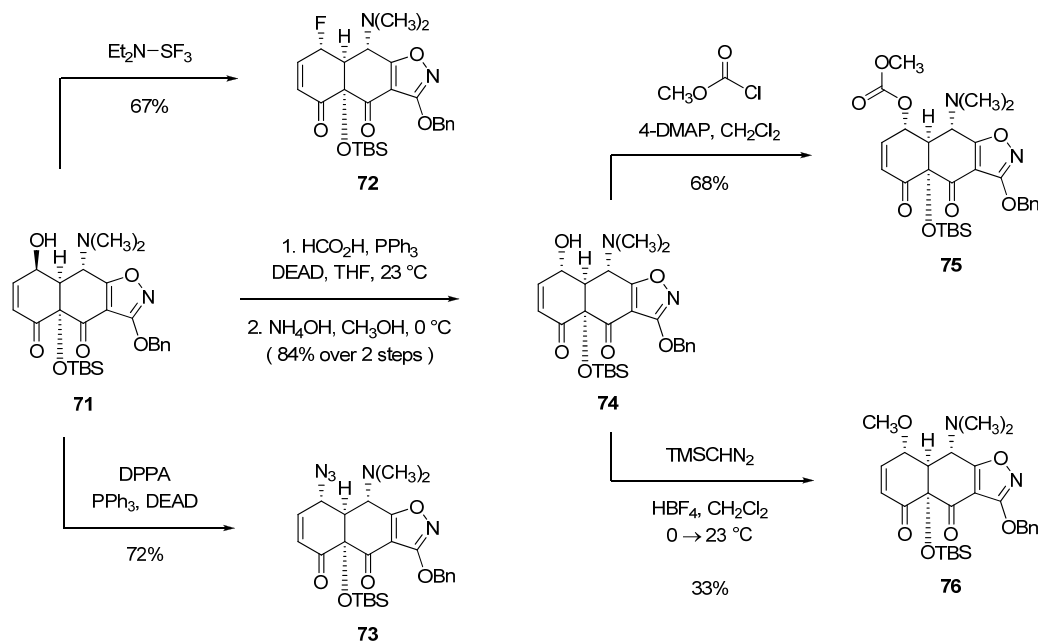
93% yield (11-g batch). Crucially, treatment of a solution of γ -iodo enone **70** in dioxane and water (5:1 mixture) with silver (I) trifluoroacetate (1 equiv) and heating of this mixture at 45 °C provided γ -(β)-hydroxy AB enone **71** in 51% yield.



Scheme 3.6. Two-step synthesis of γ -(β)-hydroxy AB enone **71** from *tert*-butyldimethylsilyl dienol ether **68**.

γ -(β)-Hydroxy enone **71** was then transformed into a diverse range of γ -substituted AB precursors (Scheme 3.7). Activation of the γ -hydroxy group of **71** followed by nucleophilic displacement provided enone products with various substituents on the “lower” face at the γ -position. Treatment of a solution of **71** in dichloromethane with diethylamino sulfur trifluoride (DAST) at 0 °C following by warming to 23 °C afforded γ -fluoro AB enone **72** in 67% yield. Similarly, sequential addition of triphenylphosphine, diethyl azodicarboxylate (DEAD) and diphenyl phosphoryl azide (DPPA) to a solution of **71** in THF at 23 °C provided γ -azido AB enone **73** (72% yield). Furthermore, the γ -hydroxy substituent of enone **71** could be straightforwardly inverted by Mitsunobu reaction with formic acid followed by deformylation of the formate ester intermediate upon treatment with ammonium hydroxide in methanol at 0 °C, providing γ -

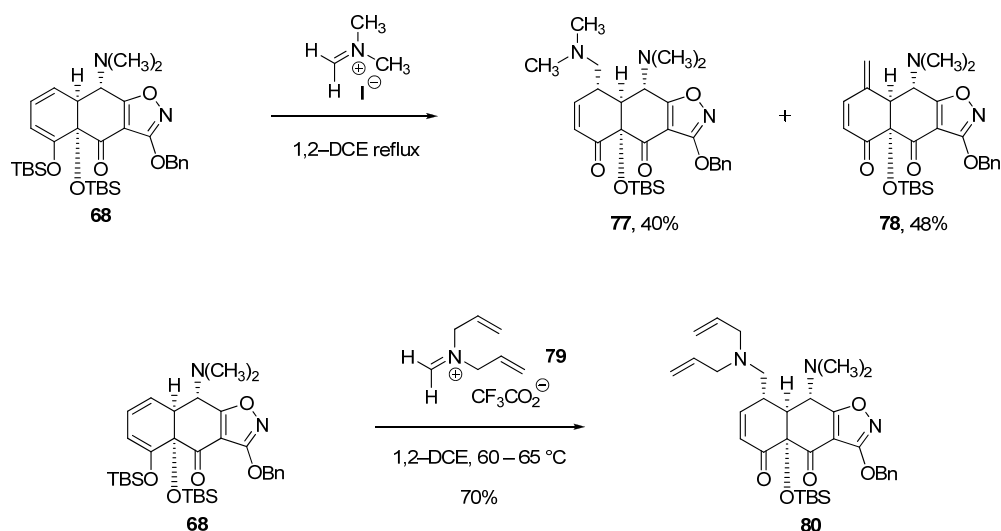
(α)-hydroxy AB enone **74**. The hydroxyl group of **74** was then straightforwardly alkylated and acylated to provide new AB precursors **75** and **76** (Scheme 3.7).



Scheme 3.7. Synthesis of diverse γ -substituted AB precursors from γ -(β)-hydroxy enone **71**.

tert-Butyldimethylsilyl dienol ether **68** also served as a precursor to AB enones with one-carbon extensions at the γ -position (Scheme 3.8). Addition of *N,N*-dimethylmethyleneiminium chloride (Eschenmoser's salt, 1.2 equiv) to a solution of silyl dienol ether **68** in 1,2-dichloroethane and heating of this mixture at reflux for 14 h afforded a mixture of γ -dimethylaminomethyl AB enone **77** (40%) and γ -exo-methylene enone **78** (48%). This useful reactivity was then harnessed to provide an enone with a protected aminomethyl substituent at the γ -position (**80**). In this case, aminoalkylation

was achieved using a diallylimmonium trifluoroacetate salt (**79**) developed by Knochel.⁹² Formation of the γ -exo-methylene enone by-product (**78**) in this reaction was minimized by: (1) adding electrophile **79** (4 equiv) in a portionwise manner, and (2) employing a lower reaction temperature (60–65 °C). These procedural modifications enabled isolation of γ -diallylaminomethyl AB precursor **80** in 70% yield.



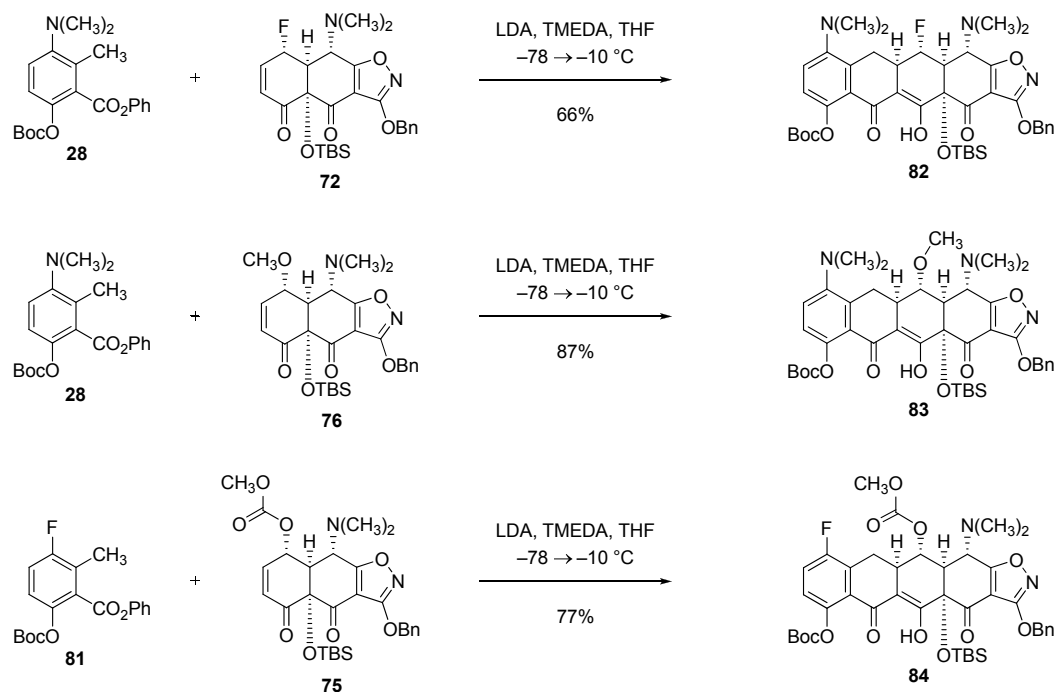
Scheme 3.8. Aminoalkylation reactions of *tert*-butyldimethylsilyl dienol ether **68**.

With a diverse collection of modified AB precursors in hand, the next task was to transform these substrates into the corresponding fully synthetic tetracyclines. The D-ring precursors corresponding to minocycline and 7-fluorotetracyclines (**28** and **81**, respectively) were chosen as suitable substrates for these investigations.⁹³ AB enones

⁹² Millot, N.; Piazza, C.; Avolio, S.; Knochel, P. *Synthesis* **2000**, 7, 941–948.

⁹³ 7-Fluorotetracyclines were discovered and developed by Tetrphase Pharmaceuticals using the fully synthetic platform developed in the Myers laboratory. The synthesis and utility of fluorinated D-ring

with “lower” face γ -substituents were found to undergo highly efficient Michael–Claisen cyclizations with benzylic anions formed by LDA deprotonation of **28** and **81** in the presence of TMEDA, affording tetracycline precursors with a range of substituents at C5. A selection of these cyclization reactions is presented in Scheme 3.9.

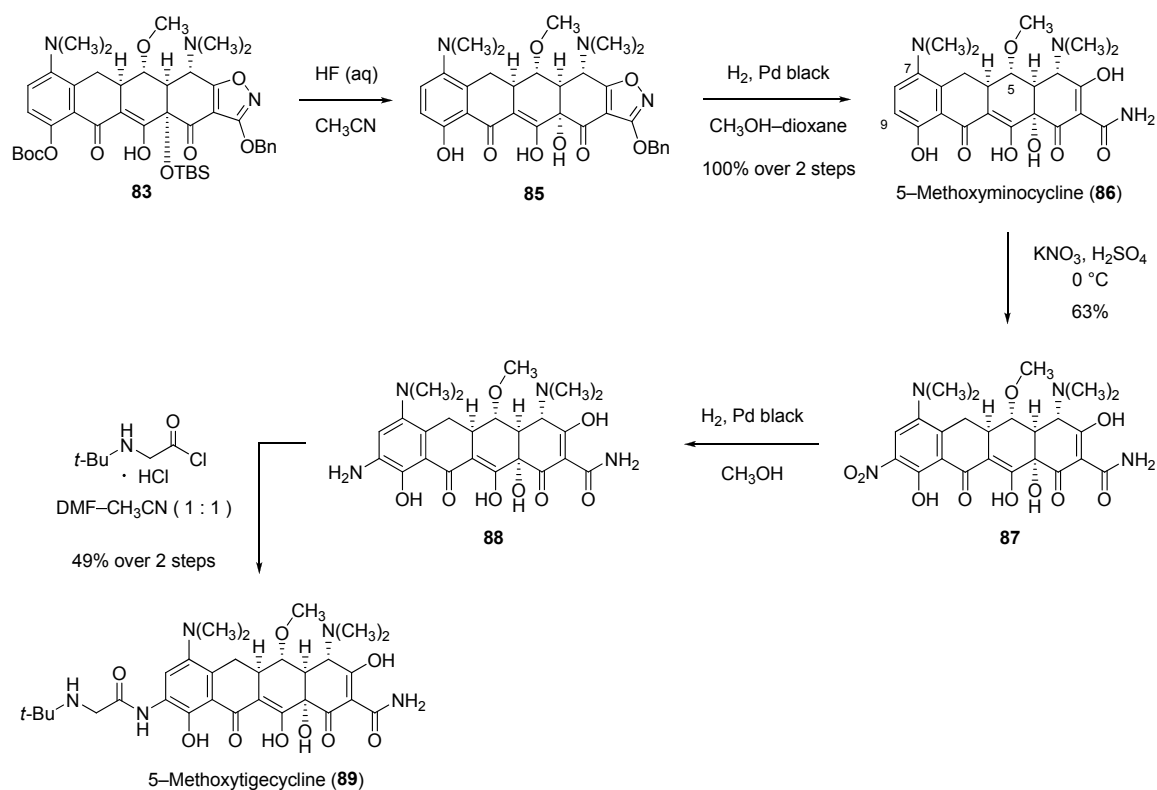


Scheme 3.9. Michael–Claisen cyclizations of *o*-toluate ester anions with AB precursors possessing fluoro (**72**), methoxy (**76**) and methyl carbonate (**75**) substituents at the γ -position.

Two-step deprotection of the Michael–Claisen cyclization products shown in Scheme 3.9 under typical conditions provided fully synthetic tetracyclines with

precursor **81** is described here: C7-Fluoro Substituted Tetracycline Compounds. PCT International Application Serial No. US2009/053142.

unprecedented modifications at C5.^{54b} For example, treatment of 5-methoxy cycloadduct **83** with hydrofluoric acid in acetonitrile at 23 °C, followed by hydrogenolysis of the crude reaction product (**85**) in the presence of palladium black under an atmosphere of hydrogen in methanol–dioxane at 23 °C and subsequent purification by rp-HPLC afforded 5-methoxyiminocycline (**86**, 100% over two steps, Scheme 3.10).

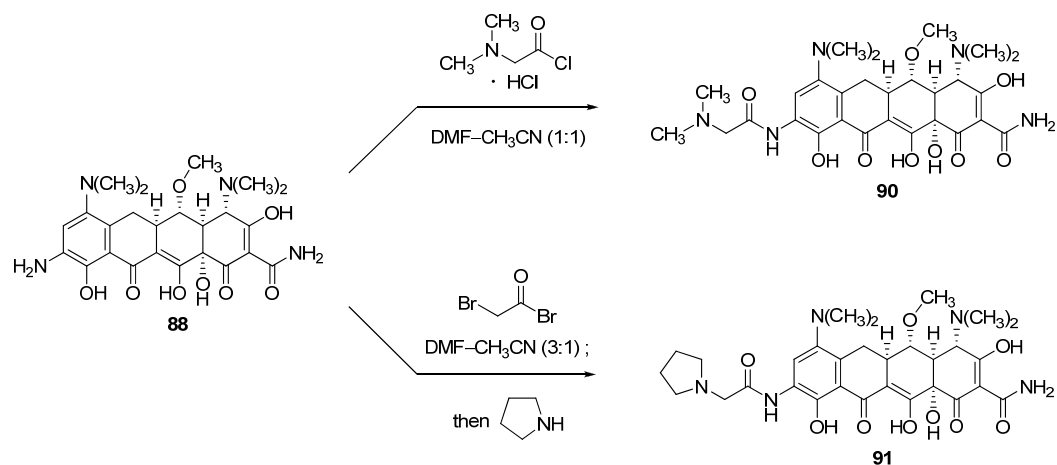


Scheme 3.10. Synthesis of 5-methoxyiminocycline (**86**) by two-step deprotection of Michael–Claisen product **83** and transformation of **86** into 5-methoxytigecycline (**89**).

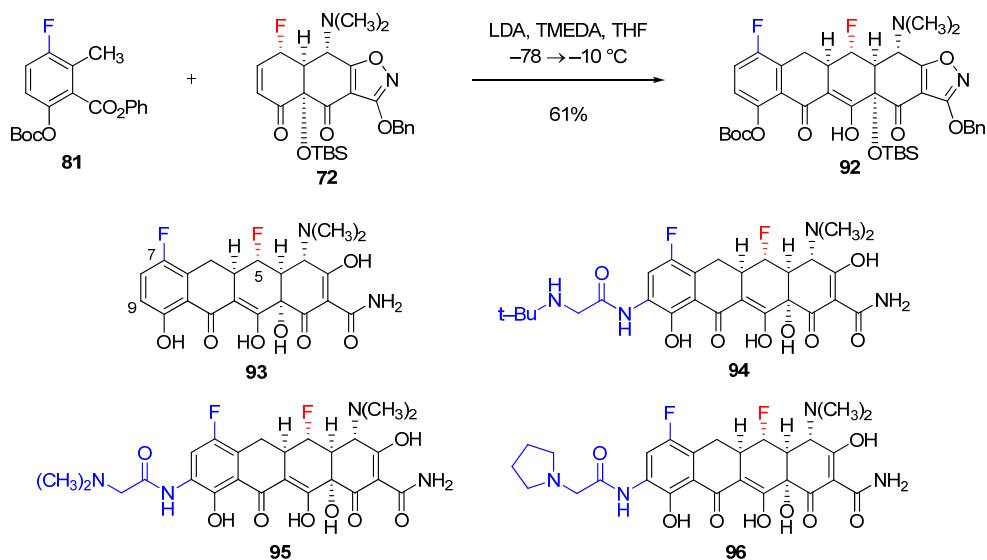
The goal of multiplicatively expanding the pool of fully synthetic tetracyclines was then efficiently advanced by employing “semisynthetic” strategies.⁹⁴ Selective nitration at C9 of 5-methoxyminocycline (**86**) was achieved by addition of potassium nitrate (1.1 equiv) to an ice-cold solution of **86** in concentrated sulfuric acid, affording 9-nitro-5-methoxyminocycline (**87**) in 63% yield after purification by rp-HPLC (Scheme 3.10 above). Reduction of the nitro group of **87** by palladium-catalyzed hydrogenation followed by treatment of a solution of the crude aniline product (**88**) in dimethylformamide and acetonitrile (1:1 mixture) with 2-(*tert*-butylamino)acetyl chloride hydrochloride afforded 5-methoxytigecycline (**89**, 49% yield over two steps).

A number of glycylicyclines with different C9 side chains were straightforwardly prepared by reaction of 9-amino “branch points” such as **88** with various different electrophiles (Scheme 3.11 below). Furthermore, the three-step sequence described above for transformation of a C5-substituted minocycline analog into the corresponding tigecycline compound (nitration–nitro reduction–side chain attachment) was also effective for the synthesis of 9-glycylamido derivatives of 7-fluorotetracyclines from the corresponding C9-unsubstituted compounds.⁹³ For example, numerous 5,7-difluorotetracyclines (compounds **93–96**) with different substitution patterns at C9 were conveniently prepared from a single Michael–Claisen cycloadduct (**92**) by deprotection followed by C9 functionalization (Scheme 3.12).

⁹⁴ (a) Sum, P.-E.; Lee, V. J.; Testa, R. T.; Hlavka, J. J.; Ellestad, G. A.; Bloom, J. D.; Gluzman, Y.; Tally, F. P. *J. Med. Chem.* **1994**, *37*, 184–188. (b) Sum, P.-E.; Petersen, P. *Bioorg. Med. Chem. Lett.* **1999**, *9*, 1459–1462.



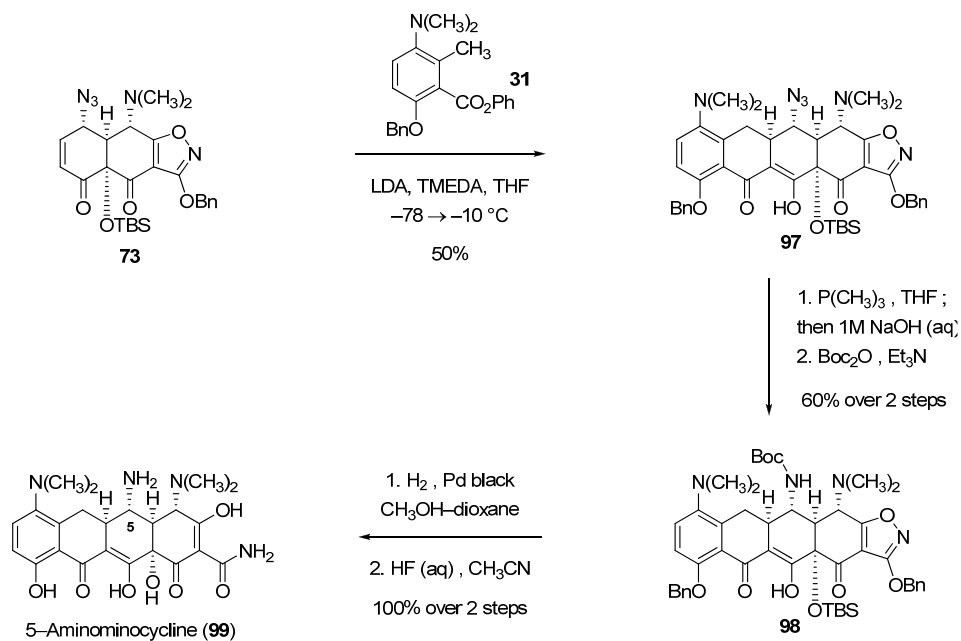
Scheme 3.11. Synthesis of diverse glycyclcyclines by final step diversification of 9-amino-5-methoxyminocycline (**88**).



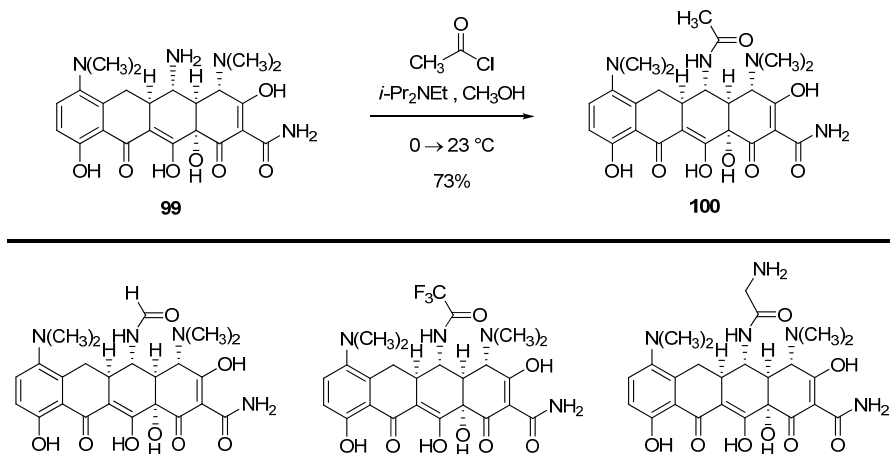
Scheme 3.12. 5,7-Difluorotetracyclines (**93–96**) prepared from a single Michael–Claisen cyclization product (**92**) by deprotection followed by C9 functionalization (nitration–nitro reduction–side chain attachment).

Fully synthetic tetracyclines possessing amino and aminomethyl substituents at C5 were also targeted for synthesis. We anticipated that these compounds could serve as substrates for late-stage diversification, thus allowing maximally expedient exploration of chemical space at C5. 5-Aminominocycline (**99**) was prepared in five synthetic operations from γ -azido AB enone **73** (Scheme 3.13). C-ring-forming cyclization of **73** with D-ring precursor **31** afforded the desired Michael–Claisen product (**97**) in 50% yield. Staudinger reduction was achieved by treatment of a solution of azide **97** in THF with trimethylphosphine followed by hydrolysis of the iminophosphorane intermediate with 1M aqueous sodium hydroxide solution. The resulting primary amine was then protected by treatment with di-*tert*-butyl dicarbonate and triethylamine, providing *tert*-butyl carbamate **98** in 60% yield from azide **97**.⁹⁵ Two-step deprotection using the inverted sequence afforded 5-aminominocycline (**99**) after purification by rp-HPLC (100% yield over two steps). Fully synthetic 5-amido derivatives of 5-aminominocycline (**99**) are presented in Scheme 3.14 below.

⁹⁵ Prior research had shown that the hydrogenolysis deprotection step is slow and low-yielding in the presence of free primary amines. For this reason, the hydrogenolysis reaction was performed on a substrate in which the primary amine was protected as a *tert*-butyl carbamate.

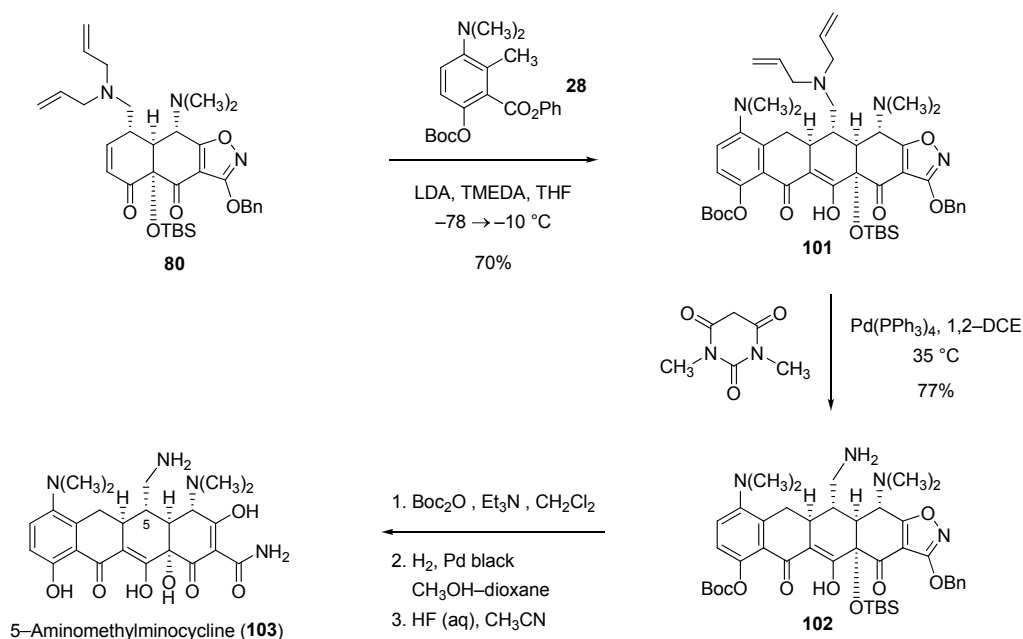


Scheme 3.13. Synthesis of 5-aminominocycline (**99**) from γ -azido AB enone **73**.

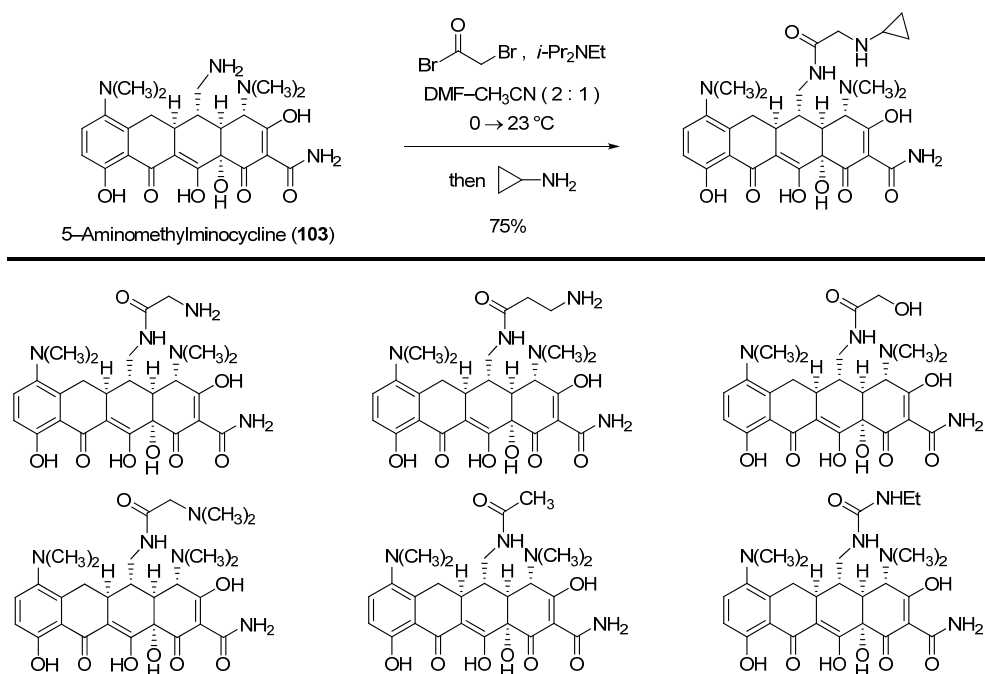


Scheme 3.14. Fully synthetic 5-amido derivatives of 5-aminominocycline (**99**).

5-Aminomethylminocycline (**103**) was prepared in five steps from γ -diallylaminomethyl AB enone **80** (Scheme 3.15). Michael–Claisen reaction of **80** and the minocycline D-ring precursor **28** provided the cyclization product **101** in 70% yield. Bis-deallylation of **101** was achieved by treatment with a catalytic amount of palladium tetrakis-(triphenylphosphine) and an excess of dimethylbarbituric acid (DCE, 35 °C). The resulting primary amine (**102**) was protected as a *tert*-butyl carbamate prior to two-step deprotection (hydrogenolysis followed by hydrofluoric acid treatment), affording 5-aminomethylminocycline (**103**). With this fully synthetic tetracycline in hand, it was straightforward to rapidly synthesize a collection of related analogs possessing extended substituents at C5 (Scheme 3.16).

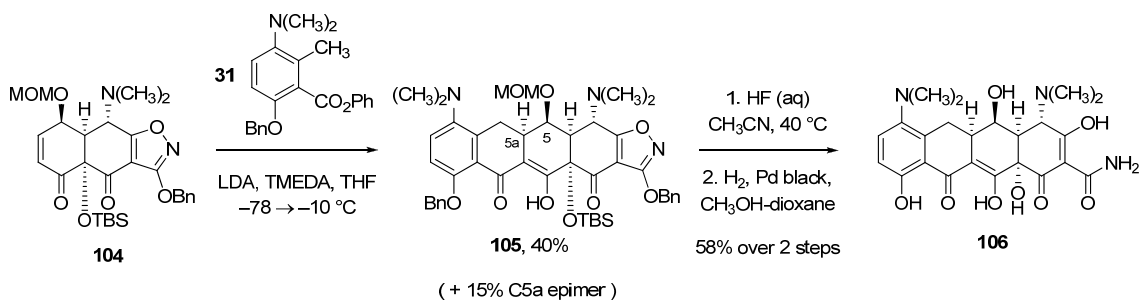


Scheme 3.15. Synthesis of 5-aminomethylminocycline (**103**) from γ -diallylaminomethyl AB enone **80**.



Scheme 3.16. Fully synthetic 5-amido derivatives of 5-aminomethylminocycline (**103**).

Finally, it is worth noting that the C-ring-forming Michael–Claisen cyclization of an AB precursor possessing an “upper” face (or β -face) substituent at the γ -position can also be stereoselective, albeit to a lesser extent (Scheme 3.17). Michael–Claisen reaction of enone **104** (with a protected hydroxy substituent on the upper face at the γ -position) with minocycline D-ring precursor **31** afforded the desired cyclization product **105** in 40% yield. The stereochemistry of **105** was confirmed by X-ray crystallography (Figure 3.2 below). A minor diastereomer, believed to be epimeric at C5a, was isolated separately (15% yield). Two-step deprotection of Michael–Claisen product **105** provided 5-(β)-hydroxyminocycline (**106**, 58% over two steps).



Scheme 3.17. Three-step synthesis of 5-(β)-hydroxyaminocycline (**106**) from an AB enone with a protected hydroxy substituent on the upper face at the γ-position (**104**).

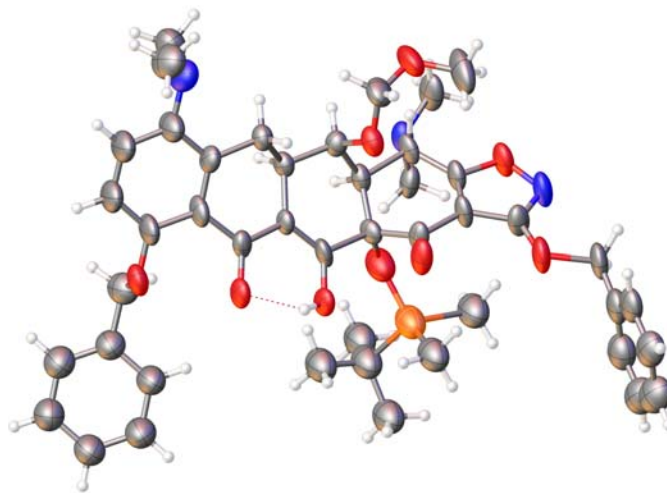


Figure 3.2. X-ray crystal structure of Michael–Claisen cyclization product **105**.

Antibacterial Activities

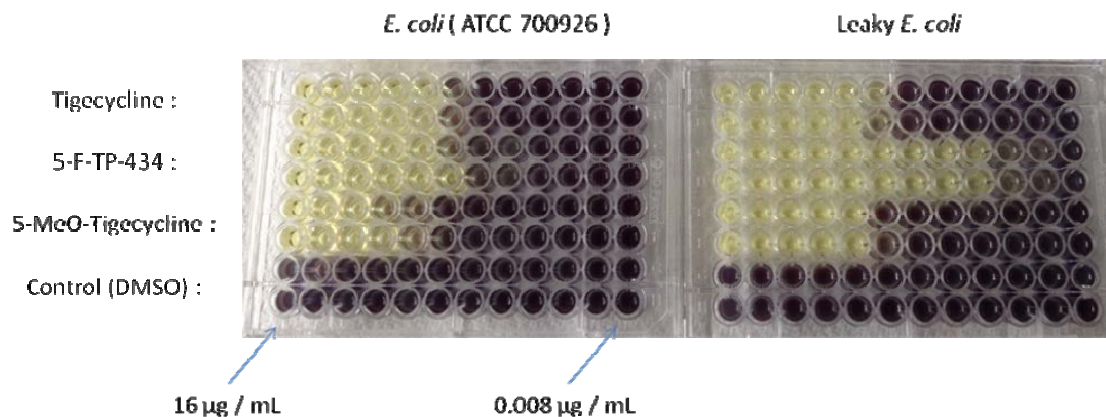
Minimum inhibitory concentrations (MIC) values were determined for all C5-substituted tetracyclines against a broad panel of tetracycline-sensitive and tetracycline-resistant Gram-positive and Gram-negative bacteria. In summary, numerous fully

synthetic C5-modified tetracyclines exhibited good activity against Gram-positive bacteria (including tetracycline-resistant organisms) and weak activity against some Gram-negative organisms, however C5 substitution provided compounds which were less active (to greater and lesser extents) than the corresponding C5-unsubstituted compounds (e.g. minocycline, tigecycline). Specific examples are discussed here and complete antibacterial activity data for all C5-substituted analogs is presented in the tables below (pages 176–184).

MIC assays for tigecycline (**9**), 5-fluoro-TP-434 (**96**)⁹⁶ and 5-methoxytigecycline (**89**) against tetracycline-susceptible *E. coli* and leaky *E. coli* strains are depicted in Figure 3.3 below. As discussed in Chapter 2, leaky *E. coli* has a more permeable outer membrane than *E. coli* (due to knockout of a lipopolysaccharide gene) and so provides some insight as to the effect of outer membrane penetration on antibacterial activity. The results of these MIC assays revealed that both synthetic analogs possess antibacterial activity and that 5-fluoro-glycylcycline **96** has similar activity to tigecycline (**9**) in this *E. coli* strain and is 16-fold more active than tigecycline in leaky *E. coli*. Thus, fully synthetic C5-fluoro-substituted tetracycline **96** was found to exhibit significantly greater potency than tigecycline against a tetracycline-susceptible strain with a permeabilized outer membrane. Unfortunately this improvement in activity (vs. tigecycline) was not common to other bacteria. Determination of antibacterial activities against a broad panel of Gram-positive and Gram-negative bacteria (including tetracycline-resistant organisms)

⁹⁶ TP-434 is a fully synthetic tetracycline antibiotic discovered and developed by Tetraphase Pharmaceuticals that is currently undergoing a Phase 2 clinical trial.

showed that **96** is significantly less active than tigecycline against most bacterial strains (see tables below for complete data).



	<i>E. coli</i>	Leaky <i>E. coli</i>
Tigecycline (9 , rows 1 & 2)	1	1
5-Fluoro-TP-434 (96 , rows 3 & 4)	1	0.063
5-Methoxytigecycline (89 , rows 5 & 6)	4	1

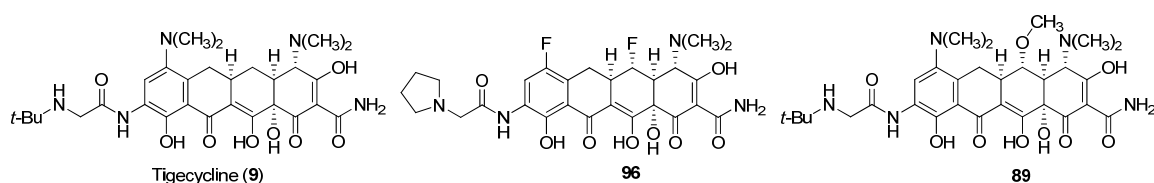


Figure 3.3. Minimum inhibitory concentration (MIC) assays and values in $\mu\text{g} / \text{mL}$ for tigecycline (**9**), 5-fluoro-TP-434 (**96**) and 5-methoxytigecycline (**89**) against *E. coli* and leaky *E. coli* strains.

active in others. 5-Methoxyminocycline and 5-aminominocycline were substantially less active against Gram-positive bacteria such as *S. aureus* and slightly less active than minocycline against Gram-negative organisms. 5-Aminomethylminocycline and its derivatives were found to be almost completely inactive as antibiotics, indicating that the introduction of extended substituents at C5 is not a promising strategy for the discovery of new tetracycline antibiotics. The discovery that 5-fluorominocycline has similar antibacterial activity to minocycline led to optimism regarding the activity of 5-fluorotigecycline. Unfortunately this compound was found to be significantly less potent than tigecycline (the corresponding 5-unsubstituted compound, Chart 3.2 below). The finding that fluoro-substitution has different effects on the activity of minocycline and tigecycline is one of many “non-linear” effects we have observed. In the case of tigecycline, 5-methoxy and 5-fluoro substitution were found to be similarly detrimental to antibacterial activity.

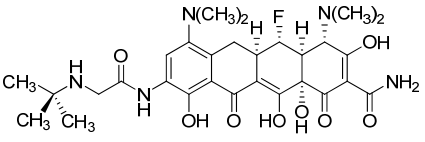
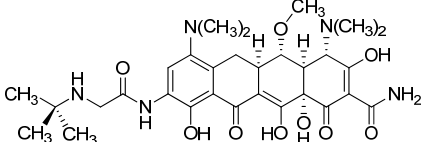
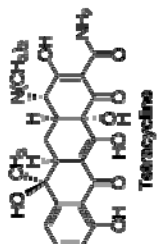
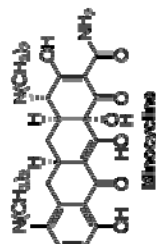
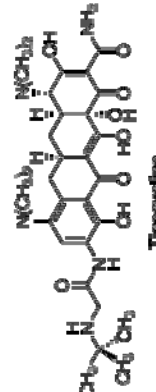
	GP				GN				
	SA101	SA158 tetK	EF404 tetM	SP160 tetM	EC107 tetM	EC155 tetA	EC878 tolC	KP457	PA555
Tigecycline	0.063	0.031	≤0.016	≤0.016	0.031	0.5	0.063	1	8
	1	0.5	0.25	0.125	0.5	>32	0.25	8	32
	1	0.5	0.125	0.031	1	>32	0.25	8	32

Chart 3.2. MIC values in µg/mL for tigecycline and selected C5-substituted tigecycline analogs (see Chart 3.1 for abbreviations).

Table 3.1. Minimum inhibitory concentration (MIC) values for tetracycline, minocycline and tigecycline (µg/mL)

	GP						GN											
	SA101	SA161	SA168	EF327	EF404	SP160	EC107	EC155	EC378	KP457	PA336	PA555	PA558	EC303	AB250	SH256	BC240	
	mg/L	mg/L	mg/L	mg/L	mg/L	mg/L	mg/L	mg/L	mg/L	mg/L	mg/L	mg/L	mg/L	mg/L	mg/L	mg/L	mg/L	
 Tetracycline	1	>32	32	>32	32	>32	2	>32	1	8	32	32	0.125	>32	>32	32	32	
 Minocycline	0.051	8	≤0.016	16	16	4	0.25	8	0.25	4	16	32	0.25	>32	8	0.25	4	
 Tigecycline	0.063	0.25	0.031	0.031	<0.016	<0.016	0.051	0.5	0.063	1	2	8	0.25	2	4	1	8	

Abbreviations: GP, Gram-positive; GN, Gram-negative; organisms – SA, *Staphylococcus aureus*; EF, *Enterococcus faecalis*; SP, *Streptococcus pneumoniae*; EC, *Escherichia coli*; KP, *Klebsiella pneumoniae*; PM, *Proteus mirabilis*; PA, *Pseudomonas aeruginosa*; AB, *Acinetobacter baumannii*; SM, *Stenotrophomonas maltophilia*; BC, *Burkholderia cenocepacia*; resistance determinants – tetM, ribosomal protection proteins; tetA, tetB, tetK, tetL, tetracycline efflux proteins; KO, multiple efflux pump knockout; ESB, extended-spectrum beta-lactamase; tolC, multiple efflux pump knockout.

Table 3.2. Minimum inhibitory concentration (MIC) values for 5-fluorotetracyclines (µg/mL)

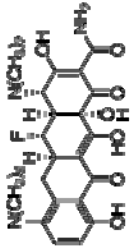
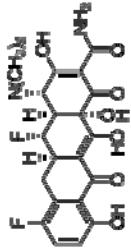
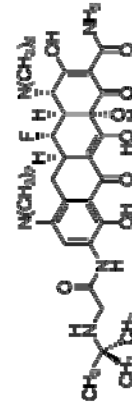


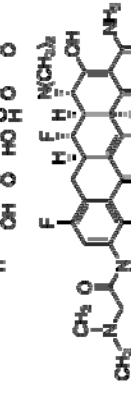
	GP						GN											
	SA101 SA151 SA158 EF327 EF404 SP160						EC107 EC155 EC378 IP457 PA355 PA556 EC303 AB250 SA256 BC240											
	W8A	W8K	W8A	W8A	W8A	W8A	W8A	W8A	W8A	W8A	ESBL	KO	W8A	W8A	W8A			
	0.063	16	≤0.016	32	16	8	0.25	16	0.125	16	>32	32	0.25	>32	>32	1	8	
	2	4	4	8	8	8	1	32	1	4	>32	32	1	>32	>32	8	8	
	1	8	0.5	0.25	0.25	0.125	0.5	>32	0.25	8	16	32	1	32	>32	32	>32	
	16	16	0.5	1	0.125	≤0.016	0.5	>32	0.25	8	8	32	0.25	>32	>32	>32	>32	
	2	8	0.5	0.5	0.063	≤0.016	0.5	>32	0.125	4	4	32	0.125	>32	>32	32	32	
	1	4	1	1	0.063	≤0.016	0.5	>32	0.125	4	16	32	0.063	>32	>32	>32	>32	

Table 3.3. Minimum inhibitory concentration (MIC) values for 5-methoxytetracyclines (µg/mL)






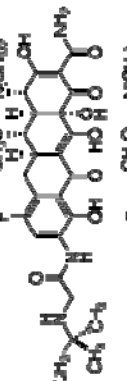

	G ⁻										G ⁺										
	SA101	SA181	SA188	FF97	FF04	SP180	NSM	NRK	NSL	NSM	EC107	FC155	FC378	IP-67	PA586	PA555	PA556	FC305	AB250	SMP66	RC240
	0.5	>32	0.5	32	16	16					1	>32	0.25	16	>32	32	0.5	>32	>32	-	8
	1	0.25	0.5	0.25	0.125	0.051					1	>32	0.25	8	16	32	1	32	>32	18	>32
	0.5	0.25	0.5	0.125	0.125	<0.016					0.25	>32	0.125	4	16	32	0.5	32	32	8	>32
	0.5	0.25	1	0.125	0.125	<0.016					0.5	>32	0.125	8	>32	32	0.5	>32	32	8	>32
	1	8	4	8	16	8					2	32	2	16	>32	>32	4	>32	>32	8	16
	16	16	0.5	0.5	0.25	<0.016					0.5	>32	0.25	4	16	32	0.5	>32	>32	32	>32
	8	8	2	0.5	0.058	<0.016					0.5	>32	0.25	8	>32	32	0.5	>32	>32	32	>32

Table 3.4. Minimum inhibitory concentration (MIC) values for 5-aminomycyclins and derivatives (µg/mL)

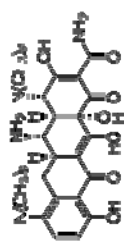
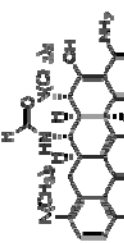
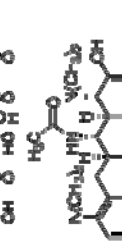
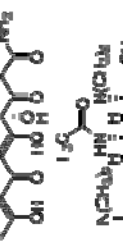
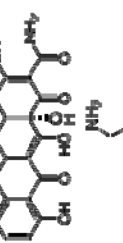
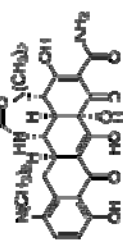
	GP						GS											
	BA101	SA18*	SA158	EF227	EF404	SP160	EC107	EC163	EC278	KP457	PK385	PA385	PA388	EC303	AB280	BA282	BC340	
	MMI	MMI	MMI	MMI	MMI	MMI	MMI	MMI	MMI	MMI	MMI	MMI	MMI	MMI	MMI	MMI	MMI	
	2	>32	2	32	32	32	1	>32	1	8	>32	16	1	>32	>32	16	32	
	2	>32	16	>32	>32	>32	2	>32	0.5	16	>32	32	0.5	>32	>32	>32	>32	
	2	>32	16	>32	>32	>32	4	>32	1	16	>32	>32	2	>32	>32	32	>32	
	-	32	0.5	>32	32	32	2	32	4	32	>32	>32	>6	>32	4	2	16	
	>32	>32	>32	>32	>32	>32	>32	>32	>32	>32	>32	>32	6	>32	>32	>32	>32	
	4	>32	2	>32	>32	>32	4	>32	1	32	>32	32	1	>32	>32	>32	>32	

Table 3.6 Minimum inhibitory concentration (MIC) values for 5-aminomethyliminocycline and derivatives (µg/mL)

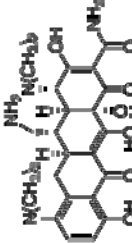
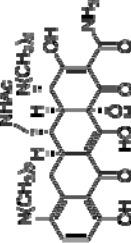

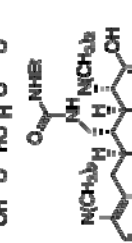
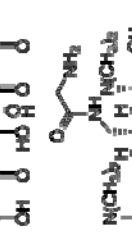
	GP						GN																							
	SA101						SA158						EF327						EF404						SP180					
	µgM	µgK	µgM	µgM	µgM	µgM	µgM	µgM	µgM	µgM	µgM	µgM	µgM	µgM	µgM	µgM	µgM	µgM	µgM	µgM	µgM	µgM	µgM	µgM	µgM	µgM	µgM	µgM		
	32	>32	16	32	>32	>32	>32	>32	>32	>32	>32	>32	>32	>32	>32	>32	>32	>32	>32	>32	>32	>32	>32	>32	>32	>32	>32	>32		
	16	>32	8	>32	>32	>32	>32	>32	>32	>32	>32	>32	>32	>32	>32	>32	>32	>32	>32	>32	>32	>32	>32	>32	>32	>32	>32	>32		
	>32	>32	16	>32	>32	>32	>32	>32	>32	>32	>32	>32	>32	>32	>32	>32	>32	>32	>32	>32	>32	>32	>32	>32	>32	>32	>32	>32		
	>32	>32	8	>32	>32	>32	>32	>32	>32	>32	>32	>32	>32	>32	>32	>32	>32	>32	>32	>32	>32	>32	>32	>32	>32	>32	>32	>32		
	>32	>32	16	>32	>32	>32	>32	>32	>32	>32	>32	>32	>32	>32	>32	>32	>32	>32	>32	>32	>32	>32	>32	>32	>32	>32	>32	>32		

Table 3.7. Minimum inhibitory concentration (MIC) values for derivatives of 5-aminomethylminocycline (µg/mL)

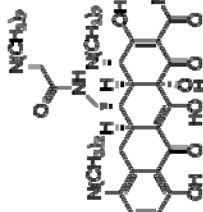
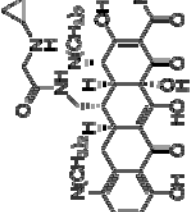
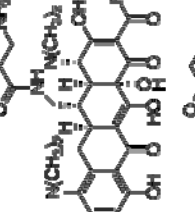
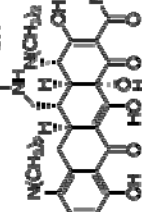
	GP						GN											
	SA101	SA161	SA168	EF327	EF404	SP160	EC107	EC155	EC378	KP457	PA385	PA555	PA558	EC603	A2250	SA2595	BC240	
	NSM	NSM	NSM	NSM	NSM	NSM	NSM	NSM	NSM	NSM	ESBL	ESBL	ESBL	NSM	NSM	NSM	NSM	
	32	>32	4	>32	>32	32	8	>32	8	>32	>32	>32	4	>32	32	32	>32	
	32	>32	4	>32	>32	>32	8	>32	4	>32	>32	>32	8	>32	32	32	>32	
	>32	>32	>32	>32	>32	>32	>32	>32	>32	>32	>32	>32	>32	>32	>32	>32	>32	
	>32	>32	>32	>32	>32	>32	>32	>32	8	>32	>32	>32	4	>32	>32	>32	>32	

Table 3.8. Minimum inhibitory concentration (MIC) values for miscellaneous C5-substituted tetracyclines (µg/mL)

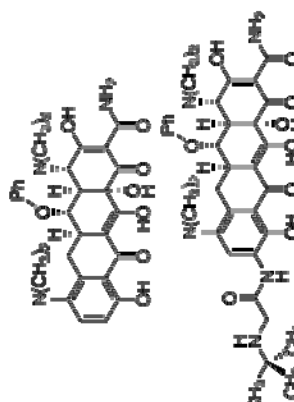
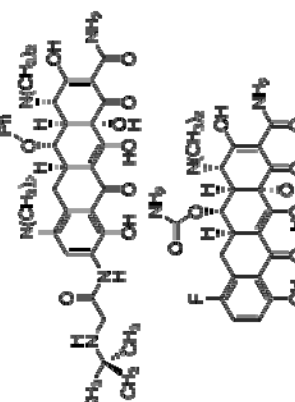
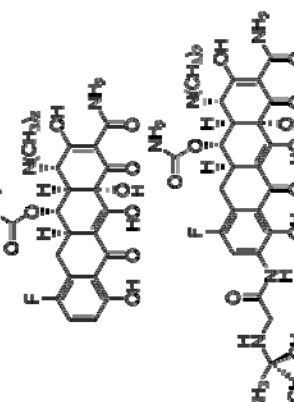
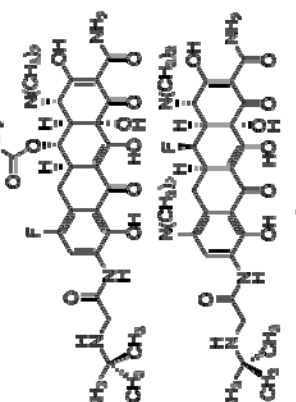
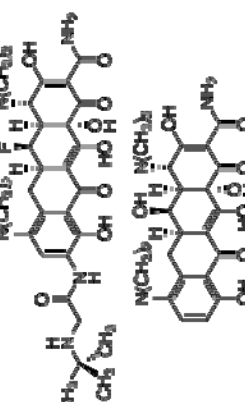

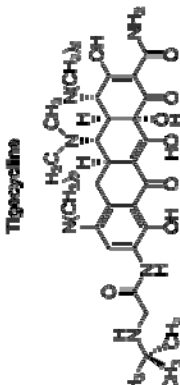
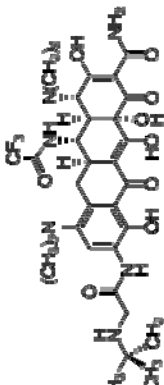
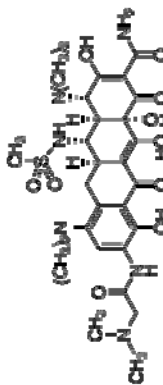
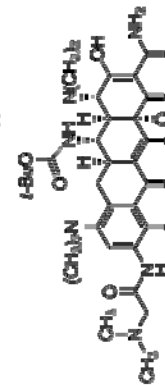

	GP						GN											
	SA101	SA151	SA158	EF327	EF404	SP160	EC107	EC165	EC378	KP457	PA385	PA555	PA588	EC903	AB250	SM258	BC240	
	0.5	4	4	0.5	4	4	16	>32	32	>32	>32	>32	>32	>32	16	8	>32	
	1	4	0.25	0.125	0.031	±0.016	1	32	1	32	32	>32	16	>32	32	8	>32	
	>32	>32	>32	>32	>32	>32	>32	>32	>32	>32	>32	>32	>32	>32	>32	>32	>32	
	>32	>32	>32	>32	>32	8	>32	>32	16	>32	>32	>32	16	>32	>32	>32	>32	
	8	>32	4	4	4	1	4	>32	2	32	>32	>32	2	>32	32	>32	>32	
	>32	>32	16	-	-	>32	>32	>32	-	>32	-	>32	16	-	>32	>32	>32	

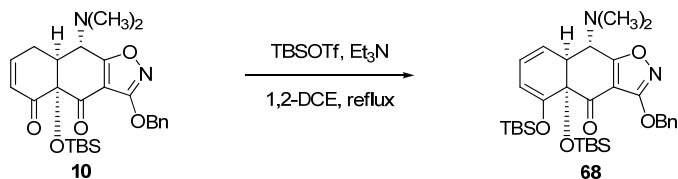
Table 3.9. Minimum inhibitory concentration (MIC) values for miscellaneous C5-substituted glycylicylines (µg/mL)

	GP						GM															
	SA10 ⁺	SA101	SA150	TT377	TT304	SP312	GC-07	EC155	EC078	KP457	PA0365	PA0358	PA0394	PA0590	EC003	AB280	SA0258	BC240				
	NSM	NSM	NSM	NSM	NSM	NSM	NSM	NSM	NSM	NSM	ESBL	KO	NSM	NSM	NSM	NSM	NSM					
	0.083	0.5	0.031	0.031	0.031	<0.016	0.031	<0.016	<0.016	0.031	0.5	0.031	1	2	8	0.125	0.031	0.5	1	4	0.5	8
	2	16	1	1	1	0.25	0.5	0.5	1	16	1	32	>32	>32	>32	2	16	32	>32	>32	16	>32
	2	16	2	0.5	0.25	0.083	0.125	0.5	2	0.5	16	>32	16	>32	>32	4	0.5	16	32	32	32	>32
	8	16	8	4	4	2	1	4	32	2	32	>32	>32	>32	>32	4	4	32	>32	>32	>32	>32
	2	4	2	0.083	0.125	0.031	<0.016	1	8	1	32	>32	>32	>32	>32	8	0.5	32	>32	16	8	>32

Conclusion

In conclusion, we have developed new chemical pathways for the synthesis of diverse γ -substituted AB enones from the γ -unsubstituted AB enone **10**. These modified AB precursors were then transformed into more than 40 fully synthetic tetracyclines with unprecedented substitutions at C5 by coupling with various D-ring precursors followed by deprotection and late-stage “branch point” diversification. Many of the modified AB precursors served as precursors to small libraries of tetracyclines with a given substituent at C5 and different D-ring portions, thereby multiplicatively expanding the pool of fully synthetic tetracyclines. Many fully synthetic C5-substituted tetracyclines demonstrated good activity against Gram-positive bacteria (including tetracycline-resistant organisms), however most compounds were significantly less active than the corresponding C5-unsubstituted tetracyclines against both Gram-positive and Gram-negative bacteria.

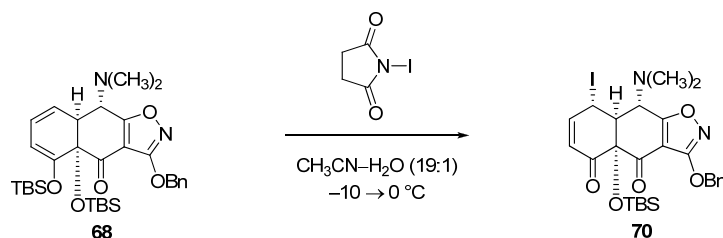
C5-Substituted Tetracyclines: Experimental Section



***tert*-Butyldimethylsilyl dienol ether 68.** Triethylamine (13.0 mL, 93.0 mmol, 3.0 equiv) and *tert*-butyldimethylsilyl trifluoromethanesulfonate (10.7 mL, 46.6 mmol, 1.5 equiv) were added sequentially to a stirring solution of AB enone **10** (15.0 g, 31.1 mmol, 1 equiv) in 1,2-dichloroethane (120 mL) at 23 °C. The reaction mixture was heated to reflux and stirred at this temperature for 18 h. The reaction solution was allowed to cool, then was poured into saturated aqueous sodium bicarbonate solution (350 mL). The resulting mixture was extracted with ethyl acetate (2 x 350 mL). The organic extracts were combined and the combined extracts were dried over anhydrous sodium sulfate. The dried solution was filtered and the filtrate was concentrated. The crude product was purified by flash-column chromatography (4% ethyl acetate–hexanes, grading to 6%), affording *tert*-butyldimethylsilyl dienol ether **68** as an off-white solid (14.5 g, 78%).

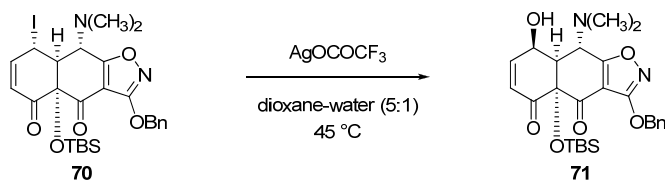
R_f = 0.68 (20% ethyl acetate–hexanes); ¹H NMR (500 MHz, CDCl₃) δ 7.48 (d, 2H, J = 7.8 Hz), 7.35 (m, 3H), 5.98 (dd, 1H, J = 9.3, 5.9 Hz), 5.87 (dd, 1H, J = 9.3, 5.9 Hz), 5.32 (m, 2H), 5.25 (d, 1H, J = 5.8 Hz), 3.78 (d, 1H, J = 10.3 Hz), 2.83 (dd, 1H, J = 9.8, 5.9 Hz), 2.48 (s, 6H), 0.82 (s, 9H), 0.77 (s, 9H), 0.15 (s, 6H), 0.13 (s, 3H), –0.04 (s, 3H); ¹³C NMR (500 MHz, CDCl₃) δ 188.7, 181.8, 167.7, 151.0, 139.3, 135.1, 128.9, 128.5, 128.4, 123.0, 122.9, 107.9, 103.4, 94.7, 81.7, 72.3, 64.2, 48.1, 42.4, 25.8, 25.4, 18.9, 17.8, –2.8,

−3.4, −4.5, −5.3; FTIR (neat film) 2929, 1716, 1510, 1247 cm^{-1} ; HRMS–ESI (m/z) calcd for $\text{C}_{32}\text{H}_{49}\text{N}_2\text{O}_5\text{Si}_2$, 597.3175; found, 596.3179.



γ -(α)-Iodo AB enone 70. Light was excluded throughout the synthesis, work-up and purification of γ -(α)-iodo AB enone **70**. *N*-Iodosuccinimide (4.83 g, 20.4 mmol, 1.05 equiv) was added in one portion to a stirring solution of *tert*-butyldimethylsilyl dienol ether **68** (11.6 g, 19.4 mmol, 1 equiv) in acetonitrile (171 mL) and water (9.0 mL) at -10 °C. The resulting mixture was stirred at this temperature for 5 min, then was allowed to warm to 0 °C. After stirring at 0 °C for 4 h, the reaction solution was partitioned between saturated aqueous sodium thiosulfate solution and ethyl acetate (300 mL each). The phases were separated and the aqueous phase was extracted with ethyl acetate (300 mL). The organic extracts were combined and the combined solution was dried over anhydrous sodium sulfate. The dried solution was filtered and the filtrate was concentrated. The crude product was purified by flash-column chromatography (12% ethyl acetate–hexanes, grading to 15%), providing the γ -(α)-iodo AB enone **70** as a yellow solid (11.0 g, 93%).

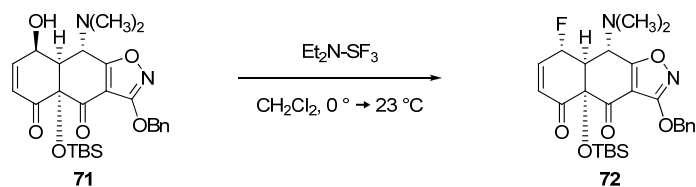
R_f = 0.59 (30% ethyl acetate–hexanes); ^1H NMR (500 MHz, CDCl_3) δ 7.49 (d, 2H, J = 7.3 Hz), 7.40–7.34 (m, 3H), 6.91 (ddd, 1H, J = 10.1, 4.6, 1.4 Hz), 6.03 (d, 1H, J = 10.1 Hz), 5.74 (d, 1H, J = 4.6 Hz), 5.36 (AB quartet, 2H), 3.52 (d, 1H, J = 11.0 Hz), 3.23 (d, 1H, J = 11.0 Hz), 2.50 (s, 6H), 0.99 (s, 9H), 0.20 (s, 3H), 0.11 (s, 3H); ^{13}C NMR (125 MHz, CDCl_3) δ 193.1, 186.4, 179.0, 167.4, 147.7, 134.9, 128.6, 128.5, 128.4, 126.1, 108.3, 83.1, 72.6, 60.8, 53.9, 41.9, 26.8, 19.5, 11.9, -2.2 , -2.2 ; HRMS–ESI (m/z): $[\text{M}+\text{H}]^+$ calcd for $\text{C}_{26}\text{H}_{34}\text{IN}_2\text{O}_5\text{Si}$, 609.1276; found, 609.1304.



γ -(β)-Hydroxy AB enone 71. Light was excluded throughout the reaction and work-up in this procedure. Silver (I) trifluoroacetate (2.59 g, 11.5 mmol, 1 equiv) was added in one portion to a solution of the γ -(α)-iodo AB enone **70** (7.0 g, 11.5 mmol, 1 equiv) in dioxane (85 mL) and water (17 mL) at 23 °C. The resulting mixture was heated to 45 °C and stirred at this temperature for 14 h. The reaction mixture was allowed to cool to 23 °C, then was partitioned between saturated aqueous sodium thiosulfate solution and ethyl acetate (250 mL each). The phases were separated and the organic phase was washed with saturated aqueous sodium bicarbonate solution (100 mL). The aqueous phases were combined and the combined aqueous mixture was extracted with ethyl acetate (250 mL, then 100 mL). The organic extracts were combined and the combined solution was dried over anhydrous sodium sulfate. The dried solution was filtered and the filtrate was concentrated. The crude product was purified by flash-column chromatography (20% ethyl acetate–hexanes, grading to 25%), affording the γ -(β)-hydroxy AB enone **71** as an off-white solid (2.90 g, 51%).

R_f = 0.40 (30% ethyl acetate–hexanes); ^1H NMR (500 MHz, CDCl_3) δ 7.48 (d, 2H, J = 7.3 Hz), 7.39–7.34 (m, 3H), 7.07 (d, 1H, J = 10.5 Hz), 6.05 (dd, 1H, J = 10.5, 2.3 Hz), 5.35 (AB quartet, 2H), 5.20 (brs, 1H), 4.37 (d, 1H, J = 11.0 Hz), 3.26–3.24 (m, 1H), 2.53 (brs, 6H), 0.83 (s, 9H), 0.26 (s, 3H), 0.03 (s, 3H); ^{13}C NMR (125 MHz, CDCl_3) δ 191.9, 186.0, 178.7, 167.4, 154.2, 134.7, 128.6, 128.5, 128.4, 126.4, 108.6, 83.8, 72.7, 68.3,

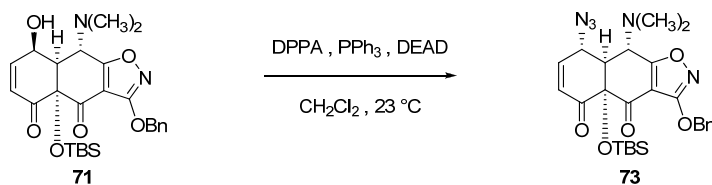
59.0, 50.7, 25.9, 19.0, -2.5, -4.1; FTIR (neat film), 2930 (w), 2857 (w), 1722 (s), 1684 (m), 1613 (w), 1512 (m), 1022 (s), 837 (s) cm^{-1} ; HRMS-ESI (m/z): $[\text{M}+\text{H}]^+$ calcd for $\text{C}_{26}\text{H}_{35}\text{N}_2\text{O}_6\text{Si}$, 499.2259; found, 499.2278.



γ -(α)-Fluoro AB enone **72.** Diethylaminosulfur trifluoride (74 μL , 0.562 mmol, 1.1 equiv) was added dropwise to a solution of the γ -(β)-hydroxy enone **71** (255 mg, 0.511 mmol, 1 equiv) in dichloromethane (10 mL) at 0 $^\circ\text{C}$. The resulting orange solution was allowed to warm to 23 $^\circ\text{C}$. After stirring at this temperature for 10 min, the reaction mixture was diluted with dichloromethane (10 mL) and washed with saturated aqueous sodium bicarbonate solution (20 mL). The phases were separated and the aqueous phase was extracted with dichloromethane (20 mL). The organic extracts were combined and the combined solution was dried over anhydrous sodium sulfate. The dried solution was filtered and filtrate was concentrated. The product was purified by flash-column chromatography (15% ethyl acetate–hexanes), providing the γ -(α)-fluoro AB enone **72** as a yellow solid (171 mg, 67%).

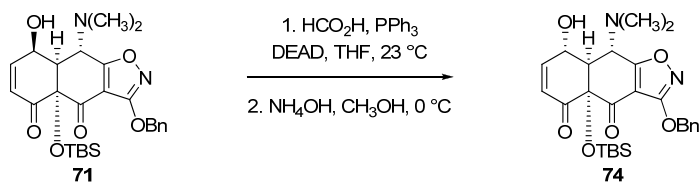
R_f = 0.40 (25% ethyl acetate–hexanes); ^1H NMR (500 MHz, CDCl_3) δ 7.51 (d, 2H, J = 7.0 Hz), 7.41–7.35 (m, 3H), 6.95–6.91 (m, 1H), 6.18 (dd, 1H, J = 10.5, 2.0 Hz), 5.43 (dd, 1H, J = 43.5, 4.0 Hz), 5.37 (AB quartet, 2H), 3.47 (dd, 1H, J = 11.0, 1.5 Hz), 3.08–3.01 (m, 1H), 2.51 (s, 6H), 0.85 (s, 9H), 0.25 (s, 3H), 0.04 (s, 3H); ^{13}C NMR (125 MHz, CDCl_3) δ 193.9 (d, J = 2.7 Hz), 186.6, 180.0 (d, J = 3.7 Hz), 167.4, 141.0 (d, J = 17.4 Hz), 134.8, 129.7 (d, J = 8.2 Hz), 128.6, 128.5, 128.5, 108.3, 83.8, 82.1 (d, J = 73.2 Hz), 72.7, 59.1 (d, J = 7.3 Hz), 50.4 (d, J = 17.4 Hz), 42.0, 25.9, 19.1, –2.4, –3.9; ^{19}F NMR (300 MHz, CDCl_3) δ –170.1; FTIR (neat film), 2930 (w), 1721 (s), 1692 (m), 1512 (m),

1474 (m), 1188 (w), 1051 (m), 936 (s), 839 (s) cm^{-1} ; HRMS–ESI (m/z): $[\text{M}+\text{H}]^+$ calcd for $\text{C}_{26}\text{H}_{34}\text{FN}_2\text{O}_5\text{Si}$, 501.2216; found, 501.2245.



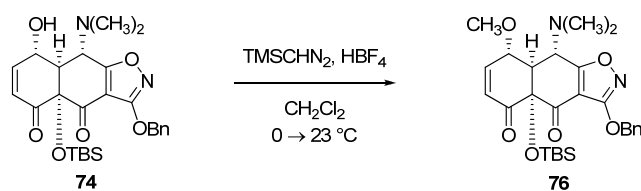
γ -(α)-Azido AB enone **73.** Triphenylphosphine (631 mg, 2.41 mmol, 1.2 equiv), a solution of diethyl azodicarboxylate (40% in toluene, 1.10 mL, 2.41 mmol, 1.2 equiv) and diphenyl phosphoryl azide (535 μ L, 2.41 mmol, 1.2 equiv) were added sequentially to a solution of γ -(β)-hydroxy AB enone **71** (1.00 g, 2.01 mmol, 1 equiv) in dichloromethane (25 mL) at 23 °C. After stirring at this temperature for 1 h, the reaction mixture was concentrated. The crude product was purified by flash-column chromatography (7% acetone–hexanes), affording the γ -(α)-azido AB enone **73** as an off-white solid (802 mg, 76%).

R_f = 0.08 (8% acetone–hexanes); ^1H NMR (500 MHz, CDCl_3) δ 7.50 (d, 2H, J = 7.8 Hz), 7.40–7.34 (m, 3H), 6.74 (dd, 1H, J = 9.8, 3.9 Hz), 6.14 (d, 1H, J = 9.8 Hz), 5.37 (AB quartet, 2H), 4.83 (d, 1H, J = 3.9 Hz), 3.54 (d, 1H, J = 11.7 Hz), 2.86 (d, 1H, J = 10.7 Hz), 2.50 (s, 6H), 0.89 (s, 9H), 0.27 (s, 3H), 0.03 (s, 3H); ^{13}C NMR (125 MHz, CDCl_3) δ 193.4, 186.5, 179.9, 167.3, 142.4, 134.8, 128.8, 128.6, 128.5, 128.4, 108.3, 81.9, 72.6, 59.7, 55.0, 49.4, 41.8, 25.8, 19.1, –2.5, –3.6; FTIR (neat film), 2099 (s), 1722 (s), 1688 (m), 1611 (w), 1506 (m), 1248 (m), 839 (s), 737 (s) cm^{-1} ; HRMS–ESI (m/z): $[\text{M}+\text{H}]^+$ calcd for $\text{C}_{26}\text{H}_{34}\text{N}_5\text{O}_5\text{Si}$, 524.2324; found, 524.2324.



γ -(α)-Hydroxy AB enone **74.** A solution of diethyl azodicarboxylate (40% in toluene, 396 μL , 1.01 mmol, 1.4 equiv) was added dropwise via syringe to a stirred solution of the γ -(β)-hydroxy AB enone **71** (360 mg, 0.722 mmol, 1 equiv), triphenylphosphine (265 mg, 1.01 mmol, 1.4 equiv) and formic acid (38.1 μL , 1.01 mmol, 1.4 equiv) in tetrahydrofuran (2.0 mL) at 23 $^\circ\text{C}$. After stirring at this temperature for 5 h, the reaction mixture was diluted with dichloromethane (20 mL) and washed with saturated aqueous sodium bicarbonate solution (20 mL). The phases were separated and the aqueous phase was extracted with dichloromethane (20 mL). The organic extracts were combined and the combined solution was dried over anhydrous sodium sulfate. The dried solution was filtered and filtrate was concentrated, providing a green oil. The crude formate ester product was dissolved in methanol (15 mL) and the resulting solution was cooled to 0 $^\circ\text{C}$. Aqueous ammonia (30% solution, 127 μL , 0.978 mmol, 1.35 equiv) was added to the cooled solution. The reaction was stirred at 0 $^\circ\text{C}$ for 25 min, then was diluted with dichloromethane (80 mL) and washed with saturated aqueous sodium bicarbonate solution (60 mL). The phases were separated and the aqueous phase was extracted with dichloromethane (80 mL). The organic extracts were combined and the combined solution was dried over anhydrous sodium sulfate. The dried solution was filtered and filtrate was concentrated, affording a brown-red oil. The product was purified by flash-column chromatography (17% ethyl acetate–hexanes), providing the γ -(α)-hydroxy AB enone **74** as a white solid (302 mg, 84%, two steps).

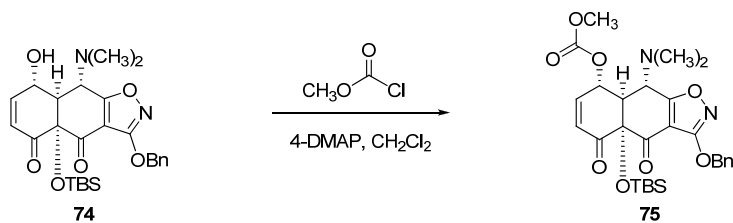
$R_f = 0.23$ (25% ethyl acetate–hexanes); ^1H NMR (500 MHz, CDCl_3) δ 7.51–7.50 (m, 2H), 7.41–7.35 (m, 3H), 7.02–6.98 (m, 1H), 6.11 (d, 1H, $J = 10.2$ Hz), 5.37 (AB quartet, 2H), 4.71–4.67 (m, 1H), 3.63 (d, 1H, $J = 11.2$ Hz), 3.57 (d, 1H, $J = 11.2$ Hz), 2.93–2.91 (m, 1H), 2.49 (s, 6H), 0.88 (s, 9H), 0.32 (s, 3H), 0.08 (s, 3H); ^{13}C NMR (125 MHz, CDCl_3) δ 193.2, 186.5, 180.7, 167.3, 146.9, 134.9, 128.6, 128.5, 128.5, 127.2, 108.2, 84.3, 72.7, 64.5, 59.6, 51.8, 41.9, 26.2, 19.1, –2.3, –3.6; HRMS–ESI (m/z): $[\text{M}+\text{H}]^+$ calcd for $\text{C}_{26}\text{H}_{35}\text{N}_2\text{O}_6\text{Si}$, 499.2259; found, 499.2270.



γ -(α)-Methoxy AB enone 76. Trimethylsilyldiazomethane (320 μ L, 0.64 mmol, 2.5 equiv) was added dropwise in three portions (2 x 120 μ L, then 80 μ L) over 10 min to a solution of the γ -(α)-hydroxy AB enone **74** (127 mg, 0.255 mmol, 1 equiv) and tetrafluoroboric acid (60 μ L, 0.458 mmol, 1.8 mmol) in dichloromethane (3.0 mL) at 0 °C. The resulting mixture was allowed to warm to 23 °C. After stirring at this temperature for 3 h, more trimethylsilyldiazomethane (120 μ L) was added to the reaction mixture. The resulting solution was stirred at 23 °C for a further 1 h, then was diluted with dichloromethane (20 mL) and poured into water (20 mL). Saturated aqueous sodium bicarbonate solution (10 mL) was added and the phases were separated. The aqueous phase was then extracted with dichloromethane (20 mL). The organic extracts were combined and the combined solution was dried over anhydrous sodium sulfate. The dried solution was filtered and the filtrate was concentrated. The crude product was purified by flash-column chromatography (13% ethyl acetate–hexanes), affording the γ -(α)-methoxy AB enone **76** as a white solid (43 mg, 33%).

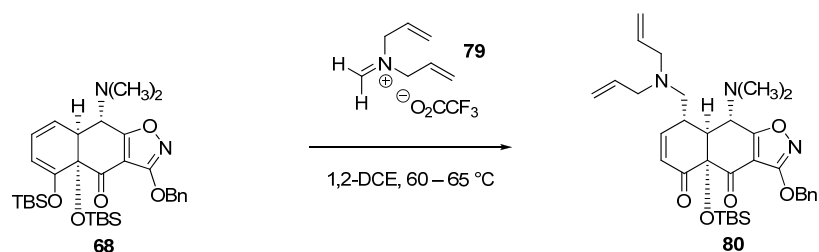
$R_f = 0.32$ (25% ethyl acetate–hexanes); ^1H NMR (500 MHz, CDCl_3) δ 7.50 (d, 2H, $J = 7.3$ Hz), 7.40–7.34 (m, 3H), 6.91 (dd, 1H, $J = 10.1, 4.1$ Hz), 6.08 (d, $J = 10.1$ Hz), 5.37 (AB quartet, 2H), 4.21 (s, 1H), 3.47 (d, 1H, $J = 10.5$ Hz), 3.41 (s, 3H), 2.88 (d, 1H, $J = 9.6$ Hz), 2.50 (s, 6H), 0.84 (s, 9H), 0.22 (s, 3H), 0.03 (s, 3H); ^{13}C NMR (125 MHz, CDCl_3) δ 194.5, 187.5, 180.4, 167.4, 144.7, 135.0, 128.5, 128.5, 128.4, 127.8, 108.2,

82.3, 73.9, 72.6, 59.6, 57.0, 48.3, 42.2, 25.8, 19.1, -2.4, -3.7; HRMS-ESI (m/z): $[M+H]^+$
calcd for $C_{27}H_{37}N_2O_6Si$, 513.2415; found, 513.2414.



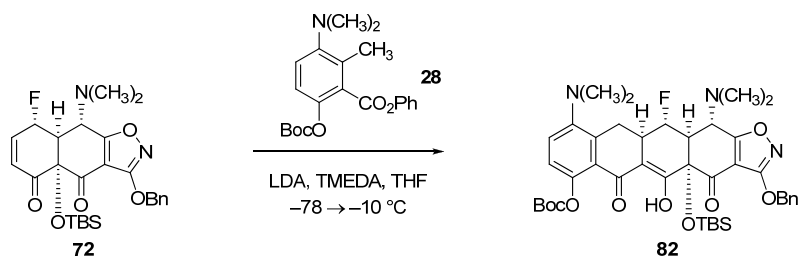
γ -(α)-Oxycarbonyloxymethyl AB Enone **75.** Methyl chloroformate (233 μ L, 3.00 mmol, 2.2 equiv) and 4-dimethylaminopyridine (367 mg, 3.00 mmol, 2.2 equiv) were added sequentially to a solution of the γ -(α)-hydroxy AB enone **74** (680 mg, 1.36 mmol, 1 equiv) in dichloromethane (15 mL) at 23 °C. The reaction mixture was stirred at this temperature for 13 h, then was diluted with dichloromethane (50 mL) and poured into saturated aqueous sodium bicarbonate solution (50 mL). The phases were separated and the aqueous phase was extracted with dichloromethane (50 mL). The organic extracts were combined and the combined solution was dried over anhydrous sodium sulfate. The dried solution was filtered and the filtrate was concentrated. The crude product was purified by flash-column chromatography, providing methyl carbonate **75** (517 mg, 68%).

R_f = 0.18 (20% ethyl acetate–hexanes); ^1H NMR (500 MHz, CDCl_3) δ 7.51–7.50 (m, 2H), 7.41–7.35 (m, 3H), 6.93 (ddd, 1H, J = 10.3, 4.7, 1.8 Hz), 6.19 (dd, 1H, J = 10.3, 1.0 Hz), 5.71 (m, 1H), 5.37 (AB quartet, 2H), 3.82 (s, 3H), 3.57 (d, 1H, J = 11.3 Hz), 3.02–2.99 (m, 1H), 2.51 (s, 6H), 0.86 (s, 9H), 0.26 (s, 3H), 0.02 (s, 3H); ^{13}C NMR (125 MHz, CDCl_3) δ 193.8, 186.6, 180.3, 167.4, 155.4, 141.4, 134.9, 129.7, 128.6, 128.5, 128.5, 108.3, 82.0, 72.7, 69.1, 59.7, 55.0, 49.9, 42.0, 25.9, 19.1, –2.4, –3.7.



γ -(α)-*N,N*-Diallylaminomethyl-substituted AB enone **80.** A freshly prepared solution of immonium trifluoroacetate salt **79** in anhydrous 1,2-dichloroethane (0.6 M, 4.3 mL, 2.58 mmol, 1.5 equiv)⁹² was added dropwise to a solution of *tert*-butyldimethylsilyl dienol ether **68** (1.01 g, 1.69 mmol, 1 equiv) in anhydrous 1,2-dichloroethane (10 mL) at 23 °C. The reaction mixture was heated to 60–65 °C. After stirring at this temperature for 1 h, a second portion of immonium trifluoroacetate solution (0.6 M, 4.3 mL, 2.58 mmol, 1.5 equiv) was added dropwise to the reaction solution. The resulting solution was stirred at 60–65 °C for 1 h, whereupon a final portion of immonium trifluoroacetate solution (0.6 M, 2.8 mL, 1.68 mmol, 1 equiv) was added dropwise. After stirring at 60–65 °C for a further 30 min, the reaction solution was allowed to cool to 23 °C. The cooled solution was poured into saturated aqueous sodium bicarbonate solution (60 mL). Dichloromethane (60 mL) was added and the phases were separated. The aqueous phase was extracted with dichloromethane (60 mL). The organic extracts were combined and the combined solution was dried over anhydrous sodium sulfate. The dried solution was filtered and the filtrate was concentrated, affording a brown oil. The crude product was purified by flash-column chromatography (dichloromethane flush, then 1% ether–dichloromethane, grading to 3% ether–dichloromethane), affording the γ -(α)-*N,N*-diallylaminomethyl-substituted AB enone **80** as a pale yellow solid (699 mg, 70%).

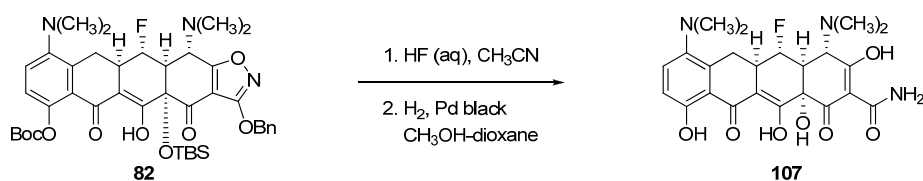
^1H NMR (500 MHz, CDCl_3) δ 7.50 (d, 2H, $J = 6.8$ Hz), 7.40–7.34 (m, 3H), 6.94 (ddd, 1H, $J = 10.3, 4.9, 1.5$ Hz), 6.06 (dd, 1H, $J = 10.3, 2.0$ Hz), 5.87–5.79 (m, 2H), 5.36 (2H, AB quartet), 5.18–5.13 (m, 4H), 3.57 (d, 1H, $J = 11.2$ Hz), 3.21–3.16 (m, 5H), 2.89 (dd, 1H, $J = 12.7, 7.3$ Hz), 2.83 (dd, 12.7, 7.3 Hz), 2.76 (d, 1H, $J = 11.2$ Hz), 2.48 (s, 9H), 0.86 (s, 9H), 0.24 (s, 3H), 0.01 (s, 3H); HRMS–ESI (m/z): $[\text{M}+\text{H}]^+$ calcd for $\text{C}_{33}\text{H}_{46}\text{N}_3\text{O}_5\text{Si}$, 592.3201; found, 592.3212.



Michael–Claisen cyclization product 82. A freshly prepared solution of lithium diisopropylamide (1.0 M, 3.30 mL, 3.30 mmol, 3.0 equiv) was added dropwise via syringe to a solution of minocycline D-ring precursor **28** (1.22 g, 3.30 mmol, 3.0 equiv) and *N,N,N',N'*-tetramethylethylenediamine (TMEDA, 995 μ L, 6.59 mmol, 6.0 equiv) in tetrahydrofuran (40 mL) at -78 $^{\circ}$ C, forming a dark red solution. After stirring at -78 $^{\circ}$ C for 35 min, a solution of γ -(α)-fluoro AB enone **72** (550 mg, 1.10 mmol, 1 equiv) in tetrahydrofuran (5 mL) was added dropwise via syringe to the reaction solution. The resulting mixture was allowed to warm slowly to -10 $^{\circ}$ C over 100 min, then was partitioned between aqueous potassium phosphate buffer solution (pH 7.0, 0.2 M, 100 mL) and dichloromethane (100 mL). The phases were separated and the aqueous phase was further extracted with dichloromethane (2 x 50 mL). The organic extracts were combined and the combined solution was dried over anhydrous sodium sulfate. The dried solution was filtered and the filtrate was concentrated, affording a dark green oil. The product was purified by flash-column chromatography (13% ethyl acetate–hexanes), providing the Michael–Claisen cyclization product **82** as a yellow solid (560 mg, 66%).

R_f = 0.43 (25% ethyl acetate–hexanes); ^1H NMR (500 MHz, CDCl_3) δ 15.70 (s, 1H), 7.51 (d, 2H, J = 6.8 Hz), 7.41–7.35 (m, 3H), 7.28 (d, 1H, J = 8.8 Hz), 7.05 (d, 1H, J = 8.8 Hz), 5.38 (AB quartet, 2H), 5.07 (dd, 1H, J = 47.9, 2.0 Hz), 3.83 (dd, 1H, J = 15.6, 5.9 Hz),

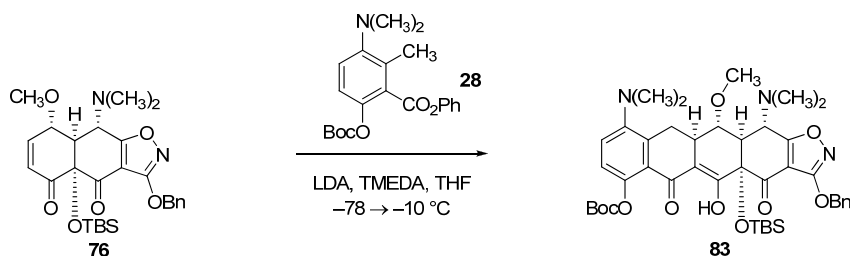
3.69 (d, 1H, $J = 11.7$ Hz), 3.37 (ddd, 1H, $J = 30.3, 15.7, 4.9, 3.9$ Hz), 2.94 (dd, 1H, $J = 20.5, 10.8$ Hz), 2.68 (s, 6H), 2.52 (s, 6H), 2.34 (dd, 1H, $J = 15.7, 14.7$ Hz), 1.54 (s, 9H), 0.83 (s, 9H), 0.24 (s, 3H), 0.09 (s, 3H); ^{13}C NMR (125 MHz, CDCl_3) δ 186.4, 185.8, 180.8, 180.1 (d, $J = 3.7$ Hz), 167.5, 152.1, 149.7, 145.3, 135.8, 135.0, 128.6, 128.5, 128.5, 124.7, 123.1, 122.5, 108.4, 104.4 (d, $J = 7.3$ Hz), 92.4 (d, $J = 179.4$ Hz), 83.8, 81.8, 72.6, 59.5 (d, $J = 10.1$ Hz), 52.5 (d, $J = 19.2$ Hz), 44.3, 41.9, 37.5 (d, $J = 28.4$ Hz), 31.4 (d, $J = 1.8$ Hz), 27.7, 25.9, 19.0, $-2.4, -3.4$; FTIR (neat film), 1759 (m), 1722 (m), 1614 (w), 1512 (m), 1234 (s), 1148 (w), 735 (w) cm^{-1} ; HRMS–ESI (m/z): $[\text{M}+\text{H}]^+$ calcd for $\text{C}_{41}\text{H}_{53}\text{FN}_3\text{O}_9\text{Si}$, 778.3530; found, 778.3533.



5-(α)-Fluorominocycline (107). Concentrated aqueous hydrofluoric acid solution (48 wt%, 3.0 mL) was added to a solution of the Michael–Claisen cyclization product **82** (522 mg, 0.671 mmol, 1 equiv) in acetonitrile (4.5 mL) in a polypropylene reaction vessel at 23 °C. The reaction solution was stirred vigorously at 23 °C for 13 ½ h, then was poured into water (150 mL) containing dipotassium hydrogenphosphate trihydrate (30 g). The resulting mixture was extracted with ethyl acetate (150 mL, then 2 x 100 mL). The organic extracts were combined and the combined solution was dried over anhydrous sodium sulfate. The dried solution was filtered and the filtrate was concentrated, affording a brownish yellow solid. Methanol (4.0 mL) and dioxane (4.0 mL) were added to the crude product. Palladium black (28.6 mg, 0.268 mmol, 0.4 equiv) was added in one portion to the resulting solution at 23 °C. An atmosphere of hydrogen was introduced by briefly evacuating the flask, then flushing with pure hydrogen (1 atm). The reaction mixture was stirred at 23 °C for 75 min, then was filtered through a plug of Celite. The filtrate was concentrated. The product was purified by preparative HPLC on an Agilent Prep C18 column [10 μ m, 250 x 21.2 mm, UV detection at 350 nm, Solvent A: 0.1% trifluoroacetic acid in water, Solvent B: acetonitrile, 2 batches, injection volume: 8.0 mL (6.0 mL 0.1% trifluoroacetic acid in water, 2.0 mL acetonitrile), gradient elution with 20→40% B over 40 min, flow rate: 15 mL/min]. Fractions eluting at 6–13 min were collected and concentrated, then re-purified by preparative HPLC [10 μ m, 250 x 21.2 mm, UV detection at 350 nm, Solvent A: 0.1% trifluoroacetic acid in water, Solvent B:

acetonitrile, 2 batches, injection volume: 8.0 mL (7.0 mL 0.1% trifluoroacetic acid in water, 1.0 mL acetonitrile), gradient elution with 5→40% B over 50 min, flow rate: 7.5 mL/min]. Fractions eluting 23–30 min were collected and concentrated, affording 5-(α)-fluorominocycline trifluoroacetate (**107**) as a yellow solid (321 mg, 81%, two steps).

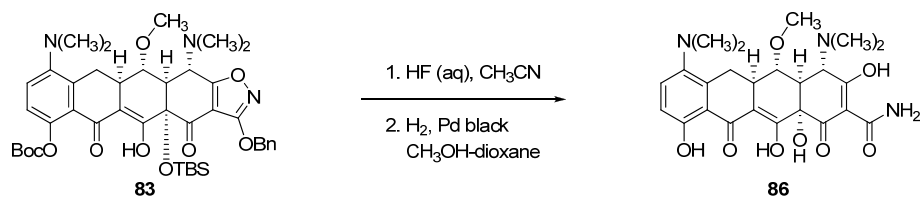
^1H NMR (500 MHz, CD_3OD , trifluoroacetate) δ 7.83 (d, 1H, $J = 9.3$ Hz), 7.03 (d, 1H, $J = 9.3$ Hz), 4.59 (ddd, 1H, $J = 48.8, 11.7, 9.3$ Hz), 4.57 (d, 1H, $J = 1.0$ Hz), 3.66 (dd, 1H, $J = 15.6, 4.4$ Hz), 3.36–3.26 (m, 2H), 3.13 (s, 6H), 2.94 (s, 6H), 2.65 (dd, 1H, $J = 14.6, 14.2$ Hz); HRMS–ESI (m/z): $[\text{M}+\text{H}]^+$ calcd for $\text{C}_{23}\text{H}_{27}\text{FN}_3\text{O}_7$, 476.1828; found, 476.1843.



Michael–Claisen cyclization product 83. A freshly prepared solution of lithium diisopropylamide (1.0 M, 2.06 mL, 2.06 mmol, 3.0 equiv) was added dropwise via syringe to a solution of the minocycline D-ring precursor **28** (765 mg, 2.06 mmol, 3.0 equiv) and TMEDA (622 μ L, 4.12 mmol, 6.0 equiv) in tetrahydrofuran (17 mL) at -78 $^{\circ}$ C, forming a dark red solution. After stirring at -78 $^{\circ}$ C for 45 min, a solution of γ -(α)-methoxy AB enone **76** (352 mg, 0.687 mmol, 1 equiv) in tetrahydrofuran (2.5 mL) was added dropwise via syringe to the reaction solution. The resulting mixture was allowed to warm slowly to -10 $^{\circ}$ C over 100 min, then was partitioned between aqueous potassium phosphate buffer solution (pH 7.0, 0.2 M, 70 mL) and dichloromethane (70 mL). The phases were separated and the aqueous phase was further extracted with dichloromethane (70 mL). The organic extracts were combined and the combined solution was dried over anhydrous sodium sulfate. The dried solution was filtered and the filtrate was concentrated. The product was purified by flash-column chromatography (15% ethyl acetate–hexanes), providing the Michael–Claisen cyclization product **83** as a yellow solid (473 mg, 87%).

R_f = 0.24 (20% ethyl acetate–hexanes); ^1H NMR (500 MHz, CDCl_3) δ 15.70 (s, 1H), 7.52–7.50 (m, 2H), 7.41–7.34 (m, 3H), 7.26 (d, 1H, J = 8.8 Hz), 7.02 (d, 1H, J = 8.3 Hz), 5.37 (AB quartet, 2H), 3.80 (d, 1H, J = 3.9 Hz), 3.72 (dd, 1H, J = 15.6, 5.4 Hz), 3.64 (d,

1H, $J = 10.7$ Hz), 3.38 (s, 3H), 3.17 (ddd, 1H, $J = 14.6, 5.4, 4.4$ Hz), 2.79 (d, 1H, $J = 10.3$ Hz), 2.67 (s, 6H), 2.51 (s, 6H), 2.34 (dd, 1H, $J = 15.1, 14.6$ Hz), 1.53 (s, 9H), 0.83 (s, 9H), 0.23 (s, 3H), 0.05 (s, 3H); ^{13}C NMR (125 MHz, CDCl_3) δ 187.3, 186.3, 180.6, 180.5, 167.4, 152.1, 149.6, 145.2, 136.4, 135.0, 128.5, 128.5, 128.4, 124.4, 123.2, 122.2, 108.5, 106.0, 83.6, 82.5, 81.7, 72.5, 60.4, 56.2, 50.1, 44.4, 41.9, 37.5, 32.4, 27.7, 25.9, 19.0, -2.4, -3.4; HRMS-ESI (m/z): $[\text{M}+\text{H}]^+$ calcd for $\text{C}_{42}\text{H}_{56}\text{N}_3\text{O}_{10}\text{Si}$, 790.3730; found, 790.3736.

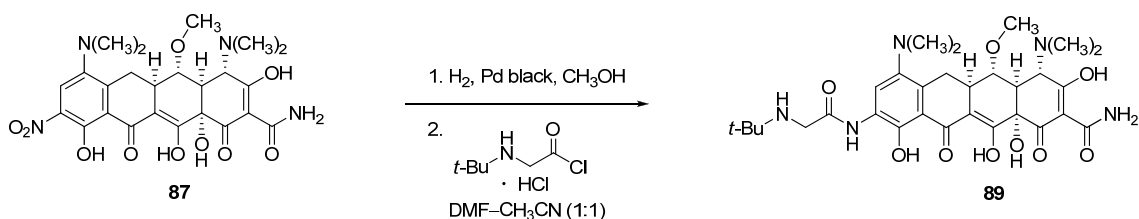


5-(α)-Methoxyminocycline (86). Concentrated aqueous hydrofluoric acid solution (48 wt%, 3.0 mL) was added to a solution of the Michael–Claisen cyclization product **83** (472 mg, 0.597 mmol, 1 equiv) in acetonitrile (4.5 mL) in a polypropylene reaction vessel at 23 °C. The reaction solution was stirred vigorously at 23 °C for 14 h, then was poured into water (150 mL) containing dipotassium hydrogenphosphate trihydrate (30 g). The resulting mixture was extracted with ethyl acetate (150 mL, then 2 x 100 mL). The organic extracts were combined and the combined solution was dried over anhydrous sodium sulfate. The dried solution was filtered and the filtrate was concentrated, affording an orange-brown solid. Methanol (4.0 mL) and dioxane (4.0 mL) were added to the crude product. Palladium black (25.4 mg, 0.239 mmol, 0.4 equiv) was added in one portion to the resulting solution at 23 °C. An atmosphere of hydrogen was introduced by briefly evacuating the flask, then flushing with pure hydrogen (1 atm). The reaction mixture was stirred at 23 °C for 75 min, then was filtered through a plug of Celite. The filtrate was concentrated. The crude product was purified by preparative HPLC on an Agilent Prep C18 column [10 μ m, 250 x 21.2 mm, UV detection at 350 nm, Solvent A: 0.1% trifluoroacetic acid in water, Solvent B: acetonitrile, 2 batches, injection volume: 8.0 mL (6.0 mL 0.1% trifluoroacetic acid in water, 2.0 mL acetonitrile), gradient elution with 20→40% B over 40 min, flow rate: 15 mL/min]. Fractions eluting at 4–9 min were

collected and concentrated, affording 5-(α)-methoxyminocycline trifluoroacetate (**86**) as a yellow solid (359 mg, 100%, 2 steps).

^1H NMR (600 MHz, CD_3OD , trifluoroacetate) δ 7.83 (d, 1H, J = 9.4 Hz), 7.03 (dd, 1H, J = 9.2, 0.7 Hz), 4.25 (d, 1H, J = 1.2 Hz), 3.67 (s, 3H), 3.62 (dd, 1H, J = 15.2, 4.4 Hz), 3.22 (dd, 1H, J = 11.4, 9.1 Hz), 3.16 (s, 6H), 3.07–3.02 (m, 1H), 2.99 (dd, 1H, J = 11.4, 9.3 Hz), 2.94 (s, 6H), 2.66 (dd, 1H, J = 14.5, 14.4 Hz); HRMS–ESI (m/z): $[\text{M}+\text{H}]^+$ calcd for $\text{C}_{24}\text{H}_{30}\text{N}_3\text{O}_8$, 488.2027; found, 488.2052.

(m, 2H), 2.94 (brs, 6H), 2.73 (s, 6H), 2.55 (dd, 1H, $J = 15.7, 13.6$ Hz); HRMS–ESI (m/z):
[M+H]⁺ calcd for C₂₄H₂₉N₄O₁₀, 533.1878; found, 533.1881.

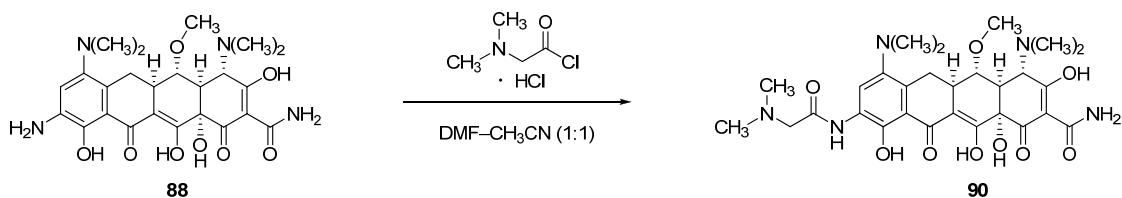


5-(α)-Methoxytigecycline (89). Palladium black (14.8 mg, 0.139 mmol, 0.4 equiv) was added in one portion to a solution of 9-nitro-5-(α)-methoxyiminocycline trifluoroacetate (**87**, 225 mg, 0.348 mmol, 1 equiv) in methanol (8.0 mL) at 23 °C. An atmosphere of hydrogen was introduced by briefly evacuating the flask, then flushing with pure hydrogen (1 atm). The reaction mixture was stirred at 23 °C for 1 ½ h, then was filtered through a plug of Celite. The filtrate was concentrated. The crude aniline product (**88**) was then divided into 8 equal portions (0.0435 mmol each, assuming 100% yield for nitro reduction) and used in diversifying steps without further purification.

2-(*tert*-Butylamino)acetyl chloride hydrochloride (16.2 mg, 0.087 mmol, 2.0 equiv) was added in one portion to a solution of crude 9-amino-5-(α)-methoxyiminocycline trifluoroacetate (0.0435 mmol, 1 equiv) in *N,N*-dimethylformamide (200 μ L) and acetonitrile (200 μ L) at 23 °C. The reaction mixture was stirred at this temperature for 2 h, whereupon 0.1% aqueous trifluoroacetic acid solution was added (6.0 mL). The resulting crude product solution was filtered and then purified by preparative HPLC by loading directly onto an Agilent Prep C18 column [10 μ m, 250 x 21.2 mm, UV detection at 350 nm, Solvent A: 0.1% trifluoroacetic acid in water, Solvent B: acetonitrile, gradient elution with 5→40% B over 50 min, flow rate: 7.5 mL/min]. Fractions eluting 21-24 min were collected and concentrated, affording 5-(α)-methoxytigecycline bistrifluoroacetate

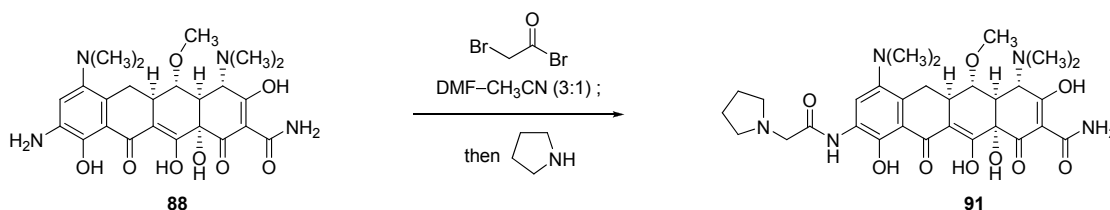
(**89**) as a yellow solid (18.0 mg, 49% over 2 steps from 9-nitro-5-(α)-methoxyminocycline).

^1H NMR (600 MHz, CD_3OD , bistrifluoroacetate) δ 8.48 (s, 1H), 4.26 (d, 1H, $J = 1.2$ Hz), 4.09 (s, 2H), 3.71 (dd, 1H, $J = 15.2, 4.5$ Hz), 3.68 (s, 3H), 3.23 (dd, 1H, $J = 11.6, 8.9$ Hz), 3.00–2.94 (m, 2H), 2.94 (brs, 6H), 2.88 (s, 6H), 2.51 (dd, 1H, $J = 15.2, 13.6$ Hz), 1.43 (s, 9H); HRMS–ESI (m/z): $[\text{M}+\text{H}]^+$ calcd for $\text{C}_{30}\text{H}_{42}\text{N}_5\text{O}_9$, 616.2977; found, 616.2969.



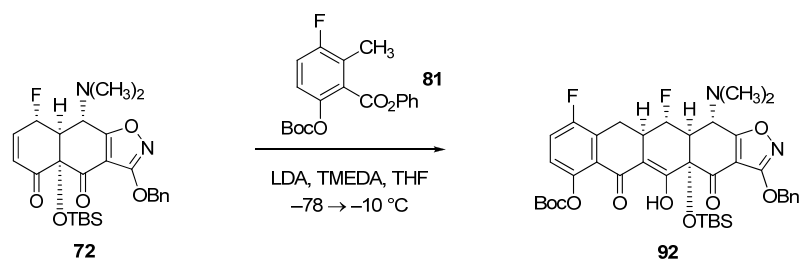
9-(*N,N*-dimethylglycylamido)-5-(α)-methoxyiminocycline (90). 2-(Dimethylamino)-acetyl chloride hydrochloride (13.7 mg, 0.087 mmol, 2.0 equiv) was added in one portion to a solution of crude 9-amino-5-(α)-methoxyiminocycline trifluoroacetate (**88**, 0.0435 mmol, 1 equiv) in *N,N*-dimethylformamide (200 μ L) and acetonitrile (200 μ L) at 23 °C. The reaction mixture was stirred at this temperature for 3 h, whereupon 0.1% aqueous trifluoroacetic acid solution was added (6.0 mL). The resulting crude product solution was filtered and then purified by preparative HPLC by loading directly onto an Agilent Prep C18 column [10 μ m, 250 x 21.2 mm, UV detection at 350 nm, Solvent A: 0.1% trifluoroacetic acid in water, Solvent B: acetonitrile, gradient elution with 5 \rightarrow 40% B over 50 min, flow rate: 7.5 mL/min]. Fractions eluting 18-20 min were collected and concentrated, affording 9-(*N,N*-dimethylglycylamido)-5-(α)-methoxyiminocycline bistrifluoroacetate (**90**) as a yellow solid (15.0 mg, 42% over 2 steps from 9-nitro-5-(α)-methoxyiminocycline).

^1H NMR (600 MHz, CD_3OD , bistrifluoroacetate) δ 8.49 (s, 1H), 4.25 (d, 1H, J = 1.0 Hz), 4.25 (s, 2H), 3.71–3.68 (m, 1H), 3.68 (s, 3H), 3.23 (dd, 1H, J = 11.4, 9.1 Hz), 3.02 (s, 6H), 3.02–2.94 (m, 2H), 2.94 (s, 6H), 2.92 (s, 6H), 2.53 (dd, 1H, J = 15.1, 13.6 Hz); HRMS–ESI (m/z): $[\text{M}+\text{H}]^+$ calcd for $\text{C}_{28}\text{H}_{38}\text{N}_5\text{O}_9$, 588.2664; found, 588.2663.



9-(Pyrrolidinoglycylamido)-5-(α)-methoxyiminocycline (91). Bromoacetyl bromide (4.5 μ L, 0.052 mmol, 1.2 equiv) was added dropwise to a mixture of crude 9-amino-5-(α)-methoxyiminocycline trifluoroacetate (**88**, 0.0435 mmol, 1 equiv) and sodium carbonate (23 mg, 0.22 mmol, 5.0 equiv) in *N,N*-dimethylformamide (300 μ L) and acetonitrile (100 μ L) at 23 °C. The resulting mixture was stirred at this temperature for 15 min, whereupon pyrrolidine (36.0 μ L, 0.435 mmol, 10.0 equiv) was added. The reaction mixture was stirred at 23 °C for a further 2 h, then 0.1% aqueous trifluoroacetic acid solution was added (6.0 mL). The resulting crude product solution was filtered and then purified by preparative HPLC by loading directly onto an Agilent Prep C18 column [10 μ m, 250 x 21.2 mm, UV detection at 350 nm, Solvent A: 0.1% trifluoroacetic acid in water, Solvent B: acetonitrile, gradient elution with 5 \rightarrow 40% B over 50 min, flow rate: 7.5 mL/min]. Fractions eluting 20–23 min were collected and concentrated, providing 9-(pyrrolidino)acetamido-5-(α)-methoxyiminocycline bistrifluoroacetate (**91**) as a yellow solid (14.5 mg, 40% yield over 2 steps from 9-nitro-5-(α)-methoxyiminocycline).

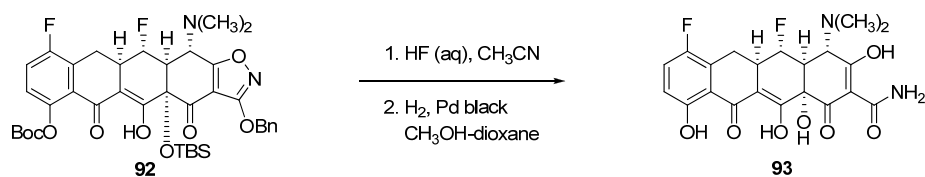
^1H NMR (600 MHz, CD_3OD , bistrifluoroacetate) δ 8.56 (s, 1H), 4.34 (s, 2H), 4.25 (d, 1H, $J = 1.2$ Hz), 3.80 (brs, 2H), 3.68 (s, 3H), 3.69–3.65 (m, 1H), 3.24–3.18 (brm, 2H), 3.23 (dd, 1H, $J = 11.5, 9.0$ Hz), 3.03–2.94 (m, 2H), 3.00 (s, 6H), 2.94 (s, 6H), 2.57 (dd, 1H, $J = 15.1, 13.6$ Hz), 2.18 (brs, 2H), 2.09 (brs, 2H); HRMS–ESI (m/z): $[\text{M}+\text{H}]^+$ calcd for $\text{C}_{30}\text{H}_{40}\text{N}_5\text{O}_9$, 614.2821; found, 614.2823.



Michael–Claisen cyclization product 92. A freshly prepared solution of lithium diisopropylamide (1.0 M, 3.45 mL, 3.45 mmol, 3.0 equiv) was added dropwise via syringe to a solution of phenyl ester **81** (1.19 g, 3.45 mmol, 3.0 equiv) and TMEDA (1.04 mL, 6.89 mmol, 6.0 equiv) in tetrahydrofuran (40 mL) at $-78\text{ }^\circ\text{C}$, forming a dark red solution. After stirring at $-78\text{ }^\circ\text{C}$ for 45 min, a solution of γ -(α)-fluoro AB enone **72** (575 mg, 1.15 mmol, 1 equiv) in tetrahydrofuran (5 mL) was added dropwise via syringe to the reaction solution. The resulting mixture was allowed to warm slowly to $-10\text{ }^\circ\text{C}$ over 100 min, then was partitioned between aqueous potassium phosphate buffer solution (pH 7.0, 0.2 M, 125 mL) and dichloromethane (125 mL). The phases were separated and the aqueous phase was further extracted with dichloromethane (2 x 50 mL). The organic extracts were combined and the combined solution was dried over anhydrous sodium sulfate. The dried solution was filtered and the filtrate was concentrated, affording a brown oil. The product was purified by flash-column chromatography (8% ethyl acetate–hexanes), providing the Michael–Claisen cyclization product **92** as a greenish-yellow solid (523 mg, 61%).

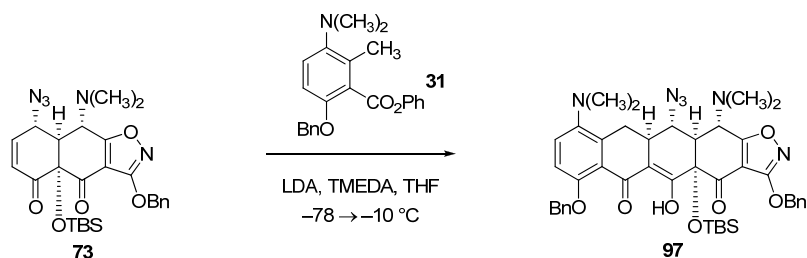
$R_f = 0.48$ (25% ethyl acetate–hexanes); ^1H NMR (500 MHz, CDCl_3) δ 15.64 (s, 1H), 7.52–7.50 (m, 2H), 7.41–7.35 (m, 3H), 7.25 (dd, 1H, $J = 8.3, 8.3$ Hz), 7.07 (dd, 1H, $J = 9.0, 4.5$ Hz), 5.38 (AB quartet, 2H), 5.03 (ddd, 1H, $J = 47.8, 3.5, 1.0$ Hz), 3.67 (dd, 1H, J

= 15.6, 5.4 Hz), 3.62 (d, 1H, J = 11.2 Hz), 3.56–3.45 (m, 1H), 2.93 (ddd, 1H, J = 22.0, 10.8, 1.0 Hz), 2.52 (s, 6H), 2.48 (dd, 1H, J = 15.6, 15.6 Hz), 1.53 (s, 9H), 0.83 (s, 9H), 0.24 (s, 3H), 0.09 (s, 3H); ^{13}C NMR (125 MHz, CDCl_3) δ 188.0, 186.0, 180.1 (d, J = 4.7 Hz), 178.1, 167.4, 156.6 (d, J = 244.4 Hz), 151.6, 146.1 (d, J = 2.7 Hz), 134.9, 128.6, 128.5, 128.5, 127.8 (d, J = 19.2 Hz), 123.6 (d, J = 8.2 Hz), 123.5 (d, J = 3.7 Hz), 120.6 (d, J = 23.8 Hz), 108.4, 104.0 (d, J = 8.2 Hz), 92.4 (d, J = 180.3 Hz), 84.2, 81.9, 72.7, 59.6 (d, J = 10.1 Hz), 52.5 (d, J = 20.1 Hz), 41.9, 36.8 (d, J = 28.4 Hz), 27.9, 27.6, 25.9, 19.0, –2.4, –3.4; ^{19}F NMR (300 MHz, CDCl_3) δ –115.1, –159.8; FTIR (neat film), 1763 (w), 1721 (m), 1614 (w), 1508 (m), 1452 (m), 1144 (m), 733 (s) cm^{-1} ; HRMS–ESI (m/z): $[\text{M}+\text{H}]^+$ calcd for $\text{C}_{39}\text{H}_{47}\text{F}_2\text{N}_2\text{O}_9\text{Si}$, 753.3013; found, 753.3023.



7-Fluoro-5-(α)-fluorosancycline (93). Concentrated aqueous hydrofluoric acid solution (48 wt%, 3.0 mL) was added to a solution of the Michael–Claisen cyclization product **92** (416 mg, 0.553 mmol, 1 equiv) in acetonitrile (4.5 mL) in a polypropylene reaction vessel at 23 °C. The reaction solution was stirred vigorously at 23 °C for 16 h, then was poured into water (150 mL) containing dipotassium hydrogenphosphate trihydrate (30 g). The resulting mixture was extracted with ethyl acetate (150 mL, then 2 x 50 mL). The organic extracts were combined and the combined solution was dried over anhydrous sodium sulfate. The dried solution was filtered and the filtrate was concentrated. Methanol (4.0 mL) and dioxane (4.0 mL) were added to the crude product. Palladium black (23.5 mg, 0.221 mmol, 0.4 equiv) was added in one portion to the resulting solution at 23 °C. An atmosphere of hydrogen was introduced by briefly evacuating the flask, then flushing with pure hydrogen (1 atm). The reaction mixture was stirred at 23 °C for 1 h, then was filtered through a plug of Celite. The filtrate was concentrated. The product was purified by preparative HPLC on an Agilent Prep C18 column [10 μ m, 250 x 21.2 mm, UV detection at 350 nm, Solvent A: 0.1% trifluoroacetic acid in water, Solvent B: acetonitrile, 2 batches, injection volume: 8.0 mL (6.0 mL 0.1% trifluoroacetic acid in water, 2.0 mL acetonitrile), gradient elution with 20→40% B over 40 min, flow rate: 15 mL/min]. Fractions eluting at 15–25 min were collected and concentrated, affording 7-fluoro-5-(α)-fluorosancycline trifluoroacetate (**93**) as a yellow solid (310 mg, 99%, two steps).

^1H NMR (600 MHz, CD_3OD , trifluoroacetate) δ 7.32 (dd, 1H, $J = 9.1, 8.9$ Hz), 6.85 (dd, 1H, $J = 9.2, 4.2$ Hz), 4.57 (ddd, 1H, $J = 48.8, 11.8, 9.0$ Hz), 4.56 (s, 1H), 3.49 (dd, 1H, $J = 15.7, 4.7$ Hz), 3.32 (dd, 1H, $J = 11.9, 5.5$ Hz), 3.28–3.21 (m, 1H), 2.93 (brs, 6H), 2.48 (dd, 1H, $J = 14.8, 14.4$ Hz); HRMS–ESI (m/z): $[\text{M}+\text{H}]^+$ calcd for $\text{C}_{21}\text{H}_{21}\text{F}_2\text{N}_2\text{O}_7$, 451.1311; found, 451.1312.



Michael–Claisen cyclization product 97. A freshly prepared solution of lithium diisopropylamide (1.0 M, 2.31 mL, 2.31 mmol, 3.1 equiv) was added dropwise via syringe to a solution of phenyl ester **31** (808 mg, 2.23 mmol, 3.0 equiv) and TMEDA (670 μ L, 4.47 mmol, 6.0 equiv) in tetrahydrofuran (20 mL) at -78 $^\circ\text{C}$, forming a dark red solution. After stirring at -78 $^\circ\text{C}$ for 40 min, a solution of γ -(α)-azido-substituted AB enone **73** (390 mg, 0.745 mmol, 1 equiv) in tetrahydrofuran (4.0 mL) was added dropwise via syringe to the reaction solution. The resulting mixture was stirred at -78 $^\circ\text{C}$ for 10 min, then was allowed to warm slowly to -10 $^\circ\text{C}$ over 100 min. Aqueous potassium phosphate buffer solution (pH 7.0, 0.2 M, 50 mL) was added and the resulting mixture was allowed to warm to 23 $^\circ\text{C}$. Dichloromethane (50 mL) was added to the crude product mixture and the phases were separated. The aqueous phase was further extracted with dichloromethane (50 mL). The organic extracts were combined and the combined solution was dried over anhydrous sodium sulfate. The dried solution was filtered and the filtrate was concentrated. The product was purified first by flash-column chromatography (12% ethyl acetate–hexanes), then by preparative HPLC on an Agilent Prep C18 column [10 μ m, 250 x 21.2 mm, UV detection at 350 nm, Solvent A: water, Solvent B: methanol, 3 batches, gradient elution with 95 \rightarrow 100% B over 50 min, flow rate: 15 mL/min].

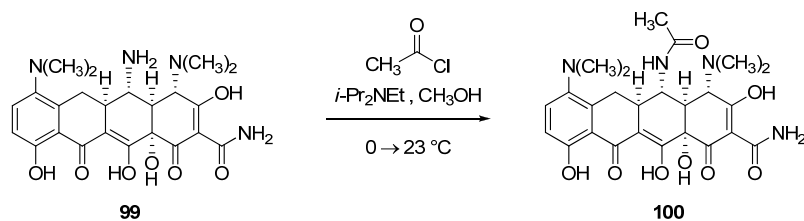
Fractions eluting at 16–22 min were collected and concentrated, providing the Michael–Claisen cyclization product **97** as a yellow solid (294 mg, 50%).

R_f = 0.28 (20% ethyl acetate–hexanes); ^1H NMR (500 MHz, CDCl_3) δ 15.82 (s, 1H), 7.53 (d, 2H, J = 6.8 Hz), 7.45 (d, 2H, J = 6.8 Hz), 7.42–7.29 (m, 6H), 7.22 (d, 1H, J = 8.8 Hz), 6.89 (d, 1H, J = 8.8 Hz), 5.40 (s, 2H), 5.16 (AB quartet, 2H), 4.14 (d, 1H, J = 5.9 Hz), 3.80 (dd, 1H, J = 15.6, 5.9 Hz), 3.74 (d, 1H, J = 10.7 Hz), 3.07–3.01 (m, 1H), 2.82 (d, 1H, J = 11.7 Hz), 2.65 (s, 6H), 2.55 (s, 6H), 2.26 (app t, 1H, J = 15.6, 14.7 Hz), 0.86 (s, 9H), 0.28 (s, 3H), 0.08 (s, 3H); ^{13}C NMR (125 MHz, CDCl_3) δ 187.3, 186.7, 180.6, 180.1, 167.5, 154.9, 145.1, 136.9, 136.5, 135.0, 128.5, 128.5, 128.5, 128.4, 127.7, 126.8, 125.3, 119.7, 114.0, 108.6, 105.1, 82.6, 72.6, 71.4, 62.7, 61.6, 52.5, 44.8, 41.9, 36.7, 32.3, 26.0, 19.1, -2.3, -3.1; FTIR (neat film), 2097 (s), 1722 (m), 1611 (m), 1512 (s), 1250 (s), 833 (s) cm^{-1} ; HRMS–ESI (m/z): $[\text{M}+\text{H}]^+$ calcd for $\text{C}_{43}\text{H}_{51}\text{N}_6\text{O}_7\text{Si}$, 791.3583; found, 791.3605.

Solvent A: water, Solvent B: methanol, gradient elution with 95→100% B over 50 min, flow rate: 15 mL/min]. Fractions eluting at 14–18 min were collected and concentrated, affording *tert*-butyl carbamate **98** as a yellow solid (18.4 mg, 60%).

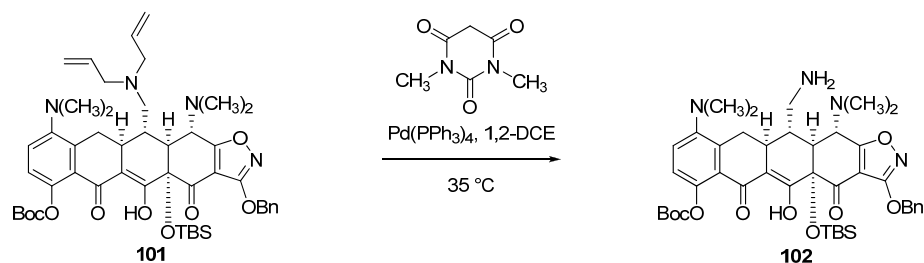
^1H NMR (500 MHz, CDCl_3) δ 16.28, 7.51 (d, 2H, $J = 7.3$ Hz), 7.47 (d, 2H, $J = 7.3$ Hz), 7.41–7.29 (m, 6H), 7.19 (d, 1H, $J = 8.8$ Hz), 6.87 (d, 1H, $J = 8.8$ Hz), 5.38 (s, 2H), 5.18 (AB quartet, 2H), 4.55 (d, 1H, $J = 9.8$ Hz), 3.95 (dd, 1H, $J = 15.7, 4.9$ Hz), 3.94 (d, 1H, $J = 10.8$ Hz), 2.83–2.79 (m, 1H), 2.67–2.63 (m, 1H), 2.63 (s, 6H), 2.52 (s, 6H), 2.35 (appt, 1H, $J = 15.1, 15.1$ Hz), 1.41 (s, 9H), 0.93 (s, 9H), 0.36 (s, 3H), 0.08 (s, 3H); ^{13}C NMR (125 MHz, CDCl_3) δ 186.5, 184.4, 181.2, 181.1, 167.4, 155.2, 154.8, 145.3, 138.0, 136.9, 135.0, 128.5, 128.5, 128.5, 128.4, 127.7, 126.8, 125.2, 120.6, 113.6, 108.4, 106.7, 83.1, 79.1, 72.6, 71.3, 60.8, 52.7, 48.5, 44.7, 41.8, 40.2, 33.2, 28.3, 26.3, 19.1, -2.5, -2.6; FTIR (neat film), 1717 (s), 1611 (w), 1512 (m), 1474 (m), 1171 (m) cm^{-1} ; HRMS–ESI (m/z): $[\text{M}+\text{H}]^+$ calcd for $\text{C}_{48}\text{H}_{61}\text{N}_4\text{O}_9\text{Si}$, 865.4202; found, 865.4246.

3.26 (m, 1H), 3.27 (s, 6H), 3.09 (brs, 1H), 2.92 (s, 6H), 2.92-2.90 (m, 1H); HRMS–ESI
(*m/z*): [M+H]⁺ calcd for C₂₃H₂₉N₄O₇, 473.2031; found, 473.2052.



5-*N*-Acetylaminoiminocycline (100). *N,N*-Diisopropylethylamine (6.0 μL , 0.034 mmol, 5.0 equiv) and acetyl chloride (1.9 μL , 0.027 mmol, 4.0 equiv) were added sequentially to solution of 5-aminominocycline trifluoroacetate (**99**, 4.0 mg, 0.0068 mmol, 1 equiv) in methanol (200 μL) at 0 $^\circ\text{C}$. The resulting solution was allowed to warm to 23 $^\circ\text{C}$ over 5 min. The reaction mixture was stirred at this temperature for 40 min, then was concentrated. The product was purified by preparative HPLC on an Agilent Prep C18 column [10 μm , 250 x 21.2 mm, UV detection at 350 nm, Solvent A: 0.1% trifluoroacetic acid in water, Solvent B: acetonitrile, injection volume: 5.0 mL (4.0 mL 0.1% trifluoroacetic acid in water, 1.0 mL acetonitrile), gradient elution with 5 \rightarrow 40% B over 50 min, flow rate: 7.5 mL/min]. Fractions eluting at 24-27 min were collected and concentrated, affording 5-*N*-acetylaminoiminocycline trifluoroacetate (**100**) as a yellow solid (3.1 mg, 73%).

^1H NMR (600 MHz, CD_3OD , trifluoroacetate) δ 7.69 (d, 1H, J = 9.2 Hz), 6.97 (d, 1H, J = 9.2 Hz), 4.00 (brs, 1H), 3.92 (s, 1H), 3.41 (dd, 1H, J = 15.4, 4.1 Hz), 3.03-2.92 (m, 2H), 2.98 (s, 6H), 2.95 (s, 6H), 2.38 (appt, 1H, J = 14.8, 14.3 Hz), 2.13 (s, 3H); HRMS–ESI (m/z): $[\text{M}+\text{H}]^+$ calcd for $\text{C}_{25}\text{H}_{31}\text{N}_4\text{O}_8$, 515.2136; found 515.2128.



5-Aminomethyliminocycline precursor 102. Michael–Claisen cyclization product **101** (815 mg, 0.938 mmol, 1 equiv) was dissolved in 1,2-dichloroethane (10 mL) and argon was bubbled through the resulting solution for 2 min. The solution was then transferred to a round-bottomed flask containing tetrakis(triphenylphosphine)palladium (108 mg, 0.094 mmol, 0.1 equiv) and 1,3-dimethylbarbituric acid (878 mg, 5.63 mmol, 6.0 equiv). The yellow homogeneous reaction solution was heated to 35 °C. After stirring at this temperature for 80 min, the reaction solution was allowed to cool to 23 °C. The cooled solution was diluted with ethyl acetate (50 mL) and the resulting solution was poured into saturated aqueous sodium bicarbonate solution (50 mL). The phases were separated and the aqueous phase was further extracted with ethyl acetate (2 x 50 mL). The organic extracts were combined and the combined solution was dried over anhydrous sodium sulfate. The dried solution was filtered and the filtrate was concentrated. The crude product was purified by flash-column chromatography (1.5% methanol–dichloromethane, grading to 5%), affording amine **102** as a golden brown solid (571 mg, 77%).

R_f = 0.26 (5% methanol–dichloromethane); ^1H NMR (500 MHz, CDCl_3) δ 7.50 (d, 2H, J = 6.8 Hz), 7.39–7.32 (m, 3H), 7.23 (d, 1H, J = 8.8 Hz), 7.01 (d, 1H, J = 8.3 Hz), 5.37 (AB quartet, 2H), 3.71 (d, 1H, J = 10.7 Hz), 3.60 (dd, 1H, J = 15.4, 5.2 Hz), 3.09–3.00 (m, 2H), 2.77 (d, 1H, J = 10.3 Hz), 2.75–2.70 (m, 1H), 2.66 (s, 6H), 2.50 (s, 6H), 2.29

(dd, 1H, $J = 15.2, 15.1$ Hz), 2.22–2.18 (m, 1H), 1.52 (s, 9H), 0.87 (s, 9H), 0.24 (s, 3H), –
0.03 (s, 3H); ^{13}C NMR (125 MHz, CDCl_3) δ 187.3, 187.2, 181.0, 180.1, 167.3, 152.0,
149.4, 145.1, 136.3, 135.0, 128.4, 128.4, 128.3, 124.1, 123.2, 122.1, 108.5, 107.4, 83.6,
83.5, 72.4, 62.6, 53.4, 48.4, 47.7, 44.4, 43.0, 41.8, 33.7, 33.5, 27.6, 26.4, 19.1, –2.5, –2.6;
HRMS–ESI (m/z): $[\text{M}+\text{H}]^+$ calcd for $\text{C}_{42}\text{H}_{57}\text{N}_4\text{O}_9\text{Si}$, 789.3889; found, 789.3920.

X-Ray Crystallography (Michael–Claisen cyclization product 105): A crystal mounted on a diffractometer was collected data at 100 K. The intensities of the reflections were collected by means of a Bruker APEX II CCD along with the D8 Diffractometer (30 KeV, $\lambda = 0.413280 \text{ \AA}$), and equipped with an Oxford Cryosystems nitrogen open flow apparatus. The collection method involved 0.5° scans in Φ at -5° in 2θ . Data integration down to 0.82 \AA resolution was carried out using SAINT V7.46 A (Bruker diffractometer, 2009) with reflection spot size optimisation. Absorption corrections were made with the program SADABS (Bruker diffractometer, 2009). The structure was solved by the direct methods procedure and refined by least-squares methods again F^2 using SHELXS-97 and SHELXL-97 (Sheldrick, 2008). Non-hydrogen atoms were refined anisotropically, and hydrogen atoms were allowed to ride on the respective atoms. Crystal data as well as details of data collection and refinement are summarized in Table 3.10, geometric parameters are shown in Tables 3.11, and hydrogen-bond parameters are listed in Table 3.12. The Ortep plots produced with SHELXL-97 program, and the other drawings were produced with Accelrys DS Visualizer 2.0 (Accelrys, 2007).

Acknowledgement: We thank Dr. Yu-Sheng Chen at ChemMatCARS, APS, for his assistance with single-crystal data. ChemMatCARS Sector 15 is principally supported by the National Science Foundation/Department of Energy under grant number NSF/CHE-0822838. Use of the Advanced Photon Source was supported by the U. S. Department of Energy, Office of Science, Office of Basic Energy Sciences, under Contract No. DE-AC02-06CH11357.

Table 3.10. Experimental details

	IV-PMW-117
Crystal data	
Chemical formula	C ₉₀ H ₁₁₀ N ₆ O ₁₈ Si ₂
M_r	1620.02
Crystal system, space group	Triclinic, <i>P</i> 1
Temperature (K)	100
a, b, c (Å)	8.5526 (8), 13.1550 (12), 20.6010 (19)
α, β, γ (°)	106.209 (2), 90.871 (2), 105.015 (2)
V (Å ³)	2140.1 (3)
Z	1
Radiation type	Synchrotron, $\lambda = 0.41328$ Å
μ (mm ⁻¹)	0.07
Crystal size (mm)	0.03 × 0.03 × 0.02
Data collection	
Diffractometer	Bruker D8 goniometer with CCD area detector diffractometer
Absorption correction	Multi-scan <i>SADABS</i>
T_{\min}, T_{\max}	0.998, 0.999
No. of measured, independent and observed [$I > 2\sigma(I)$] reflections	34033, 12277, 9207
R_{int}	0.042
Refinement	
$R[F^2 > 2\sigma(F^2)], wR(F^2), S$	0.096, 0.211, 1.10
No. of reflections	12277
No. of parameters	1169
No. of restraints	499
H-atom treatment	H-atom parameters constrained
$\Delta\rho_{\text{max}}, \Delta\rho_{\text{min}}$ (e Å ⁻³)	0.94, -0.51
Absolute structure	Flack H D (1983), Acta Cryst. A39, 876-881
Flack parameter	-0.4 (12)

Computer programs: *APEX2* v2009.3.0 (Bruker-AXS, 2009), *SAINT* 7.46A (Bruker-AXS, 2009), *SHELXS97* (Sheldrick, 2008), *SHELXL97* (Sheldrick, 2008), Bruker *SHELXTL* (Sheldrick, 2008).

Table 3.11. Geometric parameters (Å, °)

O1—C1	1.369 (7)	O16—H16	0.8400
O1—N1	1.422 (9)	O17—C66	1.418 (10)
O2—C22	1.398 (9)	O17—Si2B	1.651 (10)
O2—C4	1.443 (8)	O17—Si2	1.723 (8)
O4—C26	1.305 (11)	O18—C67	1.200 (9)
O4—C11	1.346 (10)	O19—C69	1.315 (10)
O5—C13	1.288 (9)	O19—C89	1.530 (16)
O6—C15	1.286 (9)	O19—C89B	1.550 (12)
O6—H6	0.8400	N11—C69	1.256 (10)
O7—C16	1.419 (9)	N12—C58	1.420 (11)
O7—Si1B	1.655 (9)	N12—C74	1.460 (12)
O7—Si1	1.674 (9)	N12—C75	1.467 (13)
O8—C17	1.179 (8)	C51—C68	1.282 (11)
O9—C19	1.290 (9)	C51—C52	1.512 (11)
O9—C39B	1.518 (18)	C52—N13	1.409 (11)
O9—C39	1.520 (9)	C52—C53	1.580 (9)
N1—C19	1.304 (10)	C52—H52	1.0000
N2—C2	1.451 (9)	C53—C54	1.509 (11)
N2—C20	1.453 (10)	C53—C66	1.524 (11)
N2—C21	1.467 (10)	C53—H53	1.0000
N3—C25	1.292 (14)	C54—C55	1.523 (9)
N3—C25B	1.35 (2)	C54—H54	1.0000
N3—C8	1.403 (12)	C55—C64	1.462 (10)
N3—C24B	1.42 (2)	C55—C56	1.529 (11)
N3—C24	1.453 (14)	C55—H55	1.0000
C1—C18	1.313 (10)	C56—C57	1.511 (10)
C1—C2	1.459 (10)	C56—H56A	0.9900

Table 3.11. (Continued)			
C2—C3	1.566 (8)	C56—H56B	0.9900
C2—H2	1.0000	C57—C62	1.353 (11)
C3—C16	1.513 (10)	C57—C58	1.416 (11)
C3—C4	1.541 (9)	N13—C70	1.449 (10)
C3—H3	1.0000	N13—C71	1.462 (11)
C4—C5	1.512 (9)	C58—C59	1.424 (12)
C4—H4	1.0000	C59—C60	1.359 (13)
C5—C14	1.523 (10)	C59—H59	0.9500
C5—C6	1.543 (9)	C60—C61	1.389 (12)
C5—H5	1.0000	C60—H60	0.9500
C6—C7	1.500 (9)	C61—O14	1.335 (10)
C6—H6A	0.9900	C61—C62	1.424 (10)
C6—H6B	0.9900	C62—C63	1.487 (11)
C7—C8	1.392 (11)	C63—C64	1.420 (9)
C7—C12	1.396 (11)	C64—C65	1.390 (10)
C8—C9	1.367 (11)	C65—C66	1.520 (9)
C9—C10	1.364 (12)	C66—C67	1.559 (11)
C9—H9	0.9500	C67—C68	1.471 (10)
C10—C11	1.367 (11)	C68—C69	1.439 (10)
C10—H10	0.9500	C70—H70A	0.9800
C11—C12	1.403 (9)	C70—H70B	0.9800
C12—C13	1.455 (10)	C70—H70C	0.9800
C13—C14	1.412 (9)	C71—H71A	0.9800
C14—C15	1.340 (10)	C71—H71B	0.9800
C15—C16	1.537 (9)	C71—H71C	0.9800
C16—C17	1.520 (10)	C72—O13	1.366 (12)
C17—C18	1.491 (9)	C72—H72A	0.9900
C18—C19	1.434 (10)	C72—H72B	0.9900
C20—H20A	0.9800	O13—C73	1.439 (12)
C20—H20B	0.9800	C73—H73A	0.9800
C20—H20C	0.9800	C73—H73B	0.9800

Table 3.11. (Continued)			
C21—H21A	0.9800	C73—H73C	0.9800
C21—H21B	0.9800	C72B—O13B	1.36 (2)
C21—H21C	0.9800	C72B—H72C	0.9900
C22—O3	1.347 (10)	C72B—H72D	0.9900
C22—H22A	0.9900	O13B—C73B	1.44 (2)
C22—H22B	0.9900	C73B—H73D	0.9800
O3—C23	1.382 (12)	C73B—H73E	0.9800
C23—H23A	0.9800	C73B—H73F	0.9800
C23—H23B	0.9800	C74—H74A	0.9800
C23—H23C	0.9800	C74—H74B	0.9800
C24—H24A	0.9800	C74—H74C	0.9800
C24—H24B	0.9800	C75—H75A	0.9800
C24—H24C	0.9800	C75—H75B	0.9800
C25—H25A	0.9800	C75—H75C	0.9800
C25—H25B	0.9800	O14—C76	1.449 (10)
C25—H25C	0.9800	C76—C77	1.471 (11)
C24B—H24D	0.9800	C76—C77B	1.475 (18)
C24B—H24E	0.9800	C76—H76A	0.9900
C24B—H24F	0.9800	C76—H76B	0.9900
C25B—H25D	0.9800	C76—H76C	0.9900
C25B—H25E	0.9800	C76—H76D	0.9900
C25B—H25F	0.9800	C77—C78	1.3900
C26—C27	1.508 (10)	C77—C82	1.3900
C26—H26A	0.9900	C78—C79	1.3900
C26—H26B	0.9900	C78—H78	0.9500
C27—C28	1.3900	C79—C80	1.3900
C27—C32	1.3900	C79—H79	0.9500
C28—C29	1.3900	C80—C81	1.3900
C28—H28	0.9500	C80—H80	0.9500
C29—C30	1.3900	C81—C82	1.3900
C29—H29	0.9500	C81—H81	0.9500
C30—C31	1.3900	C82—H82	0.9500

Table 3.11. (Continued)			
C30—H30	0.9500	C77B—C78B	1.3900
C31—C32	1.3900	C77B—C82B	1.3900
C31—H31	0.9500	C78B—C79B	1.3900
C32—H32	0.9500	C78B—H78A	0.9500
Si1—C35	1.875 (17)	C79B—C80B	1.3900
Si1—C33	1.918 (19)	C79B—H79A	0.9500
Si1—C34	1.951 (15)	C80B—C81B	1.3900
C33—H33A	0.9800	C80B—H80A	0.9500
C33—H33B	0.9800	C81B—C82B	1.3900
C33—H33C	0.9800	C81B—H81A	0.9500
C34—H34A	0.9800	C82B—H82A	0.9500
C34—H34B	0.9800	Si2—C85	1.794 (16)
C34—H34C	0.9800	Si2—C83	1.94 (2)
C35—C38	1.38 (2)	Si2—C84	1.942 (15)
C35—C37	1.44 (2)	C83—H83A	0.9800
C35—C36	1.53 (2)	C83—H83B	0.9800
C36—H36A	0.9800	C83—H83C	0.9800
C36—H36B	0.9800	C84—H84A	0.9800
C36—H36C	0.9800	C84—H84B	0.9800
C37—H37A	0.9800	C84—H84C	0.9800
C37—H37B	0.9800	C85—C88	1.476 (19)
C37—H37C	0.9800	C85—C86	1.490 (19)
C38—H38A	0.9800	C85—C87	1.69 (2)
C38—H38B	0.9800	C86—H86A	0.9800
C38—H38C	0.9800	C86—H86B	0.9800
Si1B—C35B	1.908 (19)	C86—H86C	0.9800
Si1B—C34B	1.935 (19)	C87—H87A	0.9800
Si1B—C33B	1.965 (18)	C87—H87B	0.9800
Si1B—C38B	2.33 (2)	C87—H87C	0.9800
C34B—H34D	0.9800	C88—H88A	0.9800
C34B—H34E	0.9800	C88—H88B	0.9800
C34B—H34F	0.9800	C88—H88C	0.9800

Table 3.11. (Continued)			
C33B—H33D	0.9800	Si2B—C85B	1.786 (19)
C33B—H33E	0.9800	Si2B—C84B	1.918 (19)
C33B—H33F	0.9800	Si2B—C83B	2.07 (2)
C35B—C38B	1.38 (2)	C83B—H83D	0.9800
C35B—C37B	1.40 (2)	C83B—H83E	0.9800
C35B—C36B	1.53 (2)	C83B—H83F	0.9800
C36B—H36D	0.9800	C84B—H84D	0.9800
C36B—H36E	0.9800	C84B—H84E	0.9800
C36B—H36F	0.9800	C84B—H84F	0.9800
C37B—H37D	0.9800	C85B—C86B	1.45 (2)
C37B—H37E	0.9800	C85B—C88B	1.50 (2)
C37B—H37F	0.9800	C85B—C87B	1.70 (3)
C38B—H38D	0.9800	C86B—H86D	0.9800
C38B—H38E	0.9800	C86B—H86E	0.9800
C38B—H38F	0.9800	C86B—H86F	0.9800
C39—C40	1.425 (12)	C87B—H87D	0.9800
C39—H39A	0.9900	C87B—H87E	0.9800
C39—H39B	0.9900	C87B—H87F	0.9800
C40—C41	1.3900	C88B—H88D	0.9800
C40—C45	1.3900	C88B—H88E	0.9800
C41—C42	1.3900	C88B—H88F	0.9800
C41—H41	0.9500	C89—C90	1.453 (19)
C42—C43	1.3900	C89—H89A	0.9900
C42—H42	0.9500	C89—H89B	0.9900
C43—C44	1.3900	C90—C91	1.3900
C43—H43	0.9500	C90—C95	1.3900
C44—C45	1.3900	C91—C92	1.3900
C44—H44	0.9500	C91—H91	0.9500
C45—H45	0.9500	C92—C93	1.3900
C39B—C40B	1.434 (19)	C92—H92	0.9500
C39B—H39C	0.9900	C93—C94	1.3900
C39B—H39D	0.9900	C93—H93	0.9500

Table 3.11. (Continued)			
C40B—C41B	1.3900	C94—C95	1.3900
C40B—C45B	1.3900	C94—H94	0.9500
C41B—C42B	1.3900	C95—H95	0.9500
C41B—H41A	0.9500	C89B—C90B	1.463 (18)
C42B—C43B	1.3900	C89B—H89C	0.9900
C42B—H42A	0.9500	C89B—H89D	0.9900
C43B—C44B	1.3900	C90B—C91B	1.3900
C43B—H43A	0.9500	C90B—C95B	1.3900
C44B—C45B	1.3900	C91B—C92B	1.3900
C44B—H44A	0.9500	C91B—H91A	0.9500
C45B—H45A	0.9500	C92B—C93B	1.3900
O11—C51	1.363 (8)	C92B—H92A	0.9500
O11—N11	1.409 (9)	C93B—C94B	1.3900
O12—C54	1.431 (10)	C93B—H93A	0.9500
O12—C72	1.453 (10)	C94B—C95B	1.3900
O12—C72B	1.47 (2)	C94B—H94A	0.9500
O15—C63	1.267 (9)	C95B—H95A	0.9500
O16—C65	1.287 (9)		
C1—O1—N1	107.8 (5)	C58—N12—C75	110.3 (8)
C22—O2—C4	114.6 (7)	C74—N12—C75	107.7 (9)
C26—O4—C11	113.4 (7)	C68—C51—O11	111.1 (7)
C15—O6—H6	109.5	C68—C51—C52	131.6 (6)
C16—O7—Si1B	142.6 (6)	O11—C51—C52	116.8 (7)
C16—O7—Si1	131.4 (6)	N13—C52—C51	121.5 (7)
C19—O9—C39B	119.7 (12)	N13—C52—C53	112.2 (6)
C19—O9—C39	115.5 (7)	C51—C52—C53	106.2 (6)
C19—N1—O1	105.7 (5)	N13—C52—H52	105.2
C2—N2—C20	114.3 (6)	C51—C52—H52	105.2
C2—N2—C21	112.5 (7)	C53—C52—H52	105.2
C20—N2—C21	112.4 (6)	C54—C53—C66	112.0 (6)
C25—N3—C8	111.7 (11)	C54—C53—C52	109.6 (6)

Table 3.11. (Continued)			
C25B—N3—C8	114 (2)	C66—C53—C52	117.5 (6)
C25—N3—C24B	124 (2)	C54—C53—H53	105.6
C25B—N3—C24B	111 (3)	C66—C53—H53	105.6
C8—N3—C24B	124 (2)	C52—C53—H53	105.6
C25—N3—C24	117.2 (11)	O12—C54—C53	106.8 (6)
C25B—N3—C24	81 (3)	O12—C54—C55	110.3 (6)
C8—N3—C24	112.6 (9)	C53—C54—C55	112.1 (6)
C18—C1—O1	109.8 (6)	O12—C54—H54	109.2
C18—C1—C2	129.9 (6)	C53—C54—H54	109.2
O1—C1—C2	120.0 (6)	C55—C54—H54	109.2
N2—C2—C1	118.3 (6)	C64—C55—C54	112.8 (6)
N2—C2—C3	112.0 (5)	C64—C55—C56	108.7 (6)
C1—C2—C3	109.7 (6)	C54—C55—C56	113.7 (6)
N2—C2—H2	105.2	C64—C55—H55	107.1
C1—C2—H2	105.2	C54—C55—H55	107.1
C3—C2—H2	105.2	C56—C55—H55	107.1
C16—C3—C4	110.9 (6)	C57—C56—C55	107.6 (7)
C16—C3—C2	115.9 (6)	C57—C56—H56A	110.2
C4—C3—C2	108.4 (6)	C55—C56—H56A	110.2
C16—C3—H3	107.1	C57—C56—H56B	110.2
C4—C3—H3	107.1	C55—C56—H56B	110.2
C2—C3—H3	107.1	H56A—C56—H56B	108.5
O2—C4—C5	112.8 (6)	C62—C57—C58	122.9 (7)
O2—C4—C3	107.1 (5)	C62—C57—C56	119.4 (7)
C5—C4—C3	110.7 (6)	C58—C57—C56	117.7 (8)
O2—C4—H4	108.7	C52—N13—C70	114.0 (7)
C5—C4—H4	108.7	C52—N13—C71	113.0 (7)
C3—C4—H4	108.7	C70—N13—C71	110.5 (7)
C4—C5—C14	111.6 (6)	C57—C58—N12	121.1 (7)
C4—C5—C6	112.3 (5)	C57—C58—C59	115.0 (9)
C14—C5—C6	108.0 (5)	N12—C58—C59	123.6 (8)
C4—C5—H5	108.3	C60—C59—C58	122.3 (8)

Table 3.11. (Continued)			
C14—C5—H5	108.3	C60—C59—H59	118.8
C6—C5—H5	108.3	C58—C59—H59	118.8
C7—C6—C5	109.9 (6)	C59—C60—C61	121.5 (8)
C7—C6—H6A	109.7	C59—C60—H60	119.2
C5—C6—H6A	109.7	C61—C60—H60	119.2
C7—C6—H6B	109.7	O14—C61—C60	123.3 (7)
C5—C6—H6B	109.7	O14—C61—C62	119.2 (7)
H6A—C6—H6B	108.2	C60—C61—C62	117.6 (9)
C8—C7—C12	120.3 (7)	C57—C62—C61	120.3 (8)
C8—C7—C6	119.8 (7)	C57—C62—C63	119.6 (6)
C12—C7—C6	119.8 (6)	C61—C62—C63	120.0 (8)
C9—C8—C7	119.3 (9)	O15—C63—C64	122.7 (7)
C9—C8—N3	121.0 (8)	O15—C63—C62	121.4 (6)
C7—C8—N3	119.7 (7)	C64—C63—C62	115.9 (7)
C10—C9—C8	120.8 (8)	C65—C64—C63	116.8 (7)
C10—C9—H9	119.6	C65—C64—C55	123.9 (6)
C8—C9—H9	119.6	C63—C64—C55	119.2 (7)
C9—C10—C11	121.1 (8)	O16—C65—C64	124.0 (6)
C9—C10—H10	119.4	O16—C65—C66	114.3 (6)
C11—C10—H10	119.4	C64—C65—C66	121.7 (7)
O4—C11—C10	120.5 (7)	O17—C66—C65	109.1 (6)
O4—C11—C12	119.9 (7)	O17—C66—C53	109.6 (6)
C10—C11—C12	119.5 (8)	C65—C66—C53	111.5 (6)
C7—C12—C11	118.7 (7)	O17—C66—C67	105.1 (6)
C7—C12—C13	117.7 (6)	C65—C66—C67	110.1 (6)
C11—C12—C13	123.5 (8)	C53—C66—C67	111.3 (6)
O5—C13—C14	119.8 (6)	O18—C67—C68	125.4 (7)
O5—C13—C12	119.6 (6)	O18—C67—C66	125.1 (6)
C14—C13—C12	120.6 (7)	C68—C67—C66	109.3 (7)
C15—C14—C13	120.5 (7)	C51—C68—C69	104.4 (7)
C15—C14—C5	122.7 (6)	C51—C68—C67	121.7 (7)
C13—C14—C5	116.5 (6)	C69—C68—C67	133.9 (8)

Table 3.11. (Continued)			
O6—C15—C14	122.7 (6)	N11—C69—O19	125.0 (7)
O6—C15—C16	114.0 (6)	N11—C69—C68	111.4 (8)
C14—C15—C16	123.3 (7)	O19—C69—C68	123.4 (7)
O7—C16—C3	107.4 (6)	N13—C70—H70A	109.5
O7—C16—C17	106.0 (6)	N13—C70—H70B	109.5
C3—C16—C17	114.4 (6)	H70A—C70—H70B	109.5
O7—C16—C15	108.3 (6)	N13—C70—H70C	109.5
C3—C16—C15	111.0 (6)	H70A—C70—H70C	109.5
C17—C16—C15	109.5 (6)	H70B—C70—H70C	109.5
O8—C17—C18	123.9 (6)	N13—C71—H71A	109.5
O8—C17—C16	126.8 (6)	N13—C71—H71B	109.5
C18—C17—C16	109.3 (6)	H71A—C71—H71B	109.5
C1—C18—C19	106.0 (6)	N13—C71—H71C	109.5
C1—C18—C17	121.1 (6)	H71A—C71—H71C	109.5
C19—C18—C17	132.8 (7)	H71B—C71—H71C	109.5
O9—C19—N1	124.1 (7)	O13—C72—O12	112.9 (8)
O9—C19—C18	125.3 (7)	O13—C72—H72A	109.0
N1—C19—C18	110.6 (7)	O12—C72—H72A	109.0
N2—C20—H20A	109.5	O13—C72—H72B	109.0
N2—C20—H20B	109.5	O12—C72—H72B	109.0
H20A—C20—H20B	109.5	H72A—C72—H72B	107.8
N2—C20—H20C	109.5	C72—O13—C73	112.0 (10)
H20A—C20—H20C	109.5	O13—C73—H73A	109.5
H20B—C20—H20C	109.5	O13—C73—H73B	109.5
N2—C21—H21A	109.5	H73A—C73—H73B	109.5
N2—C21—H21B	109.5	O13—C73—H73C	109.5
H21A—C21—H21B	109.5	H73A—C73—H73C	109.5
N2—C21—H21C	109.5	H73B—C73—H73C	109.5
H21A—C21—H21C	109.5	O13B—C72B—O12	110 (3)
H21B—C21—H21C	109.5	O13B—C72B—H72C	109.7
O3—C22—O2	114.7 (7)	O12—C72B—H72C	109.7
O3—C22—H22A	108.6	O13B—C72B—H72D	109.7

Table 3.11. (Continued)			
O2—C22—H22A	108.6	O12—C72B—H72D	109.7
O3—C22—H22B	108.6	H72C—C72B—H72D	108.2
O2—C22—H22B	108.6	C72B—O13B—C73B	117 (4)
H22A—C22—H22B	107.6	O13B—C73B—H73D	109.5
C22—O3—C23	112.1 (9)	O13B—C73B—H73E	109.5
O3—C23—H23A	109.5	H73D—C73B—H73E	109.5
O3—C23—H23B	109.5	O13B—C73B—H73F	109.5
H23A—C23—H23B	109.5	H73D—C73B—H73F	109.5
O3—C23—H23C	109.5	H73E—C73B—H73F	109.5
H23A—C23—H23C	109.5	N12—C74—H74A	109.5
H23B—C23—H23C	109.5	N12—C74—H74B	109.5
N3—C24—H24A	109.5	H74A—C74—H74B	109.5
N3—C24—H24B	109.5	N12—C74—H74C	109.5
H24A—C24—H24B	109.5	H74A—C74—H74C	109.5
N3—C24—H24C	109.5	H74B—C74—H74C	109.5
H24A—C24—H24C	109.5	N12—C75—H75A	109.5
H24B—C24—H24C	109.5	N12—C75—H75B	109.5
N3—C25—H25A	109.5	H75A—C75—H75B	109.5
N3—C25—H25B	109.5	N12—C75—H75C	109.5
H25A—C25—H25B	109.5	H75A—C75—H75C	109.5
N3—C25—H25C	109.5	H75B—C75—H75C	109.5
H25A—C25—H25C	109.5	C61—O14—C76	120.1 (6)
H25B—C25—H25C	109.5	O14—C76—C77	109.3 (7)
N3—C24B—H24D	109.5	O14—C76—C77B	108.6 (11)
N3—C24B—H24E	109.5	O14—C76—H76A	109.8
H24D—C24B—H24E	109.5	C77—C76—H76A	109.8
N3—C24B—H24F	109.5	C77B—C76—H76A	103.9
H24D—C24B—H24F	109.5	O14—C76—H76B	109.8
H24E—C24B—H24F	109.5	C77—C76—H76B	109.8
N3—C25B—H25D	109.5	C77B—C76—H76B	116.2
N3—C25B—H25E	109.5	H76A—C76—H76B	108.3
H25D—C25B—H25E	109.5	O14—C76—H76C	110.0

Table 3.11. (Continued)			
N3—C25B—H25F	109.5	C77—C76—H76C	115.6
H25D—C25B—H25F	109.5	C77B—C76—H76C	110.0
H25E—C25B—H25F	109.5	H76B—C76—H76C	102.1
O4—C26—C27	108.8 (8)	O14—C76—H76D	110.0
O4—C26—H26A	109.9	C77—C76—H76D	103.4
C27—C26—H26A	109.9	C77B—C76—H76D	110.0
O4—C26—H26B	109.9	H76A—C76—H76D	114.3
C27—C26—H26B	109.9	H76C—C76—H76D	108.3
H26A—C26—H26B	108.3	C78—C77—C82	120.0
C28—C27—C32	120.0	C78—C77—C76	120.5 (6)
C28—C27—C26	121.6 (5)	C82—C77—C76	119.1 (6)
C32—C27—C26	118.2 (6)	C77—C78—C79	120.0
C27—C28—C29	120.0	C77—C78—H78	120.0
C27—C28—H28	120.0	C79—C78—H78	120.0
C29—C28—H28	120.0	C80—C79—C78	120.0
C28—C29—C30	120.0	C80—C79—H79	120.0
C28—C29—H29	120.0	C78—C79—H79	120.0
C30—C29—H29	120.0	C79—C80—C81	120.0
C31—C30—C29	120.0	C79—C80—H80	120.0
C31—C30—H30	120.0	C81—C80—H80	120.0
C29—C30—H30	120.0	C82—C81—C80	120.0
C30—C31—C32	120.0	C82—C81—H81	120.0
C30—C31—H31	120.0	C80—C81—H81	120.0
C32—C31—H31	120.0	C81—C82—C77	120.0
C31—C32—C27	120.0	C81—C82—H82	120.0
C31—C32—H32	120.0	C77—C82—H82	120.0
C27—C32—H32	120.0	C78B—C77B—C82B	120.0
O7—Si1—C35	104.6 (7)	C78B—C77B—C76	125.3 (16)
O7—Si1—C33	118.2 (7)	C82B—C77B—C76	105.4 (16)
C35—Si1—C33	115.3 (9)	C77B—C78B—C79B	120.0
O7—Si1—C34	107.0 (7)	C77B—C78B—H78A	120.0
C35—Si1—C34	106.0 (8)	C79B—C78B—H78A	120.0

Table 3.11. (Continued)			
C33—Si1—C34	104.8 (9)	C78B—C79B—C80B	120.0
Si1—C33—H33A	109.5	C78B—C79B—H79A	120.0
Si1—C33—H33B	109.5	C80B—C79B—H79A	120.0
H33A—C33—H33B	109.5	C81B—C80B—C79B	120.0
Si1—C33—H33C	109.5	C81B—C80B—H80A	120.0
H33A—C33—H33C	109.5	C79B—C80B—H80A	120.0
H33B—C33—H33C	109.5	C82B—C81B—C80B	120.0
Si1—C34—H34A	109.5	C82B—C81B—H81A	120.0
Si1—C34—H34B	109.5	C80B—C81B—H81A	120.0
H34A—C34—H34B	109.5	C81B—C82B—C77B	120.0
Si1—C34—H34C	109.5	C81B—C82B—H82A	120.0
H34A—C34—H34C	109.5	C77B—C82B—H82A	120.0
H34B—C34—H34C	109.5	O17—Si2—C85	108.6 (6)
C38—C35—C37	113.1 (17)	O17—Si2—C83	115.6 (7)
C38—C35—C36	105.9 (15)	C85—Si2—C83	100.4 (8)
C37—C35—C36	113.0 (15)	O17—Si2—C84	107.2 (7)
C38—C35—Si1	104.3 (14)	C85—Si2—C84	106.8 (8)
C37—C35—Si1	111.9 (13)	C83—Si2—C84	117.4 (9)
C36—C35—Si1	108.1 (13)	Si2—C83—H83A	109.5
C35—C36—H36A	109.5	Si2—C83—H83B	109.5
C35—C36—H36B	109.5	H83A—C83—H83B	109.5
H36A—C36—H36B	109.5	Si2—C83—H83C	109.5
C35—C36—H36C	109.5	H83A—C83—H83C	109.5
H36A—C36—H36C	109.5	H83B—C83—H83C	109.5
H36B—C36—H36C	109.5	Si2—C84—H84A	109.5
C35—C37—H37A	109.5	Si2—C84—H84B	109.5
C35—C37—H37B	109.5	H84A—C84—H84B	109.5
H37A—C37—H37B	109.5	Si2—C84—H84C	109.5
C35—C37—H37C	109.5	H84A—C84—H84C	109.5
H37A—C37—H37C	109.5	H84B—C84—H84C	109.5
H37B—C37—H37C	109.5	C88—C85—C86	118.5 (14)
C35—C38—H38A	109.5	C88—C85—C87	101.3 (14)

Table 3.11. (Continued)			
C35—C38—H38B	109.5	C86—C85—C87	105.7 (14)
H38A—C38—H38B	109.5	C88—C85—Si2	111.9 (12)
C35—C38—H38C	109.5	C86—C85—Si2	112.2 (12)
H38A—C38—H38C	109.5	C87—C85—Si2	105.6 (11)
H38B—C38—H38C	109.5	C85—C86—H86A	109.5
O7—Si1B—C35B	122.1 (7)	C85—C86—H86B	109.5
O7—Si1B—C34B	111.3 (8)	H86A—C86—H86B	109.5
C35B—Si1B—C34B	114.7 (10)	C85—C86—H86C	109.5
O7—Si1B—C33B	101.9 (8)	H86A—C86—H86C	109.5
C35B—Si1B—C33B	100.2 (9)	H86B—C86—H86C	109.5
C34B—Si1B—C33B	102.8 (11)	C85—C87—H87A	109.5
O7—Si1B—C38B	101.7 (7)	C85—C87—H87B	109.5
C34B—Si1B—C38B	102.3 (10)	H87A—C87—H87B	109.5
C33B—Si1B—C38B	136.1 (9)	C85—C87—H87C	109.5
Si1B—C34B—H34D	109.5	H87A—C87—H87C	109.5
Si1B—C34B—H34E	109.5	H87B—C87—H87C	109.5
H34D—C34B—H34E	109.5	C85—C88—H88A	109.5
Si1B—C34B—H34F	109.5	C85—C88—H88B	109.5
H34D—C34B—H34F	109.5	H88A—C88—H88B	109.5
H34E—C34B—H34F	109.5	C85—C88—H88C	109.5
Si1B—C33B—H33D	109.5	H88A—C88—H88C	109.5
Si1B—C33B—H33E	109.5	H88B—C88—H88C	109.5
H33D—C33B—H33E	109.5	O17—Si2B—C85B	124.3 (8)
Si1B—C33B—H33F	109.5	O17—Si2B—C84B	116.1 (9)
H33D—C33B—H33F	109.5	C85B—Si2B—C84B	118.0 (11)
H33E—C33B—H33F	109.5	O17—Si2B—C83B	90.7 (9)
C38B—C35B—C37B	113.7 (19)	C85B—Si2B—C83B	87.8 (11)
C38B—C35B—C36B	104.2 (17)	C84B—Si2B—C83B	104.5 (12)
C37B—C35B—C36B	108.5 (15)	Si2B—C83B—H83D	109.5
C38B—C35B—Si1B	89.0 (13)	Si2B—C83B—H83E	109.5
C37B—C35B—Si1B	129.7 (16)	H83D—C83B—H83E	109.5
C36B—C35B—Si1B	108.2 (14)	Si2B—C83B—H83F	109.5

Table 3.11. (Continued)			
C35B—C36B—H36D	109.5	H83D—C83B—H83F	109.5
C35B—C36B—H36E	109.5	H83E—C83B—H83F	109.5
H36D—C36B—H36E	109.5	Si2B—C84B—H84D	109.5
C35B—C36B—H36F	109.5	Si2B—C84B—H84E	109.5
H36D—C36B—H36F	109.5	H84D—C84B—H84E	109.5
H36E—C36B—H36F	109.5	Si2B—C84B—H84F	109.5
C35B—C37B—H37D	109.5	H84D—C84B—H84F	109.5
C35B—C37B—H37E	109.5	H84E—C84B—H84F	109.5
H37D—C37B—H37E	109.5	C86B—C85B—C88B	114.4 (18)
C35B—C37B—H37F	109.5	C86B—C85B—C87B	114 (2)
H37D—C37B—H37F	109.5	C88B—C85B—C87B	96.2 (17)
H37E—C37B—H37F	109.5	C86B—C85B—Si2B	126.4 (16)
C35B—C38B—Si1B	54.9 (11)	C88B—C85B—Si2B	105.2 (16)
C35B—C38B—H38D	109.5	C87B—C85B—Si2B	95.4 (14)
Si1B—C38B—H38D	82.3	C85B—C86B—H86D	109.5
C35B—C38B—H38E	109.5	C85B—C86B—H86E	109.5
Si1B—C38B—H38E	163.7	H86D—C86B—H86E	109.5
H38D—C38B—H38E	109.5	C85B—C86B—H86F	109.5
C35B—C38B—H38F	109.5	H86D—C86B—H86F	109.5
Si1B—C38B—H38F	75.4	H86E—C86B—H86F	109.5
H38D—C38B—H38F	109.5	C85B—C87B—H87D	109.5
H38E—C38B—H38F	109.5	C85B—C87B—H87E	109.5
C40—C39—O9	109.0 (8)	H87D—C87B—H87E	109.5
C40—C39—H39A	109.9	C85B—C87B—H87F	109.5
O9—C39—H39A	109.9	H87D—C87B—H87F	109.5
C40—C39—H39B	109.9	H87E—C87B—H87F	109.5
O9—C39—H39B	109.9	C85B—C88B—H88D	109.5
H39A—C39—H39B	108.3	C85B—C88B—H88E	109.5
C41—C40—C45	120.0	H88D—C88B—H88E	109.5
C41—C40—C39	118.1 (9)	C85B—C88B—H88F	109.5
C45—C40—C39	121.9 (9)	H88D—C88B—H88F	109.5
C40—C41—C42	120.0	H88E—C88B—H88F	109.5

Table 3.11. (Continued)			
C40—C41—H41	120.0	C90—C89—O19	97.5 (13)
C42—C41—H41	120.0	C90—C89—H89A	112.3
C41—C42—C43	120.0	O19—C89—H89A	112.3
C41—C42—H42	120.0	C90—C89—H89B	112.3
C43—C42—H42	120.0	O19—C89—H89B	112.3
C44—C43—C42	120.0	H89A—C89—H89B	109.9
C44—C43—H43	120.0	C91—C90—C95	120.0
C42—C43—H43	120.0	C91—C90—C89	104 (2)
C43—C44—C45	120.0	C95—C90—C89	136 (2)
C43—C44—H44	120.0	C92—C91—C90	120.0
C45—C44—H44	120.0	C92—C91—H91	120.0
C44—C45—C40	120.0	C90—C91—H91	120.0
C44—C45—H45	120.0	C91—C92—C93	120.0
C40—C45—H45	120.0	C91—C92—H92	120.0
C40B—C39B—O9	107 (2)	C93—C92—H92	120.0
C40B—C39B—H39C	110.3	C94—C93—C92	120.0
O9—C39B—H39C	110.3	C94—C93—H93	120.0
C40B—C39B—H39D	110.3	C92—C93—H93	120.0
O9—C39B—H39D	110.3	C93—C94—C95	120.0
H39C—C39B—H39D	108.5	C93—C94—H94	120.0
C41B—C40B—C45B	120.00 (7)	C95—C94—H94	120.0
C41B—C40B—C39B	129 (2)	C94—C95—C90	120.0
C45B—C40B—C39B	110 (3)	C94—C95—H95	120.0
C42B—C41B—C40B	120.0	C90—C95—H95	120.0
C42B—C41B—H41A	120.0	C90B—C89B—O19	111.0 (13)
C40B—C41B—H41A	120.0	C90B—C89B—H89C	109.4
C41B—C42B—C43B	120.0	O19—C89B—H89C	109.4
C41B—C42B—H42A	120.0	C90B—C89B—H89D	109.4
C43B—C42B—H42A	120.0	O19—C89B—H89D	109.4
C42B—C43B—C44B	120.00 (6)	H89C—C89B—H89D	108.0
C42B—C43B—H43A	120.0	C91B—C90B—C95B	120.0
C44B—C43B—H43A	120.0	C91B—C90B—C89B	125.8 (14)

Table 3.11. (Continued)			
C45B—C44B—C43B	120.0	C95B—C90B—C89B	114.2 (14)
C45B—C44B—H44A	120.0	C92B—C91B—C90B	120.0
C43B—C44B—H44A	120.0	C92B—C91B—H91A	120.0
C44B—C45B—C40B	120.0	C90B—C91B—H91A	120.0
C44B—C45B—H45A	120.0	C93B—C92B—C91B	120.0
C40B—C45B—H45A	120.0	C93B—C92B—H92A	120.0
C51—O11—N11	106.4 (6)	C91B—C92B—H92A	120.0
C54—O12—C72	113.1 (7)	C92B—C93B—C94B	120.0
C54—O12—C72B	139 (3)	C92B—C93B—H93A	120.0
C65—O16—H16	109.5	C94B—C93B—H93A	120.0
C66—O17—Si2B	135.8 (7)	C93B—C94B—C95B	120.0
C66—O17—Si2	135.7 (7)	C93B—C94B—H94A	120.0
C69—O19—C89	108.4 (12)	C95B—C94B—H94A	120.0
C69—O19—C89B	117.7 (9)	C94B—C95B—C90B	120.0
C69—N11—O11	106.4 (7)	C94B—C95B—H95A	120.0
C58—N12—C74	118.4 (8)	C90B—C95B—H95A	120.0
C1—O1—N1—C19	-0.3 (8)	O11—C51—C52—N13	47.7 (11)
N1—O1—C1—C18	2.1 (9)	C68—C51—C52—C53	-10.7 (14)
N1—O1—C1—C2	175.8 (7)	O11—C51—C52—C53	177.5 (7)
C20—N2—C2—C1	-77.7 (9)	N13—C52—C53—C54	-114.7 (8)
C21—N2—C2—C1	52.2 (8)	C51—C52—C53—C54	110.3 (8)
C20—N2—C2—C3	153.2 (7)	N13—C52—C53—C66	115.9 (8)
C21—N2—C2—C3	-76.9 (7)	C51—C52—C53—C66	-19.0 (10)
C18—C1—C2—N2	-143.3 (8)	C72—O12—C54—C53	135.4 (7)
O1—C1—C2—N2	44.4 (10)	C72B—O12—C54—C53	156 (3)
C18—C1—C2—C3	-13.1 (12)	C72—O12—C54—C55	-102.5 (8)
O1—C1—C2—C3	174.6 (6)	C72B—O12—C54—C55	-82 (3)
N2—C2—C3—C16	118.9 (7)	C66—C53—C54—O12	61.1 (7)
C1—C2—C3—C16	-14.6 (9)	C52—C53—C54—O12	-71.2 (8)
N2—C2—C3—C4	-115.7 (7)	C66—C53—C54—C55	-59.9 (8)
C1—C2—C3—C4	110.8 (7)	C52—C53—C54—C55	167.9 (7)

Table 3.11. (Continued)			
C22—O2—C4—C5	-101.7 (7)	O12—C54—C55—C64	-75.7 (8)
C22—O2—C4—C3	136.3 (6)	C53—C54—C55—C64	43.2 (9)
C16—C3—C4—O2	59.9 (7)	O12—C54—C55—C56	48.6 (9)
C2—C3—C4—O2	-68.3 (7)	C53—C54—C55—C56	167.5 (7)
C16—C3—C4—C5	-63.4 (7)	C64—C55—C56—C57	-59.4 (8)
C2—C3—C4—C5	168.3 (6)	C54—C55—C56—C57	174.1 (7)
O2—C4—C5—C14	-72.7 (7)	C55—C56—C57—C62	37.3 (10)
C3—C4—C5—C14	47.2 (8)	C55—C56—C57—C58	-142.4 (8)
O2—C4—C5—C6	48.8 (8)	C51—C52—N13—C70	-78.2 (10)
C3—C4—C5—C6	168.7 (6)	C53—C52—N13—C70	154.7 (7)
C4—C5—C6—C7	179.4 (6)	C51—C52—N13—C71	49.1 (9)
C14—C5—C6—C7	-57.0 (7)	C53—C52—N13—C71	-78.0 (8)
C5—C6—C7—C8	-143.2 (8)	C62—C57—C58—N12	178.9 (8)
C5—C6—C7—C12	33.9 (10)	C56—C57—C58—N12	-1.5 (13)
C12—C7—C8—C9	-1.3 (15)	C62—C57—C58—C59	-7.7 (13)
C6—C7—C8—C9	175.7 (9)	C56—C57—C58—C59	172.0 (8)
C12—C7—C8—N3	176.6 (9)	C74—N12—C58—C57	155.2 (9)
C6—C7—C8—N3	-6.3 (14)	C75—N12—C58—C57	-80.2 (10)
C25—N3—C8—C9	-84.1 (13)	C74—N12—C58—C59	-17.6 (14)
C25B—N3—C8—C9	-40 (3)	C75—N12—C58—C59	106.9 (10)
C24B—N3—C8—C9	101 (3)	C57—C58—C59—C60	3.0 (14)
C24—N3—C8—C9	50.2 (15)	N12—C58—C59—C60	176.2 (9)
C25—N3—C8—C7	98.0 (13)	C58—C59—C60—C61	1.0 (15)
C25B—N3—C8—C7	142 (3)	C59—C60—C61—O14	179.4 (9)
C24B—N3—C8—C7	-77 (3)	C59—C60—C61—C62	-0.7 (13)
C24—N3—C8—C7	-127.7 (11)	C58—C57—C62—C61	8.3 (13)
C7—C8—C9—C10	-2.1 (16)	C56—C57—C62—C61	-171.3 (7)
N3—C8—C9—C10	-180.0 (11)	C58—C57—C62—C63	-175.4 (8)
C8—C9—C10—C11	5.2 (17)	C56—C57—C62—C63	4.9 (12)
C26—O4—C11—C10	90.5 (11)	O14—C61—C62—C57	176.0 (8)
C26—O4—C11—C12	-87.5 (10)	C60—C61—C62—C57	-3.8 (12)
C9—C10—C11—O4	177.2 (9)	O14—C61—C62—C63	-0.2 (12)

Table 3.11. (Continued)			
C9—C10—C11—C12	-4.8 (16)	C60—C61—C62—C63	179.9 (7)
C8—C7—C12—C11	1.7 (13)	C57—C62—C63—O15	154.4 (8)
C6—C7—C12—C11	-175.4 (7)	C61—C62—C63—O15	-29.3 (11)
C8—C7—C12—C13	-175.8 (8)	C57—C62—C63—C64	-25.2 (11)
C6—C7—C12—C13	7.1 (11)	C61—C62—C63—C64	151.1 (7)
O4—C11—C12—C7	179.4 (8)	O15—C63—C64—C65	4.0 (11)
C10—C11—C12—C7	1.4 (13)	C62—C63—C64—C65	-176.4 (7)
O4—C11—C12—C13	-3.3 (13)	O15—C63—C64—C55	179.3 (7)
C10—C11—C12—C13	178.7 (9)	C62—C63—C64—C55	-1.2 (10)
C7—C12—C13—O5	154.7 (7)	C54—C55—C64—C65	-14.8 (11)
C11—C12—C13—O5	-22.6 (12)	C56—C55—C64—C65	-141.8 (7)
C7—C12—C13—C14	-24.4 (11)	C54—C55—C64—C63	170.3 (7)
C11—C12—C13—C14	158.2 (8)	C56—C55—C64—C63	43.3 (9)
O5—C13—C14—C15	3.6 (11)	C63—C64—C65—O16	-5.5 (11)
C12—C13—C14—C15	-177.3 (7)	C55—C64—C65—O16	179.4 (7)
O5—C13—C14—C5	177.9 (6)	C63—C64—C65—C66	176.7 (7)
C12—C13—C14—C5	-2.9 (10)	C55—C64—C65—C66	1.7 (12)
C4—C5—C14—C15	-18.7 (9)	Si2B—O17—C66—C65	-31.1 (11)
C6—C5—C14—C15	-142.7 (7)	Si2—O17—C66—C65	-81.4 (8)
C4—C5—C14—C13	167.0 (6)	Si2B—O17—C66—C53	-153.4 (8)
C6—C5—C14—C13	43.1 (8)	Si2—O17—C66—C53	156.3 (6)
C13—C14—C15—O6	-3.4 (11)	Si2B—O17—C66—C67	86.9 (9)
C5—C14—C15—O6	-177.5 (7)	Si2—O17—C66—C67	36.6 (9)
C13—C14—C15—C16	177.7 (6)	O16—C65—C66—O17	44.3 (9)
C5—C14—C15—C16	3.7 (11)	C64—C65—C66—O17	-137.7 (8)
Si1B—O7—C16—C3	-152.6 (8)	O16—C65—C66—C53	165.4 (7)
Si1—O7—C16—C3	159.0 (6)	C64—C65—C66—C53	-16.6 (10)
Si1B—O7—C16—C17	84.7 (10)	O16—C65—C66—C67	-70.5 (8)
Si1—O7—C16—C17	36.3 (8)	C64—C65—C66—C67	107.4 (8)
Si1B—O7—C16—C15	-32.7 (12)	C54—C53—C66—O17	165.7 (6)
Si1—O7—C16—C15	-81.1 (8)	C52—C53—C66—O17	-66.0 (8)
C4—C3—C16—O7	164.5 (5)	C54—C53—C66—C65	44.9 (8)

Table 3.11. (Continued)			
C2—C3—C16—O7	-71.4 (7)	C52—C53—C66—C65	173.1 (7)
C4—C3—C16—C17	-78.2 (7)	C54—C53—C66—C67	-78.5 (7)
C2—C3—C16—C17	45.9 (8)	C52—C53—C66—C67	49.7 (9)
C4—C3—C16—C15	46.3 (7)	O17—C66—C67—O18	-108.5 (8)
C2—C3—C16—C15	170.4 (6)	C65—C66—C67—O18	8.8 (11)
O6—C15—C16—O7	45.5 (9)	C53—C66—C67—O18	133.0 (8)
C14—C15—C16—O7	-135.5 (7)	O17—C66—C67—C68	67.2 (7)
O6—C15—C16—C3	163.2 (6)	C65—C66—C67—C68	-175.5 (6)
C14—C15—C16—C3	-17.9 (10)	C53—C66—C67—C68	-51.3 (8)
O6—C15—C16—C17	-69.6 (8)	O11—C51—C68—C69	-4.1 (10)
C14—C15—C16—C17	109.3 (8)	C52—C51—C68—C69	-176.2 (10)
O7—C16—C17—O8	-109.7 (9)	O11—C51—C68—C67	178.5 (7)
C3—C16—C17—O8	132.2 (8)	C52—C51—C68—C67	6.3 (16)
C15—C16—C17—O8	6.9 (12)	O18—C67—C68—C51	-158.2 (9)
O7—C16—C17—C18	69.0 (8)	C66—C67—C68—C51	26.1 (11)
C3—C16—C17—C18	-49.2 (8)	O18—C67—C68—C69	25.2 (15)
C15—C16—C17—C18	-174.5 (7)	C66—C67—C68—C69	-150.5 (10)
O1—C1—C18—C19	-2.8 (9)	O11—N11—C69—O19	-179.9 (9)
C2—C1—C18—C19	-175.8 (8)	O11—N11—C69—C68	-4.2 (11)
O1—C1—C18—C17	-179.1 (7)	C89—O19—C69—N11	6 (2)
C2—C1—C18—C17	7.9 (13)	C89B—O19—C69—N11	-13.7 (17)
O8—C17—C18—C1	-157.3 (8)	C89—O19—C69—C68	-169.1 (17)
C16—C17—C18—C1	24.0 (10)	C89B—O19—C69—C68	171.1 (12)
O8—C17—C18—C19	27.6 (14)	C51—C68—C69—N11	5.3 (12)
C16—C17—C18—C19	-151.1 (8)	C67—C68—C69—N11	-177.7 (9)
C39B—O9—C19—N1	18 (2)	C51—C68—C69—O19	-178.9 (9)
C39—O9—C19—N1	-5.4 (13)	C67—C68—C69—O19	-1.9 (17)
C39B—O9—C19—C18	-163.1 (19)	C54—O12—C72—O13	-80.9 (9)
C39—O9—C19—C18	173.7 (9)	C72B—O12—C72—O13	126 (4)
O1—N1—C19—O9	177.9 (8)	O12—C72—O13—C73	-79.7 (11)
O1—N1—C19—C18	-1.4 (9)	C54—O12—C72B—O13B	-87 (4)
C1—C18—C19—O9	-176.6 (8)	C72—O12—C72B—O13B	-47 (3)

Table 3.11. (Continued)			
C17—C18—C19—O9	-0.9 (15)	O12—C72B—O13B—C73B	-99 (6)
C1—C18—C19—N1	2.7 (10)	C60—C61—O14—C76	35.5 (12)
C17—C18—C19—N1	178.3 (8)	C62—C61—O14—C76	-144.4 (8)
C4—O2—C22—O3	-78.6 (9)	C61—O14—C76—C77	162.2 (7)
O2—C22—O3—C23	-79.8 (10)	C61—O14—C76—C77B	154.7 (14)
C11—O4—C26—C27	-178.9 (6)	O14—C76—C77—C78	-49.8 (10)
O4—C26—C27—C28	104.0 (8)	C77B—C76—C77—C78	36 (9)
O4—C26—C27—C32	-71.8 (8)	O14—C76—C77—C82	137.4 (6)
C32—C27—C28—C29	0.0	C77B—C76—C77—C82	-137 (10)
C26—C27—C28—C29	-175.7 (8)	C82—C77—C78—C79	0.0
C27—C28—C29—C30	0.0	C76—C77—C78—C79	-172.7 (8)
C28—C29—C30—C31	0.0	C77—C78—C79—C80	0.0
C29—C30—C31—C32	0.0	C78—C79—C80—C81	0.0
C30—C31—C32—C27	0.0	C79—C80—C81—C82	0.0
C28—C27—C32—C31	0.0	C80—C81—C82—C77	0.0
C26—C27—C32—C31	175.9 (7)	C78—C77—C82—C81	0.0
C16—O7—Si1—C35	135.3 (8)	C76—C77—C82—C81	172.8 (8)
Si1B—O7—Si1—C35	9.4 (8)	O14—C76—C77B—C78B	11 (2)
C16—O7—Si1—C33	5.5 (10)	C77—C76—C77B—C78B	-86 (9)
Si1B—O7—Si1—C33	-120.4 (9)	O14—C76—C77B—C82B	156.6 (13)
C16—O7—Si1—C34	-112.5 (9)	C77—C76—C77B—C82B	60 (9)
Si1B—O7—Si1—C34	121.6 (10)	C82B—C77B—C78B—C79B	0.0
O7—Si1—C35—C38	-62.0 (15)	C76—C77B—C78B—C79B	142 (2)
C33—Si1—C35—C38	69.6 (16)	C77B—C78B—C79B—C80B	0.0
C34—Si1—C35—C38	-174.9 (15)	C78B—C79B—C80B—C81B	0.0
O7—Si1—C35—C37	60.6 (13)	C79B—C80B—C81B—C82B	0.0
C33—Si1—C35—C37	-167.9 (12)	C80B—C81B—C82B—C77B	0.0
C34—Si1—C35—C37	-52.4 (15)	C78B—C77B—C82B—C81B	0.0
O7—Si1—C35—C36	-174.4 (11)	C76—C77B—C82B—C81B	-148 (2)
C33—Si1—C35—C36	-42.8 (14)	C66—O17—Si2—C85	136.8 (9)
C34—Si1—C35—C36	72.7 (14)	Si2B—O17—Si2—C85	28.0 (9)
C16—O7—Si1B—C35B	-77.6 (12)	C66—O17—Si2—C83	24.9 (10)

Table 3.11. (Continued)			
Si1—O7—Si1B—C35B	13.0 (8)	Si2B—O17—Si2—C83	-83.9 (9)
C16—O7—Si1B—C34B	63.2 (14)	C66—O17—Si2—C84	-108.2 (10)
Si1—O7—Si1B—C34B	153.8 (12)	Si2B—O17—Si2—C84	143.0 (11)
C16—O7—Si1B—C33B	172.1 (11)	O17—Si2—C85—C88	-49.4 (15)
Si1—O7—Si1B—C33B	-97.2 (9)	C83—Si2—C85—C88	72.3 (15)
C16—O7—Si1B—C38B	-45.2 (11)	C84—Si2—C85—C88	-164.7 (14)
Si1—O7—Si1B—C38B	45.5 (7)	O17—Si2—C85—C86	174.6 (12)
O7—Si1B—C35B—C38B	63.0 (14)	C83—Si2—C85—C86	-63.7 (14)
C34B—Si1B—C35B—C38B	-76.6 (16)	C84—Si2—C85—C86	59.3 (16)
C33B—Si1B—C35B—C38B	174.1 (13)	O17—Si2—C85—C87	59.9 (10)
O7—Si1B—C35B—C37B	-176.5 (17)	C83—Si2—C85—C87	-178.4 (10)
C34B—Si1B—C35B—C37B	44 (2)	C84—Si2—C85—C87	-55.4 (12)
C33B—Si1B—C35B—C37B	-65 (2)	C66—O17—Si2B—C85B	-103.4 (13)
C38B—Si1B—C35B—C37B	120 (2)	Si2—O17—Si2B—C85B	4.9 (11)
O7—Si1B—C35B—C36B	-41.6 (16)	C66—O17—Si2B—C84B	62.3 (16)
C34B—Si1B—C35B—C36B	178.8 (14)	Si2—O17—Si2B—C84B	170.6 (16)
C33B—Si1B—C35B—C36B	69.5 (15)	C66—O17—Si2B—C83B	168.8 (11)
C38B—Si1B—C35B—C36B	-104.6 (18)	Si2—O17—Si2B—C83B	-82.9 (10)
C37B—C35B—C38B—Si1B	-133.6 (19)	O17—Si2B—C85B—C86B	-175 (2)
C36B—C35B—C38B—Si1B	108.5 (15)	C84B—Si2B—C85B—C86B	20 (3)
O7—Si1B—C38B—C35B	-129.6 (12)	C83B—Si2B—C85B—C86B	-86 (2)
C34B—Si1B—C38B—C35B	115.3 (14)	O17—Si2B—C85B—C88B	-38 (2)
C33B—Si1B—C38B—C35B	-8.4 (18)	C84B—Si2B—C85B—C88B	156.8 (18)
C19—O9—C39—C40	-169.5 (8)	C83B—Si2B—C85B—C88B	51.5 (18)
C39B—O9—C39—C40	84 (4)	O17—Si2B—C85B—C87B	60.2 (16)
O9—C39—C40—C41	97.5 (10)	C84B—Si2B—C85B—C87B	-105.3 (16)
O9—C39—C40—C45	-85.5 (10)	C83B—Si2B—C85B—C87B	149.5 (15)
C45—C40—C41—C42	0.0	C69—O19—C89—C90	-146 (2)
C39—C40—C41—C42	177.1 (8)	C89B—O19—C89—C90	-25 (4)
C40—C41—C42—C43	0.0	O19—C89—C90—C91	-100 (2)
C41—C42—C43—C44	0.0	O19—C89—C90—C95	83 (3)
C42—C43—C44—C45	0.0	C95—C90—C91—C92	0.0

Table 3.11. (Continued)			
C43—C44—C45—C40	0.0	C89—C90—C91—C92	-177.7 (15)
C41—C40—C45—C44	0.0	C90—C91—C92—C93	0.0
C39—C40—C45—C44	-177.0 (8)	C91—C92—C93—C94	0.0
C19—O9—C39B—C40B	-163 (2)	C92—C93—C94—C95	0.0
C39—O9—C39B—C40B	-79 (4)	C93—C94—C95—C90	0.0
O9—C39B—C40B—C41B	42 (4)	C91—C90—C95—C94	0.0
O9—C39B—C40B—C45B	-129 (2)	C89—C90—C95—C94	177 (2)
C45B—C40B—C41B—C42B	0.0	C69—O19—C89B—C90B	-178.1 (14)
C39B—C40B—C41B—C42B	-170 (3)	C89—O19—C89B—C90B	115 (7)
C40B—C41B—C42B—C43B	0.0	O19—C89B—C90B—C91B	-97.3 (14)
C41B—C42B—C43B—C44B	0.0	O19—C89B—C90B—C95B	85.1 (17)
C42B—C43B—C44B—C45B	0.0	C95B—C90B—C91B—C92B	0.0
C43B—C44B—C45B—C40B	0.0	C89B—C90B—C91B—C92B	-177.5 (14)
C41B—C40B—C45B—C44B	0.0	C90B—C91B—C92B—C93B	0.0
C39B—C40B—C45B—C44B	172 (2)	C91B—C92B—C93B—C94B	0.0
C51—O11—N11—C69	1.7 (10)	C92B—C93B—C94B—C95B	0.0
N11—O11—C51—C68	1.8 (10)	C93B—C94B—C95B—C90B	0.0
N11—O11—C51—C52	175.3 (8)	C91B—C90B—C95B—C94B	0.0
C68—C51—C52—N13	-140.4 (10)	C89B—C90B—C95B—C94B	177.8 (12)

Table 3.12. Hydrogen-bond parameters

$D-H\cdots A$	$D-H$ (Å)	$H\cdots A$ (Å)	$D\cdots A$ (Å)	$D-H\cdots A$ (°)
O6—H6 \cdots O5	0.84	1.78	2.458 (6)	136.3
O16—H16 \cdots O15	0.84	1.96	2.474 (7)	118.9

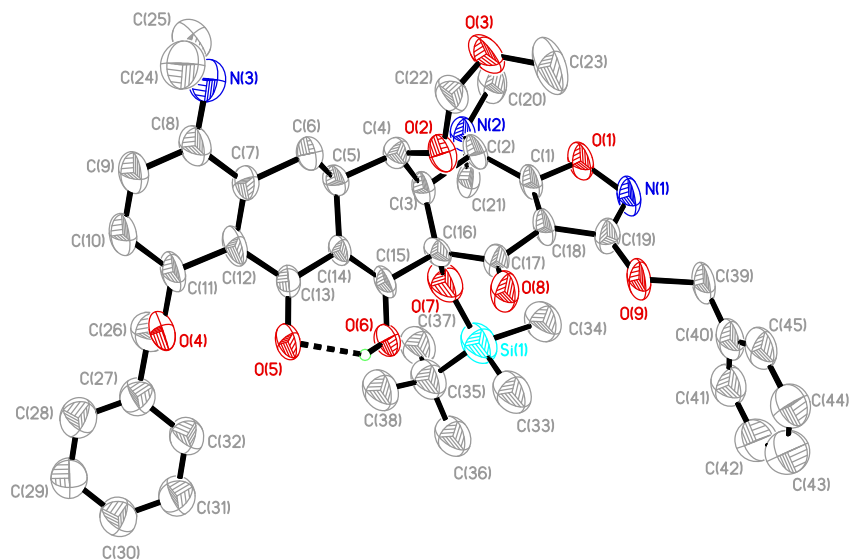


Figure 3.4a

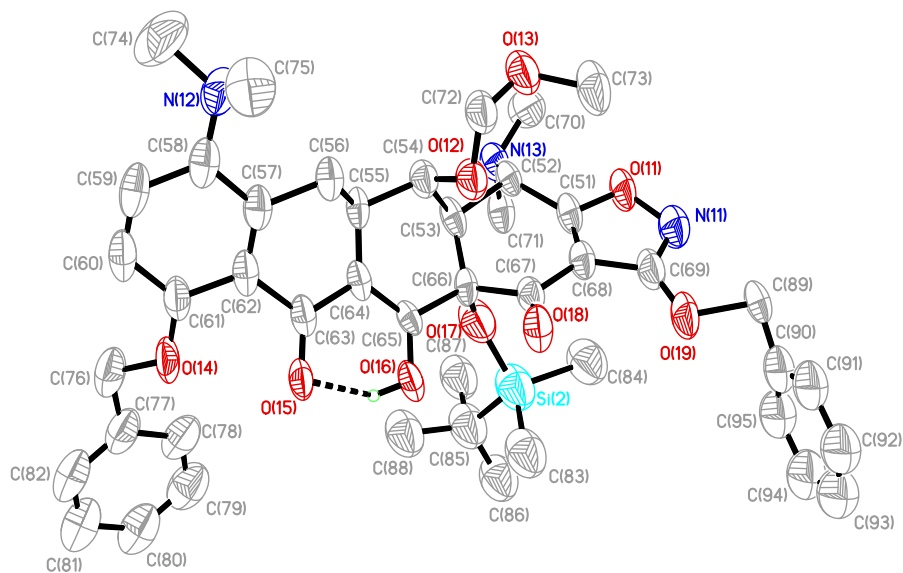


Figure 3.4b

Figure 3.4. Perspective views showing 50% probability displacement (the H atoms that rides on C atoms and the disorder parts have been omitted).

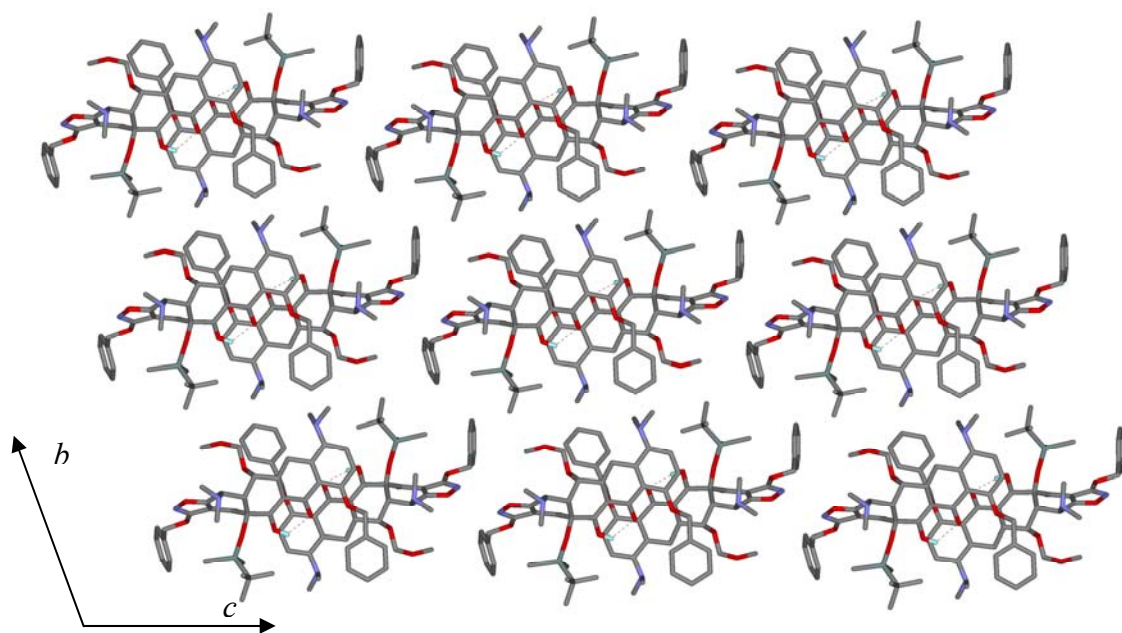
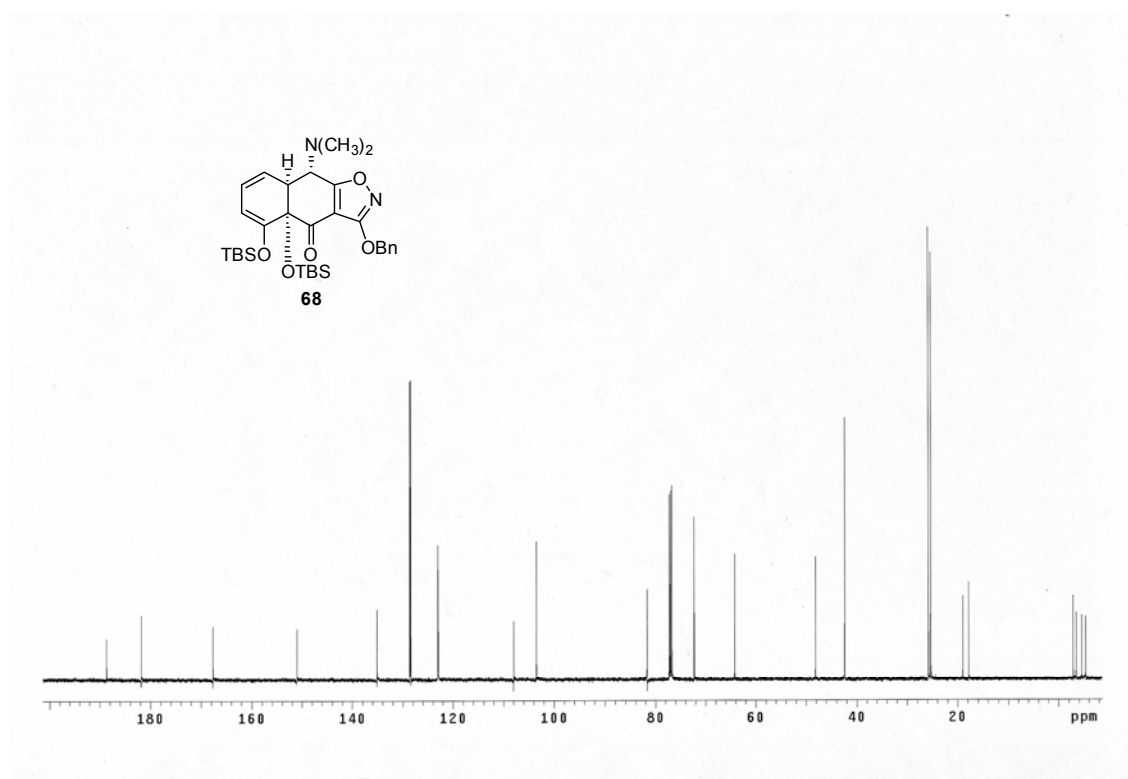
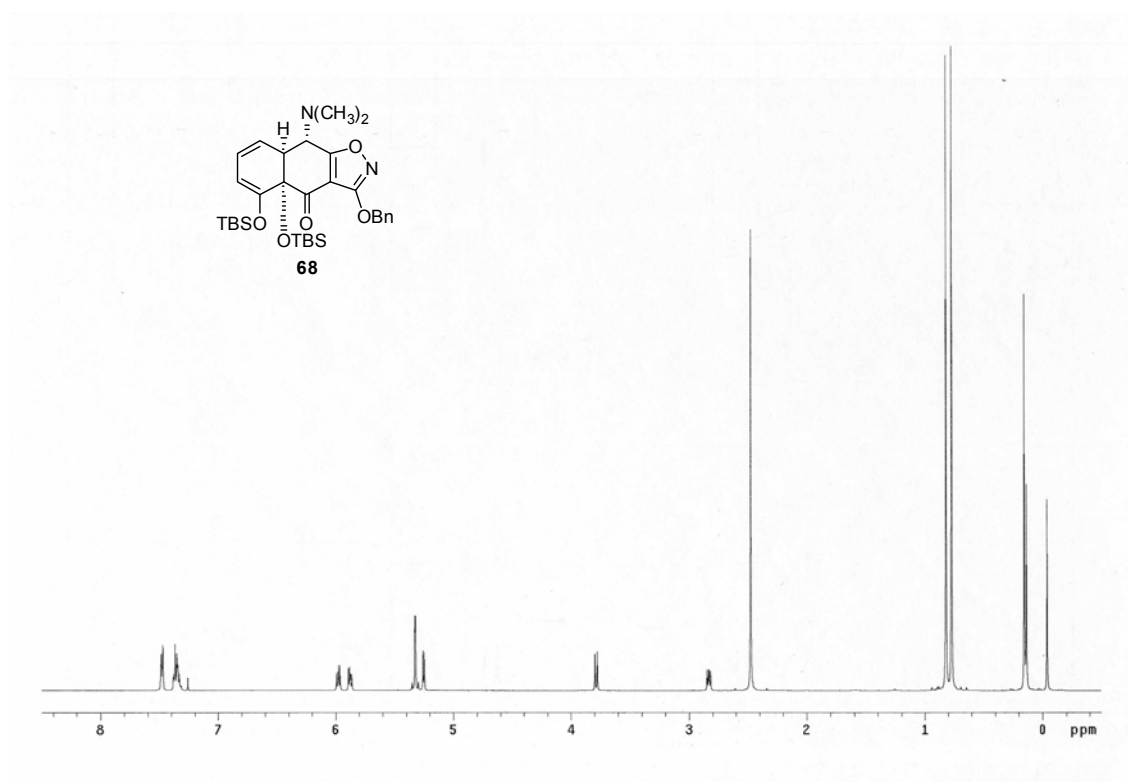
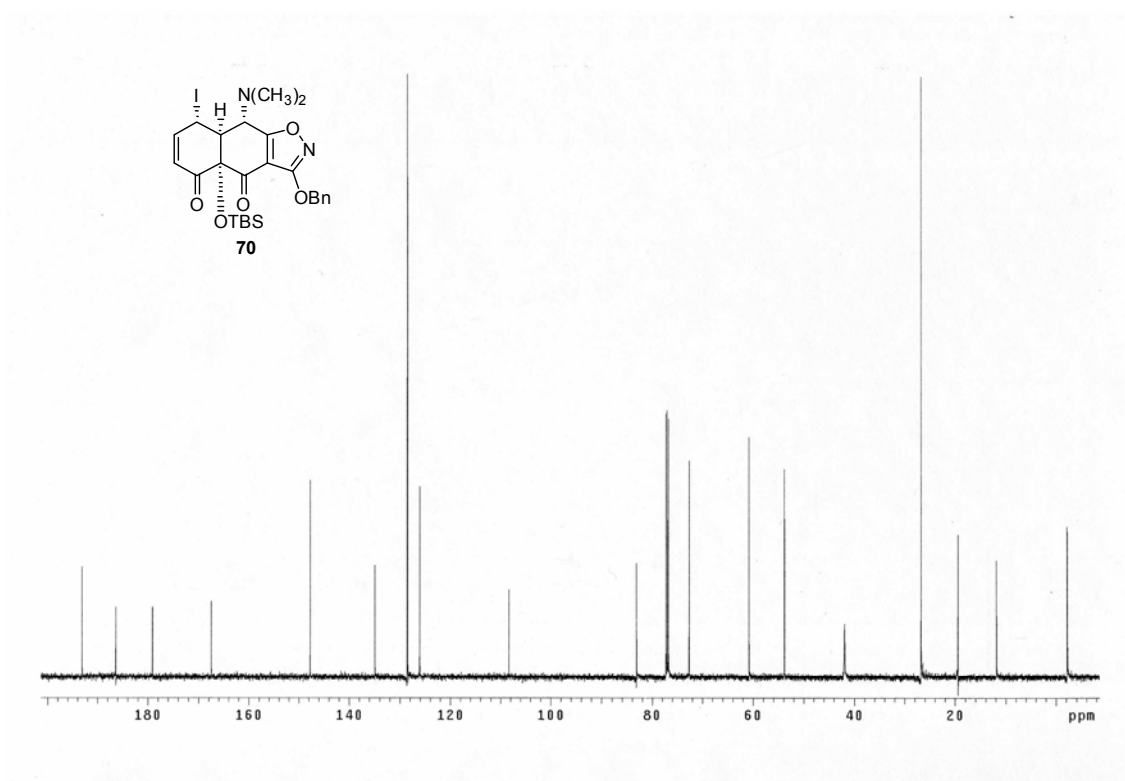
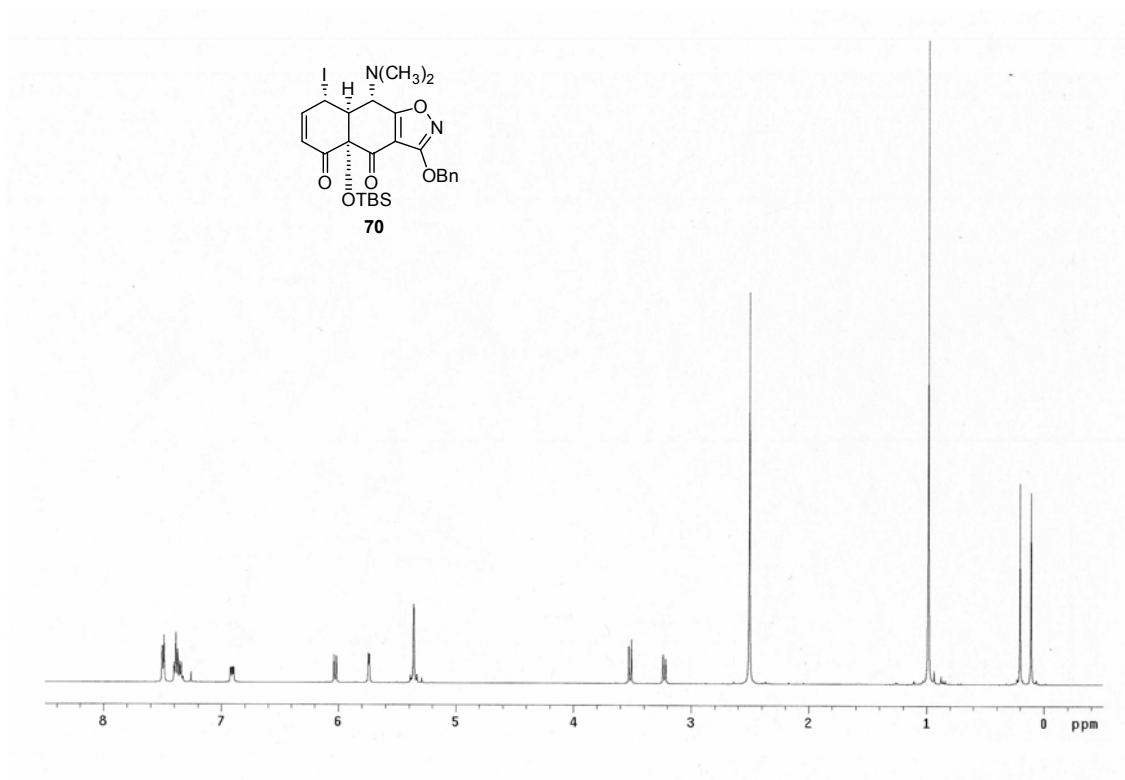
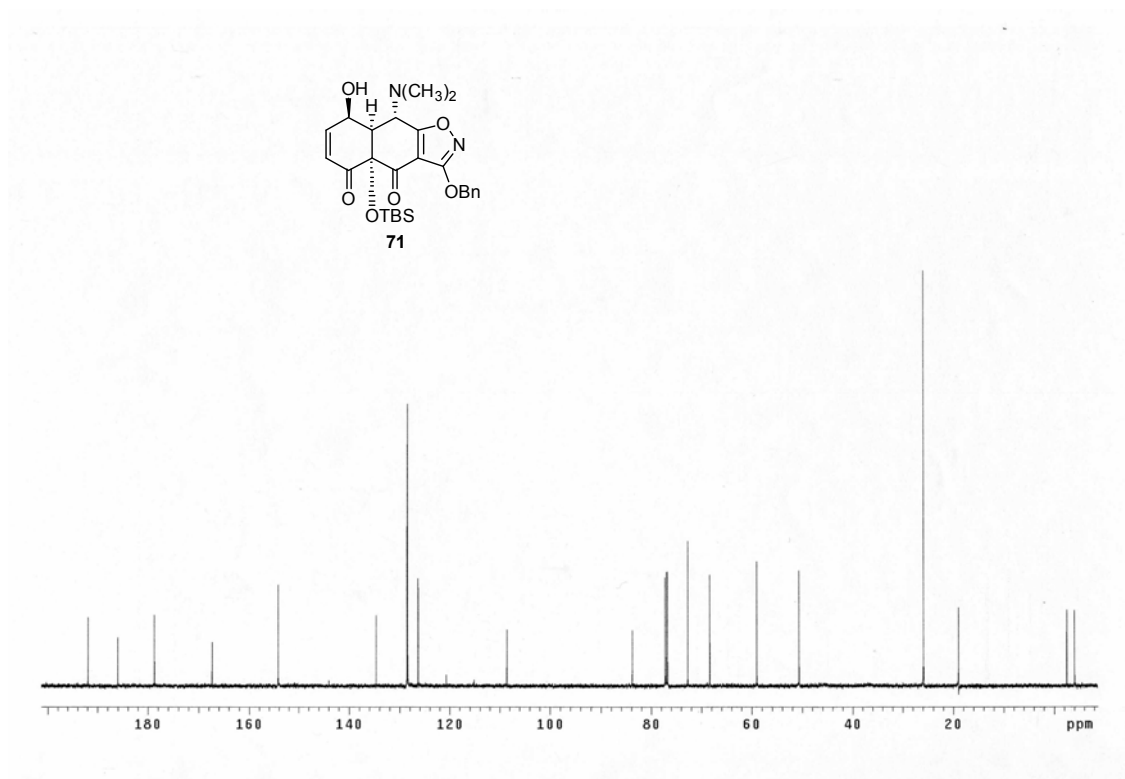
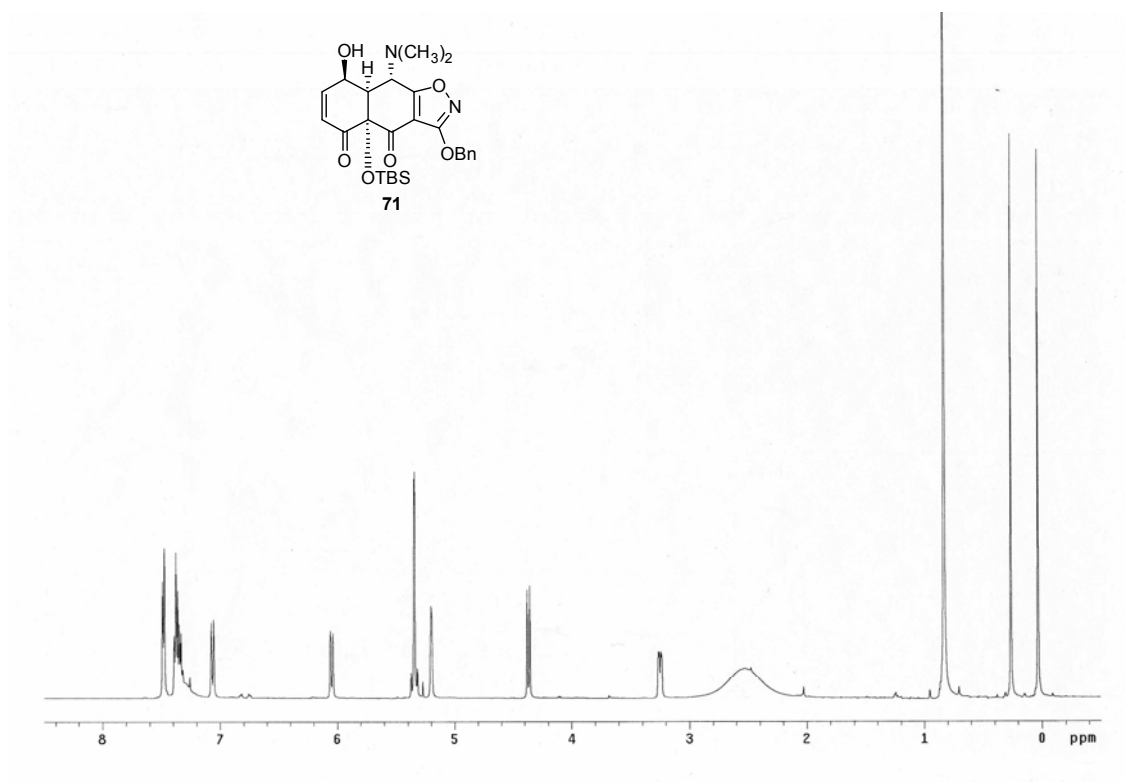


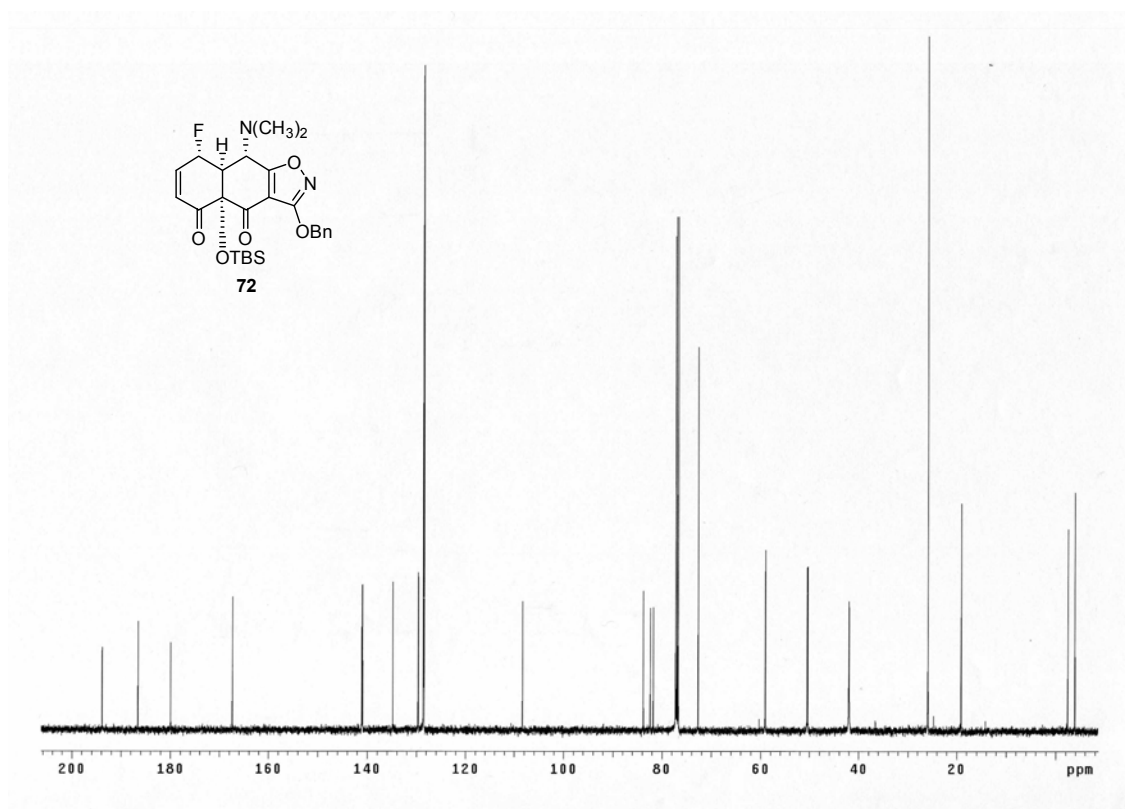
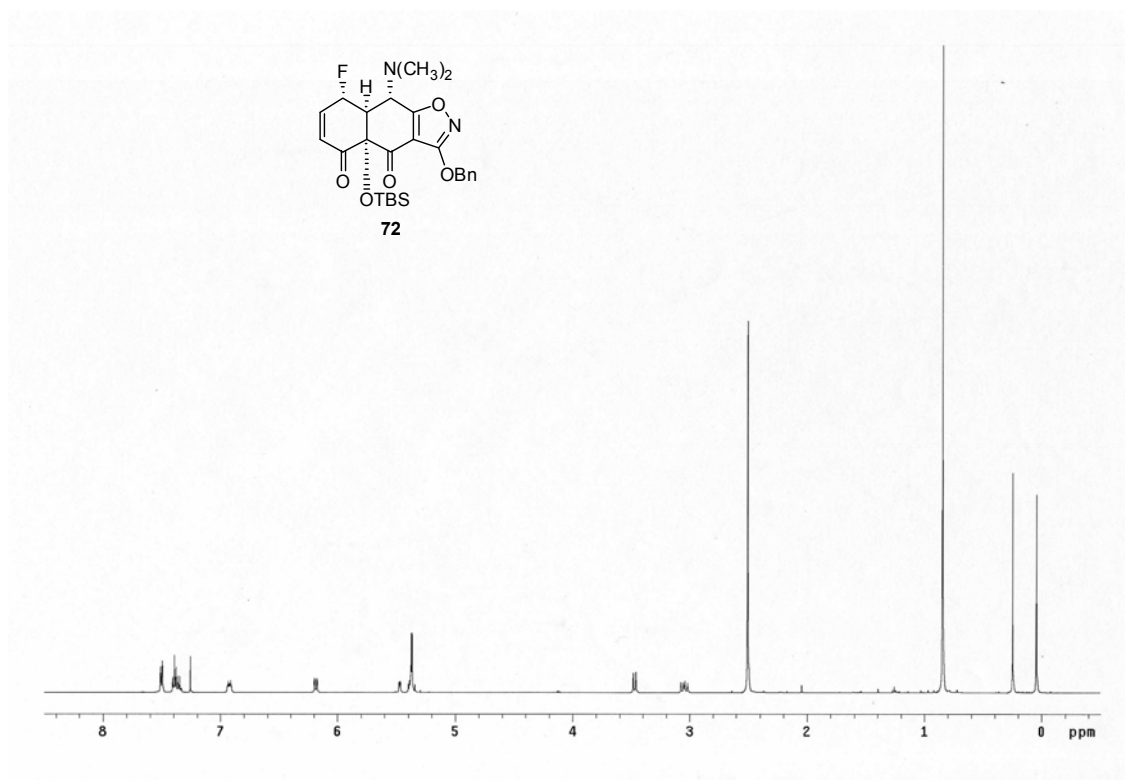
Figure 3.5. Three-dimensional supramolecular architecture viewed along the a -axis direction.

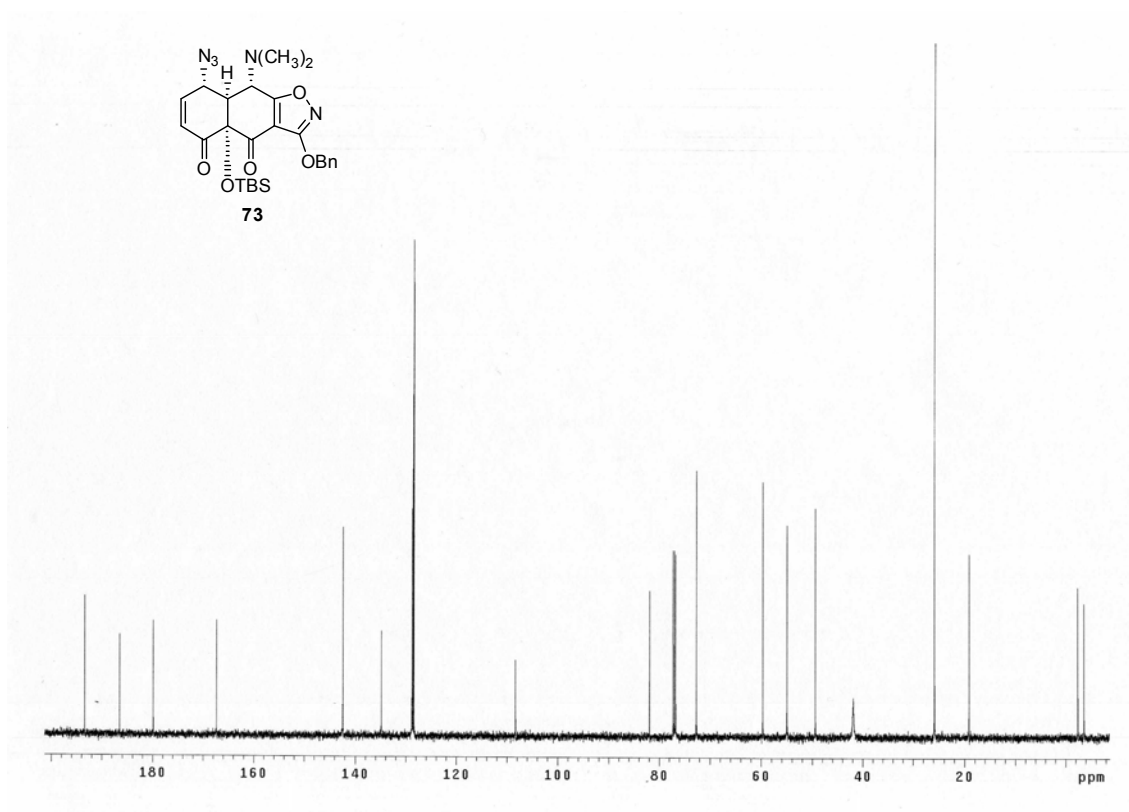
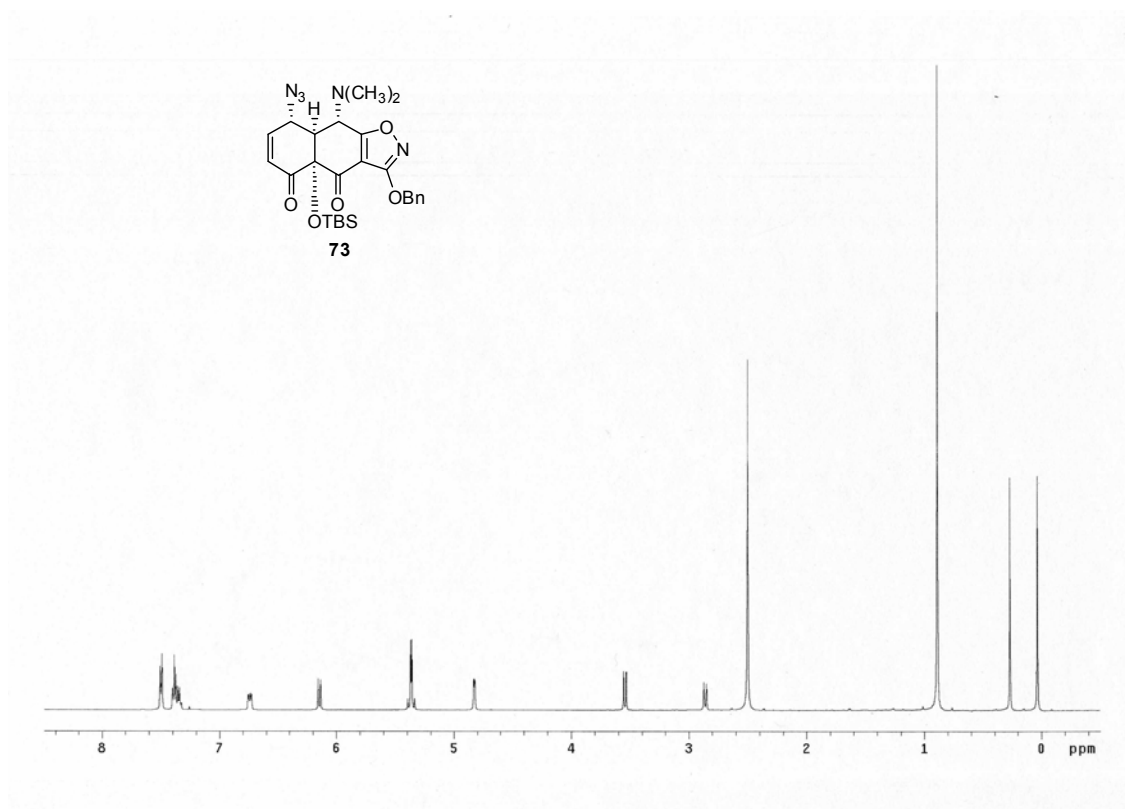
Catalog of Spectra

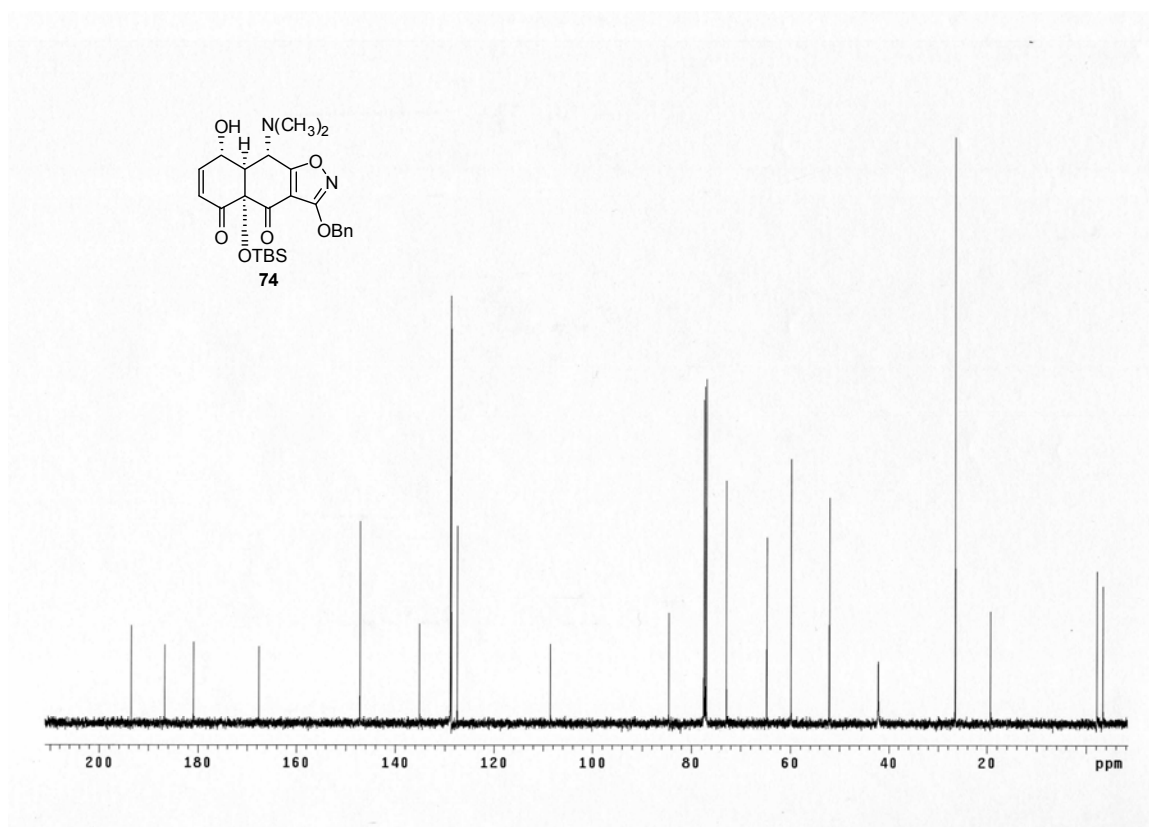
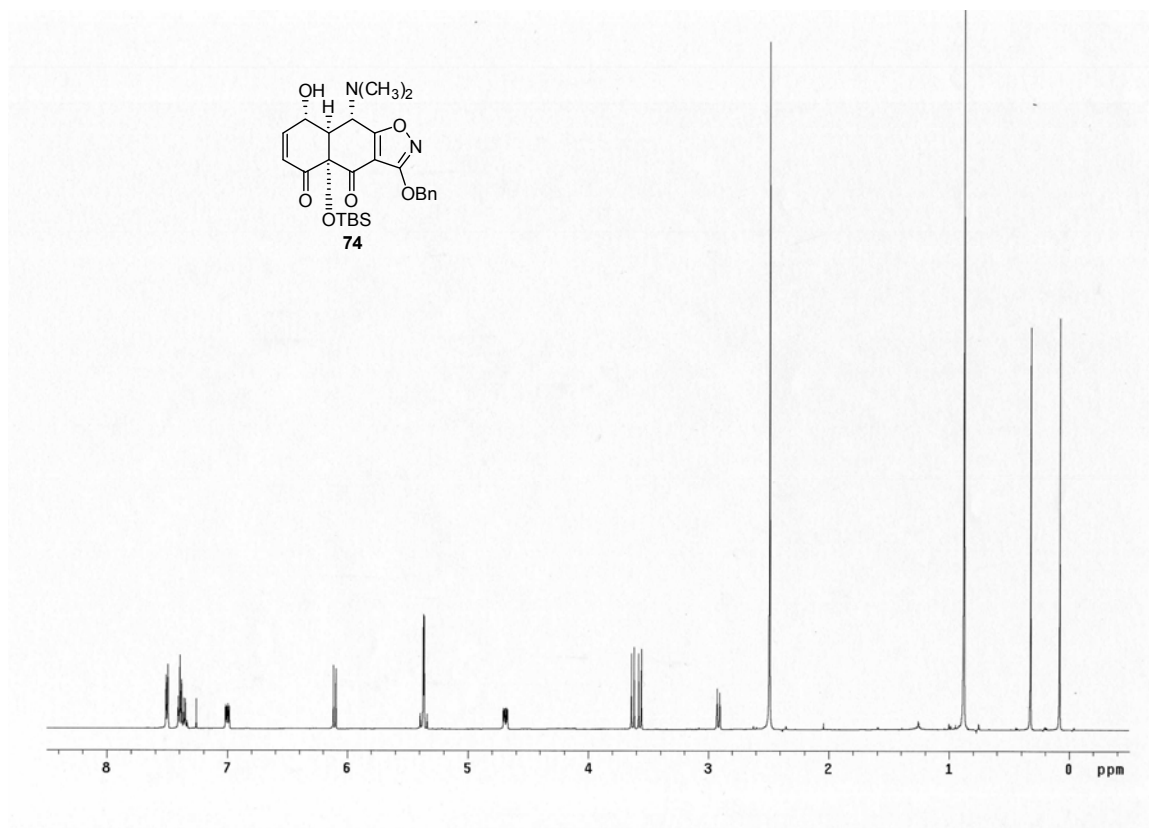


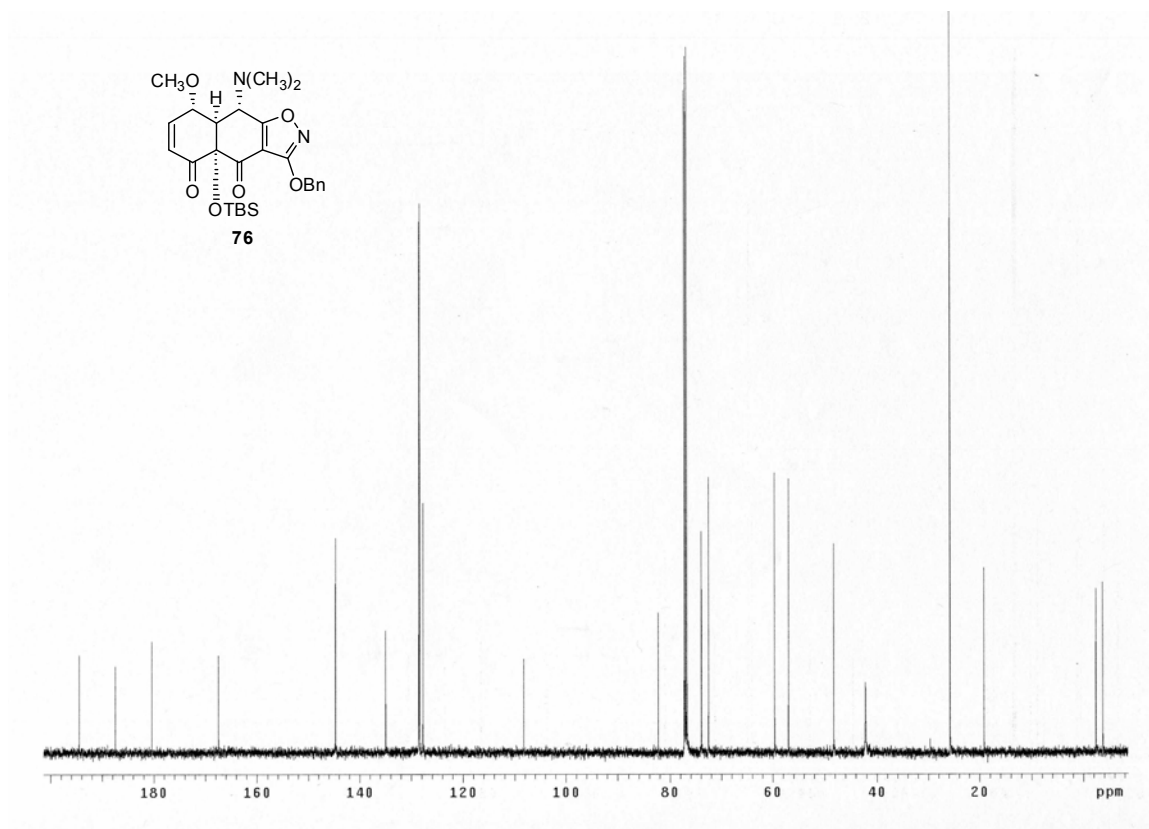
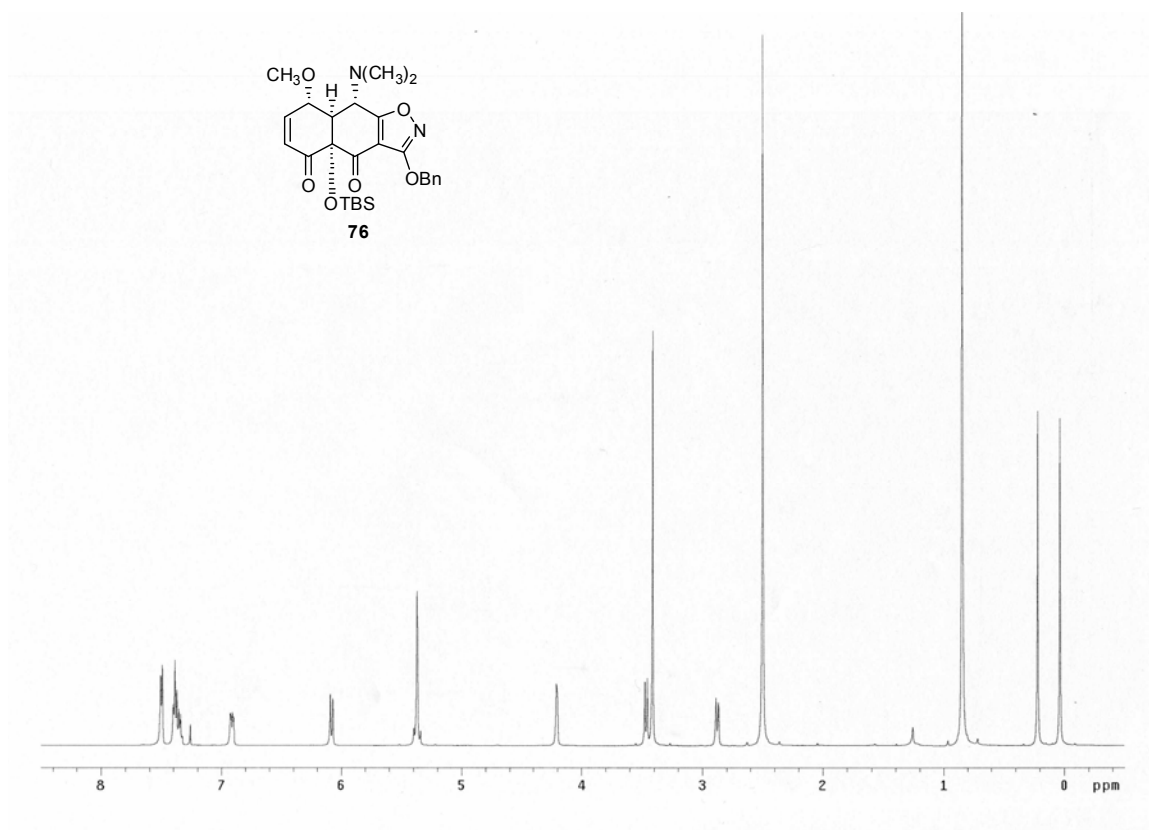


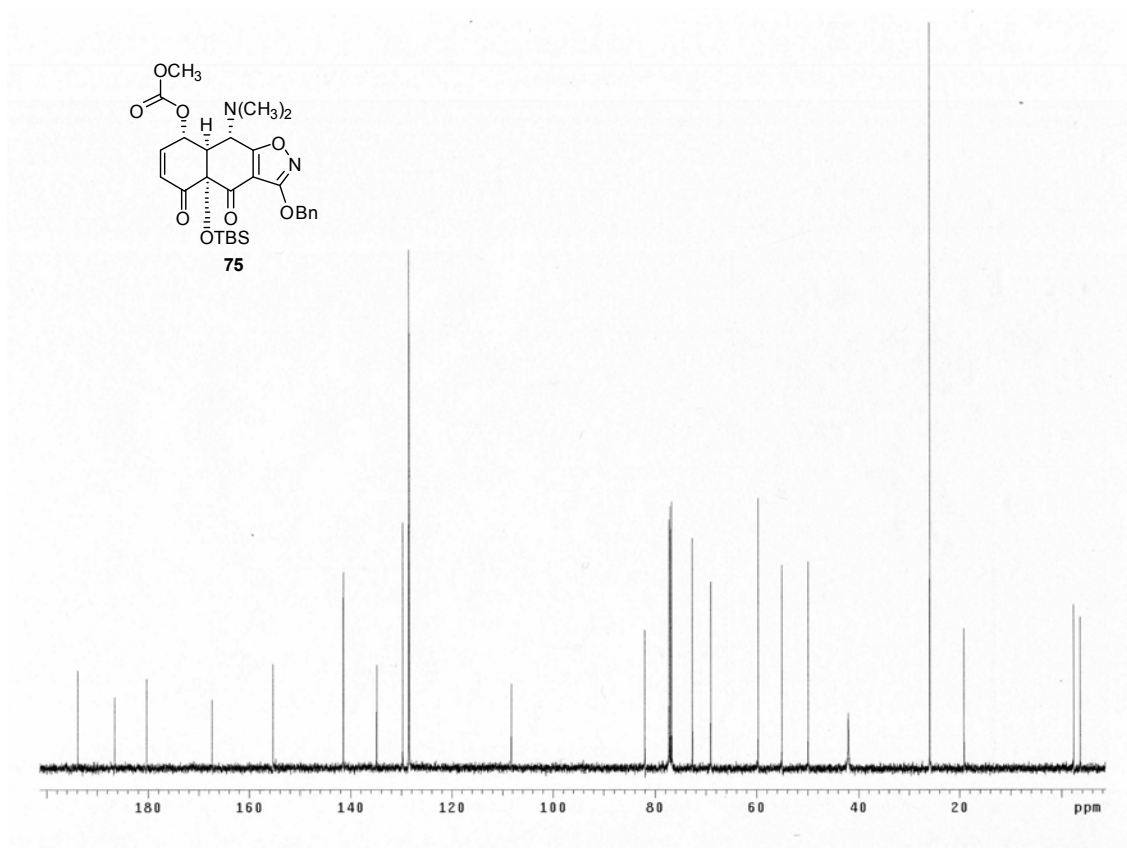
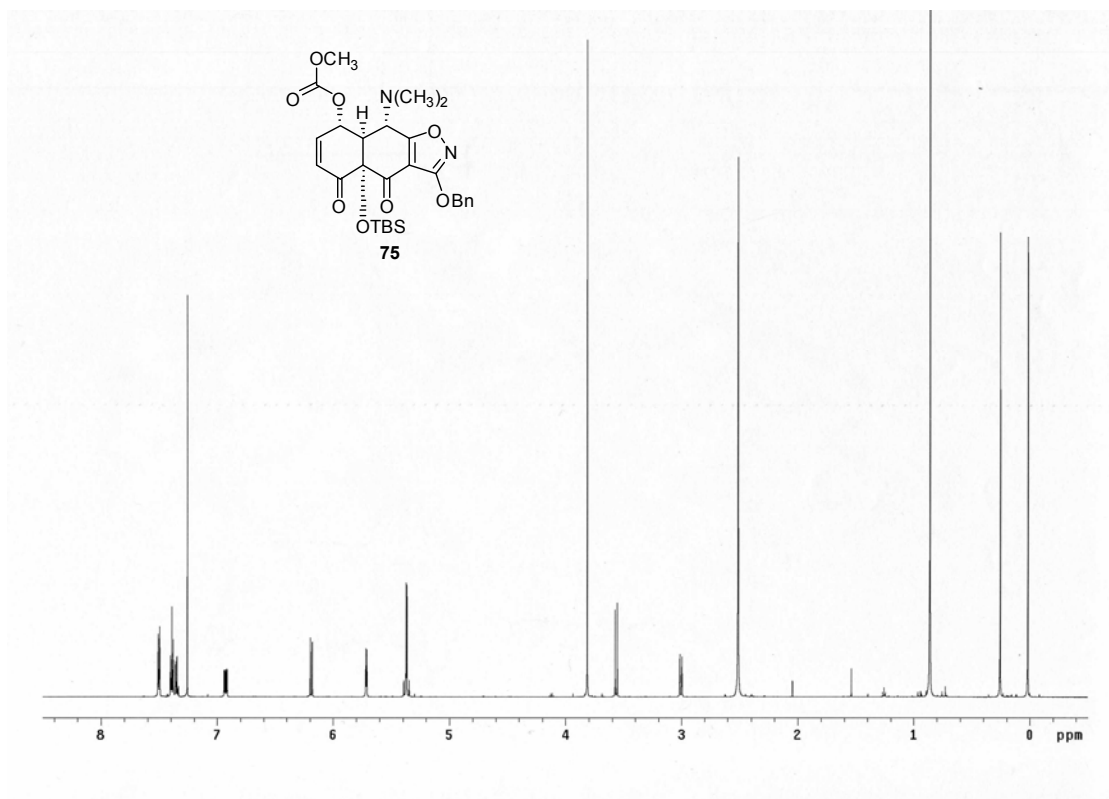


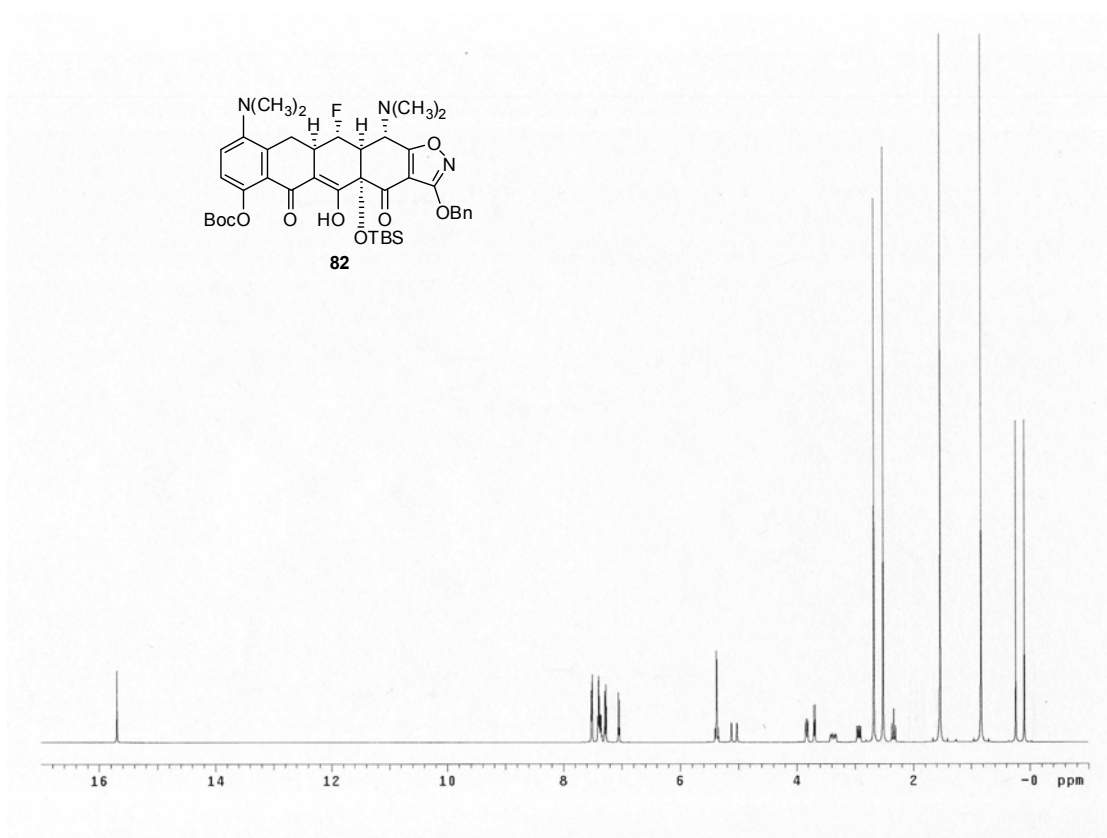
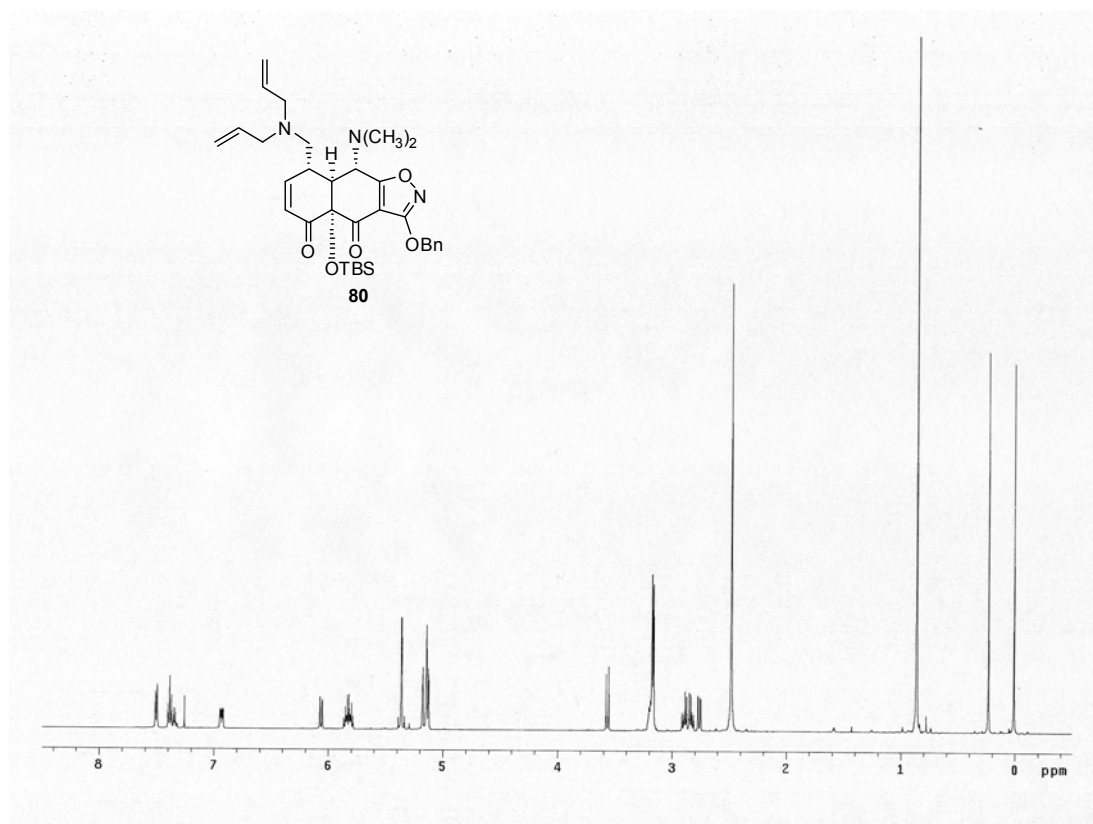


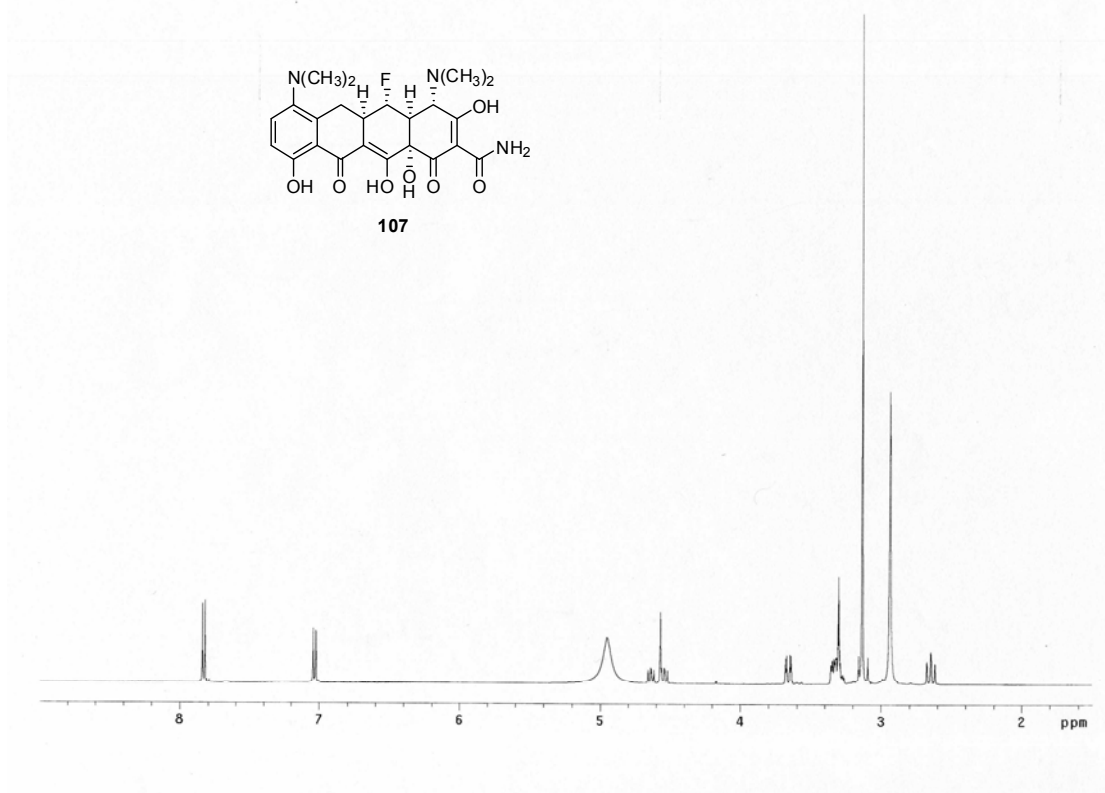
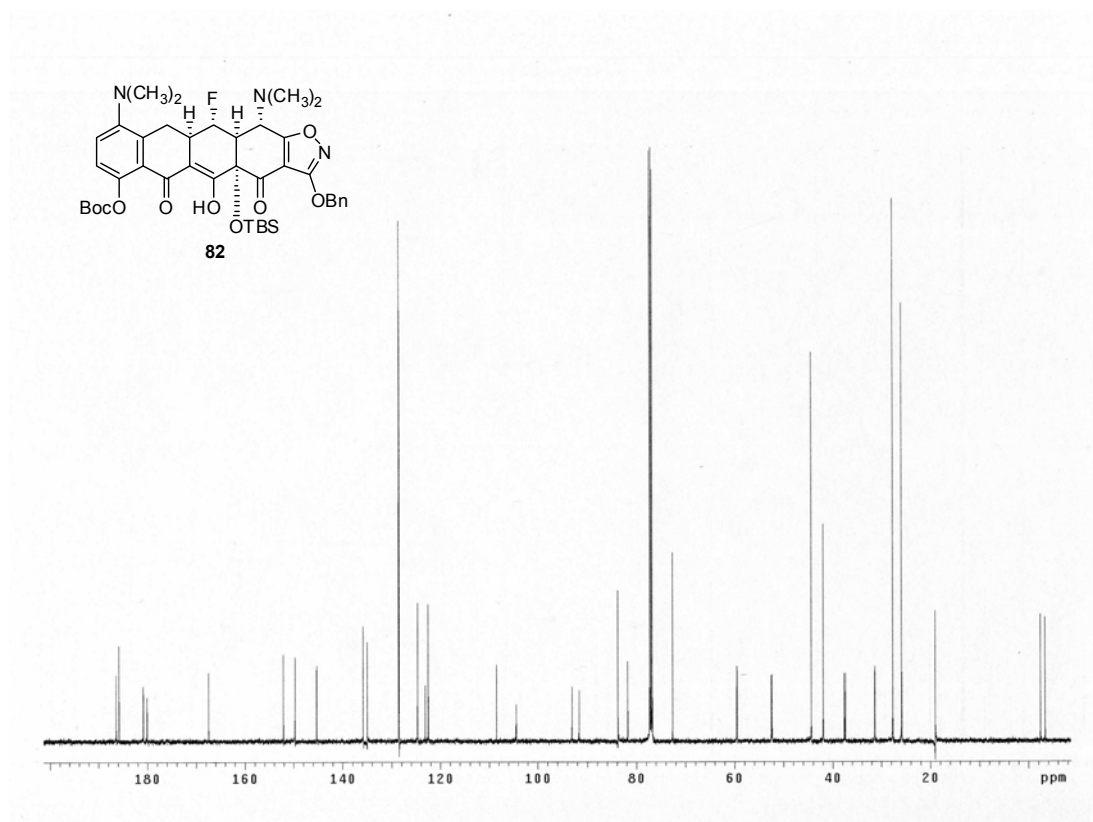


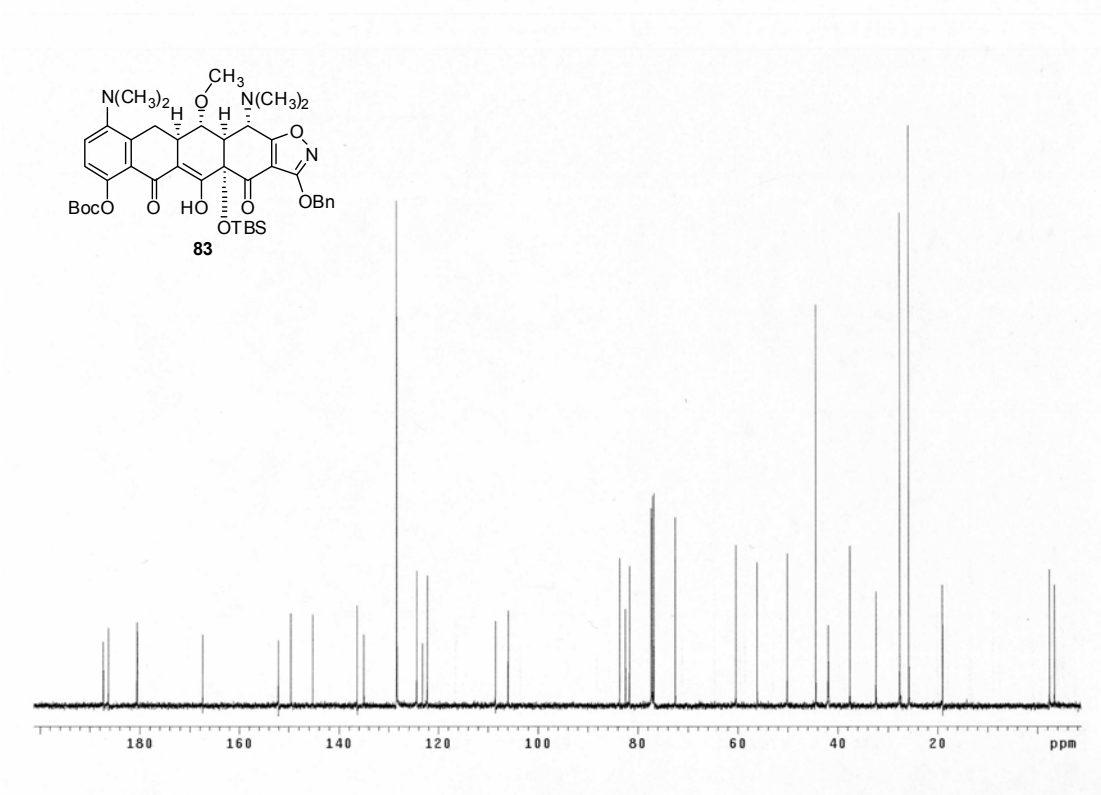
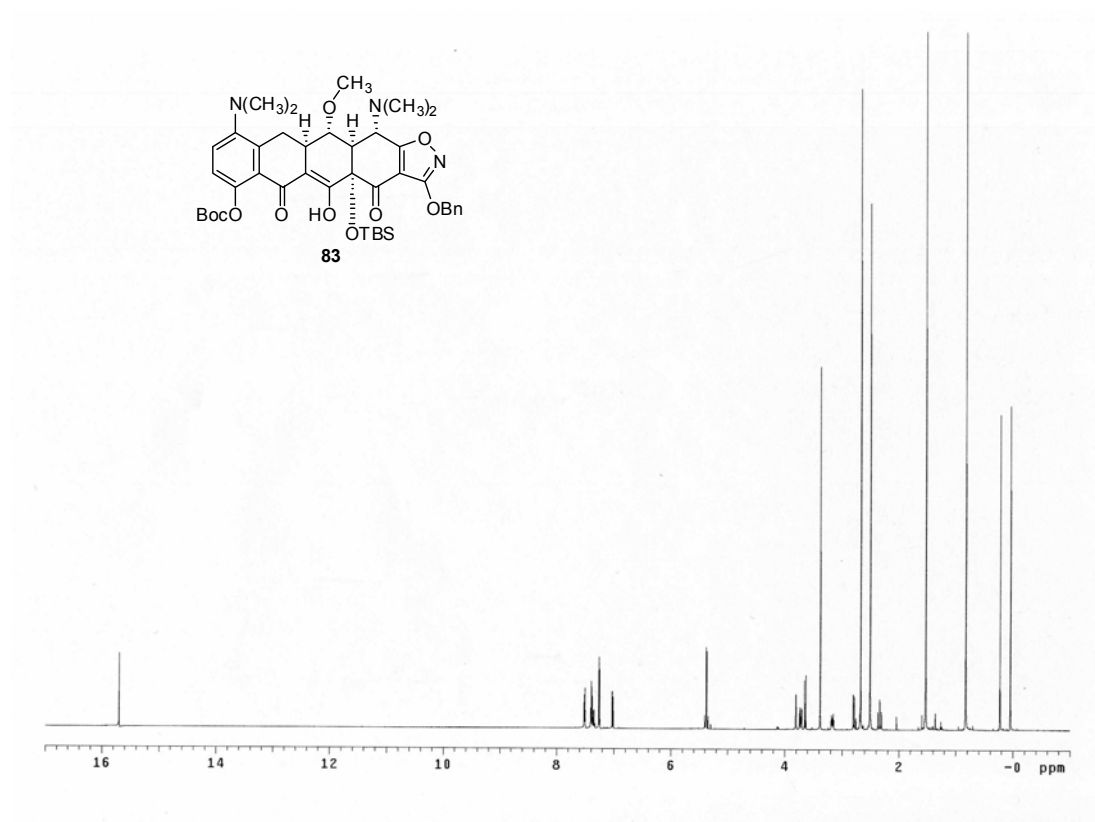


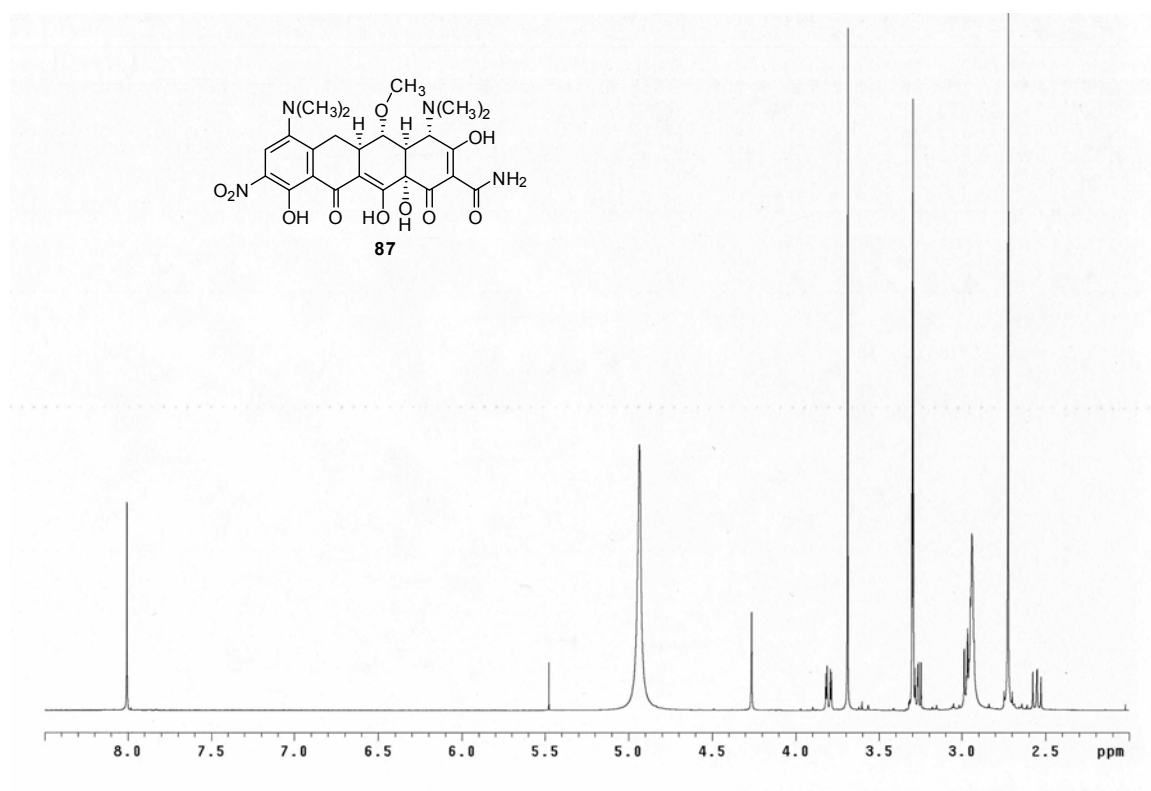
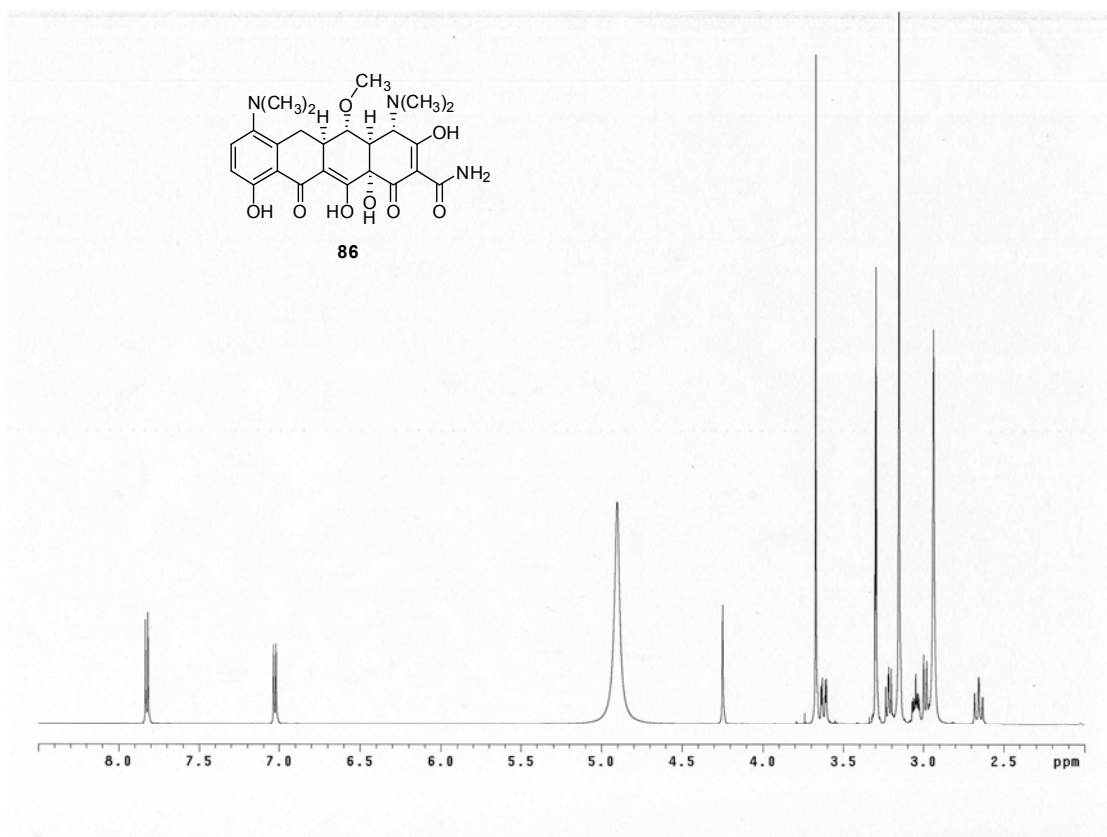


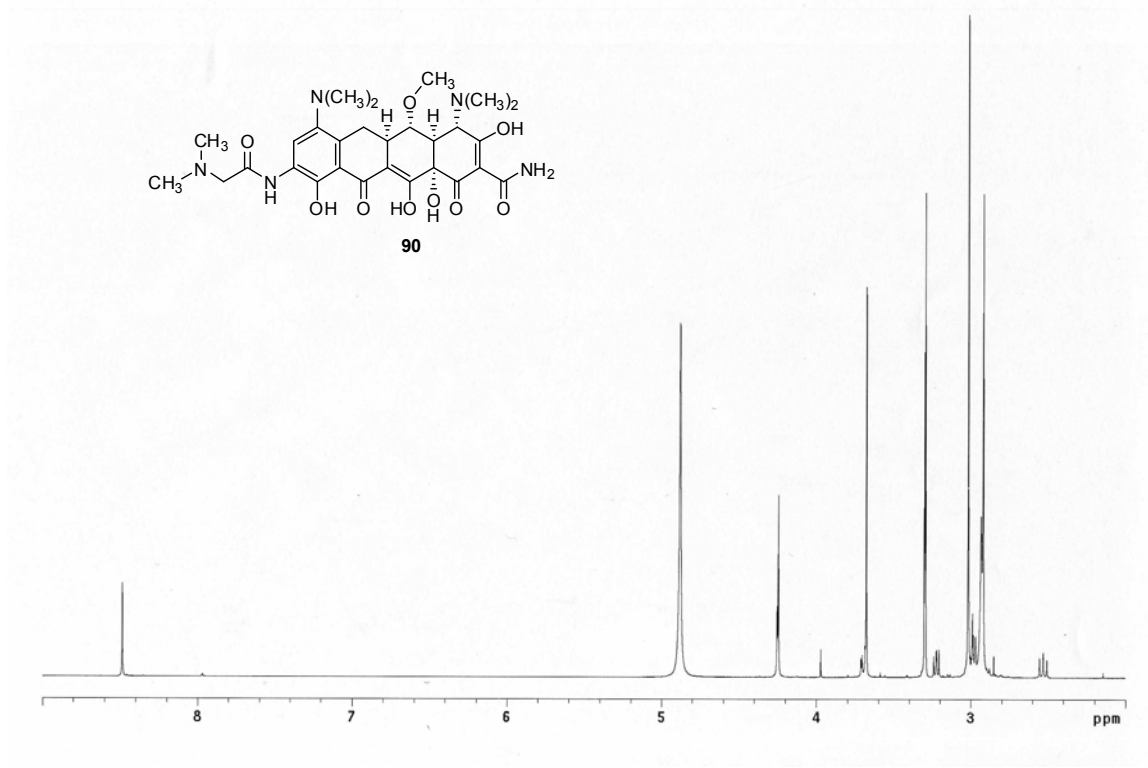
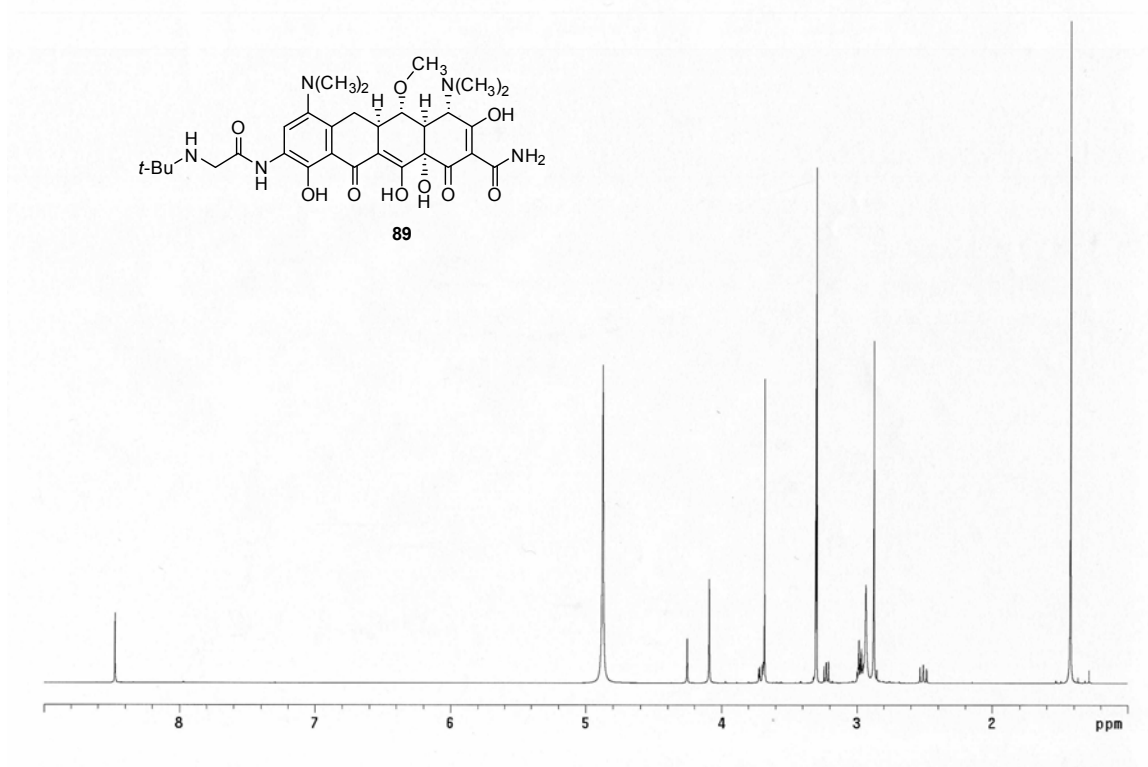


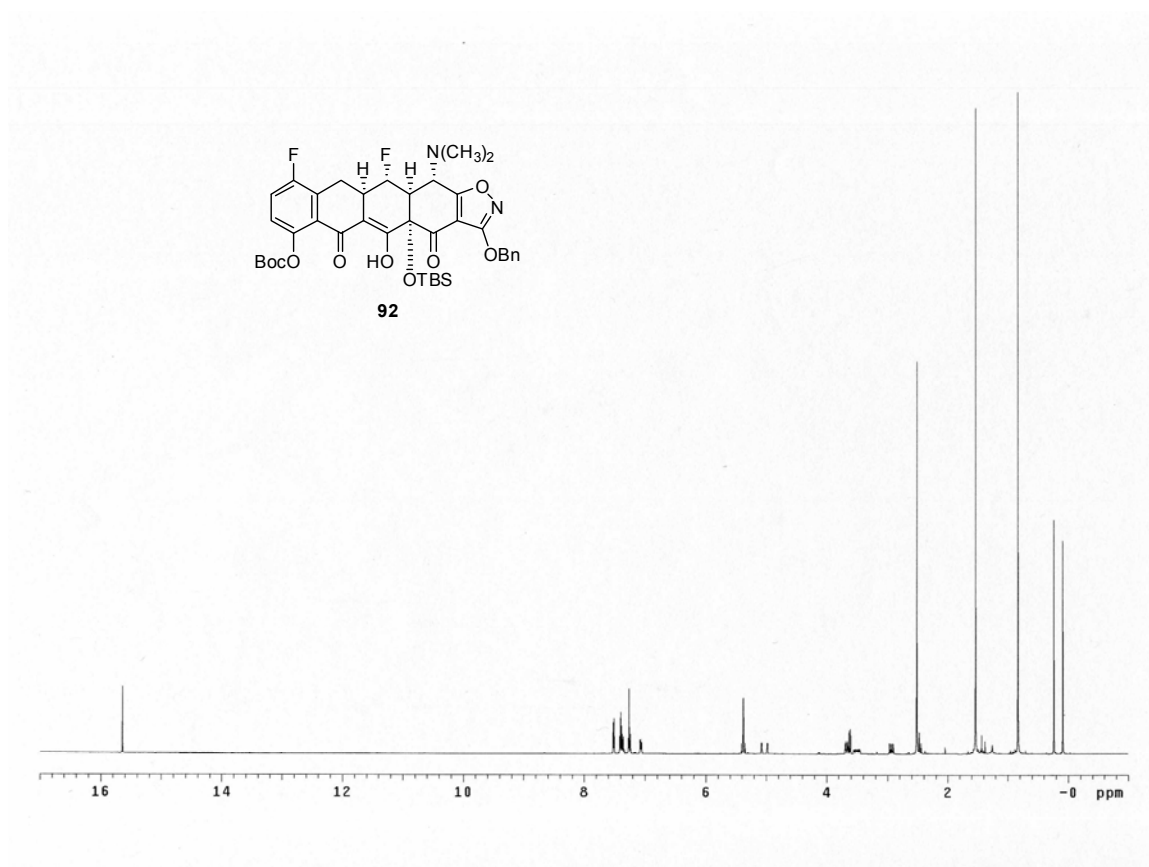
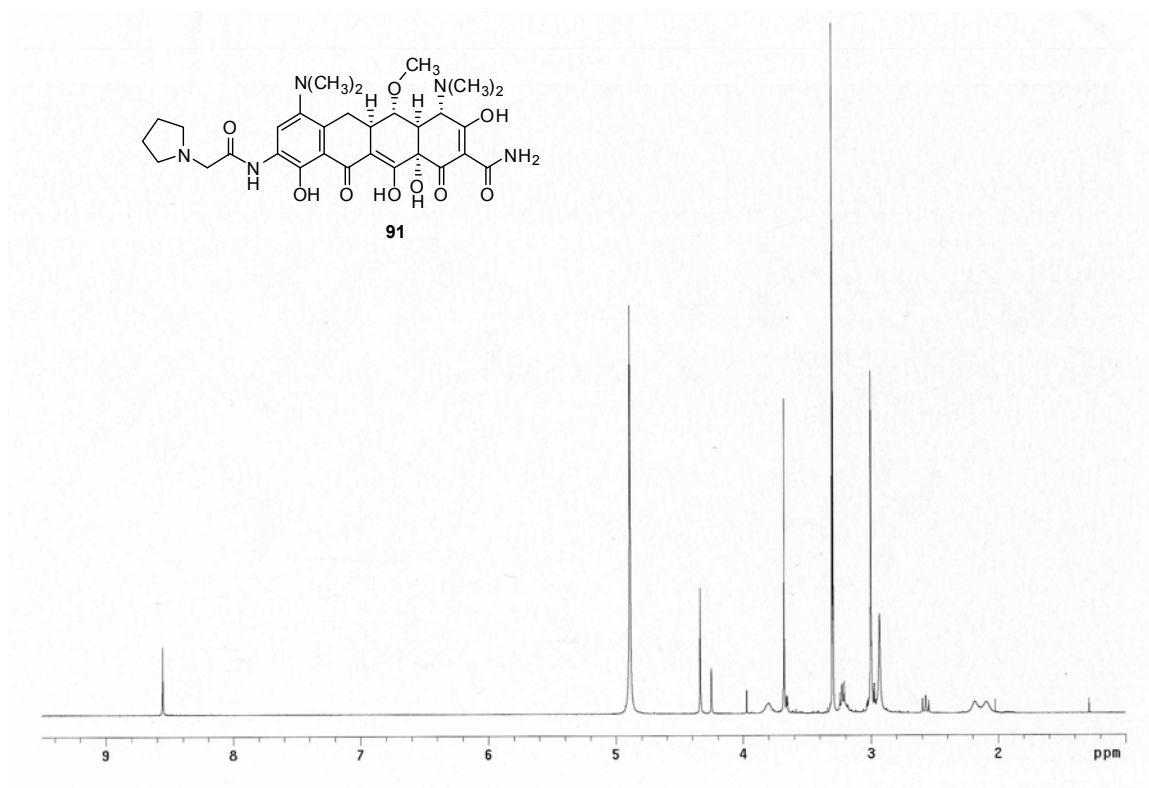


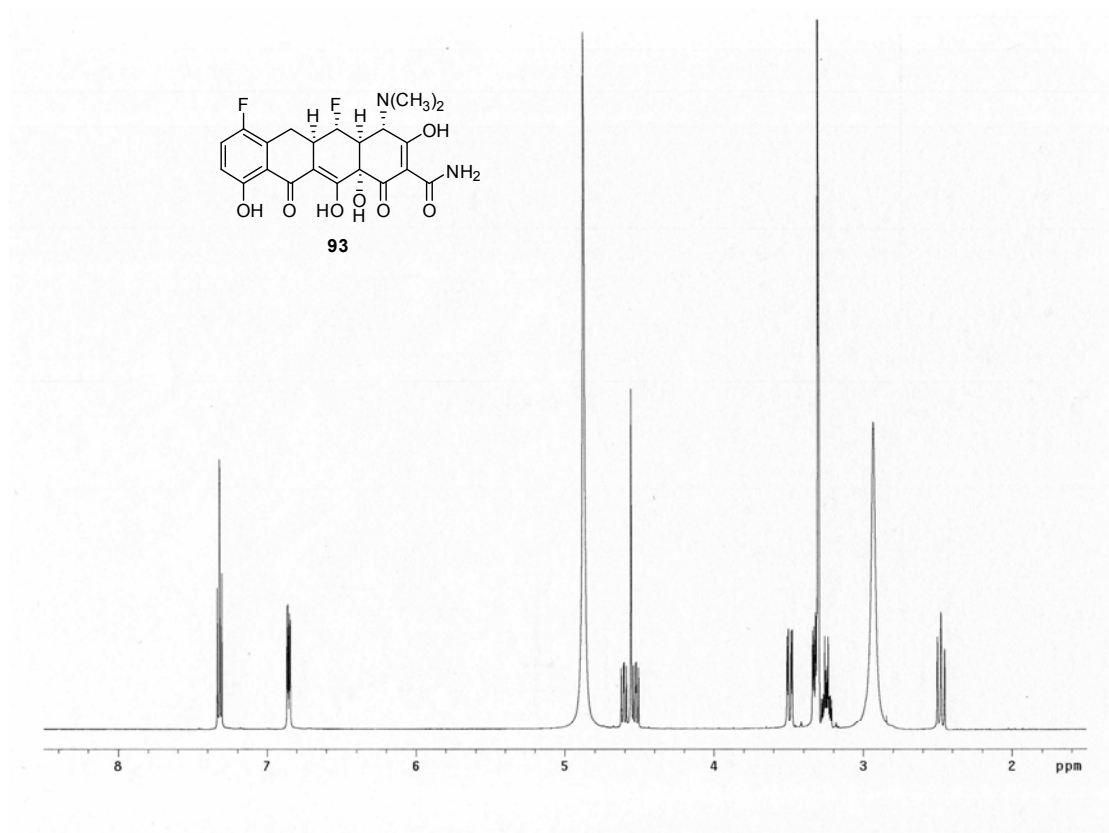
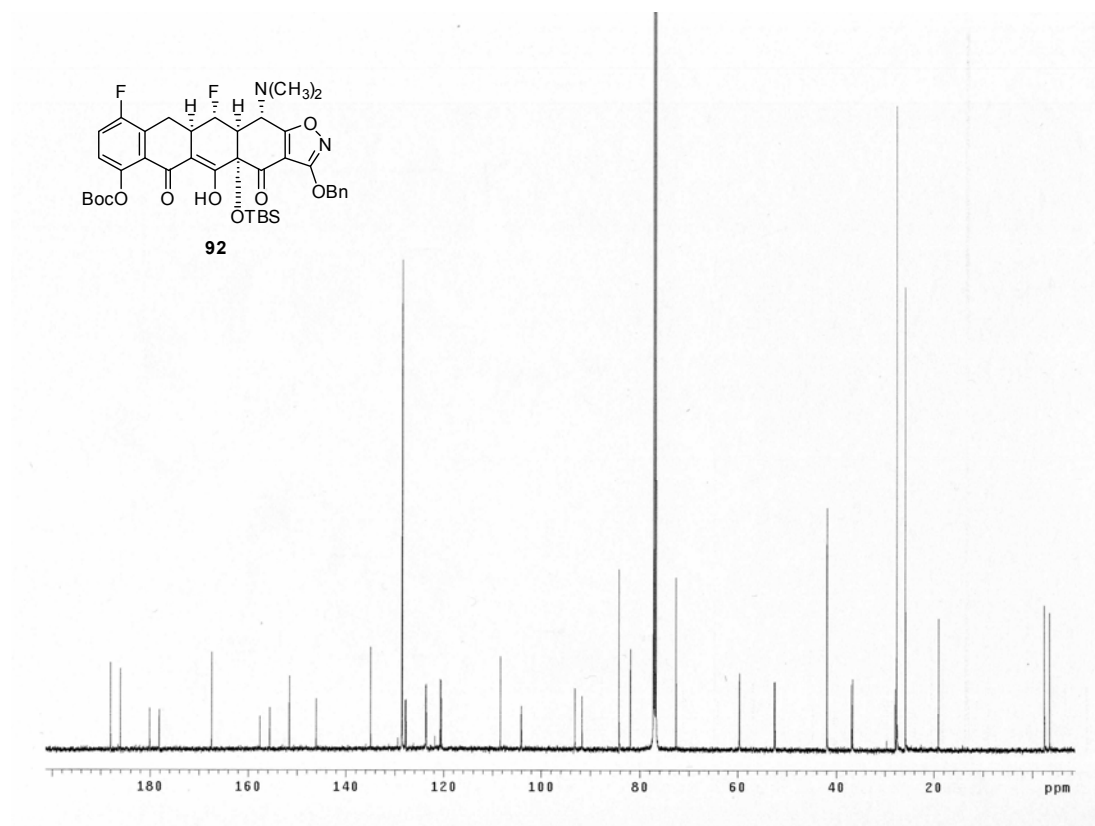


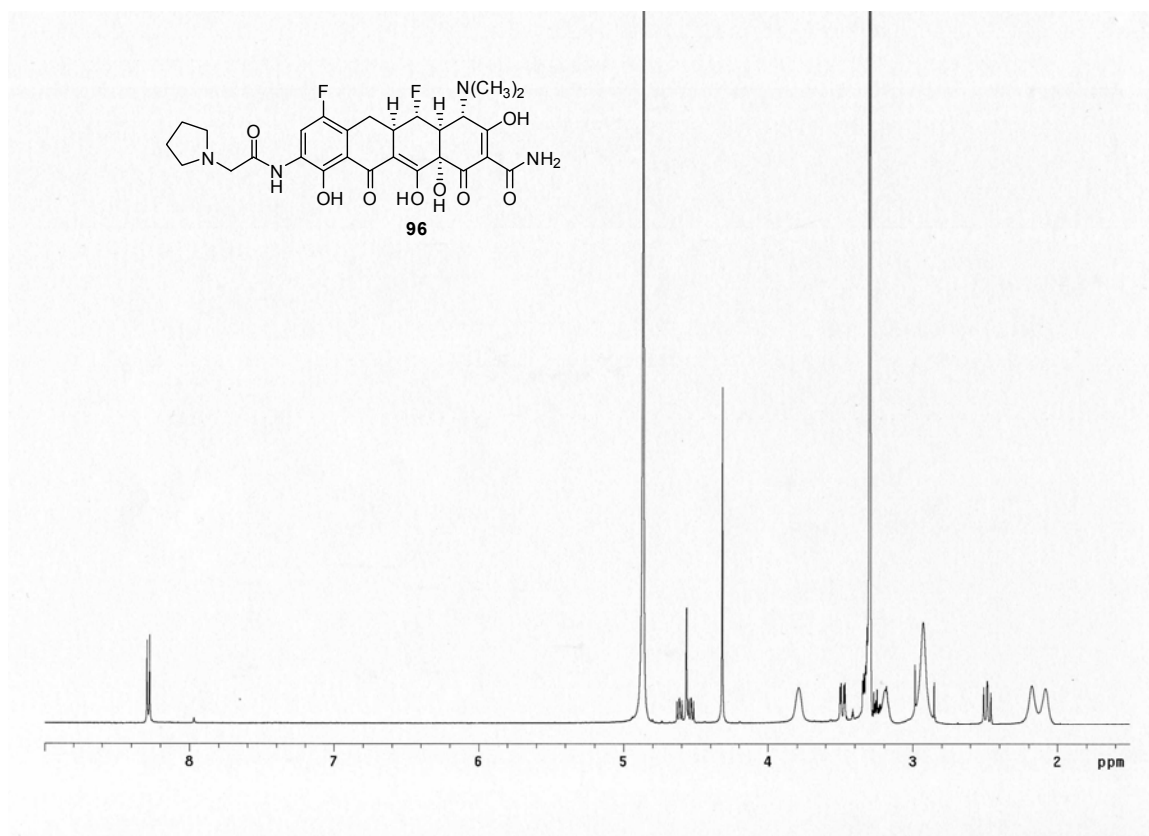
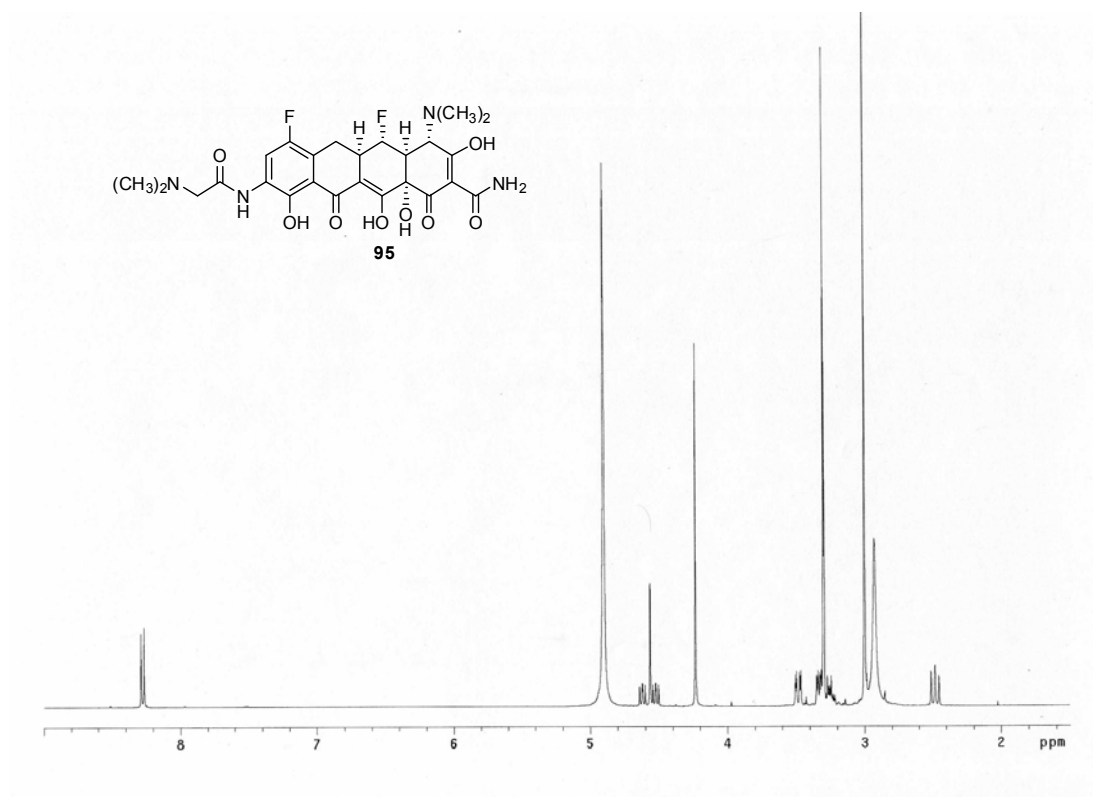


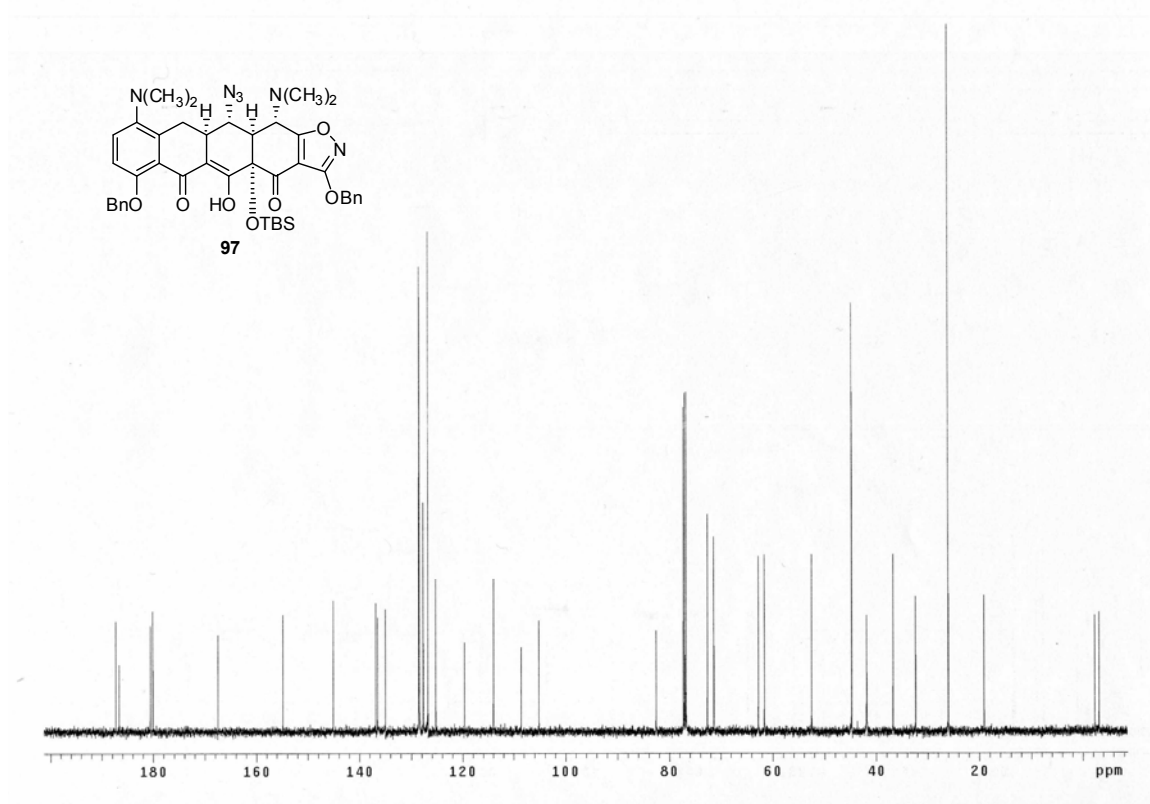
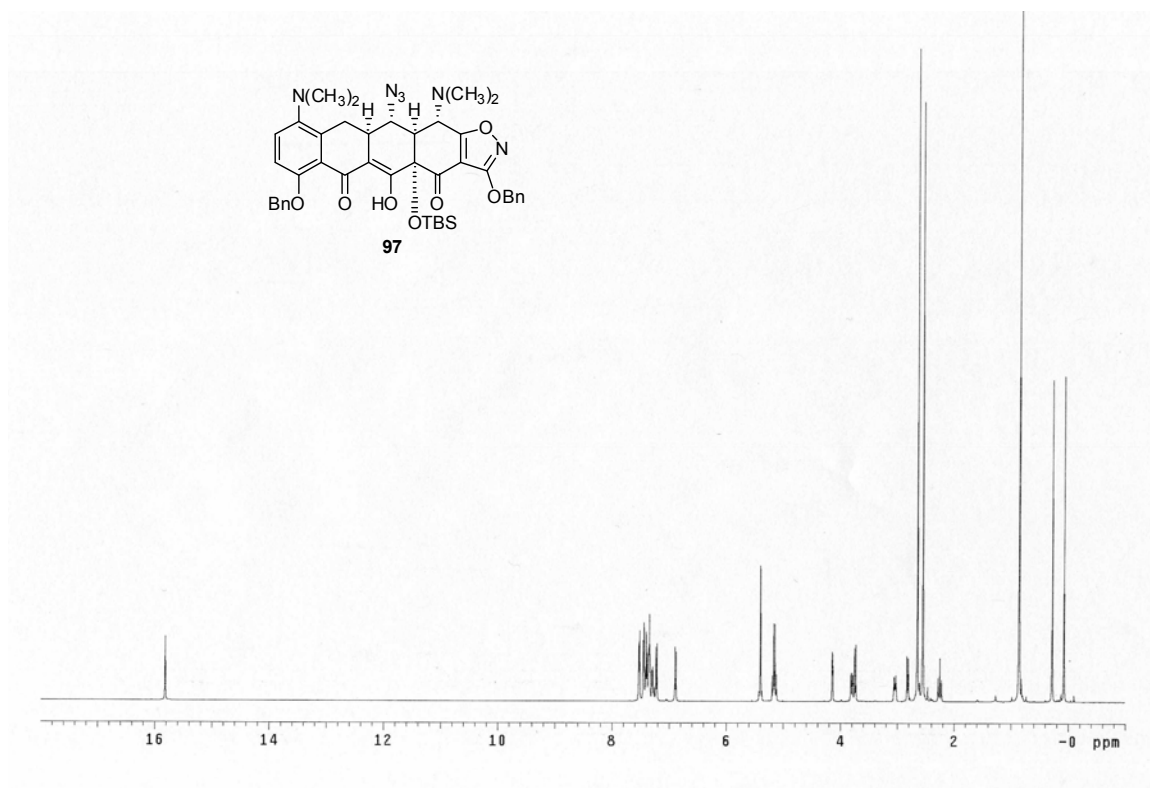


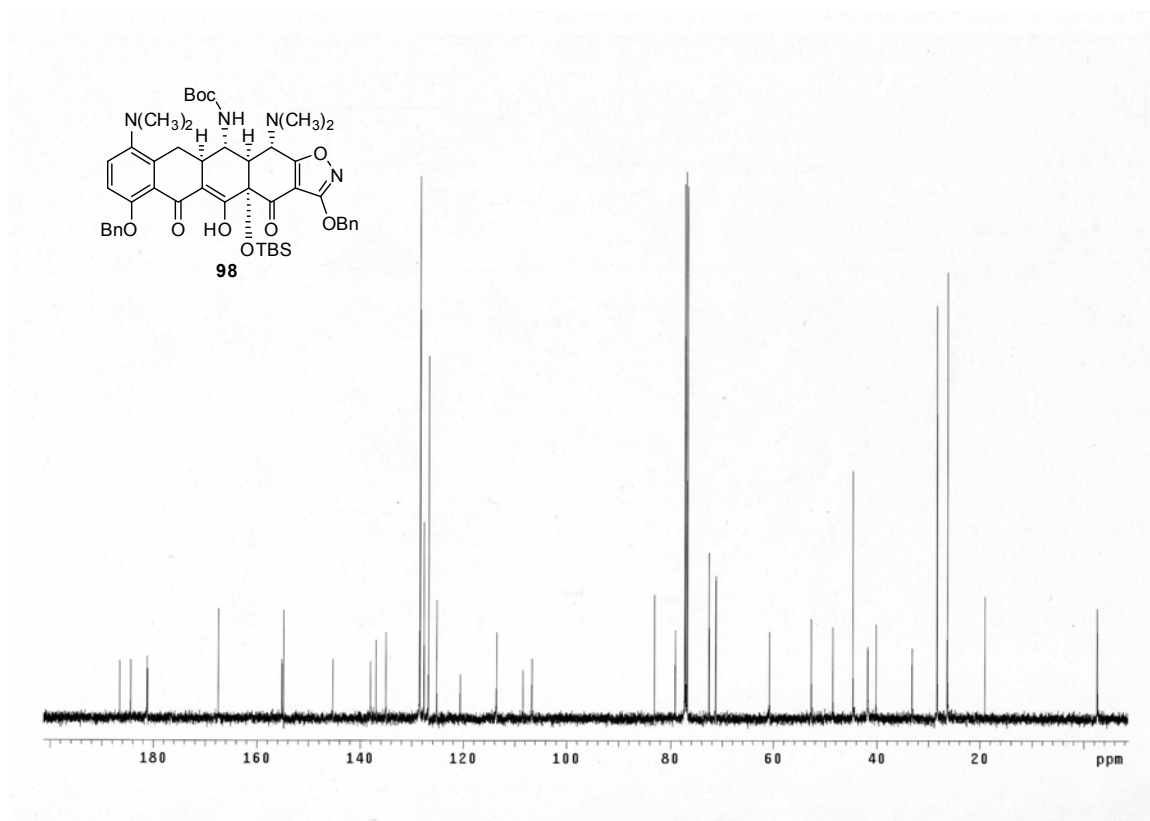
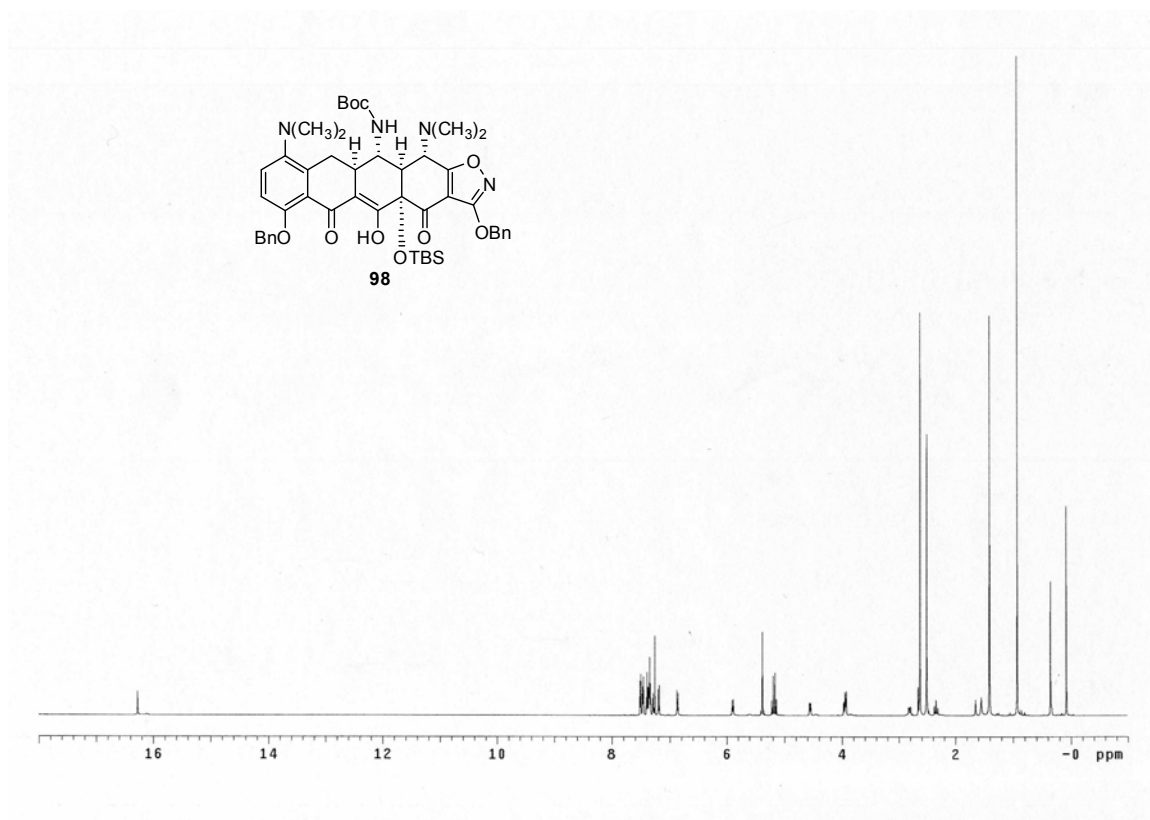


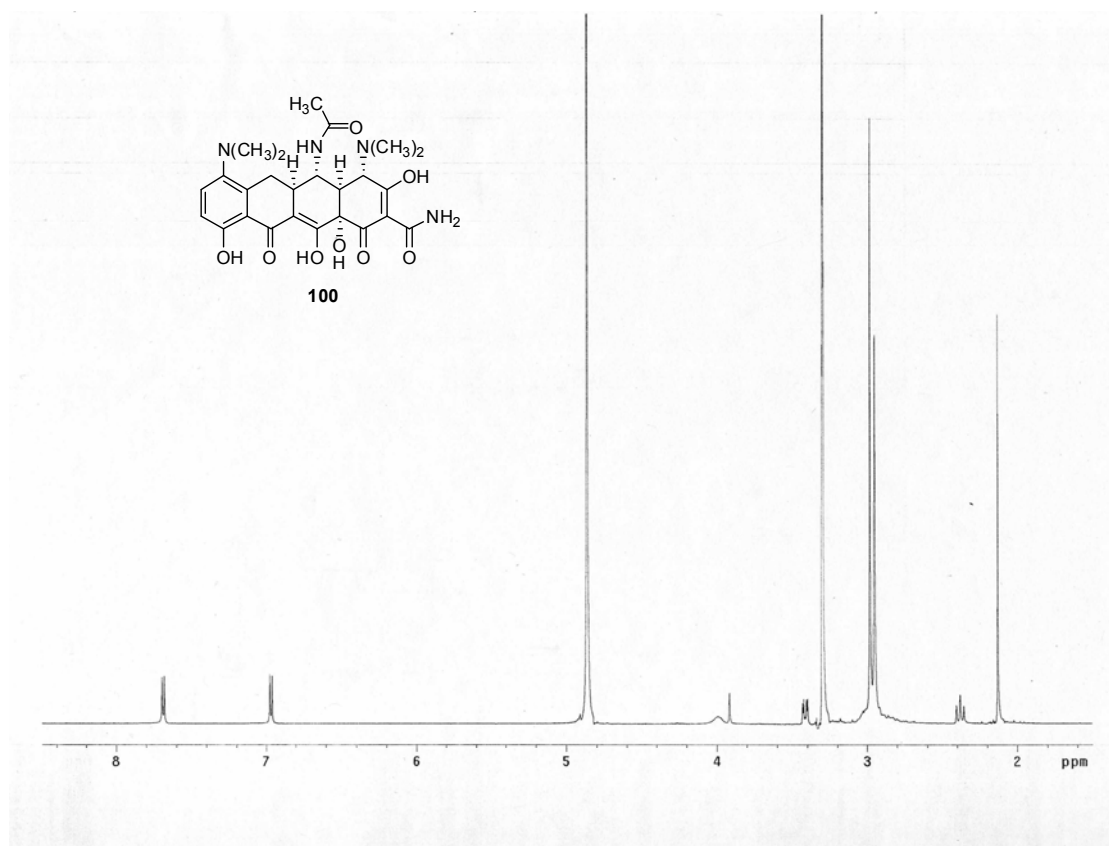
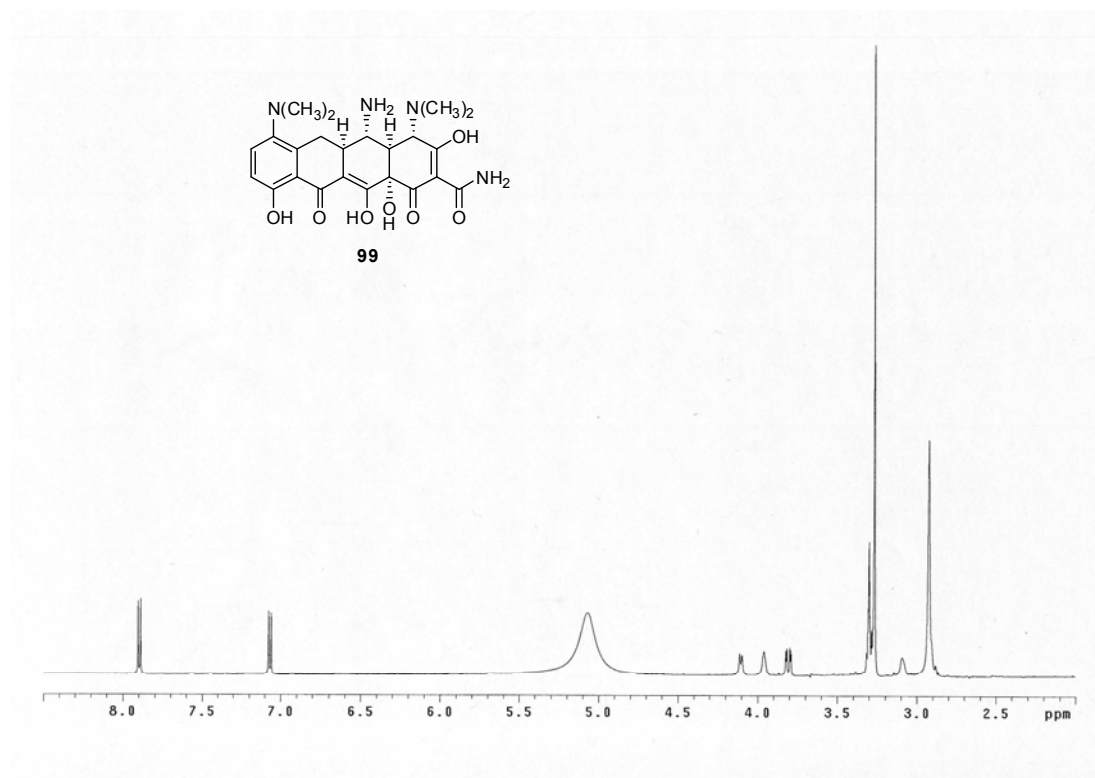


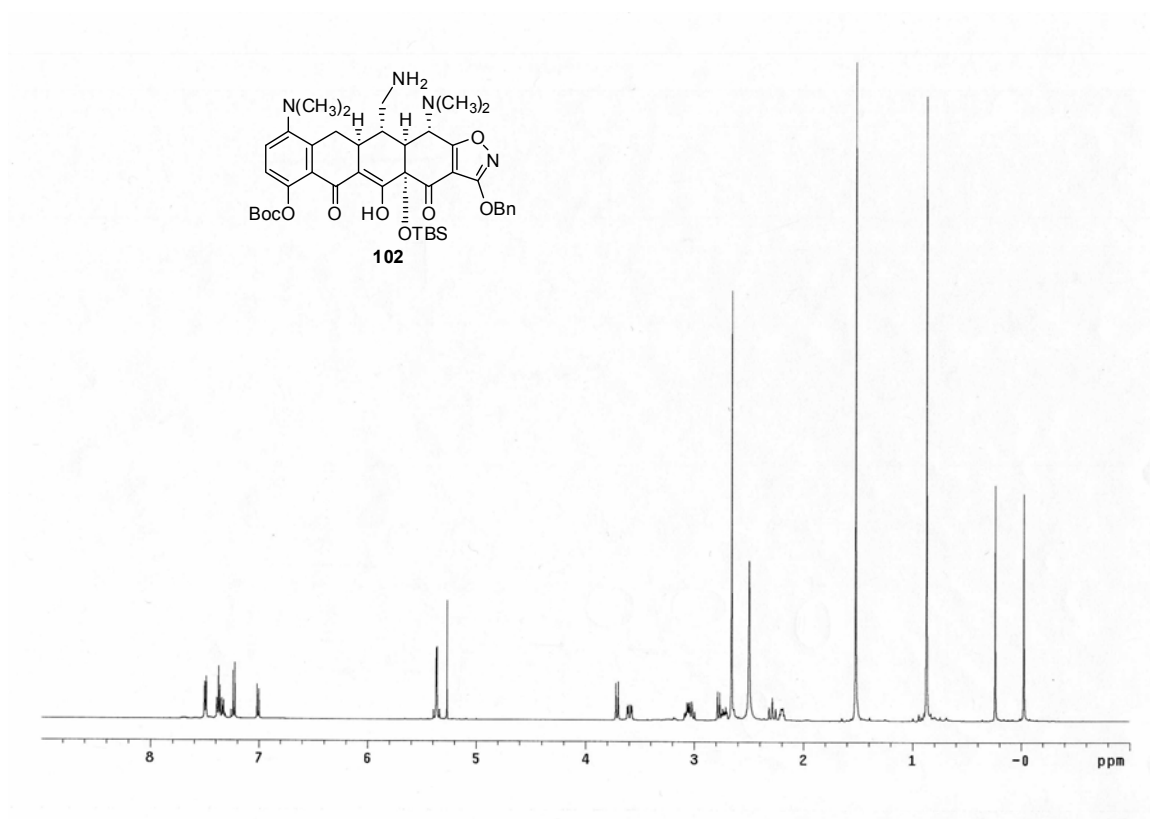
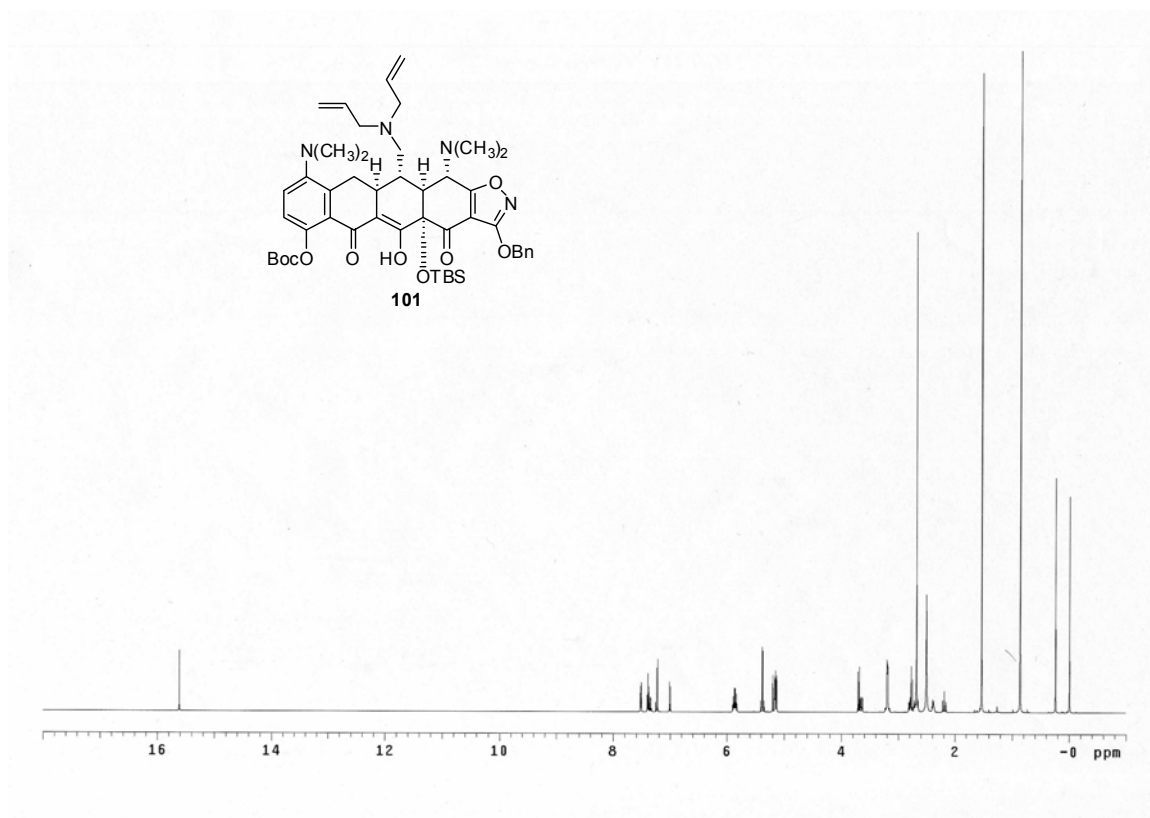


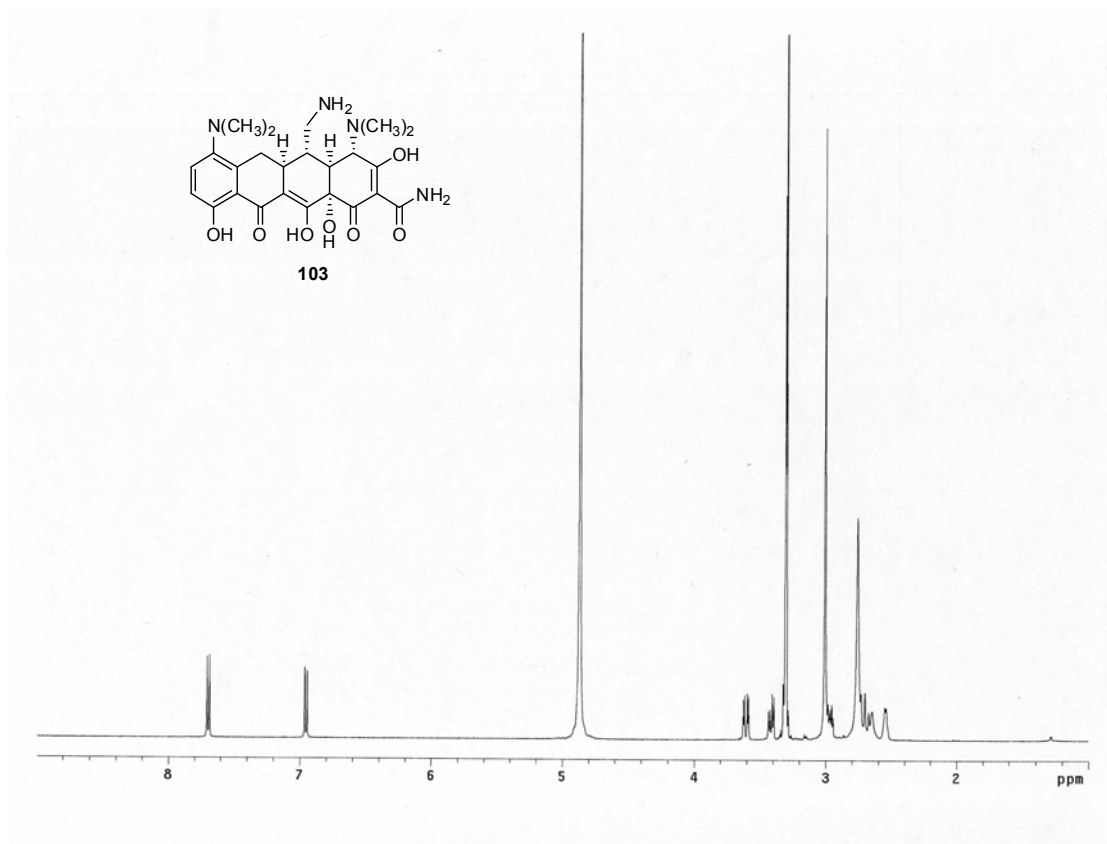
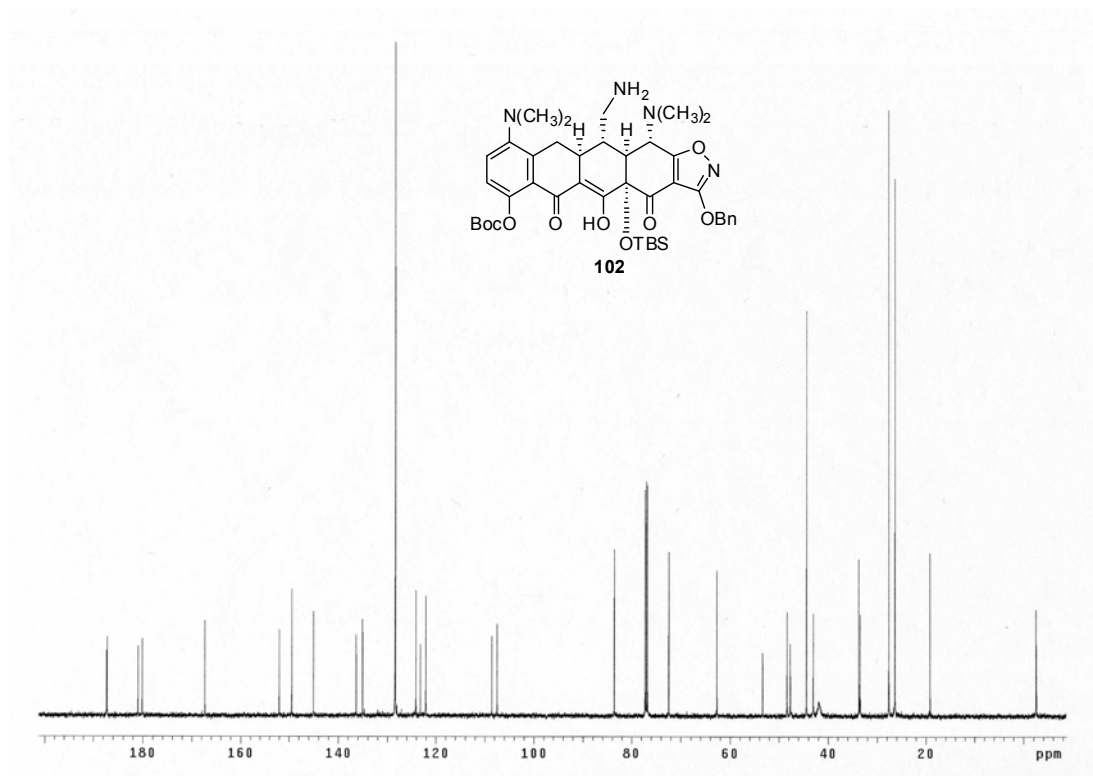


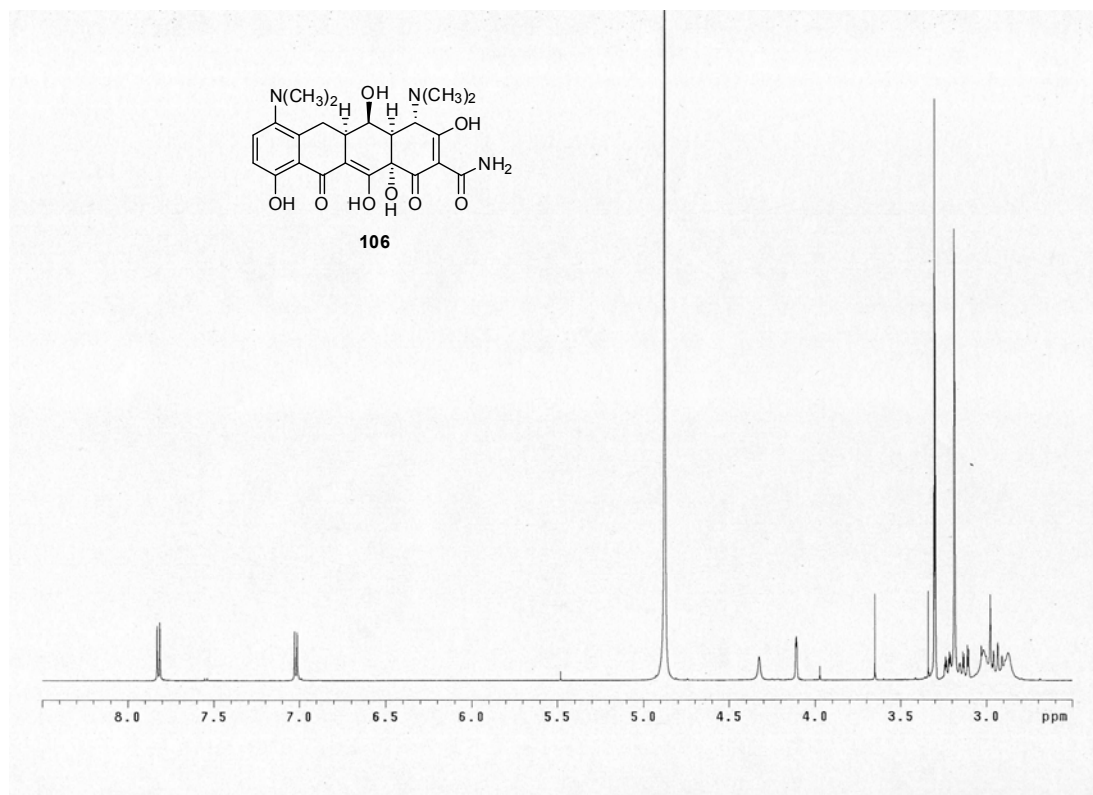












Chapter 4

Progress Toward the Synthesis of 5-Hetero-Tetracyclines

Introduction

Gram-negative bacterial cells are bounded by two permeability barriers: (1) the cytoplasmic membrane, which is permeable to uncharged, lipophilic molecules; and (2) the outer membrane, which has a different constitution and is significantly less permeable to lipophilic molecules.⁹⁷ Tetracyclines, like most antibacterials, penetrate the outer membrane of Gram-negative cells predominantly by passing through aqueous channels provided by porin proteins imbedded in the outer membrane. Antibacterial agents with activity against Gram-negative bacteria tend to have higher relative polar surface area (see Chapter 1 for discussion) and lower mean molecular mass than antibacterials which are only active against Gram-positive organisms. These requirements for Gram-negative activity are believed to be driven by the properties of porin proteins.

OmpF is one of the porin proteins found in the outer membrane of *Escherichia coli*. The X-ray crystal structure of OmpF revealed a trimer of identical subunits, each consisting of a β -barrel with 16 transmembrane β -strands.⁹⁸ At its most constricted (at about half the height of the barrel) the pore narrows to an ellipse of cross-section 11 x 7 Å. Pore diameter increases abruptly to 22 x 15 Å beyond the constriction zone (which is

⁹⁷ Nikaido, H. *Microbio. Mol. Biol. Rev.* **2003**, 67, 593-656.

⁹⁸ Cowan, S. W.; Schirmer, T.; Rummel, G.; Steiert, M.; Ghosh, R.; Paupit, R. A.; Jansonius, J. N.; Rosenbusch, J. P. *Nature* **1992**, 358, 727-733.

approximately 9 Å long). The constriction region of OmpK36, a porin found in *Klebsiella pneumoniae*, was found to be almost exactly the same size as that of OmpF.⁹⁹

In theory, the introduction of new hydrogen bond-forming substituents on the tetracycline scaffold could make the displacement of water molecules associated with passage through porin channels less disfavored. Any structural decoration would (to lesser or greater extents) increase overall size of the molecule in one or more dimensions, which in the case of larger groups could disrupt movement of the small molecule through the constricted regions of porin proteins. We were led to consider the possibility that we could increase the polarity of tetracyclines without increasing size (and thereby disrupting movement through porin channels) by incorporating a heteroatom into the polyketide-derived carbocyclic scaffold.

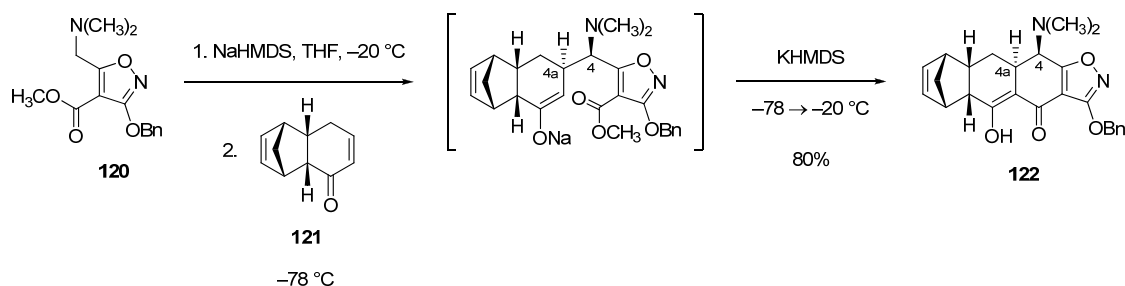
The incorporation of a heteroatom (oxygen or nitrogen) at position 5 on the tetracycline scaffold would add a hydrogen bonding substituent and increase the polar surface area of these antibacterial small molecules without significantly increasing molecular weight or size. In theory, this could make the displacement of water molecules associated with passage through porin channels less disfavored, thus making penetration of Gram-negative cells more efficient. For these reasons, we chose to consider the preparation of fully synthetic 5-oxo- and 5-aza-tetracyclines.

⁹⁹ Dutzler, R.; Rummel, G.; Alberti, S.; Hernández-Allés, S.; Phale, P. S.; Rosenbusch, J. P.; Benedi, V. J.; Schirmer, T. *Structure* **1999**, 7, 425–434.

Unlike the β - and γ -substituted AB precursors to fully synthetic 5a- and 5-substituted tetracyclines described in preceding chapters, it would not be possible to prepare “5-hetero” AB precursors directly from the AB enone **10**. We instead considered synthesizing these modified AB components by adaptation of our third-generation synthesis of the AB enone **10**.¹⁰⁰ The third-generation synthesis comprises a five-step synthetic sequence from two starting materials of near equal complexity, as measured by the number of steps required to prepare each starting material. Asymmetry is transferred from the B-ring precursor **121** to C4 and C4a via a highly diastereoselective Michael–Claisen cyclization reaction with the sodium enolate of isoxazole precursor **120** (Scheme 4.1).¹⁰¹ Michael addition proceeds by addition to the sterically more accessible face of cyclohexenone **121** (along a pseudoaxial trajectory) and with complete control of relative stereochemistry at C4 and C4a.

¹⁰⁰ Kummer, D. A.; Li, D.; Dion, A.; Myers, A. G. *Chem. Sci.* **2011**, 2, 1710–1718.

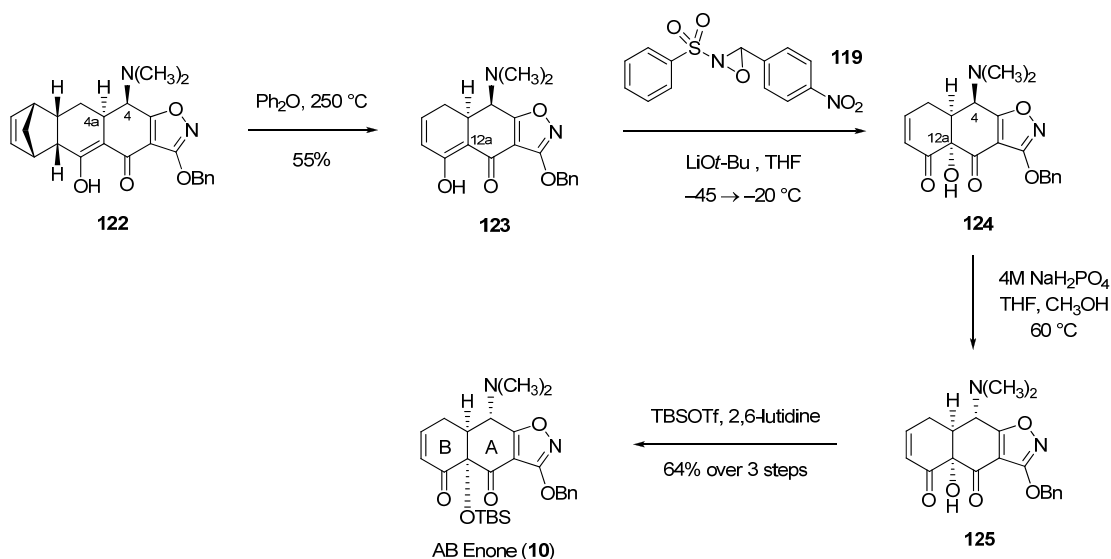
¹⁰¹ Stork reported the first synthesis of isoxazole ester **120** while developing the 5-benzyloxyisoxazole function as a protective group for the A ring of tetracyclines, an innovation that was critical to the development of the Myers tetracycline platform. For original work, see: (a) Stork, G.; Hagedorn, A. A. *J. Am. Chem. Soc.* **1978**, 100, 3609–3611. (b) Stork, G.; LaClair, J. J.; Spargo, P.; Nargund, R. P.; Totah, N. *J. Am. Chem. Soc.* **1996**, 118, 5304–5305. For an optimized protocol for the synthesis of isoxazole **120**, see: Kummer, D. A. (2011) *II. A Practical, Convergent Route to the Key Precursor to the Tetracycline Antibiotics*. Ph.D. Thesis, Harvard University.



Scheme 4.1. Diastereoselective Michael–Claisen cyclization of components **120** and **121**.

Michael–Claisen cycloadduct **122** was transformed into the AB enone **10** by the following sequence (Scheme 4.2): (1) expulsion of cyclopentadiene from **122** by retro-Diels–Alder fragmentation, (2) C12a-hydroxylation of **123** with 3-(4-nitrophenyl)-2-(phenylsulfonyl)-oxaziridine (**119**),¹⁰² (3) C4-epimerization upon heating a solution of **124** in tetrahydrofuran–methanol with sodium dihydrogen phosphate, and (4) protection of the C12a-hydroxyl group of **125** as a *tert*-butyldimethylsilyl ether. The relative stereochemical outcome of the A-ring-forming cyclization described above did not match the stereochemistry of tetracyclines at C4, but this result proved advantageous as the dimethylamino group of intermediate **123** directs the approach of oxaziridine **119** to the sterically more accessible lower face, providing hydroxylation product **124** with the required stereochemistry at C12a.

¹⁰² Vishwakarma, L. C.; Stringer, O. D.; Davis, F. A. *Organic Syntheses* **1993**, Coll. Vol. 8, 546.



Scheme 4.2. Synthesis of AB enone **10** from Michael–Claisen cycloadduct **122**.

It was well known prior to this work that various conditions could be used to effect epimerization at C4 of tetracyclines. Lederle scientists observed in 1955 that tetracycline is converted to a mixture of C4 stereoisomers in 1M sodium dihydrogen phosphate–methanol (2:1, 25 °C).¹⁰³ It has also been demonstrated that a mixture of C4 epimers of sancycline (6-deoxy-6-demethyltetracycline) can be isomerized to provide predominantly the natural stereoisomer by treatment with calcium (II) chloride in a water–butanol mixture containing ethanolamine (pH 8.5, reflux).¹⁰⁴

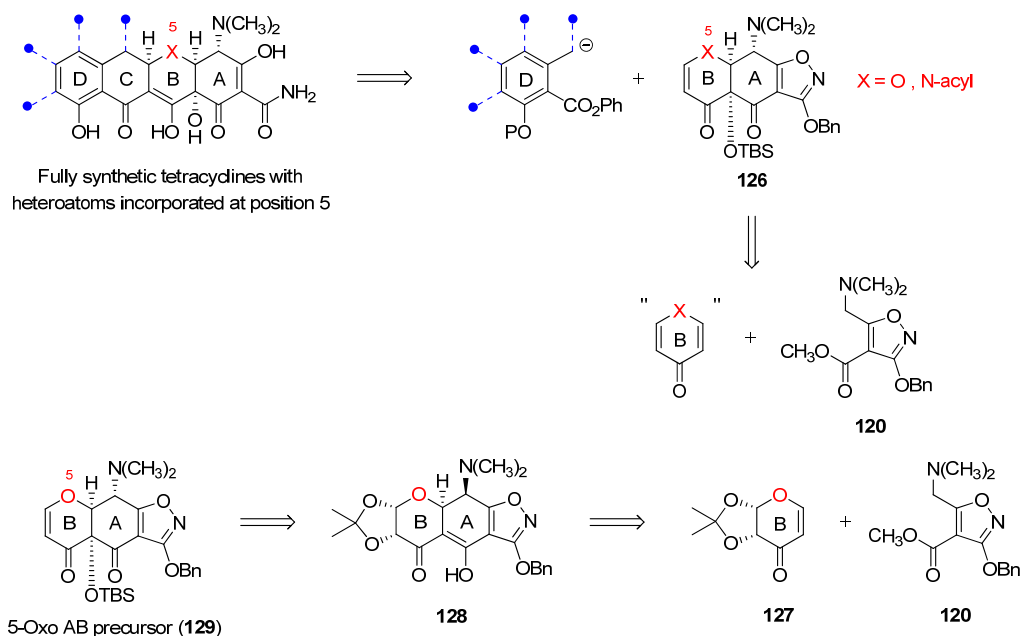
¹⁰³ (a) Doerschuk, A. P.; Bitler, B. A.; McCormick, J. R. D. *J. Am. Chem. Soc.* **1955**, 77, 4687. (b) McCormick, J. R. D.; Fox, S. M.; Smith, L. L.; Bitler, B. A.; Reichenthal, J.; Origoni, V. E.; Muller, W. H.; Winterbottom, R.; Doerschuk, A. P. *J. Am. Chem. Soc.* **1957**, 79, 2849.

¹⁰⁴ M. M. Noseworthy. U.S. Patent 3,009,956, November 21, **1961**.

Retrosynthetic Strategy and Background

We envisioned preparing 5-hetero-tetracyclines using an iterative Michael–Claisen strategy, a conceptual approach that had been successful in the third-generation synthesis of the AB enone **10**. 5-Hetero-tetracyclines could be formed by cyclization reactions of D-ring precursors with 5-hetero AB precursors (represented by structure **126**, where X is oxygen or protected nitrogen; Scheme 4.3). 5-Hetero AB precursors could in turn be accessed via A-ring-forming Michael–Claisen cyclizations of isoxazole ester anions and heterocyclic B-ring precursors. Dihydro-4-pyranone **127** was selected as a potential precursor to the B ring of 5-oxo-tetracyclines. There is literature precedent for a diastereoselective conjugate addition reaction of the enantiomer of **127** with a thiol nucleophile, with addition occurring from the face opposite the isopropylidene substituent.¹⁰⁵ An analogous stereochemical outcome in the cyclization we envisioned would provide the correct stereochemistry at C4a. Numerous challenges were anticipated in transforming the Michael–Claisen product **128** into AB precursor **129**, including removal of the B-ring isopropylidene substituent, stereoselective C12a-hydroxylation and C4-epimerization. Efforts toward the synthesis of 5-oxo AB enone **129** are described below.

¹⁰⁵ Witczak, Z. J.; Lorchak, D.; Nguyen, N. *Carbohydrates Res.* **2007**, *342*, 1929–1933.



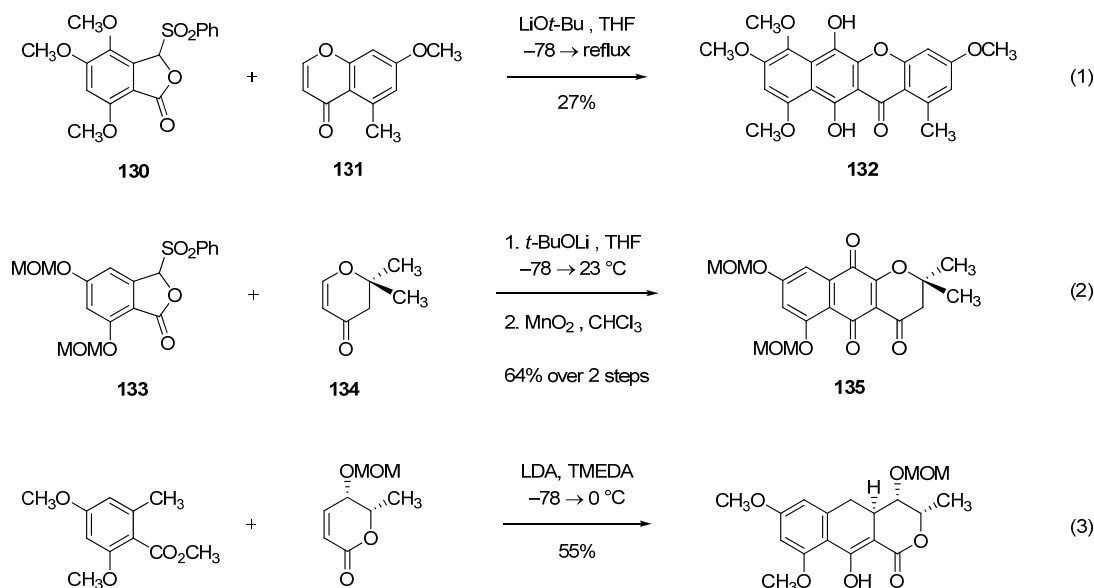
Scheme 4.3. Retrosynthesis of 5-hetero-tetracyclines: an iterative Michael–Claisen cyclization strategy.

There are a few examples in the literature that provide precedent for the Michael–Claisen cyclizations proposed in Scheme 4.3 above. Hauser described a regiospecific annulation reaction of the sulfone-stabilized phthalide anion derived from **130** with benzopyranone **131**, affording Michael–Claisen cyclization product **132** in 27% yield (eq 1, Scheme 4.4).¹⁰⁶ Tatsuta reported an efficient coupling reaction involving phthalide **133** and oxocyclic enone **134** (eq 2); oxidation of the cyclization product afforded quinone **135** in 64% yield over two steps.¹⁰⁷ This is the only example of which we are aware of an

¹⁰⁶ Hauser, F. M.; Hewawasam, P.; Baghdanov, V. M. *J. Org. Chem.* **1988**, 53, 223-224.

¹⁰⁷ Tatsuta, K.; Tanaka, Y.; Kojima, M.; Ikegami, H. *Chem. Lett.* **2002**, 14–15.

electrophile of this type (dihydro-4-pyranone) undergoing a successful Michael–Claisen reaction. There is also some precedent for cyclizations involving α,β -unsaturated lactone Michael acceptors (see eq 3 for an example).¹⁰⁸



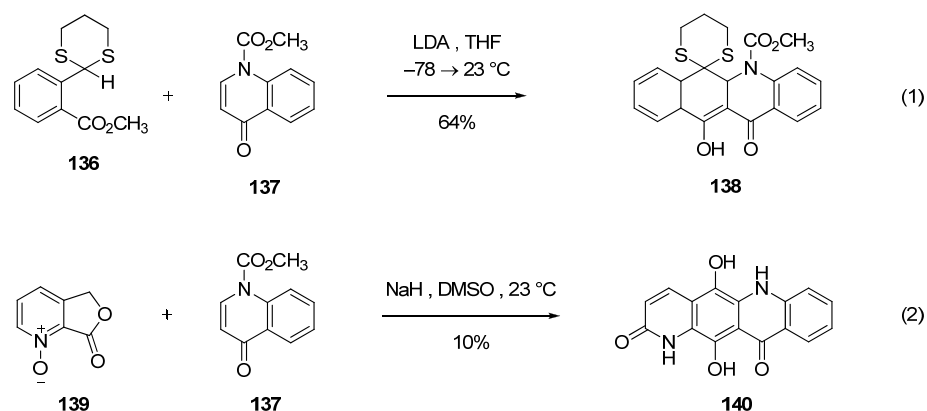
Scheme 4.4. Literature examples of Michael–Claisen and Michael–Dieckmann reaction sequences involving oxocyclic enones: benzopyranone, dihydro-4-pyranone and α,β -unsaturated lactone Michael acceptors.

There are two examples in the literature of Michael–Claisen reactions sequences of benzylic anions and azacyclic enone electrophiles.¹⁰⁹ In both examples the Michael

¹⁰⁸ Examples of Michael–Claisen reactions involving α,β -unsaturated lactones as Michael acceptors: (a) Tatsuta, K.; Yamazaki, T.; Mase, T.; Yoshimoto, T. *Tetrahedron Lett.* **1998**, 39, 1771–1772. (b) Braukmuller, S.; Brückner, R. *Eur. J. Org. Chem.* **2006**, 2110–2118.

¹⁰⁹ (a) Alvarez, M.; Ajana, W.; Lopez-Calahorra, F.; Joule, J. A. *J. Chem. Soc. Perkin Trans. 1* **1994**, 917–919. (b) Ajana, W.; Lopez-Calahorra, F.; Joule, J. A.; Alvarez, M. *Tetrahedron* **1997**, 53, 341–356.

acceptor is *N*-methoxycarbamoyl-4-quinolone (**137**). Reaction of **137** with the dithiane-stabilized benzylic anion derived from methyl ester **136** afforded Michael–Claisen product **138** in 64% yield (eq 1, Scheme 4.5). In addition, quinolone **137** was found to undergo a Michael–Claisen reaction with the phthalide anion of pyridine *N*-oxide **139**, providing the product **140** following post-cyclization transformations (eq 2). Similar cyclization reactions of 4-pyridone and dihydro-4-pyridone electrophiles have not been reported as far as we are aware, but these azacyclic enones have been shown to undergo conjugate addition reactions with organometallic reagents.^{110,111}



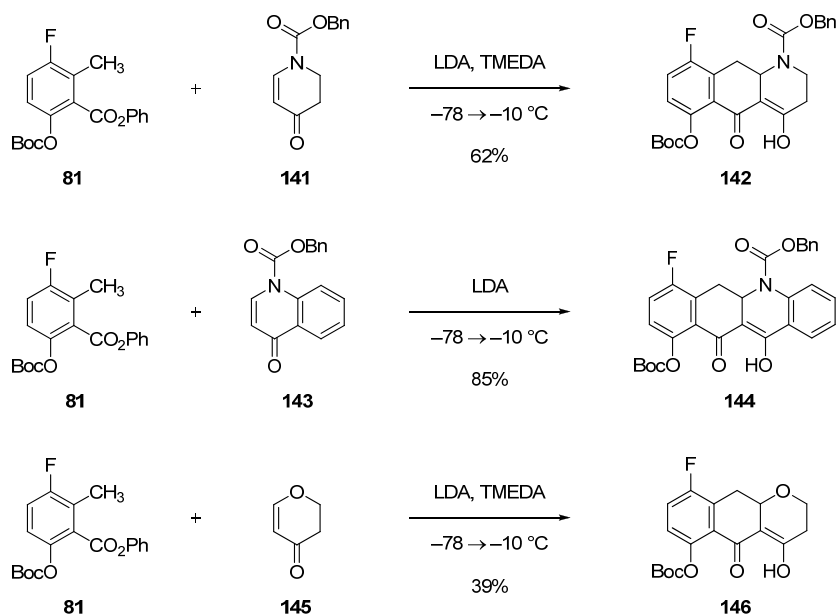
Results

Before targeting 5-hetero AB precursors it was first necessary to investigate the feasibility of constructing the C ring of 5-hetero-tetracyclines by Michael–Claisen cyclization. The results of model systems are presented in Scheme 4.6 below. Addition of *N*-benzyloxycarbamoyl-dihydro-4-pyridone **141** (1 equiv)¹¹² to a solution of the anion formed by LDA deprotonation of D-ring precursor **81** (2 equiv) in the presence of TMEDA (4 equiv) at –78 °C, followed by warming of the reaction mixture to –10 °C provided the desired Michael–Claisen product **142** in 64% yield after purification by flash-column chromatography. As far as we are aware, this is the first example of a Michael–Claisen reaction with a dihydro-4-pyridone as the conjugate acceptor. This reaction was also successful in the absence of TMEDA, although product **142** was formed in slightly lower yield. The analogous cyclization reaction of *N*-benzyloxycarbamoyl-quinolone **143** was extremely efficient without TMEDA additive, affording Michael–Claisen cycloadduct **144** in 85% yield following purification.¹¹³ The feasibility of our synthetic plan to access 5-hetero-tetracyclines using Michael–Claisen

¹¹² *N*-Benzyloxycarbamoyl-dihydro-4-pyridone **141** was prepared from 4-piperidone monohydrate hydrochloride by treatment with benzyl chloroformate (1 equiv) and sodium hydroxide (2 equiv) followed by oxidation of the acylation product, *N*-benzyloxy-4-piperidone, with *o*-iodoxybenzoic acid (IBX) in the presence of 4-methylmorpholine *N*-oxide. For oxidation conditions, see: Nicolaou, K. C.; Gray, D. L. F.; Montagnon, T.; Harrison, S. T. *Angew. Chem. Int. Ed.* **2002**, *41*, 996–1000.

¹¹³ *N*-Benzyloxycarbamoyl-4-quinolone **143** was prepared from 2'-nitroacetophenone according to procedures detailed in the following literature precedents: (a) Tois, J.; Vahermo, M.; Koskinen, A. *Tetrahedron Lett.* **2005**, *46*, 735–737. (b) Shintani, R.; Yamagami, T.; Kimura, T.; Hayashi, T. *Org. Lett.* **2005**, *7*, 5317–5319.

chemistry was further affirmed by a successful cyclization reaction of D-ring precursor **81** with dihydro-4-pyranone **145**,¹¹⁴ providing the desired product **146** in 39% yield.

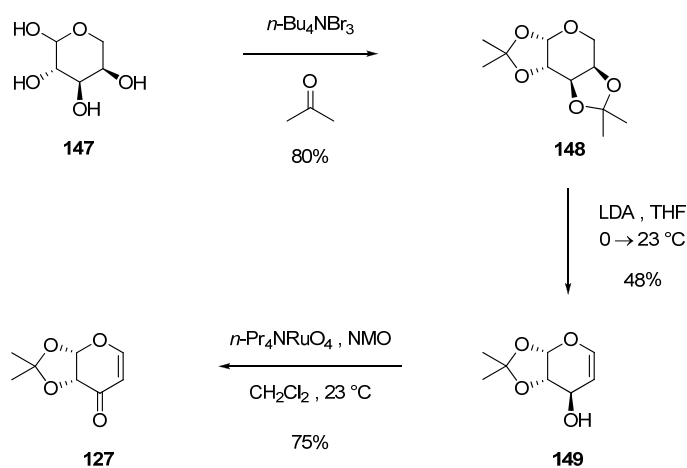


Scheme 4.6. Michael–Claisen cyclization reactions of D-ring precursor **81** with dihydro-4-pyridone, 4-quinolone and dihydro-4-pyranone electrophiles.

Once the feasibility of constructing the C ring of 5-hetero-tetracyclines using Michael–Claisen cyclizations had been established, synthetic approaches to 5-hetero AB precursors could be considered and developed. Heterocyclic enone **127** was identified as a possible precursor to the B ring of 5-oxo AB enone **129** (see Scheme 4.3 above). This potential B-ring precursor (**127**) was prepared as a single enantiomer via an efficient

¹¹⁴ For the preparation of dihydro-4-pyranone **145**, see: (a) Paquette, L. A.; Oplinger, J. A. *Tetrahedron* **1989**, *45*, 107–124. (b) Smith, A. B.; Fukui, M. *J. Am. Chem. Soc.* **1987**, *109*, 1269–1272.

three-step sequence adapted from literature precedent (Scheme 4.7). D-(–)-Arabinose (**147**) was converted into the corresponding bis-*O*-isopropylidene derivative **148** upon prolonged stirring with a catalytic quantity of tetrabutylammonium tribromide in dry acetone (80% yield, 2 d, 12-g batch).¹¹⁵ Treatment of bis-*O*-isopropylidene **148** with an excess of lithium diisopropylamide afforded allylic alcohol **149** as the product of a lithiation–elimination sequence.¹¹⁶ In a significant improvement upon a literature procedure, oxidation of allylic alcohol **149** was achieved rapidly and efficiently with tetrapropylammonium perruthenate (10 mol %) and *N*-methylmorpholine *N*-oxide (NMO, 1.5 equiv), providing the potential B–ring precursor **127** in 75% yield.¹¹⁷



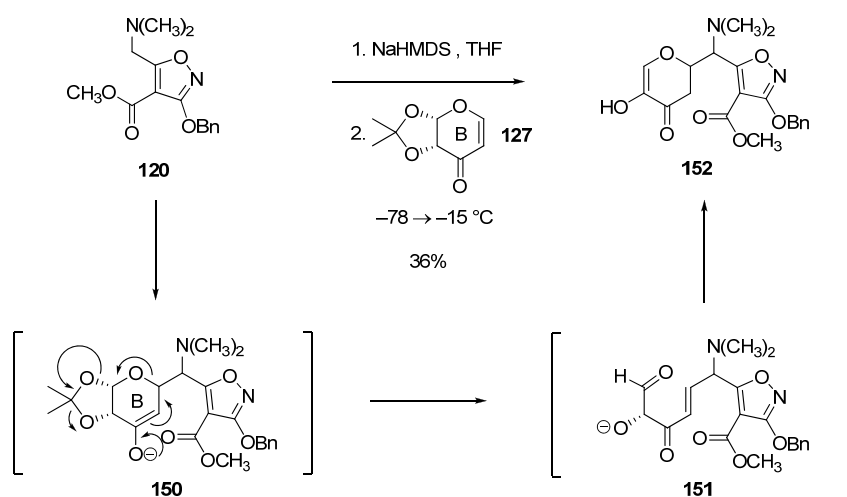
Scheme 4.7. Synthesis of heterocyclic enone **127**, a possible B-ring precursor.

¹¹⁵ Khan, A. T.; Khan, M. M.; Adhikary, A. *Carbohydrates Res.* **2011**, *346*, 673–677.

¹¹⁶ Klemer, A.; Jung, G. *Chem. Ber.* **1981**, *114*, 1192–1195.

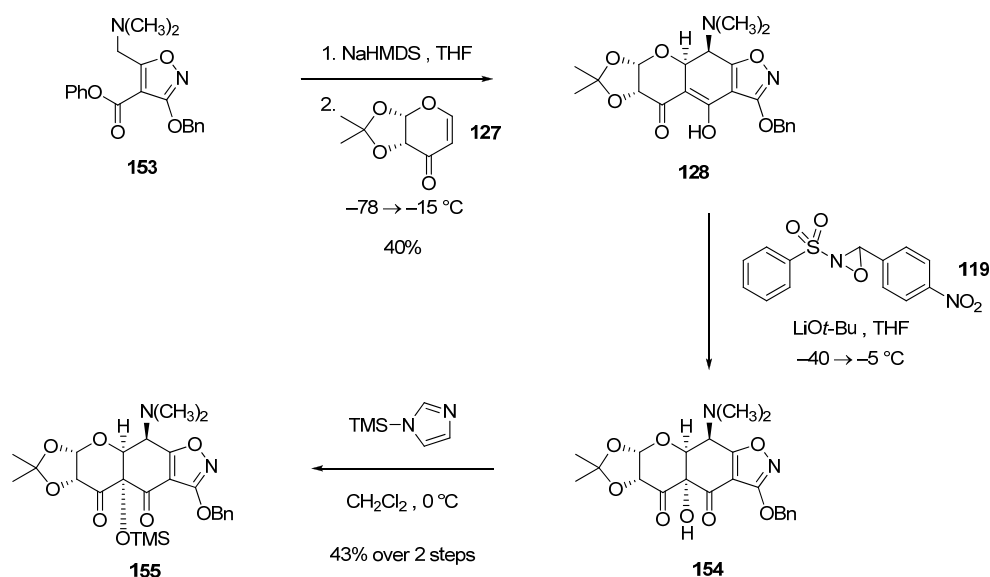
¹¹⁷ Ley, S. V.; Norman, J.; Griffith, W. P.; Marsden, S. P. *Synthesis* **1994**, *7*, 639–666.

The next challenge was to construct the A ring of 5-oxo-tetracyclines by a Michael–Claisen reaction of B-ring precursor **127** with isoxazole ester anions known from prior research to be effective nucleophiles in analogous A-ring-forming cyclizations. Attempted cyclization of **127** with the anion derived from methyl ester isoxazole **120** was not successful. The major product of this cyclization attempt was compound **152** (Scheme 4.8). A possible mechanism for the formation of **152** is presented below. This product could be formed by Michael addition of the isoxazole ester anion (to form enolate **150**) followed by sequential B-ring opening, expulsion of acetone (to give alkoxide **151**), tautomerization and cyclization to form the B ring. No Michael–Claisen products were observed in this reaction, indicating that the energy barrier for Claisen cyclization is higher than that for B-ring opening of enolate intermediate **150**.



Scheme 4.8. Unsuccessful A-ring cyclization attempt with isoxazole methyl ester **120**.

It was hoped that this problem could be overcome by increasing the electrophilicity of the isoxazole ester. Addition of B-ring precursor **127** (1 equiv) to a solution of the anion formed by NaHMDS deprotonation of the phenyl ester isoxazole **153** at $-78\text{ }^{\circ}\text{C}$, followed by warming of the reaction mixture to $-15\text{ }^{\circ}\text{C}$ and stirring at this temperature for $2\frac{1}{2}\text{ h}$ afforded the Michael–Claisen product **128** in 40% yield as a single diastereomer after purification by flash-column chromatography and rp-HPLC (Scheme 4.9 below). NMR analysis revealed trace amounts of by-products in the crude product mixture, but no diastereomers of **128** were isolated following purification. The stereochemical outcome of the cyclization is homologous with the outcome of the A-ring-forming cyclization reaction in the third-generation synthesis of the AB enone **10**.¹⁰⁰



Scheme 4.9. Synthesis of trimethylsilyl ether **155** via sequential diastereoselective reactions: Michael–Claisen coupling of isoxazole phenyl ester **153** and B-ring precursor **127**, followed by C12a-hydroxylation.

With Michael–Claisen product **128** in hand, we next sought to introduce hydroxylation at C12a using optimized conditions that were developed for the third-generation synthesis of the AB enone **10**. It was not known whether the isopropylidene substituent would block approach of the electrophilic oxidant from the lower face, potentially eroding the stereoselectivity observed in the third-generation synthesis. Fortunately, addition of lithium *tert*-butoxide to a THF solution of **128** and 3-(4-nitrophenyl)-2-(phenylsulfonyl)-oxaziridine (**119**)¹⁰² at –40 °C followed by warming of the reaction mixture to –5 °C afforded the desired C12a-hydroxylated compound **154** as the only major product (Scheme 4.9 above). Partial purification of **154** followed by protection of the C12a-hydroxyl group as a trimethylsilyl ether by treatment with 1-(trimethylsilyl)imidazole (5 equiv) at 0 °C afforded compound **155** in 43% yield over two steps. The relative stereochemical outcomes of all reactions in this synthetic sequence were confirmed by an X-ray crystal structure of C12a-hydroxylation product **154** (Figure 4.1).

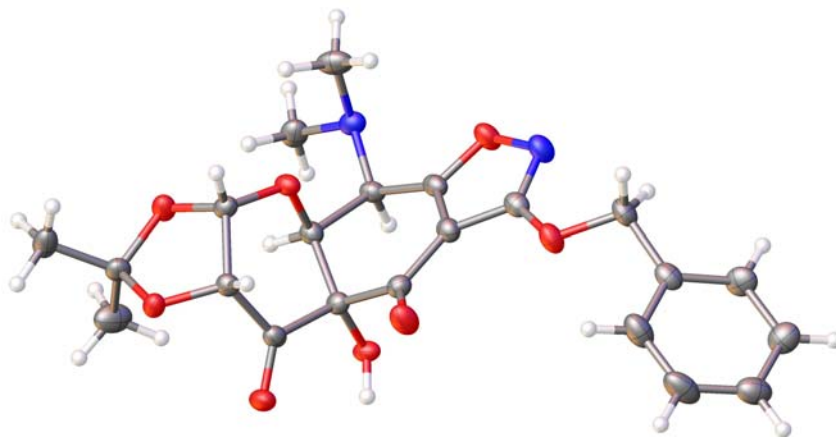
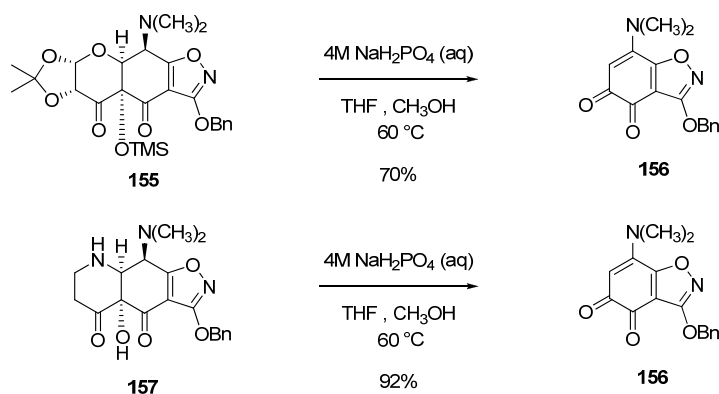


Figure 4.1. X-ray crystal structure of C12a-hydroxylation product **154**.

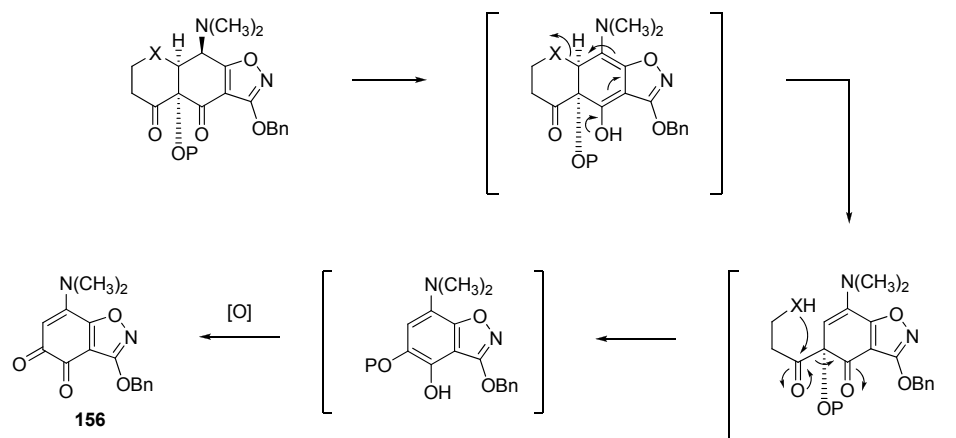
Two significant challenges remained in order to convert trimethylsilyl ether **155** (or the C12a-hydroxy compound **154**) into an AB precursor to 5-oxo-tetracyclines: (1) inversion of C4 stereochemistry, and (2) removal of the B-ring “chiral auxiliary” and formation of an enone.

Initial investigations indicate that C4-epimerization may be an intractable problem in this system. Heating of a solution of trimethylsilyl ether **155** in aqueous sodium dihydrogen phosphate, methanol and tetrahydrofuran at 60 °C quickly led to formation of a dark red reaction mixture. Following work-up and purification it was found that the starting material had been cleanly converted to a red solid which was characterized as diketone **156** (70% yield, Scheme 4.10). Interestingly, graduate researcher Fan Liu observed formation of the same decomposition product (**156**, 92% yield) from piperidone **157** (a possible precursor to 5-aza-tetracyclines) under identical conditions.



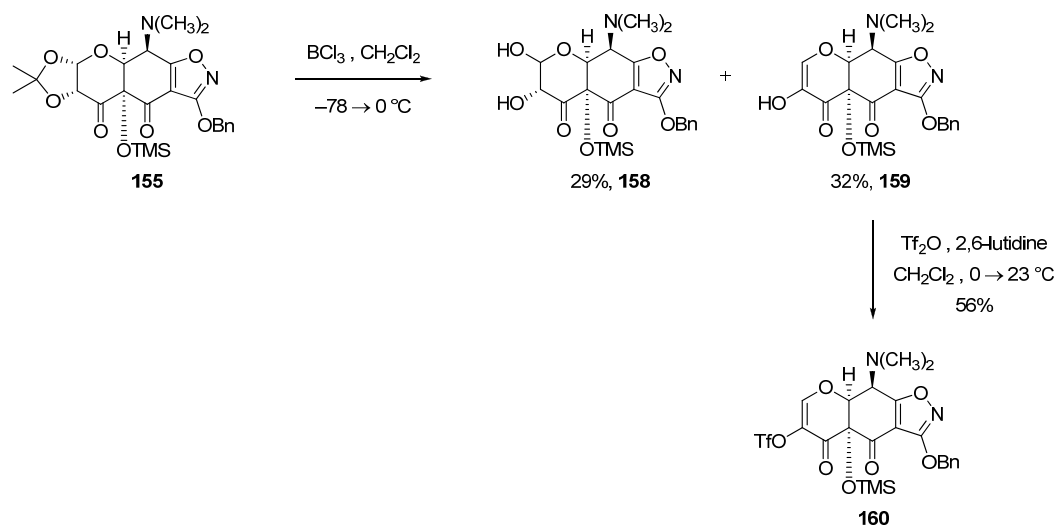
Scheme 4.10. Attempts to achieve C4-epimerization led to decomposition.

Attempts to achieve C4-epimerization using both acidic and basic conditions have led to the formation of diketone **156**. The highly distinctive dark red color of **156** has been observed upon formation of even small amounts of this product in various reaction mixtures. Treatment of substrates **154** and **155** with bases such as DBU and phosphazene $P_4-t\text{-Bu}$ in various solvents with different reaction temperatures either provided recovered starting material or led to decomposition. An attempt to form an extended C1–C4 enolate by treatment of a THF solution of **155** with an excess of NaHMDS at $-78\text{ }^{\circ}\text{C}$ afforded recovered starting material. The characteristic dark red color of diketone **156** was also observed upon prolonged exposure of 12a-hydroxylation product **154** to silica gel, and upon attempts to purify this compound by reverse-phase HPLC (methanol–water solvent system). A possible mechanism for the formation of **156** from various precursors to 5-hetero AB enones is presented in Scheme 4.11.



Scheme 4.11. Possible mechanism for the formation of decomposition product **156**.

Despite these failures, we also sought to find conditions for removal of the acetonide functionality and formation of a B-ring enone (Scheme 4.12 below). Addition of boron trichloride to a solution of acetonide **155** in dichloromethane at $-78\text{ }^{\circ}\text{C}$ followed by warming to $0\text{ }^{\circ}\text{C}$ provided diol **158** (29%) and enol **159** (32%). Treatment of enol **159** with trifluoromethanesulfonic anhydride (Trf_2O , 1.5 equiv) and 2,6-lutidine afforded enone triflate **160** in 56% yield following purification by flash-column chromatography. Diol **158** could also be converted to **160** using an excess of Trf_2O (2.5 equiv) and 2,6-lutidine (5 equiv). A dark red color was observed quickly following purification of enone triflate **160**, and complete decomposition to diketone **156** occurred upon standing overnight at $23\text{ }^{\circ}\text{C}$ under an inert atmosphere. An attempt to achieve palladium-catalyzed reduction of triflate **160** immediately following purification also led to decomposition.



Scheme 4.12. Synthesis of enone triflate **160**.

Conclusion

The chemical innovations described herein have established the viability of an iterative Michael–Claisen strategy for the synthesis of 5-hetero-tetracyclines. The substrate scope of the Michael–Claisen cyclization reaction has been expanded to include new heterocyclic enone electrophiles such as dihydro-4-pyridones.

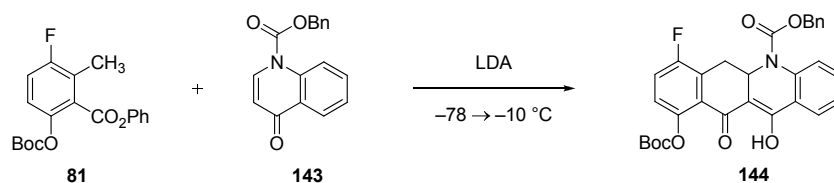
Experimental Section



Michael–Claisen cyclization product 142. A freshly prepared solution of lithium diisopropylamide in tetrahydrofuran (1.0 M, 418 μL , 0.418 mmol, 2.1 equiv) was added dropwise via syringe to a solution of phenyl ester **81** (138 mg, 0.398 mmol, 2.0 equiv) and TMEDA (120 μL , 0.796 mmol, 4.0 equiv) in tetrahydrofuran (2.5 mL) at $-78\text{ }^{\circ}\text{C}$, forming a bright red solution. After stirring at $-78\text{ }^{\circ}\text{C}$ for 45 min, a solution of *N*-benzyloxycarbamoyl-2,3-dihydro-4-pyridone **141** (46 mg, 0.199 mmol, 1 equiv) in tetrahydrofuran (0.5 mL) was added to the reaction solution dropwise via syringe. The resulting mixture was stirred at $-78\text{ }^{\circ}\text{C}$ for 10 min, then was allowed to warm slowly to $-10\text{ }^{\circ}\text{C}$ over 50 min. Aqueous potassium phosphate buffer solution (pH 7.0, 0.2 M, 25 mL) was then added to the reaction solution and the resulting mixture was allowed to warm to $23\text{ }^{\circ}\text{C}$. The product mixture was extracted with ethyl acetate (20 mL, then 10 mL). The organic extracts were combined and the combined solution was dried over anhydrous sodium sulfate. The dried solution was filtered and the filtrate was concentrated. The product was purified by flash-column chromatography (12% ethyl acetate–hexanes), providing Michael–Claisen cyclization product **142** as a pale yellow solid (60 mg, 62%).

$R_f = 0.19$ (15% ethyl acetate–hexanes); ^1H NMR (500 MHz, CDCl_3) δ 15.32 (s, 1H), 7.38–7.33 (m, 5H), 7.24 (app t, 1H, $J = 8.8\text{ Hz}$), 7.08 (dd, 1H, $J = 8.8, 3.9\text{ Hz}$), 5.20 (AB

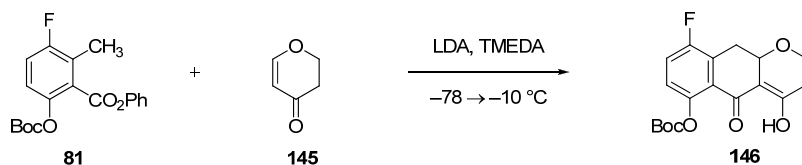
quartet, 2H), 4.88 (brd, 1H, $J = 9.8$ Hz), 4.41 (brs, 1H), 3.46 (brd, 1H, $J = 13.7$ Hz), 3.11 (app t, 1H, $J = 12.7, 11.7$ Hz), 2.61 (app t, 2H, $J = 14.6, 13.7$ Hz), 2.38 (brd, 1H, $J = 17.6$ Hz), 1.58 (s, 9H); ^{13}C NMR (125 MHz, CDCl_3) δ 184.2, 180.8, 157.3 (d, $J = 245.3$ Hz), 154.8, 151.5, 146.5 (d, $J = 2.7$ Hz), 136.1, 128.6, 128.2, 128.1, 127.7 (d, $J = 19.2$ Hz), 125.1 (d, $J = 3.7$ Hz), 123.4 (d, $J = 8.2$ Hz), 120.4 (d, $J = 23.8$ Hz), 110.6, 105.9, 84.0, 67.6, 48.9, 37.4, 31.9, 27.7; FTIR (neat film), 1761 (m), 1701 (m), 1225 (s), 1144 (s), 733 (s) cm^{-1} ; HRMS–ESI (m/z): $[\text{M}+\text{Na}]^+$ calcd for $\text{C}_{26}\text{H}_{26}\text{FNNaO}_7$, 506.1591; found, 506.1549.



Michael–Claisen cyclization product 144. A freshly prepared solution of lithium diisopropylamide in tetrahydrofuran (1.0 M, 421 μ L, 0.421 mmol, 2.1 equiv) was added dropwise via syringe to a solution of phenyl ester **81** (139 mg, 0.401 mmol, 2.0 equiv) in tetrahydrofuran (2.5 mL) at -78 $^{\circ}$ C, forming a bright red solution. After stirring at -78 $^{\circ}$ C for 35 min, a solution of *N*-benzyloxycarbamoyl-quinolone **143** (56 mg, 0.201 mmol, 1 equiv) in tetrahydrofuran (0.5 mL) was added to the reaction solution dropwise via syringe. The resulting mixture was stirred at -78 $^{\circ}$ C for 10 min, then was allowed to warm slowly to -10 $^{\circ}$ C over 75 min. Aqueous potassium phosphate buffer solution (pH 7.0, 0.2 M, 25 mL) was then added to the reaction solution and the resulting mixture was allowed to warm to 23 $^{\circ}$ C. The product mixture was extracted with ethyl acetate (2×30 mL). The organic extracts were combined and the combined solution was dried over anhydrous sodium sulfate. The dried solution was filtered and the filtrate was concentrated. The product was purified by flash-column chromatography (8% ethyl acetate–hexanes), providing Michael–Claisen cyclization product **144** as an orange-yellow solid (91 mg, 85%).

$R_f = 0.37$ (15% ethyl acetate–hexanes); ^1H NMR (500 MHz, CDCl_3) δ 14.59 (s, 1H), 7.86 (d, 1H, $J = 7.8$ Hz), 7.74 (d, 1H, $J = 8.8$ Hz), 7.42–7.33 (m, 6H), 7.24 (app t, 1H, $J = 8.8$, 7.8 Hz), 7.14 (app t, 1H, $J = 8.8$, 7.8 Hz), 7.09 (dd, 1H, $J = 8.8$, 3.9 Hz), 5.51 (dd, 1H, $J =$

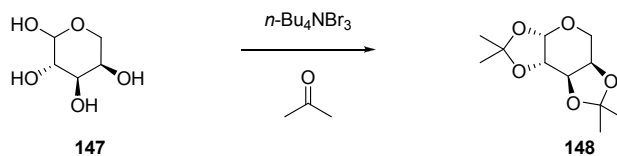
12.7, 3.9 Hz), 5.30 (AB quartet, 2H), 3.50 (dd, 1H, $J = 14.6, 3.9$ Hz), 2.92 (app t, 1H, $J = 14.6, 13.6$ Hz), 1.60 (s, 9H); ^{13}C NMR (125 MHz, CDCl_3) δ 182.8, 166.8, 157.3 (d, $J = 245.3$ Hz), 154.4, 151.5, 146.3 (d, $J = 2.7$ Hz), 138.1, 135.4, 132.8, 128.6, 128.4, 128.2, 126.6 (d, $J = 19.2$ Hz), 125.6 (d, $J = 3.7$ Hz), 124.8, 124.2, 123.8, 123.6 (d, $J = 8.2$ Hz), 121.8, 120.7 (d, $J = 24.7$ Hz), 107.0, 84.1, 68.4, 53.3, 29.6, 27.7; FTIR (neat film), 1759 (m), 1713 (m), 1285 (s), 1265 (s), 1225 (s), 1140 (s) cm^{-1} ; HRMS–ESI (m/z): $[\text{M}+\text{Na}]^+$ calcd for $\text{C}_{30}\text{H}_{26}\text{FNNaO}_7$, 554.1586; found, 554.1571.



Michael–Claisen cyclization product 146. A freshly prepared solution of lithium diisopropylamide in tetrahydrofuran (1.0 M, 171 μL , 0.171 mmol, 2.1 equiv) was added dropwise via syringe to a solution of phenyl ester **81** (56.5 mg, 0.163 mmol, 2.0 equiv) and TMEDA (49.2 μL , 0.326 mmol, 4.0 equiv) in tetrahydrofuran (1.25 mL) at $-78\text{ }^{\circ}\text{C}$, forming a bright red solution. After stirring at $-78\text{ }^{\circ}\text{C}$ for 30 min, a solution of 2,3-dihydro-4H-pyran-4-one **145** (8 mg, 0.082 mmol, 1 equiv) in tetrahydrofuran (0.25 mL) was added to the reaction solution dropwise via syringe. The resulting mixture was stirred at $-78\text{ }^{\circ}\text{C}$ for 5 min, then was allowed to warm slowly to $-10\text{ }^{\circ}\text{C}$ over 55 min. Aqueous potassium phosphate buffer solution (pH 7.0, 0.2 M, 15 mL) was then added to the reaction solution and the resulting mixture was allowed to warm to $23\text{ }^{\circ}\text{C}$. The product mixture was extracted with dichloromethane ($2 \times 15\text{ mL}$). The organic extracts were combined and the combined solution was dried over anhydrous sodium sulfate. The dried solution was filtered and the filtrate was concentrated. The product was purified by flash-column chromatography (9% ethyl acetate–hexanes, grading to 12%), providing Michael–Claisen cyclization product **146** as a pale orange-yellow solid (11 mg, 39%).

$R_f = 0.29$ (15% ethyl acetate–hexanes); ^1H NMR (500 MHz, CDCl_3) δ 15.37 (s, 1H), 7.22 (app t, 1H, $J = 8.8, 7.8\text{ Hz}$), 7.05 (dd, 1H, $J = 8.8, 4.9\text{ Hz}$), 4.56 (dd, 1H, $J = 12.7, 4.8\text{ Hz}$), 4.21 (dd, 1H, $J = 11.7, 7.8\text{ Hz}$), 3.82 (app td, 1H, $J = 11.7, 3.9\text{ Hz}$), 3.43 (dd, 1H, $J = 15.6, 5.9\text{ Hz}$), 2.85–2.78 (m, 1H), 2.62 (app t, 1H, $J = 14.7, 13.7\text{ Hz}$), 2.35 (dd, 1H, $J =$

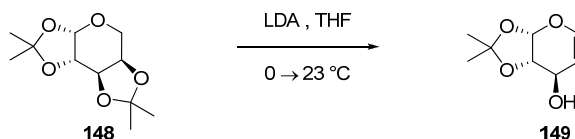
18.6, 3.9 Hz), 1.57 (s, 9H); ^{13}C NMR (125 MHz, CDCl_3) δ 182.4, 181.3, 157.1 (d, $J = 245.3$), 151.5, 146.1 (d, $J = 2.7$ Hz), 126.4 (d, $J = 19.2$ Hz), 125.1 (d, $J = 3.7$ Hz), 123.3 (d, $J = 8.3$ Hz), 120.2 (d, $J = 23.8$ Hz), 108.5, 84.0, 70.5, 63.5, 31.5, 27.9 (d, $J = 2.7$ Hz), 27.7; FTIR (neat film), 1759 (m), 1614 (w), 1279 (m), 1225 (s), 1144 (s) cm^{-1} ; HRMS–ESI (m/z): $[\text{M}+\text{H}]^+$ calcd for $\text{C}_{18}\text{H}_{19}\text{FNaO}_6$, 373.1063; found, 373.1025.



Bis-*O*-isopropylidene **148.**¹¹⁸ Tetrabutylammonium tribromide (1.29 g, 2.66 mmol, 0.04 equiv) was added in one portion to a white suspension of *D*-(-)-arabinose (**147**, 10.0 g, 66.6 mmol, 1 equiv) in dry acetone (250 mL, dried over anhydrous calcium sulfate) at 23 °C. The resulting mixture was stirred at 23 °C for 2 d, whereupon triethylamine (1.0 mL) was added carefully. The yellow product solution was concentrated. The crude product was purified by flash-column chromatography (2% acetone–hexanes, grading to 5%), affording bis-*O*-isopropylidene **148** as a white solid (12.3 g, 80%). ¹H NMR data for **148** closely matched that reported in the literature.¹¹⁹

¹¹⁸ This procedure is adapted from that of Khan et al.: Khan, A. T.; Khan, M. M.; Adhikary, A. *Carbohydrates Res.* **2011**, *346*, 673–677.

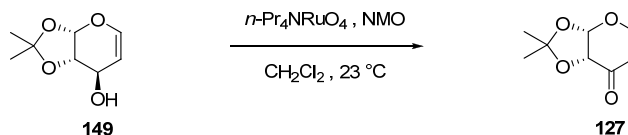
¹¹⁹ Pedatella, S.; Guaragna, A.; D'Alonzo, D.; De Nisco, M.; Palumbo, G. *Synthesis* **2006**, *2*, 305–308.



Allylic alcohol 149.¹²⁰ A round-bottomed flask containing a solution of bis-*O*-isopropylidene **148** (13.8 g, 59.9 mmol, 1 equiv) in tetrahydrofuran (500 mL) was placed in a cooling bath containing an ice–water mixture. A commercial solution of lithium diisopropylamide (2.0 M in tetrahydrofuran–heptane–ethylbenzene, 102 mL, 204 mmol, 3.4 equiv) was added carefully via cannula over 20 min to the cooled starting material solution. The resulting mixture was stirred for 30 min, whereupon the cooling bath was removed. The reaction mixture was allowed to warm to 23 °C. After stirring at this temperature for 6 h, the reaction flask was placed in a cooling water bath and water (400 mL) was added carefully. The cooling bath was removed and the product mixture was poured into a separatory funnel containing chloroform (400 mL). The phases were separated and the aqueous phase was further extracted with chloroform (400 mL, then 200 mL). The organic extracts were combined and the combined solution was dried over anhydrous sodium sulfate. The dried solution was filtered and the filtrate was concentrated. The product was purified by flash-column chromatography (20% ethyl acetate–hexanes, grading to 25%), providing allylic alcohol **149** as a pale yellow solid (5.05 g, 49%).

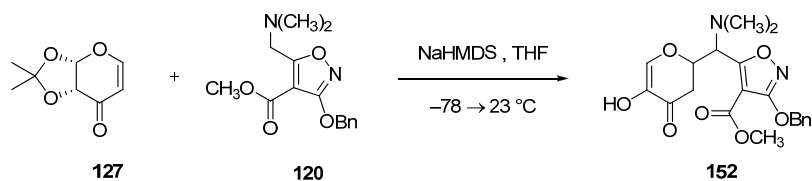
¹²⁰ This procedure is adapted from that of Klemer et al.: Klemer, A.; Jung, G. *Chem. Ber.* **1981**, *114*, 1192–1195.

$R_f = 0.22$ (30% ethyl acetate-hexanes); ^1H NMR (500 MHz, CDCl_3) δ 6.34 (d, 1H, $J = 6.3$ Hz), 5.44 (d, 1H, $J = 2.9$ Hz), 4.96-4.93 (m, 1H), 4.20-4.18 (m, 2H), 2.33 (d, 1H, $J = 4.9$ Hz), 1.45 (s, 3H), 1.39 (s, 3H); ^{13}C NMR (125 MHz, CDCl_3) δ 143.2, 111.0, 99.0, 93.4, 77.9, 60.3, 27.7, 25.8; FTIR (neat film), 3431 (br), 1651 (m), 1227 (s), 1076 (s), 1022 (s) cm^{-1} .



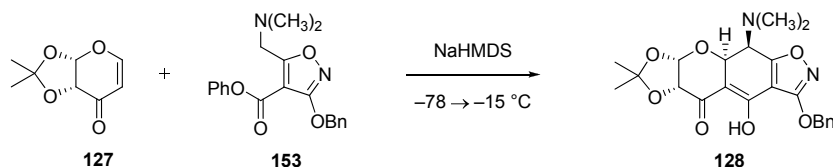
Dihydro-4-pyranone 127. Tetrapropylammonium perruthenate (343 mg, 0.976 mmol, 0.1 equiv) was added portionwise over 5 min to a cooled mixture (ice–water cooling bath) of allylic alcohol **149** (1.68 g, 9.76 mmol, 1 equiv), *N*-methylmorpholine *N*-oxide (1.72 g, 14.6 mmol, 1.5 equiv) and powdered 4Å molecular sieves in anhydrous dichloromethane (25 mL). The cooling bath was removed and the reaction mixture was allowed to warm to $23\text{ }^\circ\text{C}$. After stirring at this temperature for 20 min, the reaction mixture was filtered through a thick pad of silica gel, washing through with ethyl acetate. The filtrate was concentrated. The crude product was purified by flash-column chromatography (20% ethyl acetate–hexanes), affording dihydro-4-pyranone **127** as a very pale yellow solid (1.25 g, 75%).

$R_f = 0.26$ (30% ethyl acetate–hexanes); ^1H NMR (500 MHz, CDCl_3) δ 7.25 (d, 1H, $J = 6.0$ Hz), 5.88 (d, 1H, $J = 3.7$ Hz), 5.43 (d, 1H, $J = 6.4$ Hz), 4.19 (d, 1H, $J = 2.7$ Hz), 1.52 (s, 3H), 1.43 (s, 3H); ^{13}C NMR (125 MHz, CDCl_3) δ 186.3, 160.7, 113.3, 103.8, 101.0, 76.7, 27.4, 25.7; FTIR (neat film), 1678 (s), 1599 (s), 1223 (s), 1032 (s) cm^{-1} .



Methyl ester 152. A 1.0 M solution of sodium bis(trimethylsilyl)amide in tetrahydrofuran (197 μ L, 0.197 mmol, 2.1 equiv) was added dropwise via syringe to a solution of methyl 3-benzyloxy-5-(dimethylaminomethyl)isoxazole-4-carboxylate **120** (54.6 mg, 0.188 mmol, 2.0 equiv) in tetrahydrofuran (1.5 mL) at -78 $^{\circ}$ C (dry ice–acetone bath). The resulting yellow solution was stirred at this temperature for 5 min, then was allowed to warm to -20 $^{\circ}$ C (dry ice–acetonitrile bath). After stirring at -20 $^{\circ}$ C for 30 min, the reaction flask was placed in a dry ice–acetone bath at -78 $^{\circ}$ C. After stirring at this temperature for a further 5 min, a solution of B-ring precursor **127** (16.0 mg, 0.094 mmol, 1 equiv) in tetrahydrofuran (0.3 mL) was added slowly to the isoxazole anion solution at -78 $^{\circ}$ C. The reaction mixture was stirred at this temperature for 5 min, then was allowed to warm slowly to 23 $^{\circ}$ C over 70 min. Aqueous potassium phosphate buffer solution (pH 7.0, 0.2 M, 10 mL) and dichloromethane (10 mL) were added in sequence and the phases were separated. The aqueous phase was extracted with dichloromethane (10 mL). The organic extracts were combined and the combined solution was dried over anhydrous sodium sulfate. The dried solution was filtered and the filtrate was concentrated. The product was purified by flash-column chromatography (25% ethyl acetate–hexanes, grading to 30%), affording methyl ester **152** as a yellow solid (14.0 mg, 37%).

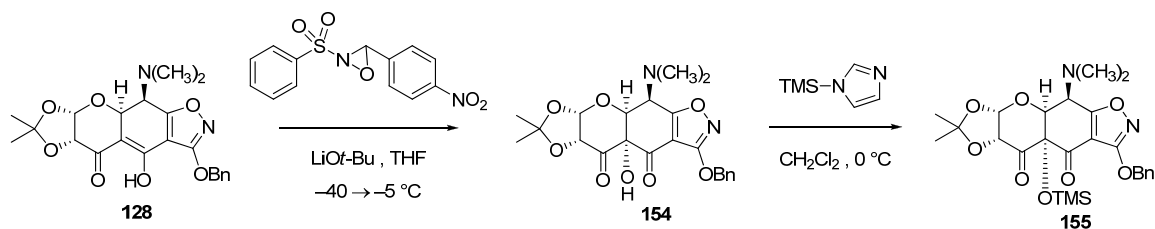
$R_f = 0.09$ (30% ethyl acetate-hexanes); ^1H NMR (500 MHz, CDCl_3) δ 7.49 (d, 2H, $J = 7.8$ Hz), 7.42-7.35 (m, 3H), 7.20 (s, 1H), 5.36 (s, 2H), 5.34 (brs, 1H), 4.94-4.89 (m, 1H), 4.80 (d, 1H, $J = 9.8$ Hz), 3.86 (s, 3H), 2.98 (dd, 1H, $J = 17.6, 3.5$ Hz), 2.74 (dd, 1H, $J = 17.6, 14.7$ Hz), 2.26 (s, 6H); ^{13}C NMR (125 MHz, CDCl_3) δ 187.5, 174.2, 168.8, 161.6, 145.0, 136.7, 135.4, 128.6, 128.4, 127.8, 104.3, 76.8, 72.0, 62.3, 51.9, 42.1, 38.2; FTIR (neat film), 1717 (m), 1674 (w), 1634 (w), 1613 (m), 1508 (m), 1173 (s), 1113 (s), 733 (s) cm^{-1} ; HRMS-ESI (m/z): $[\text{M}+\text{H}]^+$ calcd for $\text{C}_{19}\text{H}_{23}\text{N}_2\text{O}_6$, 403.1500; found, 403.1524.



Michael–Claisen cyclization product 128. A 1.0 M solution of sodium bis(trimethylsilyl)amide in tetrahydrofuran (12.1 mL, 12.1 mmol, 2.05 equiv) was added dropwise via syringe to a solution of phenyl 3-benzyloxy-5-(dimethylaminomethyl)isoxazole-4-carboxylate **153** (4.14 g, 11.8 mmol, 2.0 equiv) in tetrahydrofuran (100 mL) at $-78\text{ }^{\circ}\text{C}$ (dry ice–acetone bath). The resulting brownish yellow solution was stirred at this temperature for 5 min, then was allowed to warm to $-30\text{ }^{\circ}\text{C}$ (dry ice–acetonitrile bath). After stirring at $-30\text{ }^{\circ}\text{C}$ for 40 min, the reaction flask was placed in a dry ice–acetone bath at $-78\text{ }^{\circ}\text{C}$. After stirring at this temperature for a further 5 min, a solution of B-ring precursor **127** (1.00 g, 5.88 mmol, 1 equiv) in tetrahydrofuran (7.0 mL) was added slowly to the orange isoxazole anion solution at $-78\text{ }^{\circ}\text{C}$. The reaction mixture was stirred at this temperature for 5 min, then was allowed to warm slowly to $-15\text{ }^{\circ}\text{C}$ over 80 min. After stirring at $-15\text{ }^{\circ}\text{C}$ for a further 2 h, saturated aqueous ammonium chloride solution (30 mL) was added. The cooling bath was removed and the reaction flask was allowed to warm to $23\text{ }^{\circ}\text{C}$. Water (150 mL) and ethyl acetate (200 mL) were added and the phases were separated. The aqueous phase was extracted with ethyl acetate (200 mL). The organic extracts were combined and the combined solution was dried over anhydrous sodium sulfate. The dried solution was filtered and the filtrate was concentrated. The product was purified first by flash-column chromatography (18% acetone–hexanes, grading to 24%), then by preparative HPLC on an Agilent Prep

C18 column [10 μ m, 250 x 21.2 mm, UV detection at 350 nm, solvent A: water, solvent B: methanol, gradient elution with 70–90% B over 50 min, flow rate: 15 mL/min, 5 batches]. Fractions eluting 14–20 min were collected and concentrated, providing the Michael–Claisen cyclization product **128** as a yellow solid (1.00 g, 40%).

R_f = 0.15 (25% acetone–hexanes); ^1H NMR (500 MHz, CDCl_3) δ 13.62 (s, 1H), 7.49 (d, 2H, J = 7.8 Hz), 7.40–7.34 (m, 3H), 5.96 (d, 1H, J = 4.9 Hz), 5.37 (s, 2H), 5.10 (d, 1H, J = 6.8 Hz), 4.54 (d, 1H, J = 4.9 Hz), 4.22 (d, 1H, J = 7.8 Hz), 2.32 (s, 6H), 1.42 (s, 6H); ^{13}C NMR (125 MHz, CDCl_3) δ 182.3, 175.5, 167.3, 167.2, 134.8, 128.6, 128.6, 128.3, 109.5, 108.9, 106.5, 98.4, 72.6, 68.7, 64.6, 58.1, 42.2, 27.0, 26.8; FTIR (neat film), 2932 (w), 1699 (s), 1649 (s), 1510 (s), 1250 (s), 1125 (s), 836 (s) cm^{-1} ; HRMS–ESI (m/z): $[\text{M}+\text{H}]^+$ calcd for $\text{C}_{22}\text{H}_{24}\text{N}_2\text{O}_7$, 429.1662; found, 429.1656.



Trimethylsilyl ether 155. A commercial solution of lithium *tert*-butoxide in tetrahydrofuran (1.0 M, 305 μ L, 0.305 mmol, 0.3 equiv) was added dropwise via syringe to a stirred suspension of 3-(4-nitrophenyl)-2-(phenylsulfonyl)-oxaziridine¹⁰² (404 mg, 1.32 mmol, 1.3 equiv) and the Michael–Claisen cyclization product **128** (435 mg, 1.02 mmol, 1 equiv) in tetrahydrofuran (6.0 mL) at -40 $^{\circ}$ C. The resulting mixture was allowed to warm slowly to -5 $^{\circ}$ C over 30 min. After stirring at -5 $^{\circ}$ C for 1 h, saturated aqueous sodium bicarbonate solution (40 mL) was added and the product was extracted with ethyl acetate (2 x 40 mL). The organic extracts were combined and the combined solution was dried over anhydrous sodium sulfate. The dried solution was filtered and the filtrate was concentrated. The product was partially purified by flash-column chromatography (30% ethyl acetate–hexanes), affording impure tertiary alcohol **154** (mass of impure product = 395 mg). The impure hydroxylation product **154** was dissolved in dichloromethane (5.0 mL) and the resulting solution was cooled to 0 $^{\circ}$ C. 1-(Trimethylsilyl)imidazole (652 μ L, 4.44 mmol, 5.0 equiv) was added dropwise to the cooled solution of hydroxylation product **154**. After stirring at 0 $^{\circ}$ C for 1 h, the reaction mixture was diluted with dichloromethane (10 mL) and saturated aqueous sodium bicarbonate solution (10 mL) was added dropwise over 5 min with an ice–water cooling bath. The resulting mixture was allowed to warm to room temperature whereupon dichloromethane (10 mL) and

water (10 mL) were added. The phases were separated and the aqueous phase was extracted with dichloromethane (20 mL). The organic extracts were combined and the combined solution was dried over anhydrous sodium sulfate. The dried solution was filtered and the filtrate was concentrated. The crude product was purified by flash-column chromatography (12% ethyl acetate–hexanes, grading to 15%), providing trimethylsilyl ether **155** as a pale yellow solid (223 mg, 43% over two steps).

R_f = 0.18 (15% ethyl acetate–hexanes); ^1H NMR (500 MHz, CDCl_3) δ 7.46 (d, 2H, J = 7.3 Hz), 7.38–7.32 (m, 3H), 5.74 (d, 1H, J = 5.0 Hz), 5.37 (s, 2H), 4.79 (d, 1H, J = 2.7 Hz), 4.48 (d, 1H, J = 5.5 Hz), 4.45 (d, 1H, J = 3.2 Hz), 2.62 (s, 6H), 1.43 (s, 3H), 1.41 (s, 3H), 0.08 (s, 9H); ^{13}C NMR (125 MHz, CDCl_3) δ 200.9, 186.6, 179.4, 168.0, 134.8, 128.5, 128.5, 128.1, 110.0, 105.1, 99.4, 86.4, 77.4, 76.5, 72.4, 59.2, 43.3, 27.4, 26.9, 1.7; FTIR (neat film), 1753 (m), 1703 (m), 1512 (s), 1157 (s), 1072 (s), 849 (s) cm^{-1} ; HRMS–ESI (m/z): $[\text{M}+\text{H}]^+$ calcd for $\text{C}_{25}\text{H}_{33}\text{N}_2\text{O}_8\text{Si}$, 517.2001; found, 517.2022.

X-Ray Crystallography (C12a-hydroxylation product 154): A crystal mounted on a diffractometer was collected data at 180 K. The intensities of the reflections were collected by means of a Bruker APEX II DUO CCD diffractometer (Cu $K\alpha$ radiation, $\lambda=1.54178$ Å), and equipped with an Oxford Cryosystems nitrogen flow apparatus. The collection method involved 1.0° scans in ω at 30° , 55° , 80° and 115° in 2θ . Data integration down to 0.84 Å resolution was carried out using SAINT V7.46 A with reflection spot size optimization.¹²¹ Absorption corrections were made with the program SADABS.¹²¹ The structure was solved by the direct methods procedure and refined by least-squares methods against F^2 using SHELXS-97 and SHELXL-97.¹²² Non-hydrogen atoms were refined anisotropically, and hydrogen atoms were allowed to ride on the respective atoms. Crystal data as well as details of data collection and refinement are summarized in Table 4.1, geometric parameters are shown in Table 4.2, and hydrogen-bond parameters are listed in Table 4.3. The Ortep plots produced with SHELXL-97 program, and the other drawings were produced with Accelrys DS Visualizer 2.0.¹²³

¹²¹ Bruker AXS APEX II, Bruker AXS, Madison, Wisconsin, **2009**.

¹²² G. M. Sheldrick, Acta Cryst. **2008**, A64, 112-122.

¹²³ Accelrys DS Visualizer v2.0.1, Accelrys Software. Inc., **2007**.

Table 4.1. Experimental details

	V-PMW-526
Crystal data	
Chemical formula	C ₂₂ H ₂₄ N ₂ O ₈
M_r	444.43
Crystal system, space group	Monoclinic, $P2_1$
Temperature (K)	100
a, b, c (Å)	9.5161 (2), 17.6610 (3), 13.0462 (2)
β (°)	107.255 (1)
V (Å ³)	2093.91 (7)
Z	4
Radiation type	Cu $K\alpha$
μ (mm ⁻¹)	0.91
Crystal size (mm)	0.03 × 0.01 × 0.01
Data collection	
Diffractionmeter	Bruker D8 goniometer with CCD area detector diffractometer
Absorption correction	Multi-scan <i>SADABS</i>

Table 4.1. (Continued)	
T_{\min}, T_{\max}	0.973, 0.991
No. of measured, independent and observed [$I > 2\sigma(I)$] reflections	33387, 6774, 6441
R_{int}	0.038
Refinement	
$R[F^2 > 2\sigma(F^2)], wR(F^2), S$	0.028, 0.066, 1.05
No. of reflections	6774
No. of parameters	593
No. of restraints	1
H-atom treatment	H atoms treated by a mixture of independent and constrained refinement
$\Delta\rho_{\max}, \Delta\rho_{\min}$ (e Å ⁻³)	0.17, -0.15
Absolute structure	Flack H D (1983), Acta Cryst. A39, 876-881
Flack parameter	0.02 (10)

Computer programs: *APEX2* v2009.3.0 (Bruker-AXS, 2009), *SAINT* 7.46A (Bruker-AXS, 2009), *SHELXS97* (Sheldrick, 2008), *SHELXL97* (Sheldrick, 2008), Bruker *SHELXTL* (Sheldrick, 2008).

Table 4.2. Geometric parameters (Å, °)

C1—N1	1.307 (2)	C31—N3	1.315 (2)
C1—O1	1.328 (2)	C31—O11	1.328 (2)
C1—C2	1.429 (3)	C31—C32	1.423 (3)
C2—C11	1.360 (3)	C32—C41	1.351 (3)
C2—C3	1.447 (3)	C32—C33	1.460 (2)
C3—O2	1.217 (2)	C33—O12	1.213 (2)
C3—C4	1.549 (3)	C33—C34	1.546 (3)
C4—O3	1.408 (2)	C34—O13	1.407 (2)
C4—C5	1.521 (2)	C34—C35	1.526 (3)
C4—C9	1.542 (2)	C34—C39	1.551 (2)
C5—O4	1.202 (2)	C35—O14	1.205 (2)
C5—C6	1.527 (3)	C35—C36	1.519 (3)
C6—O5	1.407 (2)	C36—O15	1.404 (2)
C6—C8	1.531 (2)	C36—C38	1.523 (2)
C6—H6	1.0000	C36—H36	1.0000

Table 4.2. (Continued)			
C7—O5	1.434 (2)	C37—O15	1.442 (2)
C7—O6	1.446 (2)	C37—O16	1.446 (2)
C7—C20	1.505 (3)	C37—C49	1.501 (3)
C7—C19	1.511 (3)	C37—C50	1.514 (3)
C8—O7	1.394 (2)	C38—O17	1.398 (2)
C8—O6	1.416 (2)	C38—O16	1.423 (2)
C8—H8	1.0000	C38—H38	1.0000
C9—O7	1.429 (2)	C39—O17	1.425 (2)
C9—C10	1.550 (2)	C39—C40	1.549 (2)
C9—H9	1.0000	C39—H39	1.0000
C10—N2	1.464 (2)	C40—N4	1.472 (2)
C10—C11	1.501 (3)	C40—C41	1.494 (3)
C10—H10	1.0000	C40—H40	1.0000
C11—O8	1.330 (2)	C41—O18	1.333 (2)
C12—O1	1.456 (2)	C42—O11	1.457 (2)
C12—C13	1.502 (3)	C42—C43	1.501 (3)

Table 4.2. (Continued)			
C12—H12A	0.9900	C42—H42A	0.9900
C12—H12B	0.9900	C42—H42B	0.9900
C13—C18	1.380 (3)	C43—C44	1.393 (3)
C13—C14	1.394 (3)	C43—C48	1.397 (3)
C14—C15	1.390 (3)	C44—C45	1.390 (3)
C14—H14	0.9500	C44—H44	0.9500
C15—C16	1.367 (4)	C45—C46	1.375 (3)
C15—H15	0.9500	C45—H45	0.9500
C16—C17	1.372 (3)	C46—C47	1.389 (3)
C16—H16	0.9500	C46—H46	0.9500
C17—C18	1.387 (3)	C47—C48	1.382 (3)
C17—H17	0.9500	C47—H47	0.9500
C18—H18	0.9500	C48—H48	0.9500
C19—H19A	0.9800	C49—H49A	0.9800
C19—H19B	0.9800	C49—H49B	0.9800
C19—H19C	0.9800	C49—H49C	0.9800

Table 4.2. (Continued)			
C20—H20A	0.9800	C50—H50A	0.9800
C20—H20B	0.9800	C50—H50B	0.9800
C20—H20C	0.9800	C50—H50C	0.9800
C21—N2	1.458 (3)	C51—N4	1.468 (2)
C21—H21A	0.9800	C51—H51A	0.9800
C21—H21B	0.9800	C51—H51B	0.9800
C21—H21C	0.9800	C51—H51C	0.9800
C22—N2	1.466 (3)	C52—N4	1.476 (3)
C22—H22A	0.9800	C52—H52A	0.9800
C22—H22B	0.9800	C52—H52B	0.9800
C22—H22C	0.9800	C52—H52C	0.9800
N1—O8	1.448 (2)	N3—O18	1.4343 (19)
O3—H3	0.90 (3)	O13—H13	0.87 (3)
N1—C1—O1	125.05 (17)	N3—C31—O11	123.85 (16)
N1—C1—C2	112.66 (17)	N3—C31—C32	112.13 (16)

Table 4.2. (Continued)			
O1—C1—C2	122.21 (16)	O11—C31—C32	123.94 (16)
C11—C2—C1	103.57 (16)	C41—C32—C31	104.02 (15)
C11—C2—C3	123.97 (18)	C41—C32—C33	122.80 (16)
C1—C2—C3	132.43 (17)	C31—C32—C33	133.18 (16)
O2—C3—C2	125.31 (18)	O12—C33—C32	125.09 (17)
O2—C3—C4	121.30 (17)	O12—C33—C34	121.96 (16)
C2—C3—C4	113.37 (15)	C32—C33—C34	112.84 (15)
O3—C4—C5	112.00 (14)	O13—C34—C35	111.76 (14)
O3—C4—C9	110.37 (14)	O13—C34—C33	106.97 (14)
C5—C4—C9	108.76 (14)	C35—C34—C33	108.32 (15)
O3—C4—C3	107.42 (15)	O13—C34—C39	109.47 (14)
C5—C4—C3	107.85 (15)	C35—C34—C39	108.37 (14)
C9—C4—C3	110.41 (14)	C33—C34—C39	111.98 (14)
O4—C5—C4	121.55 (17)	O14—C35—C36	121.70 (17)
O4—C5—C6	121.48 (16)	O14—C35—C34	120.63 (17)
C4—C5—C6	116.96 (15)	C36—C35—C34	117.67 (14)

Table 4.2. (Continued)			
O5—C6—C5	112.59 (15)	O15—C36—C35	112.00 (14)
O5—C6—C8	103.25 (14)	O15—C36—C38	103.00 (14)
C5—C6—C8	113.72 (14)	C35—C36—C38	112.57 (15)
O5—C6—H6	109.0	O15—C36—H36	109.7
C5—C6—H6	109.0	C35—C36—H36	109.7
C8—C6—H6	109.0	C38—C36—H36	109.7
O5—C7—O6	105.33 (14)	O15—C37—O16	105.64 (13)
O5—C7—C20	108.47 (16)	O15—C37—C49	111.96 (15)
O6—C7—C20	109.71 (16)	O16—C37—C49	108.52 (16)
O5—C7—C19	111.26 (16)	O15—C37—C50	107.28 (16)
O6—C7—C19	108.58 (16)	O16—C37—C50	110.39 (15)
C20—C7—C19	113.20 (19)	C49—C37—C50	112.81 (17)
O7—C8—O6	111.22 (14)	O17—C38—O16	111.08 (14)
O7—C8—C6	115.42 (15)	O17—C38—C36	115.21 (15)
O6—C8—C6	103.12 (15)	O16—C38—C36	102.20 (14)
O7—C8—H8	108.9	O17—C38—H38	109.4

Table 4.2. (Continued)			
O6—C8—H8	108.9	O16—C38—H38	109.4
C6—C8—H8	108.9	C36—C38—H38	109.4
O7—C9—C4	107.08 (14)	O17—C39—C40	106.40 (13)
O7—C9—C10	106.36 (14)	O17—C39—C34	108.99 (14)
C4—C9—C10	113.55 (14)	C40—C39—C34	113.84 (14)
O7—C9—H9	109.9	O17—C39—H39	109.2
C4—C9—H9	109.9	C40—C39—H39	109.2
C10—C9—H9	109.9	C34—C39—H39	109.2
N2—C10—C11	113.77 (15)	N4—C40—C41	112.22 (14)
N2—C10—C9	116.78 (15)	N4—C40—C39	117.08 (15)
C11—C10—C9	106.17 (14)	C41—C40—C39	107.96 (14)
N2—C10—H10	106.5	N4—C40—H40	106.3
C11—C10—H10	106.5	C41—C40—H40	106.3
C9—C10—H10	106.5	C39—C40—H40	106.3
O8—C11—C2	110.96 (17)	O18—C41—C32	110.79 (16)
O8—C11—C10	123.03 (16)	O18—C41—C40	121.42 (15)

Table 4.2. (Continued)			
C2—C11—C10	125.95 (16)	C32—C41—C40	127.66 (16)
O1—C12—C13	108.31 (15)	O11—C42—C43	109.34 (14)
O1—C12—H12A	110.0	O11—C42—H42A	109.8
C13—C12—H12A	110.0	C43—C42—H42A	109.8
O1—C12—H12B	110.0	O11—C42—H42B	109.8
C13—C12—H12B	110.0	C43—C42—H42B	109.8
H12A—C12—H12B	108.4	H42A—C42—H42B	108.3
C18—C13—C14	118.0 (2)	C44—C43—C48	118.93 (18)
C18—C13—C12	119.89 (17)	C44—C43—C42	122.94 (17)
C14—C13—C12	122.12 (19)	C48—C43—C42	118.09 (16)
C15—C14—C13	120.4 (2)	C45—C44—C43	119.91 (18)
C15—C14—H14	119.8	C45—C44—H44	120.0
C13—C14—H14	119.8	C43—C44—H44	120.0
C16—C15—C14	120.5 (2)	C46—C45—C44	120.73 (18)
C16—C15—H15	119.7	C46—C45—H45	119.6
C14—C15—H15	119.7	C44—C45—H45	119.6

Table 4.2. (Continued)			
C15—C16—C17	119.7 (2)	C45—C46—C47	119.86 (19)
C15—C16—H16	120.2	C45—C46—H46	120.1
C17—C16—H16	120.2	C47—C46—H46	120.1
C16—C17—C18	120.1 (2)	C48—C47—C46	119.89 (19)
C16—C17—H17	119.9	C48—C47—H47	120.1
C18—C17—H17	119.9	C46—C47—H47	120.1
C13—C18—C17	121.22 (18)	C47—C48—C43	120.66 (18)
C13—C18—H18	119.4	C47—C48—H48	119.7
C17—C18—H18	119.4	C43—C48—H48	119.7
C7—C19—H19A	109.5	C37—C49—H49A	109.5
C7—C19—H19B	109.5	C37—C49—H49B	109.5
H19A—C19—H19B	109.5	H49A—C49—H49B	109.5
C7—C19—H19C	109.5	C37—C49—H49C	109.5
H19A—C19—H19C	109.5	H49A—C49—H49C	109.5
H19B—C19—H19C	109.5	H49B—C49—H49C	109.5
C7—C20—H20A	109.5	C37—C50—H50A	109.5

Table 4.2. (Continued)			
C7—C20—H20B	109.5	C37—C50—H50B	109.5
H20A—C20—H20B	109.5	H50A—C50—H50B	109.5
C7—C20—H20C	109.5	C37—C50—H50C	109.5
H20A—C20—H20C	109.5	H50A—C50—H50C	109.5
H20B—C20—H20C	109.5	H50B—C50—H50C	109.5
N2—C21—H21A	109.5	N4—C51—H51A	109.5
N2—C21—H21B	109.5	N4—C51—H51B	109.5
H21A—C21—H21B	109.5	H51A—C51—H51B	109.5
N2—C21—H21C	109.5	N4—C51—H51C	109.5
H21A—C21—H21C	109.5	H51A—C51—H51C	109.5
H21B—C21—H21C	109.5	H51B—C51—H51C	109.5
N2—C22—H22A	109.5	N4—C52—H52A	109.5
N2—C22—H22B	109.5	N4—C52—H52B	109.5
H22A—C22—H22B	109.5	H52A—C52—H52B	109.5
N2—C22—H22C	109.5	N4—C52—H52C	109.5
H22A—C22—H22C	109.5	H52A—C52—H52C	109.5

Table 4.2. (Continued)			
H22B—C22—H22C	109.5	H52B—C52—H52C	109.5
C1—N1—O8	104.29 (14)	C31—N3—O18	104.38 (13)
C21—N2—C10	111.45 (15)	C51—N4—C40	111.14 (14)
C21—N2—C22	109.98 (16)	C51—N4—C52	110.08 (15)
C10—N2—C22	117.13 (14)	C40—N4—C52	116.75 (14)
C1—O1—C12	116.77 (15)	C31—O11—C42	115.91 (14)
C4—O3—H3	109.9 (18)	C34—O13—H13	106.9 (17)
C6—O5—C7	108.05 (13)	C36—O15—C37	108.05 (13)
C8—O6—C7	109.74 (13)	C38—O16—C37	108.24 (13)
C8—O7—C9	115.50 (14)	C38—O17—C39	115.65 (13)
C11—O8—N1	108.48 (13)	C41—O18—N3	108.61 (13)
N1—C1—C2—C11	2.3 (2)	N3—C31—C32—C41	3.0 (2)
O1—C1—C2—C11	-174.62 (17)	O11—C31—C32—C41	-173.92 (16)
N1—C1—C2—C3	-175.66 (19)	N3—C31—C32—C33	-176.46 (18)
O1—C1—C2—C3	7.5 (3)	O11—C31—C32—C33	6.6 (3)

Table 4.2. (Continued)			
C11—C2—C3—O2	-168.86 (19)	C41—C32—C33—O12	-166.79 (18)
C1—C2—C3—O2	8.7 (3)	C31—C32—C33—O12	12.6 (3)
C11—C2—C3—C4	12.8 (3)	C41—C32—C33—C34	17.0 (2)
C1—C2—C3—C4	-169.64 (19)	C31—C32—C33—C34	-163.66 (18)
O2—C3—C4—O3	-95.7 (2)	O12—C33—C34—O13	-96.5 (2)
C2—C3—C4—O3	82.68 (18)	C32—C33—C34—O13	79.89 (17)
O2—C3—C4—C5	25.2 (2)	O12—C33—C34—C35	24.1 (2)
C2—C3—C4—C5	-156.42 (15)	C32—C33—C34—C35	-159.49 (15)
O2—C3—C4—C9	143.88 (18)	O12—C33—C34—C39	143.59 (17)
C2—C3—C4—C9	-37.7 (2)	C32—C33—C34—C39	-40.0 (2)
O3—C4—C5—O4	14.3 (2)	O13—C34—C35—O14	15.6 (2)
C9—C4—C5—O4	136.56 (18)	C33—C34—C35—O14	-102.0 (2)
C3—C4—C5—O4	-103.7 (2)	C39—C34—C35—O14	136.33 (18)
O3—C4—C5—C6	-166.24 (15)	O13—C34—C35—C36	-164.94 (15)
C9—C4—C5—C6	-44.0 (2)	C33—C34—C35—C36	77.47 (19)
C3—C4—C5—C6	75.77 (19)	C39—C34—C35—C36	-44.2 (2)

Table 4.2. (Continued)			
O4—C5—C6—O5	-35.2 (2)	O14—C35—C36—O15	-31.4 (2)
C4—C5—C6—O5	145.32 (15)	C34—C35—C36—O15	149.19 (15)
O4—C5—C6—C8	-152.22 (17)	O14—C35—C36—C38	-146.88 (18)
C4—C5—C6—C8	28.3 (2)	C34—C35—C36—C38	33.7 (2)
O5—C6—C8—O7	-151.86 (15)	O15—C36—C38—O17	-156.30 (15)
C5—C6—C8—O7	-29.5 (2)	C35—C36—C38—O17	-35.5 (2)
O5—C6—C8—O6	-30.37 (17)	O15—C36—C38—O16	-35.74 (17)
C5—C6—C8—O6	91.94 (17)	C35—C36—C38—O16	85.08 (17)
O3—C4—C9—O7	-176.43 (14)	O13—C34—C39—O17	178.49 (14)
C5—C4—C9—O7	60.32 (18)	C35—C34—C39—O17	56.37 (18)
C3—C4—C9—O7	-57.82 (18)	C33—C34—C39—O17	-63.05 (18)
O3—C4—C9—C10	-59.34 (19)	O13—C34—C39—C40	-62.92 (19)
C5—C4—C9—C10	177.42 (15)	C35—C34—C39—C40	174.96 (14)
C3—C4—C9—C10	59.28 (19)	C33—C34—C39—C40	55.5 (2)
O7—C9—C10—N2	-60.33 (19)	O17—C39—C40—N4	-50.47 (19)
C4—C9—C10—N2	-177.85 (15)	C34—C39—C40—N4	-170.53 (15)

Table 4.2. (Continued)			
O7—C9—C10—C11	67.73 (17)	O17—C39—C40—C41	77.28 (17)
C4—C9—C10—C11	-49.79 (19)	C34—C39—C40—C41	-42.77 (19)
C1—C2—C11—O8	-1.9 (2)	C31—C32—C41—O18	-2.6 (2)
C3—C2—C11—O8	176.28 (17)	C33—C32—C41—O18	176.91 (16)
C1—C2—C11—C10	175.38 (17)	C31—C32—C41—C40	173.18 (17)
C3—C2—C11—C10	-6.5 (3)	C33—C32—C41—C40	-7.3 (3)
N2—C10—C11—O8	-29.2 (2)	N4—C40—C41—O18	-34.4 (2)
C9—C10—C11—O8	-158.99 (16)	C39—C40—C41—O18	-164.85 (15)
N2—C10—C11—C2	153.90 (18)	N4—C40—C41—C32	150.24 (17)
C9—C10—C11—C2	24.1 (2)	C39—C40—C41—C32	19.7 (2)
O1—C12—C13—C18	143.90 (18)	O11—C42—C43—C44	-10.8 (2)
O1—C12—C13—C14	-36.4 (2)	O11—C42—C43—C48	171.70 (16)
C18—C13—C14—C15	1.1 (3)	C48—C43—C44—C45	1.0 (3)
C12—C13—C14—C15	-178.61 (19)	C42—C43—C44—C45	-176.51 (18)
C13—C14—C15—C16	0.0 (3)	C43—C44—C45—C46	-0.1 (3)
C14—C15—C16—C17	-0.6 (3)	C44—C45—C46—C47	-0.9 (3)

Table 4.2. (Continued)			
C15—C16—C17—C18	0.1 (3)	C45—C46—C47—C48	0.9 (3)
C14—C13—C18—C17	-1.6 (3)	C46—C47—C48—C43	0.0 (3)
C12—C13—C18—C17	178.11 (19)	C44—C43—C48—C47	-0.9 (3)
C16—C17—C18—C13	1.0 (3)	C42—C43—C48—C47	176.68 (18)
O1—C1—N1—O8	175.07 (17)	O11—C31—N3—O18	174.81 (16)
C2—C1—N1—O8	-1.7 (2)	C32—C31—N3—O18	-2.11 (19)
C11—C10—N2—C21	176.40 (15)	C41—C40—N4—C51	-179.95 (15)
C9—C10—N2—C21	-59.3 (2)	C39—C40—N4—C51	-54.3 (2)
C11—C10—N2—C22	-55.7 (2)	C41—C40—N4—C52	-52.6 (2)
C9—C10—N2—C22	68.5 (2)	C39—C40—N4—C52	73.1 (2)
N1—C1—O1—C12	-4.1 (3)	N3—C31—O11—C42	-8.9 (3)
C2—C1—O1—C12	172.35 (17)	C32—C31—O11—C42	167.68 (16)
C13—C12—O1—C1	-148.03 (16)	C43—C42—O11—C31	-144.68 (16)
C5—C6—O5—C7	-91.18 (16)	C35—C36—O15—C37	-90.26 (17)
C8—C6—O5—C7	31.89 (18)	C38—C36—O15—C37	30.95 (18)
O6—C7—O5—C6	-21.19 (19)	O16—C37—O15—C36	-14.48 (18)

Table 4.2. (Continued)			
C20—C7—O5—C6	-138.59 (16)	C49—C37—O15—C36	103.47 (17)
C19—C7—O5—C6	96.28 (19)	C50—C37—O15—C36	-132.25 (15)
O7—C8—O6—C7	142.43 (15)	O17—C38—O16—C37	150.94 (14)
C6—C8—O6—C7	18.15 (18)	C36—C38—O16—C37	27.55 (17)
O5—C7—O6—C8	0.52 (19)	O15—C37—O16—C38	-9.60 (18)
C20—C7—O6—C8	117.08 (17)	C49—C37—O16—C38	-129.83 (16)
C19—C7—O6—C8	-118.74 (17)	C50—C37—O16—C38	106.06 (18)
O6—C8—O7—C9	-65.49 (19)	O16—C38—O17—C39	-62.13 (19)
C6—C8—O7—C9	51.5 (2)	C36—C38—O17—C39	53.4 (2)
C4—C9—O7—C8	-67.14 (18)	C40—C39—O17—C38	172.73 (14)
C10—C9—O7—C8	171.14 (14)	C34—C39—O17—C38	-64.12 (18)
C2—C11—O8—N1	0.9 (2)	C32—C41—O18—N3	1.48 (19)
C10—C11—O8—N1	-176.38 (16)	C40—C41—O18—N3	-174.63 (15)
C1—N1—O8—C11	0.48 (19)	C31—N3—O18—C41	0.43 (18)

Table 4.3. Hydrogen-bond parameters

$D-H\cdots A$	$D-H$ (Å)	$H\cdots A$ (Å)	$D\cdots A$ (Å)	$D-H\cdots A$ (°)
$O3-H3\cdots N4^i$	0.90 (3)	2.03 (3)	2.893 (2)	161 (3)
$O13-H13\cdots N2^{ii}$	0.87 (3)	2.12 (3)	2.915 (2)	151 (2)

Symmetry code(s): (i) $x+1, y, z$; (ii) $x-1, y, z-1$.

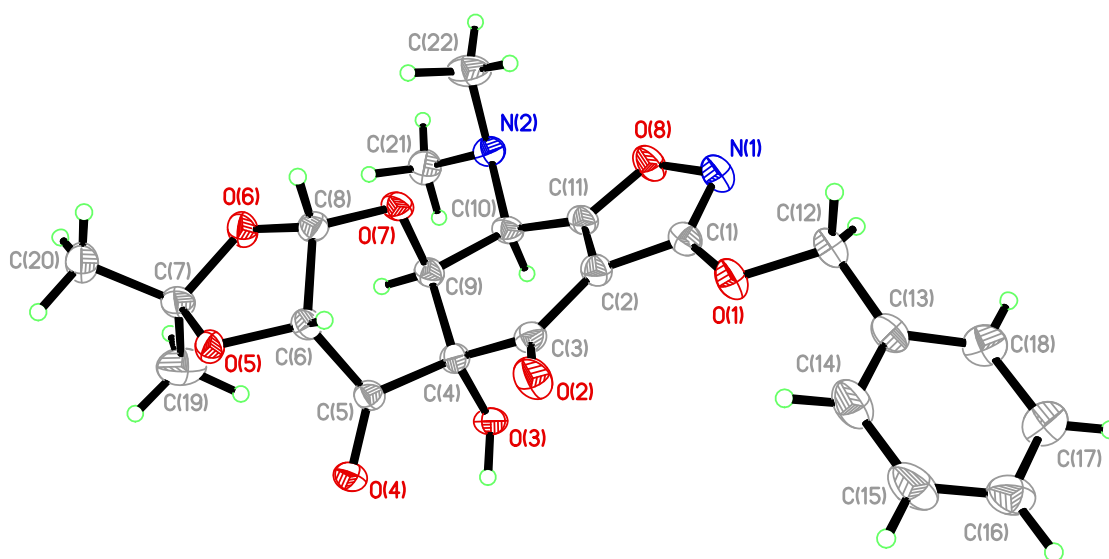


Figure 4.1a

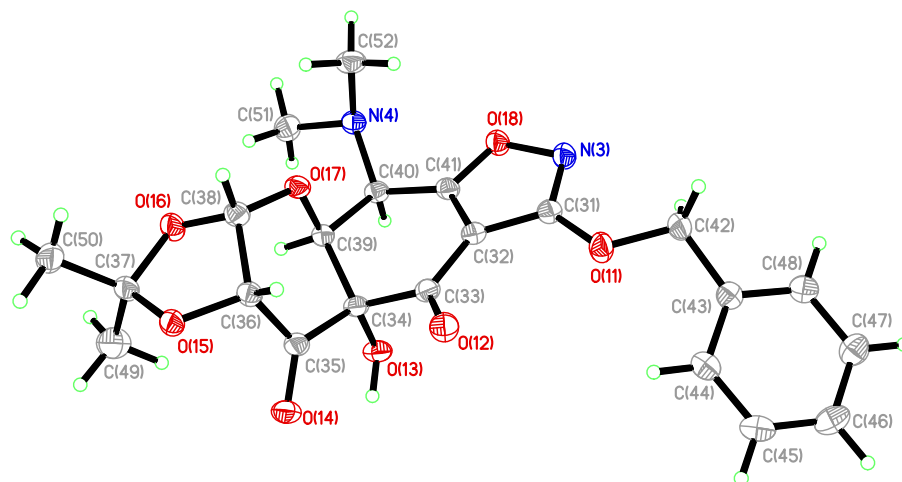


Figure 4.1b

Figure 4.1. Perspective views showing 50% probability displacement.

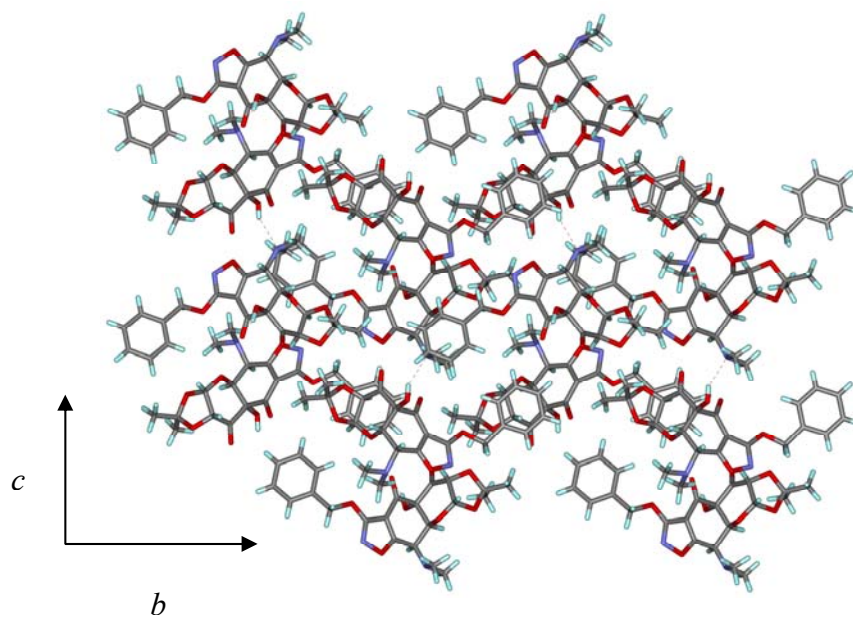


Figure 4.2. Three-dimensional supramolecular architecture viewed along the *a*-axis direction.

Catalog of Spectra

